Non-aging disruptive carbon molecular sieve membranes: preparation and characterization

Sandra Cristina Vale Rodrigues

Dissertation presented for the degree of

Doctor in Chemical and Biological Engineering

by the

University of Porto

Supervisors

Adélio Miguel Magalhães Mendes

Fernão Domingos de Montenegro Baptista Malheiro de Magalhães

LEPABE – Laboratory for Process Engineering, Environment, Biotechnology and Energy

Department of Chemical Engineering

Faculty of Engineering – University of Porto

Porto, 2017

Statement of originality

I certify that this work does not contain any material that has been used nor will be for the award of any other degree or diploma in my name or anyone, in any university or institution. In addition, I certify that, to the best of my knowledge, this work does not contain any material previously published or written by another person, expect where due reference has been made in the text.

_____

Sandra Cristina Vale Rodrigues

Statement

In order to fulfil the Rules of Ethics of the Doctoral Program of Chemical and Biological Engineering (PDEQB), we hereby declare that all the contents of the thesis presented by Sandra Cristina Vale Rodrigues, entitled 'Non-aging disruptive carbon molecular sieve membranes: preparation and characterization', is exclusively from the author with the collaborations mentioned in the thesis.

_____

Adélio Miguel Magalhães Mendes
Full Professor

_____

Fernão Domingos de Montenegro Baptista Malheiro de Magalhães
Assistant Professor

This work was the result of the projects:

(i) POCI-01-0145-FEDER-006939 (Laboratory for Process Engineering, Environment, Biotechnology and Energy – UID/EQU/00511/2013) funded by the European Regional Development Fund (ERDF), through COMPETE2020 – Programa Operacional Competitividade e Internacionalização (POCI) and by national funds, through FCT - Fundação para a Ciência e a Tecnologia.

(ii) NORTE-01-0145-FEDER-000005 – LEPABE-2-ECO-INNOVATION, supported by North Portugal Regional Operational Programme (NORTE 2020), under the Portugal 2020 Partnership Agreement, through the European Regional Development Fund (ERDF).

(iii) SFRH/BD/93779/2013 – PhD grant, through Portuguese Foundation for Science and Technology (FCT) supported by funding POPH/FSE.

Acknowledgments

First of all, I would like to acknowledge my supervisors, Prof. Adélio Mendes and Prof. Fernão Magalhães, for allowing me to carry out my PhD work. To Prof. Adélio Mendes, my most sincere gratitude for the enormous dedication, understanding, for believing in me and never letting me give up…Thank you so much for your unconditional support at the most difficult moments! To Prof. Fernão Magalhães I am very grateful for all the support and the patience during helpful discussions.

I would like to acknowledge the financial support of the Portuguese Foundation for Science and Technology (FCT) for my PhD grant (Ref. SFRH/BD/93779/2013). I would also like to thank LEPABE, DEQ and FEUP for giving me the conditions to accomplish my work.

I want to thank Dr. Jamie Moffat and Dr. Colin Marshall from Innovia Films Ltd. for their kindness, for supplying the regenerated cellulose films and all fundamental support in the development of my work. I have no words to thank all that you have done for me!

I would like to acknowledge Dr. Roger Whitley for the fruitful discussions during all these years.

I would also like to thank Dr. Alfredo Tanaka and Dr. Margot Tanco for the enormous help they gave me when they welcomed me into their research area.

A special thank you to Mr. Nelson Neves, from the company Neves&Neves, for understanding all my urgent requests and to D. Fátima Faustino for her kindness and help with administrative questions.

My thankful words also go to my lab mates for their friendship and precious help. I want to thank with a special word to Márcia Andrade for the support, affection and

for always being there with kind words and a smile. To Diana Paiva, thank you for your kindness and precious help with FTIR analysis.

I also would like to acknowledge all my friends outside FEUP for all wonderful moments and advices.

Thank you to my mother-in-law and father-in-law for trusting me, for sharing my problems and your kind words… you´re the best!

To my mother, my father and my sister Rita, thank you for all the love, patience, for not letting me down, for the encouragements, for never letting me feel alone…thank you all for the amazing people you are!

My last gratitude goes to my dear husband Tiago for all the love, comprehension and patience. Thank you for being by my side in the most difficult moments and for the serenity you give me… you make me truly happy!

To my dear husband Tiago…

To my parents…

Abstract

Gas separation/purification by membrane processes is a very challenging research area since membranes should display high adaptability, high reliability, low energy consumption and low capital cost, operation and maintenance. Presently, polymers are the dominant materials used for membranes fabrication due to easy processability and adequate permselectivity for many gas pairs; however, polymeric membranes face an "upper bound" limitation and plasticization issues in aggressive streams.

Carbon molecular sieve membranes, formed by thermal decomposition of a polymeric precursor, have been promoted as energy-efficient candidates for gas separation due to their high selectivity, permeability and stability in harsh chemical conditions. Carbon molecular sieve membranes have a highly aromatic structure comprising sp^2 hybridized carbon sheets packed imperfectly with larger micropores connected by smaller ultramicropores. Nevertheless, these membranes have not yet made into commercial products mainly because to a significant decrease in performance when exposed to humidity and/or oxygen, and poor mechanical strength.

The present thesis targets the development and characterization of carbon molecular sieve membranes with high separation performance, no pore blocking effect when treating humidified gas streams and showing minimal oxygen chemisorption.

Supported carbon molecular sieve membranes were successfully prepared by a single step dip coating process of a composite dispersion on alpha-alumina supports and subsequent carbonization at 500 °C and 550 °C; the composite dispersion was prepared by loading boehmite nanoparticles in a resorcinol-formaldehyde resin. The influence of the carbonization end temperature on the structure, morphology and performance of the membranes was examined by scanning electron microscopy, thermogravimetric analysis, CO_2 adsorption and permeation to N_2, O_2, He, H_2 and CO_2. The membranes revealed good ideal selectivities, with separation performances above the Robeson's upper bound for polymeric membranes.

Novel carbon molecular sieve membranes that do not show any noticeable pore blockage when treating humidified streams with up to *ca*. 80 % relative humidity were described for the first time; they were prepared from commercial cellophane sheets (regenerated cellulose), a renewable low-cost precursor. The obtained membranes showed a mostly linear water vapor adsorption isotherm, characteristic of a homogeneous distribution of hydrophilic sites on the pore surfaces, allowing for water molecules to hop continuously between sites and avoiding the formation of pore-blocking water clusters. Moreover, these membranes displayed high mechanical flexibility and extraordinary separation performance characteristics being situated far above Robeson's upper bound. These results represent a great contribution for bringing this type of membranes to a commercial level.

Cellophane is being produced for more than a century by the viscose process, which uses a metastable solution of cellulose xanthogenate with hazardous byproducts and generates two kilograms of waste per kilogram of cellulose obtained. Ionic liquids, as a new type of environmentally "green solvents", represent a promising alternative to the viscose process. Regenerated cellulose-based carbon molecular sieve membranes were successfully prepared using an ionic liquid process to dissolve cellulose. Robeson's upper bound for polymeric membranes was overtaken by the obtained carbon molecular sieve membranes regarding O_2/N_2, He/N_2 and H_2/N_2 separations; besides, permeation experiments performed with oxygen and nitrogen with *ca.* 80 % relative humidity showed no performance decrease demonstrating that these membranes are stable in the presence of water vapor. These promising results open the doors for the preparation of tailor made precursors able to provide carbon molecular sieve membranes with high separation performance and stability.

Sumário

A separação/purificação de gases por processos de membrana é uma área de investigação muito desafiante uma vez que as membranas prometem apresentar elevada adaptabilidade, elevada confiabilidade, baixo consumo de energia e baixo custo de capital, de operação e de manutenção. Atualmente, os polímeros são os materiais dominantes na preparação de membranas devido ao seu fácil processamento e à sua adequada permselectividade para vários pares de gases; no entanto, as membranas poliméricas enfrentam uma limitação de "limite superior" bem como problemas de plastificação em fluxos agressivos. As membranas de peneiro molecular de carbono, formadas a partir da decomposição térmica de um precursor polimérico, têm sido promovidas como candidatas eficientes em termos energéticos para a separação de gases devido à sua elevada seletividade, permeabilidade e estabilidade em condições químicas severas. As membranas de peneiro molecular de carbono têm uma estrutura altamente aromática compreendendo folhas de carbono na hibridização sp^2 acondicionadas imperfeitamente com microporos conectados a ultramicroporos. No entanto, estas membranas ainda não foram comercializadas principalmente devido à diminuição significativa no seu desempenho quando expostas à humidade e/ou oxigénio, e devido à sua baixa resistência mecânica.

A presente tese visa o desenvolvimento e caracterização de membranas de peneiro molecular de carbono que apresentem elevados desempenhos de separação, nenhum efeito de bloqueio de poros ao tratar fluxos gasosos humidificados e mínima quimissorção de oxigénio.

Foram preparadas com sucesso membranas de peneiro molecular de carbono suportadas a partir de um processo de revestimento por imersão de uma dispersão compósita em suportes de alfa-alumina com posterior carbonização a 500 °C e 550 °C; a dispersão compósita foi preparada a partir de uma resina resorcinol-formadeído com nanopartículas de boemite. A influência da temperatura de carbonização na estrutura, morfologia e no desempenho das membranas foi examinada por microcopia eletrónica

de varrimento, análise termogravimétrica, adsorção do CO_2 e permeação ao N_2, O_2, He, H_2 e CO_2. As membranas exibiram boas seletividades ideais, com desempenhos de separação acima do limite superior de Robeson para membranas poliméricas.

Membranas de carbono que não apresentam um evidente bloqueio de poros ao tratar fluxos humidificados até cerca de 80 % de humidade relativa foram descritas pela primeira vez; estas membranas foram preparadas a partir de folhas de celofane comercial (celulose regenerada), um precursor renovável de baixo custo. As membranas obtidas apresentaram uma isotérmica de adsorção do vapor de água praticamente linear, característica de uma distribuição homogénea dos locais hidrofílicos nas superfícies dos poros, permitindo às moléculas de água pularem continuamente entre estes locais e evitando a formação de aglomerados de água responsáveis pelo bloqueio dos poros. Além disso, estas membranas mostraram elevada flexibilidade mecânica e extraordinários desempenhos de separação, posicionados muito acima do limite superior de Robeson. Estes resultados representam um grande contributo para trazer este tipo de membranas a um nível comercial.

O celofane é produzido há mais de um século pelo processo viscose, o qual usa uma solução metaestável de xantogenato de celulose com subprodutos perigosos e origina dois quilos de lixo por cada quilo de celulose obtido. Os líquidos iónicos, como um novo tipo de "solventes verdes", representam uma alternativa promissora à viscose. Membranas de peneiro molecular de carbono à base de celulose regenerada foram preparadas com êxito usando um líquido iónico para dissolver a celulose. O limite superior de Robeson para membranas poliméricas foi ultrapassado pelas membranas de peneiro molecular de carbono obtidas no que respeita às separações O_2/N_2, He/N_2 e H_2/N_2; além disso, testes de permeação realizados com oxigénio e azoto com cerca de 80 % de humidade relativa mostraram que as membranas não sofriam uma queda no seu desempenho, demonstrando a sua estabilidade na presença de vapor de água. Estes resultados promissores abrem a porta para a preparação de precursores feitos por medida que são capazes de originar membranas de peneiro molecular de carbono com elevados desempenhos de separação e estabilidade.

Table of Contents

List of Figure Captions

List of Table Captions

Chapter I

Chapter 1 – Introduction

In the last few decades membranes have evolved from a research topic to a mature industrial separation technology.

Describing a little of the history of the use of membranes, the development of high-flux anisotropic membrane modules for reverse osmosis applications occurred in the late 1960s and early 1970s. Permea (now owned by Air Products and Chemicals) adapted this technology to gas separation and in 1980 launched the first industrial application. The commercialized polysulfone hollow-fiber membranes were an immediate success, especially for the separation and recovery of hydrogen from purge gas streams of ammonia plants. From this moment, Dow, Cynara, Separex and Generon followed the footsteps of Air Products and Chemicals and soon membranes of cellulose acetate for carbon dioxide removal from natural gas became commercial, as well as for producing nitrogen from air [1]. Later, Ube Industries Ltd addressed the hydrogen separation from hydrocarbons using polyimide hollow fiber membranes. Nowadays, Ube Industrials also produces these membranes for air dehumidification and nitrogen production from air. Currently, Air Liquide fabricates hollow fiber membranes (based on DuPont's fiber spinning technology) for carbon dioxide removal, hydrogen purification and air separation [2]. A milestone chart summarizing the development of membranes for gas separation is displayed in Figure 1.1.

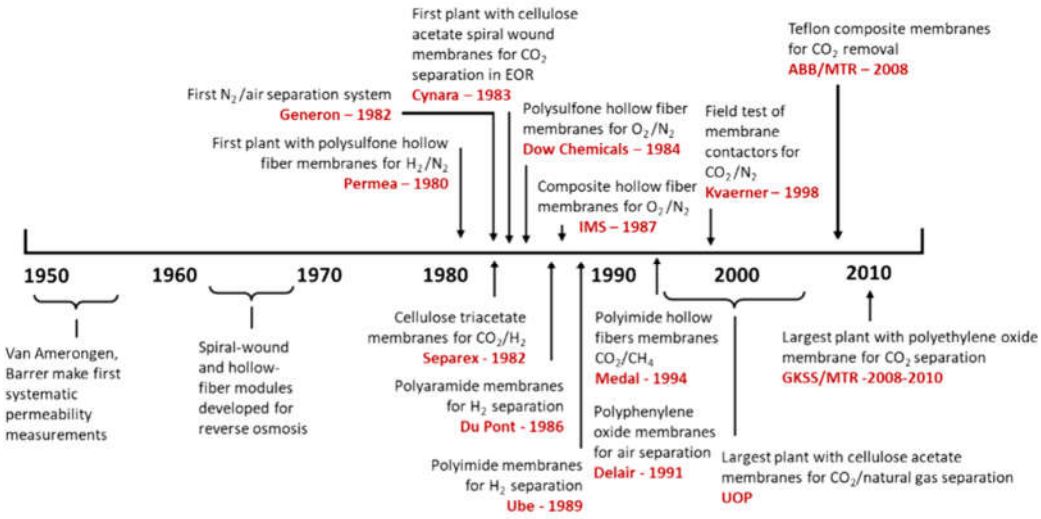

Figure 1.1. Milestones in the development of membrane gas separations (adapted from [3]).

Membrane technology for gas separations has been growing ever since, and by 2013 membrane-based gas separation market was $218 million and is projected to grow at a CAGR (Compound Annual Growth Rate) of 9.0 % from 2014 to 2019 (Figure 1.2) [4]. Most commercially available hollow fiber membranes for gas separation are made from materials developed in the 1980s, where the polymers reached the threshold technological level for that applications.

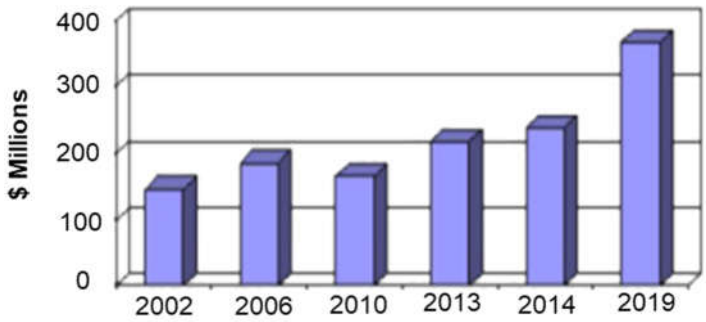

Figure 1.2. U.S. market for membrane products used in gas separation (2002-2019) [4].

A small number of polymeric materials has been used to produce around 90 % of the total installed gas separation membrane based. Table 1.1 presents a list of the main gas separation markets and the corresponding membrane materials.

Table 1.1. Gas separation markets and used membrane material (adapted from [5]).

Market	Membrane material
Nitrogen/air Hydrogen separation	Polysulfone Polyimide/polyaramide Polyimide Tetrabromo polycarbonate
Natural gas separations Carbon dioxide/methane	Cellulose acetate
Vapor/gas separation Air dehydration	Polyphenylene oxide Polyimide Silicone Rubber

1.1. Membranes

The most important component in any membrane separation process is the membrane itself. A membrane can be defined as a thin permselective barrier between two streams, with certain permeability and selectivity towards one or more components of a mixture [6, 7]. A schematic representation of a simple gas separation membrane process is shown in Figure 1.3. The feed stream, at high pressure, gets in contact with the membrane in a membrane module. Then, the more permeable gaseous species permeate preferentially across the membrane and are accumulated in the so-called permeate flow.

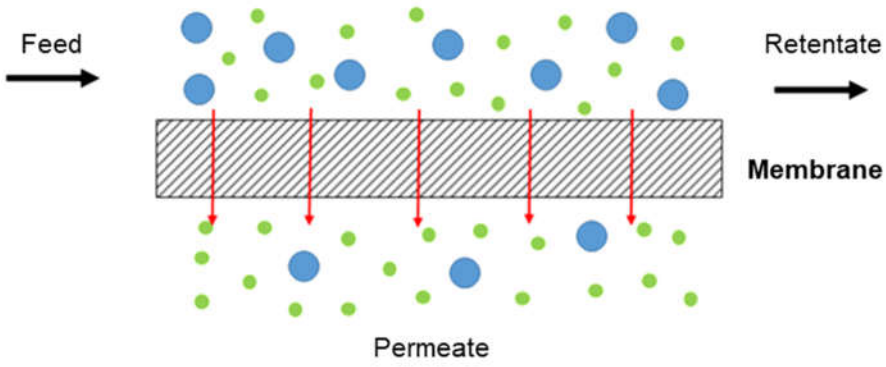

Figure 1.3. Basic representation of a membrane process.

The driving force for species permeate may be in the form of concentration difference, temperature difference or an electrical field. Normally, in gas separations, the driving force is the partial pressure difference.

Membranes can be classified by their nature as biological or synthetic. Synthetic membranes can be subdivided into mixed matrix, polymeric and inorganic membranes. Figure 1.4 presents a scheme of the general classification of membranes.

According to the International Union of Pure and Applied Chemistry (IUPAC), membranes can also be classified according to their pore dimensions as macroporous, mesoporous, microporous and dense membranes. Macroporous membranes present pore diameters above 50 nm, mesoporous display pore diameters between 2 and 50 nm, microporous have pore diameters between 0.3 and 2 nm and finally dense membranes present pore diameters below to 0.3 nm. Membrane morphology, structure and chemistry determines the separation mechanism and performance [7].

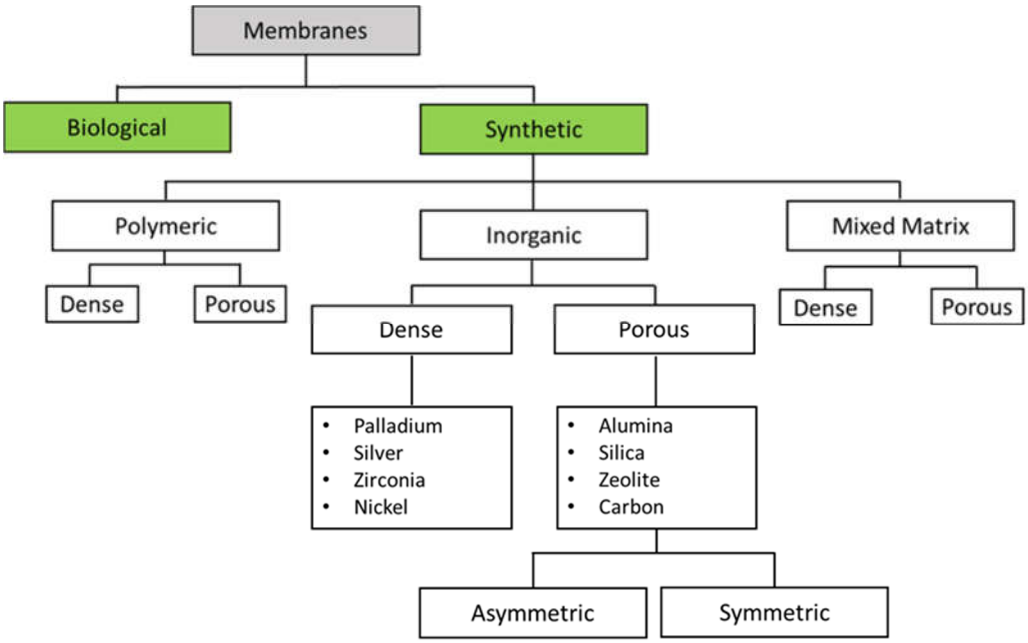

Figure 1.4. Scheme of a general classification of membranes.

1.1.1. Polymeric membranes

The most commonly used membranes in gas separation are polymeric. This is mainly due to the availability of different types of relatively low-cost polymers that can be easily processed into a membrane with good separation performance and sufficient permeation [8]. The polymers commonly used are cellulose acetate, cellulose triacetate, polyimides, polyamides, polycarbonate, polysulfone, polydimethylsiloxane and polymethylpentene [9]. Polymeric membranes are usually produced using the phase inversion method, the solvent evaporation method or the interfacial polymerization and can be subdivided in two categories: glassy and rubbery membranes [10, 11]. Glassy membranes are used at temperatures below the glass transition temperature and, normally, have relatively high selectivity and low permeability. Rubbery membranes are used at temperatures above the glass transition temperature and possess normally high permeability and low selectivity [10, 11].

Despite polymeric membranes are the most commonly used membranes in gas separation, they are not suitable for harsh environments such as those prone to corrosion and high temperatures. Besides, they have high sensitivity to swelling and compaction [8]. As a result, inorganic membranes have rapidly received global attention in being considered as one of the potential candidates to replace polymeric membranes.

1.1.2. Inorganic membranes

The interest in the development of inorganic membranes is related to their normally better selectivity and thermal and chemical stabilities, despite their higher price. Inorganic membranes are divided in two major categories based on their structure: porous membranes and dense membranes. Dense inorganic membranes have low permeability, which limits their use in industrial applications, and as a result more interest has been grown for developing porous inorganic membranes [12]. Among these membranes, attention has been focused on molecular sieve materials

such as zeolites, silica and carbon. Silica-based membranes have good selectivity to hydrogen/nitrogen mixtures, but their selectivities for similar size molecules (such as O_2 and N_2) are low [13]. Zeolite membranes display high chemical, thermal and mechanical stabilities and are able to separate isomers. However, it is difficult to obtain large, crack-free zeolite membranes [13] and, as a result, these membranes have low selectivities. Carbon molecular sieve membranes have very attractive characteristics such as superior thermal resistance, chemical stability in corrosive environments, high permeabilities as well as excellent selectivities when compared to polymeric and other inorganic membranes [14]. As a result, carbon molecular sieve membranes have emerged as promising candidates for gas separations.

1.1.3. Mixed matrix membranes

Mixed matrix membranes contain a bulk continuous phase with dispersed inorganic particles. Inorganic fillers act to create preferential permeation pathways for selective permeability while posing a barrier for undesired permeation improving the separation performance [15]. Using properties of both organic and inorganic phase, membranes with good permeability, selectivity, mechanical strength, processability and thermal and chemical stability can be prepared [16]. Many inorganic materials have been used in the preparation of mixed matrix membranes including zeolites [17, 18], carbon molecular sieves [19], activated carbons [20], mesoporous materials [21, 22], non-porous silica [23], fullerene [24], graphite [25], carbon nanotubes [26] and metal organic frameworks [27]. The common polymeric materials used include polysulfones, polycarbonates, poly(arylketones), poly(arylethers) and polyimides [28]. A harmonizing combination of inorganic materials and polymers and the elimination of interfacial defects between the two phases play an essential role on the final separation properties of the membranes. It is also important to control the filler concentration, shape and dimensions to reach the expected performance [2]. Mixed matrix

membranes offer, so, very interesting properties. However, their cost and difficulties for commercial scale manufacture remain important challenges [2].

Table 1.2 shows a brief comparison between polymeric, inorganic and mixed matrix membranes.

Table 1.2. Comparison between polymeric, inorganic and mixed matrix membranes (adapted from [29]).

	Polymeric	**Inorganic**	**Mixed matrix**
Characteristics	Present in either rubbery or glassy type. Polymer is more rigid and hard in glassy state, and more soft and flexible in rubbery state.	Made from inorganic-based materials.	Contain a bulk continuous polymeric phase with dispersed inorganic particles.
Advantages	Easy to process. Low production cost. Robust handling.	High chemical and thermal stability. Separation performance above Robeson upper limit.	High chemical and thermal stability. Excellent mechanical strength. Separation performance above Robeson upper limit. Robust handling.
Disadvantages	Can be irreversibly swollen or plasticized when exposed to CO_2 or hydrocarbons. Susceptible to corrosion and do not support high temperatures.	Brittleness. High production cost.	High production cost.

Commercial membrane applications are vast and have expanding during last two decades in industries such as natural gas processing, air separation, landfill gas recovery, among many others. Table 1.3 presents examples of commercial membrane applications and major suppliers [30].

Table 1.3. Commercial applications and current major suppliers of membrane for gas separation [30].

Gas separation	Commercial application	Current supplier
O_2/N_2	Nitrogen generation Oxygen enrichment	Permea (Air Products), Generon (IGS), IMS (Praxair), Medal (Air Liquide), Parker Gas Separation, Ube
H_2/hydrocarbons	Refinery hydrogen recovery	Air Products, Air Liquide, Praxair, Ube
H_2/CO_2	Syngas ratio adjustment	Air Products, Air Liquide, Praxair, Ube
H_2/N_2	Ammonia Purge gas	Air Products, Air Liquide, Praxair, Ube
CO_2/CH_4	Acid gas treatment Enhanced oil recovery Landfill gas upgrading	Cynara (NATCO), Kvaerner, Air Products, Ube, UOP (Separex)
H_2S/hydrocarbon	Sour gas treating	NATCO, Kvaerner, Air Products, Ube, Separex
H_2O/hydrocarbon	Natural gas dehydration	Kvaerner, Air Products
H_2O/air	Air dehydration	Air Products, Parker Balxston Ultratroc, Praxair
Hydrocarbons/air	Pollution control Hydrocarbon recovery	Borsig, MTR, GMT, NKK
Hydrocarbons from process streams	Organic solvent recovery Monomer recovery	Borsig, MTR, GMT, SIHI

Separation processes require a membrane with both high selectivity and high permeability. However, Robeson [31, 32] showed that there is a trade-off between permeability and selectivity, *i.e.*, when the selectivity increases, permeability decreases and vice-versa. The validity of the Robeson upper bound curve was demonstrated for a large number of polymeric membranes [31, 32]. As a result, the production of membranes that surpass the upper bound and achieve high selectivity while maintaining reasonable permeability still presents a major challenge in the membrane field.

1.2. Gas Separation Mechanisms

For porous membranes the permeation occurs mainly through the pores, while for a dense membrane the permeation is through the bulk of the membrane material. When permeation involves transport along ultramicropores (diameters between 0.35 and 0.7 nm), the species permeate in the adsorbed form. For dense membranes, the sorption/diffusion mechanism is the most commonly used for describing the mass transport [33]. In this mechanism, a gas molecule adsorbs at the feed side surface followed by diffusion through the bulk, and finally it desorbs at the other side of the membrane [33, 34].

In porous membranes, four types of mechanisms describe the mass transport: viscous flow, Knudsen diffusion, surface diffusion and molecular sieving (Figure 1.5). The mass transport of a gas through a porous inorganic membrane depends on their pore morphology and surface chemistry. From Figure 1.5 it can be observed that viscous flow dominates in the largest pores and yields no separation whereas molecular sieving mechanism yields a highest selectivity at the smallest pores. For a membrane with micropores, the permeation can be quite high if the membrane shows a very narrow pore size distribution and if it has a high porosity.

Viscous flow - Viscous flow occurs essentially in pores larger than 50 nm where intermolecular collisions are predominant; these collisions result in an overall pressure drop along the membrane and the transport occurs due to the establishment of a pressure difference between the two sides of the membranes. In this case, there is no selectivity [33].

Knudsen diffusion - Knudsen diffusion occurs when the pore diameter (2-50 nm) is around or smaller than the mean-free path of the gas; species collide more frequently with the pore walls than with each other. The selectivity, obtained by the square root of the reciprocal ratio between the molecular mass of the species, is low [35, 36].

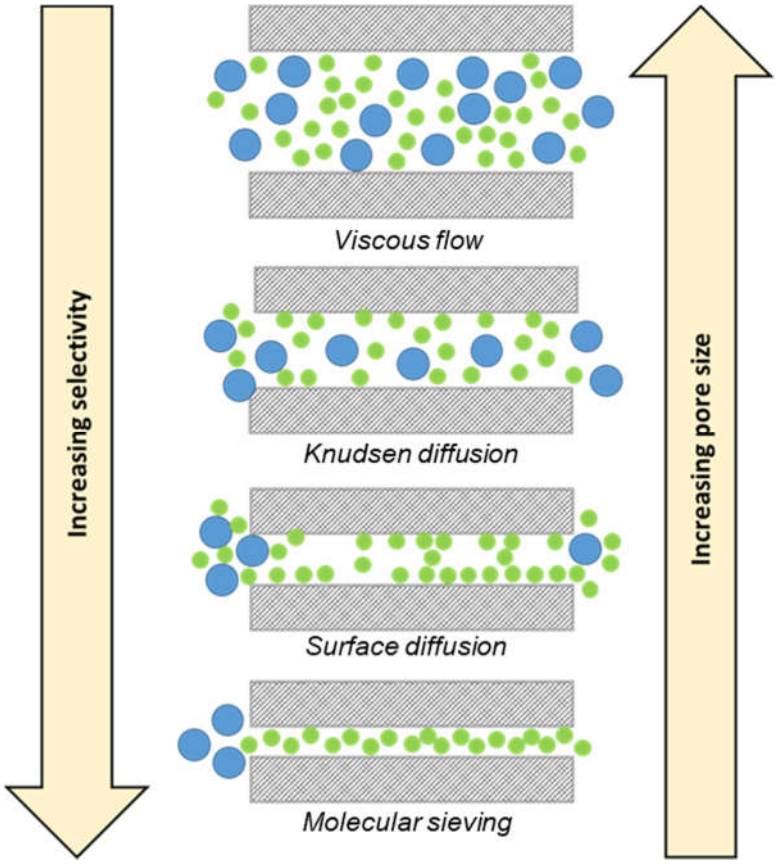

Figure 1.5. Mechanisms for permeation of gases through porous membranes.

Surface diffusion - Surface diffusion occurs when one of the gas molecules adsorbs on the pore (0.5-2 nm) walls of the membrane and migrates along the surface. Different species exhibit different adsorption rates on the surface of the pore which affects the diffusion rates along the same surface: the more adsorbable molecules permeate faster through these pores, while the transport of species with lower affinity to the surface walls is more difficult [37].

Molecular sieving - Molecular sieving occurs when the pores have sizes close to those of the permeating species (0.3-0.5 nm). For small enough pore sizes only the smallest gas molecules can permeate through the membrane while bulkier species are retained

[13]. This regime is characterized by its high selectivity and low to moderate flux. Carbon molecular sieve membranes exhibit this type of gas transport [13, 38, 39].

1.3. Carbon Molecular Sieve Membranes

Carbon can form different structures with different properties – carbon allotropes. The main reason for this diversity is the presence of four outer electrons capable of multi-bondings: sp-linear; sp^2-ring and sp^3-diamond [40]. Figure 1.6 shows a schematic representation of sp, sp^2 and sp^3 orbital configurations.

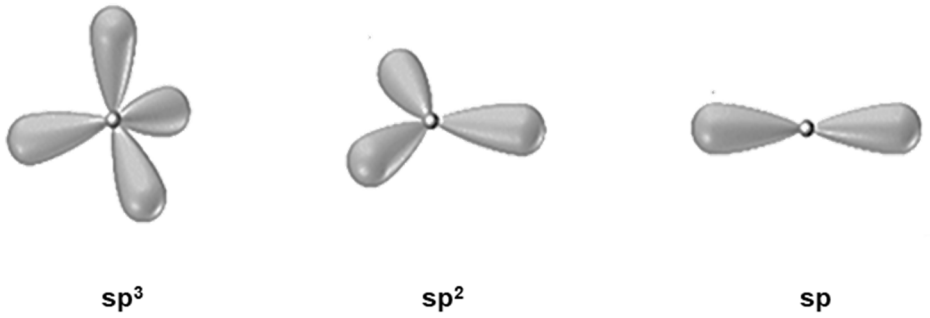

Figure 1.6. Schematic representation of sp, sp^2 and sp^3 orbital configurations (adapted from [41]).

The three molecular configurations of carbon are amorphous carbon, graphite and diamond, as shown in Figure 1.7. Graphite is the most thermodynamically stable phase of carbon at standard conditions and is a typical example of sp^2 hybridized crystal structure. Graphite has a layered, planar structure (Figure 1.7-C). In each layer, the carbon atoms are arranged in an hexagonal lattice with a distance of 0.142 nm between each other and with a distance of 0.335 nm between the layers [41]. These layers are arranged above each other in an offset ABABAB configuration and the carbons in the adjacent layers are bonded by van der Waals forces [40].

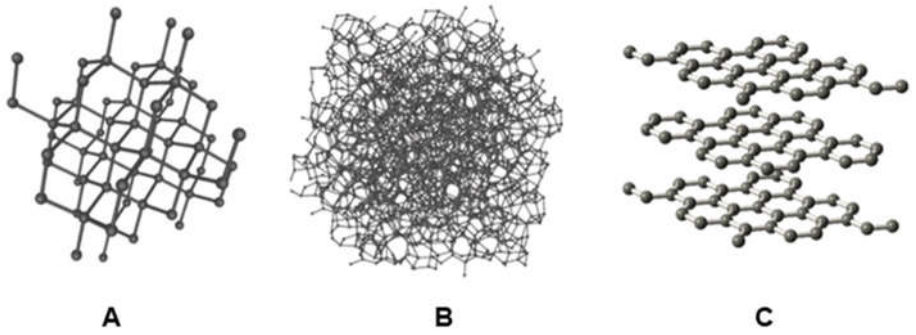

Figure 1.7. Molecular configuration of **(A)** diamond structure, **(B)** amorphous carbon structure, **(C)** graphite structure (adapted from [42]).

Franklin [43, 44] classified carbons in two types, based in their graphitizing ability: graphitizable and non-graphitizable. Graphitizable carbons are structures that upon heating may become graphitic featuring graphene layers stacked in ABABAB sequence. Non-graphitizable carbons never graphitize even upon heating [40]. In these group of carbons the graphene planes cannot rearrange to form a graphitic structure because so many bonds would need to be broken simultaneously that the activation energy becomes too high.

Carbon molecular sieve membranes (CMSM) are made of essentially non-graphitizable porous carbons. CMSM have been studied for more than 30 years as promising membranes for gas separation. CMSM are prepared by carbonization of polymeric-based precursors under controlled inert atmosphere [45, 46]. After the carbonization step, CMSM displays a highly aromatic structure comprising disordered sp^2 hybridized carbon sheets packed imperfectly [47]. Pores are formed from packing imperfections between microcrystalline regions in the material as shown in Figure 1.8; the CMSM structure is called as turbostratic and described as “slit-like” with a bimodal pore size distribution with larger micropores connecting ultramicropores [34, 48] (Figure 1.8). Micropores provide sorption sites while ultramicropores (called constrictions) enable molecular sieving, making CMSM both highly permeable and highly selective - a distinct characteristic of these materials.

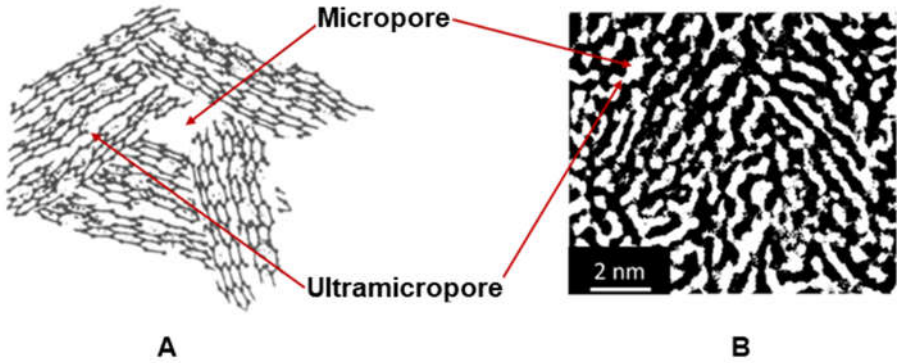

Figure 1.8. Carbon molecular sieve membranes "slit-like" pore structure: **(A)** sp^2 hybridized carbon sheets, **(B)** real high-resolution transmission electron micrograph of a CMSM.

At the constricted apertures, gas molecules are confined to the space between two carbon walls and subjected to a potential field [49]. Figure 1.9 schematizes the relative potential of a molecule within a pore or a constriction. If the pore is large enough, there is no overlap of the potential associated to the opposite walls (case A); as the pore aperture gets narrower the overlapped potential crosses a minimum (maximum adsorption energy, case B) until becomes positive and the pore becomes impermeable to the species (case D). However, if repulsive forces in the potential field dominate, sorption energy is smaller and the pore become a constriction that the diffusing molecules must overcome (case C). Except for case A, the permeating species is in the sorbed phase. For case B, the mass transport mechanism in micropores can be described by the sorption-diffusion mechanism. For case C, activated diffusion mechanism, also known as configurational diffusion [50], has to be considered. It should be emphasized, however, that different species may display different sorption behaviors for the very same pore; the transport of these two species can then follow different transport mechanisms.

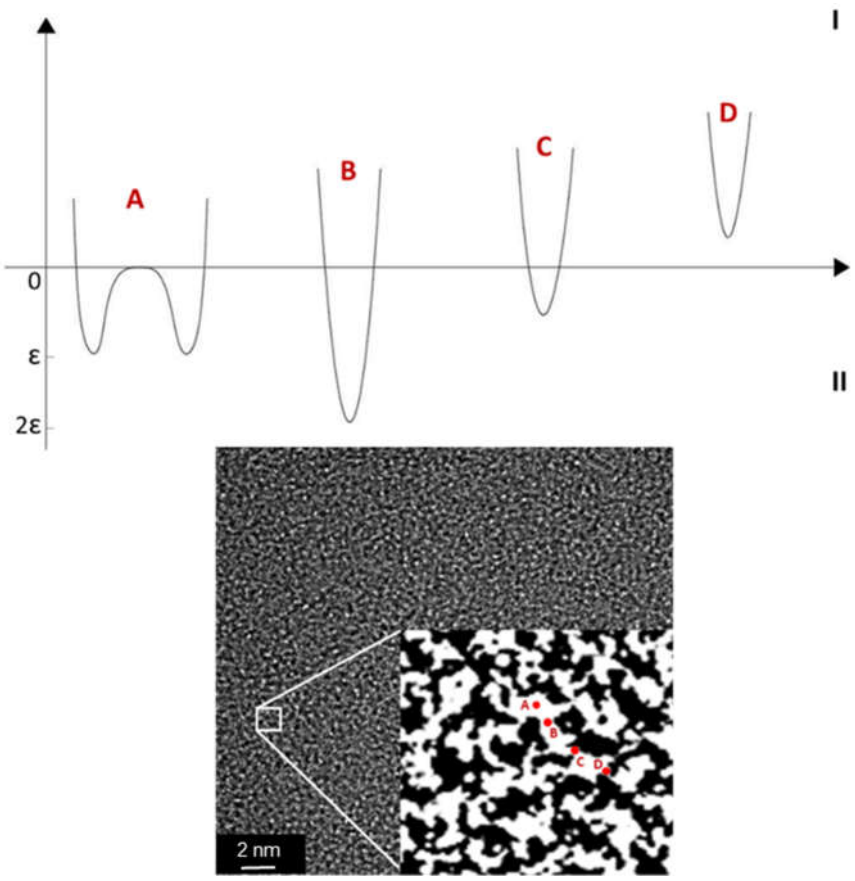

Figure 1.9. Schematic representation of the species/wall interactions within a pore/constriction: **(I)** Potential energy, E, of a specie as a function of its distance to the wall (adapted from [49]), **(II)** species in a real pore.

The precursor material and carbonization conditions, such as heating rate, end temperature, soaking time and gas atmosphere and pre-/post-treatment conditions, that will be discussed later, determine the microstructure and permeance properties of the CMSM [51-54].

1.3.1. Preparation of carbon molecular sieve membranes

The preparation of CMSM involves five steps (*i.e.*, precursor material selection, precursor preparation, pre-treatment, carbonization and post-treatment) which must be controlled and optimized. Among these steps, carbonization is the most important

and can be considered the heart of the carbon membrane production process [55-57]. The polymer precursor has also a crucial function in determining the final structure of the carbon membranes since different polymer precursors carbonized in the same conditions lead to CMSM with different properties [13, 58]. Figure 1.10 shows a schematic diagram of the CMSM fabrication process.

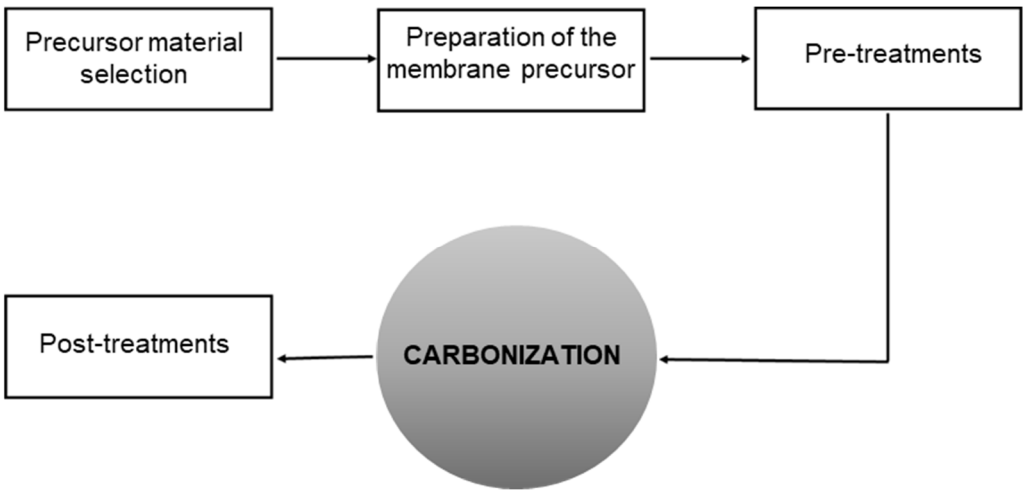

Figure 1.10. Production process of carbon membranes.

Precursor material selection

The choice of a suitable polymeric precursor is a fundamental step to guarantee the production of defect-free carbon molecular sieve membranes. A detailed investigation into the chemical structure and physical properties of the polymer should be primarily considered. The polymeric precursor should withstand high temperature treatment without much shrinkage, should be thermosetting to avoid melting or softening during any stage of carbonization and should display a high carbon yield [38]. Suitable precursors should not originate any cracks, defects or pore-holes to appear after the carbonization step. The precursor should also provide good separation performances and should have an economical price.

Numerous materials have been extensively studied as precursors to prepare CMSM such as polyimides [54, 58-63], cellulose [64, 65], polyacrylonitrile (PAN) [66],

polyfurfuryl alcohol (PFA) [67, 68], polyetherimide (PEI) [69-73], polyphenylene oxide (PPO) [74-77], phenolic resins [45, 78-82] and polymer blends [83-87]. All precursors have attractive features, but also some drawbacks. Table 1.4 shows the main advantages and disadvantages of common precursors used to prepare CMSM. It is important to note that the choice of the precursor depends on the required application (the gas mixtures to separate).

Recently, it was pointed out by our group for the first time that depending on the selected precursor material, carbon molecular sieves with two extreme sieving mechanisms can be prepared. As it will be discussed in more detail in Chapter 3.A, those mechanisms are rationalized as being gate sieving (for carbon molecular sieves having a gate-like pore shape) and tubular sieving (for carbon molecular sieves having a tubular shape pore).

Preparation of the membrane precursor

Polymeric precursors must be prepared at optimized conditions to produce good quality carbon molecular sieve membranes. Defects in the precursor membranes will be transferred to the carbon membranes, originating small pinholes or cracks that will compromise the selectivity required for gas separation.

The precursor (and consequently the CMSM) can be prepared as supported or unsupported flat membranes or hollow/capillary fibers [13]; flat membranes are envisioned almost exclusively for lab applications while hollow or capillary fibers are envisioned for industrial applications.

Unsupported membranes have the disadvantage of the intrinsic weak mechanical strength which limits their practical applications whereas supported membranes have extra mechanical strength provided by the support. For this reason supported membranes are frequently favored.

Table 1.4. Advantages and disadvantages of some precursors used to prepare CMSM.

Precursor	Advantages	Disadvantages	Ref.
Polyimides	Easy to process. Commercially available products (Kapton, Matrimid and P84 co-polymer).	Expensive. Most of them only available at laboratory scale.	[88-93]
PFA	Provide carbon membranes with narrow pore size distributions and chemically stable.	Only can be used to prepare supported membranes.	[57, 94]
PAN	Provide carbon fibers with good mechanical properties. High carbon yield.	Low O_2/N_2 selectivity.	[66]
PPO	Excellent mechanical properties. Easy modification with functional groups.	High cost.	[74, 95]
Phenolic Resins	Low-cost. High carbon yield. Simple to prepare.	Low reproducibility.	[78, 81, 82, 96, 97]
Cellulose	Low-cost. 100 % biodegradable.	Poor solubility in common organic solvents.	[64, 65, 98]
PEI	High carbon yield. Good separation factors. Good chemical stability.	High cost.	[99-101]
Polymer Blends	Enhance the gas permeabilities. Create a wide range of pore size distribution (macro, meso, micro and ultramicropores).	Limited polymer pairs for miscible polymer blends. Uncontrolled phase separation for immiscible blends.	[83-87, 102, 103]

However, from the standpoint of large scale commercial application, costs are a crucial factor and the hollow/capillary fiber geometry will be preferable because of the high packing density (membrane area per unit volume), easy module assembly and mechanical stability [104]. Hollow fiber membranes can, for example, be fabricated with asymmetric structure with a thin selective layer and a thick mechanical highly permeable support layer (self-supported membranes).

Pre-treatments

Depending on the selected precursor, a specific pre-treatment can be applied to obtain carbon membranes with improved mechanical stability and separation performance. Sometimes the precursor is subjected to more than one pre-treatment procedure to achieve the desired properties; pre-treatments can be divided into physical and chemical [56, 57]:

Physical pre-treatments - comprehends stretching or drawing the hollow fiber membranes [12]. This physical technique is occasionally referred to a post-spinning treatment, applied to remove the surface imperfections, attenuate differences in filament diameter and improve the retention of molecular orientation prior to carbonization with the purpose to obtain carbon fibers with a good equilibrium between stiffness and strength [105].

Chemical pre-treatments - comprehends the partial oxidation of the membranes surface and the use of chemical reagents for obtaining specific effects. Surface partial oxidation or thermostabilization is the most popular and commonly used method to pre-treat the membrane precursor. This pre-treatment may display a substantial influence on the resulting carbon membrane performance [12, 56, 57]. It is believed that, after oxidation under air atmosphere, membranes with greater mechanical stability are obtained; oxygen acts as a dehydrogenation agent in the conversion of C-C bonds to C=C bonds and generates oxygen-bearing groups in the polymer backbone (such as -OH and C=O) [8]. These oxygen-bearing groups promote intermolecular crosslinking of the polymer chains making the polymer structure stiffer, less prone to relaxation and more capable of withstanding the high temperatures observed during the carbonization process [8]. Avoiding excessive volatilization of elemental carbon, this pre-treatment also maximizes the final carbon yield [12, 57]. Some variables can significantly affect the performance of the final CMSM, such as oxidation temperature, oxidation atmosphere, heating rate and soaking time. Consequently, and depending of the polymeric precursor, it is necessary to optimize them.

Chemical methods using chemical reagents enhance the uniformity of the pore system formed during carbonization. The precursor is fully immersed in an appropriate solution and then washed and dried before the carbonization step. In some cases, the pores of the membranes are evacuated and filled with nitrogen before the immersion in the aqueous solution to obtain membranes with higher carbon contents [12]. The chemicals commonly used include hydrazine (improves the dimensional stability of the membrane and avoid clogging of pores during carbonization [106]) and dimethylformamide (improves mechanical properties [105]); hydrochloric acid [107], ammonium chloride [107], phosphoric acid and diammonium hydrogen phosphates are used as catalysts [12, 57], increasing the carbon yield and allowing the carbonization to be carried out at lower temperatures and faster heating rates.

Carbonization

Carbon molecular sieve membranes are formed upon the controlled carbonization of a suitable polymer precursor, following a specific temperature history under a controlled reducing atmosphere, aiming to produce amorphous carbon membrane with very narrow pore size distribution. As the polymer matrix decomposes, volatiles such as carbon dioxide, carbon monoxide, nitrogen and ammonia are released [108]. At the end of the carbonization process, a carbon matrix consisting of disordered non-homogeneous graphene-like layers is formed. The spaces between these disordered graphene-like layers are the pores of the membrane. As previously discussed, the porous network of the membrane is typically slit-like and consists of relatively wide openings (responsible for higher permeabilities) with narrow constrictions (responsible for the molecular sieving properties of the membrane).

Different variables can affect the carbonization step and small changes on these carbonization parameters have a significant impact on the final properties of CMSM. Such of that variables (carbonization end temperature, carbonization atmosphere, inert flowrate, heating rate and soaking time) are discussed in the following:

Carbonization end temperature - carbonization temperature lies between the decomposition temperature of the carbonaceous precursor and its graphitization temperature. The optimum carbonization end temperature strongly depends on the type of precursor. Generally, an increase in the carbonization end temperature results in a decrease in the gas permeability, an increase in the ideal selectivity and an increase in brittleness; higher carbonization end temperatures originate CMSM with more compact (originates the shrinkage of the membrane), crystallinity, density and smaller average interplanar spacing between the graphitic layers [8, 109].

Carbonization atmosphere - must be controlled for avoiding undesired burn off and chemical damage of the precursor. Carbonization under vacuum normally originates more selective and less permeable CMSM when compared to a carbonization under an inert atmosphere (N_2, He or Ar). CMSM prepared in an inert atmosphere have a more open porous network, which results from the removal of the by-products from the polymer decomposition (by the flow of the gas), avoiding the carbon deposition in the formed pores [57, 110].

Flowrate - when an inert gas atmosphere is used, the gas flowrate is another important parameter to consider; higher flowrates produce carbon membranes with improved permeabilities showing a minimal role on the selectivities [57].

Heating rate - during the carbonization process, the release rate of volatiles is related to the heating rate, as well as to the pore size distribution and number of connecting pores. Heating rates between 0.1 and 13.3 $°C \cdot min^{-1}$ are normally used [107, 110]; low heating rates produce CMSM with small pores, less connecting pores (smaller permeability) and enhanced crystallinity. In contrast, high heating rates can originate pinholes or cracks in the carbon matrix. Therefore, an extensive study for determining the optimum heating rate for the carbonization procedure must be carefully done.

Soaking time - is the period of time that the membrane is hold at constant carbonization end temperature before being cooled down to room temperature. The soaking time induces microstructural rearrangement which affects the pore size distribution of CMSM and therefore it can be used to fine-tune their transport properties. Larger soaking times cause pore sintering which results in a decreasing of permeability and an increase in the selectivity [8, 111].

Post-treatments

After the carbonization step, polymeric precursors are transformed into carbon membranes with varying degrees of porosity, pore size distribution and connectivity, and surface chemistry, which influence the separation properties. To improve the desired pore descriptors and to repair defects/cracks, various post-treatment methods have been applied. These include post-oxidation or activation, chemical vapor deposition, post-pyrolysis and coating [56, 57]:

Post-oxidation - removes carbon atoms from the pore walls, enlarging them; consequently, this method is performed when pore opening is needed. Membranes oxidation can be performed using different oxidizing agents such as pure oxygen, oxygen admixed with other gases, air, steam, carbon dioxide, nitrogen oxides and chlorine oxides. Solutions of oxidizing agents at elevated temperatures can also be used, such as nitric acid, mixtures of nitric and sulfuric acids, chromic acid and peroxide solutions [12, 57]. Different activation temperatures and dwell times have been applied to obtain desired pore structures in different materials [75, 112-114]; generally, when the oxidation temperature is increased, an increase in gas permeance and a decrease in permselectivity of permanent gas pairs (such as O_2/N_2 and CO_2/N_2) are observed.

Koros and Singh [115] developed recently a new oxygen doping method (*Dual* Temperature *Secondary* Oxygen Doping), where high temperature and a trace amount

of oxygen are used after carbonization to enhance the separation performance of CMSM for O_2/N_2 gas pair while the high membrane permeance is maintained.

Chemical vapor deposition (CVD) - performed to obtain a CMSM with a narrower pore size distribution. Higher selectivities are obtained through the pyrolytic decomposition of organic species such as ethane, propane, propylene, ethylene and benzene [12, 57] introduced into the porous system of the carbon membranes. The selected hydrocarbons must have high chemical stability in the gas phase and not produce intermediate species. Moreover, the carbon species should have adequate reactivity to be adsorbed and pyrolyzed on the pore mouth and must have an appropriate shape to produce a flat coating. At the end, the pore mouth narrows to the smallest dimension of the hydrocarbon molecule [116]. CVD of carbon onto a CMSM may bring about three distinct results (Figure 1.11): homogenous deposition (Figure 1.11-A), in-layer deposition (Figure 1.11-B) and adlayer deposition (Figure1.11-C). Homogenous decomposition is, in general, the preferred mode [12] . However, if the CVD conditions such as temperature, time of deposition, vapor flowrate and composition are not accurately optimized, the excess of vapor deposition blocks the pores [117].

Post-pyrolysis - used to decrease the pore volume. Generally, post-pyrolysis is performed after the post-oxidation to recuperate from an excessive pore enlargement [12, 57]. Post-oxidation and post-pyrolysis are frequently repeated several times until the desired pore size distribution be achieved.

Coating - applied to repair cracks/defects in CMSM [12]. However, coating treatments will result in a decrease of CMSM permeability [119].

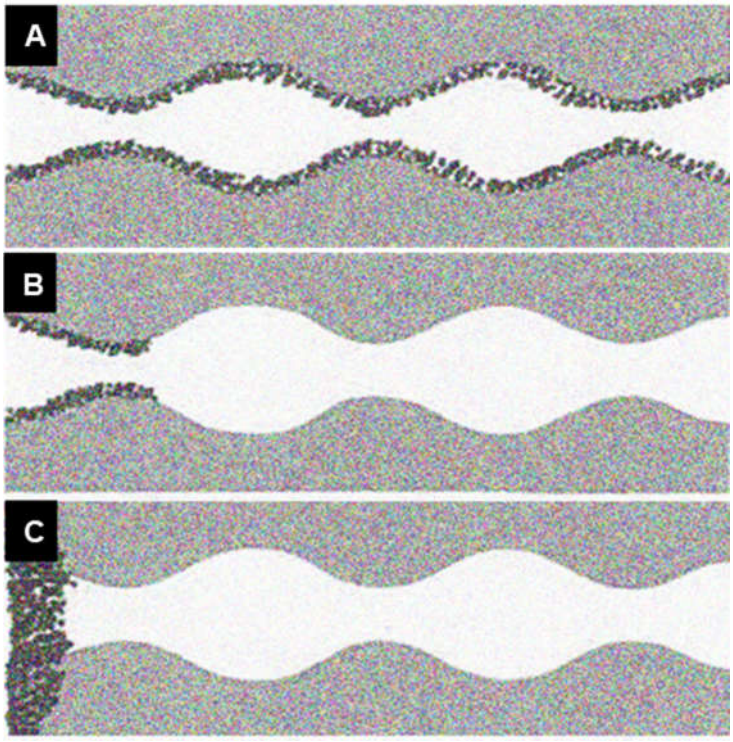

Figure 1.11. Mechanism of carbon deposition on the pore system of CMSM: **(A)** homogeneous deposition on membrane pore walls, **(B)** in-layer deposition on membrane pore wall entrances, **(C)** adlayer deposition outside membrane pores (adapted from [118]).

The ideal carbon molecular sieve membrane should present high permeability and selectivity, maintain its performance in the presence of humidity, oxygen and organic compounds, be stable under harsh thermal and chemical environments, be mechanically resistant and have a low production cost.

1.4. Challenges in Carbon Membranes Development

1.4.1. CMSM aging

Although CMSM have high thermal and chemical resistance, they may present significant problems related to their performance stability. The aging effect is the change in membrane performance over time when exposed to specific environments.

Two phenomena are particularly important on the carbon membranes stability: chemisorption and physisorption [120]. Chemisorption is the chemical bonding of a component, such as oxygen or propylene, with sites in the carbon surface. Physisorption is the physical adsorption of a gas (through Van der Waals or dispersion forces, permanent dipoles or hydrogen bonding) on the membrane surface and is mostly reversible.

Not many studies have taken into account the aging phenomenon, although it becomes really important when a carbon membrane is commercialized and therefore it must always be studied.

Exposure to humidity

The vulnerability of CMSM to humidity is a complex phenomenon considering the weak character of the water-carbon dispersion forces and the tendency of water molecules to form hydrogen bonds within the bulk phase. Water initially adsorbs onto hydrophilic sites which are much more reactive than the atoms in the interior of the carbon matrix; once the first water molecule is adsorbed onto the carbon matrix, adsorbate-adsorbate interactions promote the adsorption of further water molecules via hydrogen bonding generating a water cluster. The resulting cluster gains then enough energy to be released from the hydrophilic site and rolling until blocking a constriction [121].

Jones and Koros in 1995 [122] found that the loss of CMSM separation performance occurred in the first few hours after exposure to humidity, as water molecules are adsorbed to active sites in critical constrictions. These authors observed that at low humidity (<23 % RH) significant membrane performance was maintained while at higher humidity (85 % RH) the performance was drastically decreased [122]. Lagorsse *et al.* [123] studied the exposure of CMSM at 32.5 % of relative humidity and observed a permeance loss of about 50 % when compared to the value prior to exposure to humidity.

Exposure to oxygen

Oxygen chemisorbs at active sites forming oxygen-containing groups on the pore windows, which reduces the pore volume. Menendez and Fuertes [124] studied the permeance and permselectivity modification with time of carbon membranes after oxygen exposition. A significant permeance loss was observed with membranes stored either in lab air or dry air. By contrast, permselectivities increase slightly; after one day of storage, the permeability to N_2, O_2 and CO_2 decreased by nearly 50 % and at longer times of storage the permeance losses were around 90 %. Similarly, Lagorsse *et al*. [123] reported the long-term exposure of CMSM to different dry environments and observed membrane performance losses essentially due to chemisorption of oxygen.

Exposure to organics

Carbon membranes are organophilic and, therefore, they have a very high affinity to organic compounds [12]. Furthermore, the weak dispersion interactions between organic molecules and carbon walls are enhanced in narrow pores as the adsorption potentials of the opposite walls are overlaid. At pore constrictions, this effect is higher and molecules can actually block the pores. Jones and Koros [125] studied the effect of exposure of CMSM to several organic vapors and a decrease in oxygen flux was observed. Additionally, higher hydrocarbons exposition resulted in a complete membrane separation performance loss; higher hydrocarbons, even present in trace amounts, are prejudicial to CMSM separation performance.

1.4.2. Regeneration of carbon molecular sieve membranes

Various regeneration techniques are known in the art; these include thermal regeneration, ultrasonic regeneration, chemical regeneration, electrothermal regeneration and microwave regeneration. However, these techniques are not favored: they are time consuming, expensive and often unsuccessful. Table 1.5 presents a summary of the different conventional regeneration methods.

Table 1.5. Summary of different regeneration methods [128].

Method	Energy demand	Operation	Complexity
Thermal	High	Offline	Medium
Chemical	Medium	Offline	Medium
Electrothermal	Low	Online	Low
Ultrasonic	Low	Online	Low
Microwaves	Medium	Offline	Low

Heat treatments with hydrogen at high temperatures (passivation) where hydrogen passivates the active sites have been also proposed by several authors [123, 126, 127]. However, even after this reducing treatment, the passivation is not completely effective and still leaves reactive sites capable of re-adsorbing oxygen [123]. Moreover, passivation of carbon surfaces with hydrogen seems to be more effective at 630 °C or 1000 ^{o}C and its application to CMSM is not reasonable for the reason that may damage their specific molecular pore size distribution.

In 1994, Jones and Koros [125] proposed the use of propylene as a cleaning agent after CMSM exposition to contaminants. A few years later, Menendez and Fuertes [124] demonstrated that propylene could prevent the chemisorption of oxygen. Besides, CMSM permeabilities were not significantly affected by the treatment.

1.4.3. Mechanical stability

Another drawback of CMSM that still have to be overcome is their inherent brittleness. The elongation at break is relatively short and the membrane's elastic modulus is high. In 1999, Tanihara *et al*. [109] studied the mechanical properties of a carbon membrane produced from asymmetric polyimide hollow fiber. The elastic modulus significantly increased and the elongation at break decreased as the carbonization temperature increased from 600 °C to 1000 °C. Similar trend was also found in polyacrylonitrile-based carbon fiber studies [129, 130].

It is well known that the addition of plasticizers to polymers lead to a decrease in intermolecular forces along polymer chains improving the flexibility and chain mobility

[131]. Accordingly, these additives are used to enhance flexibility, decrease brittleness and avoid excessive shrinkage of polymeric precursor films. The carbonized membranes obtained from these precursors inherit these properties. Plasticizers commonly used include propylene glycol, ethylene glycol, polyethylene glycol, glycerol, urea, among others [132].

Currently, the production of CMSM involves high costs; carbon membranes are 10 to 100 times more expensive than conventional polymeric membranes [36, 110]. Therefore, carbon membranes must achieve a superior performance in order to compensate their higher cost.

1.5. Potential Industrial Applications for CMSM

1.5.1. Nitrogen and oxygen separation from air

The production of low-cost and high purity nitrogen from air is one the most important potential application for CMSM. Their use in the production of nitrogen from air presents some advantages: it requires low maintenance, low energy consumption, the separation modules are compact and lightweight and can be positioned either vertically or horizontally [133]. Similarly, CMSM have shown growing interest for producing oxygen-enriched streams from air, providing an alternative to conventional air separation processes such as cryogenic distillation and pressure swing adsorption that are considered energy intensive technologies [134].

1.5.2. Methane purification

Carbon membranes can be used for the purification of methane from different sources as well as in the recovery of carbon dioxide in oil fields. Additionally, carbon membranes can operate in severe environments being useful in the removal of acid gases from natural gas [12, 133].

1.5.3. Hydrogen recovery

Membranes compete with cryogenic, catalytic and pressure swing adsorption processes in the hydrogen recovery process. However, polymeric membranes require additional recompression costs [12, 133]. Carbon molecular sieve membranes can be used in the hydrogen recovery process without further compression of the feed gas.

1.5.4. Light alkenes/alkanes

Up to now, propene/propane separation has been investigated by using polymeric membranes. However, they are not thermally and chemically stable and have low permselectivity for this separation [12]. These drawbacks have led to the need of developing thermally and chemically stable membranes that exhibit better separation performances. CMSM display, in general, excellent alkenes/alkanes permselectivities making them promising materials for petrochemical industry.

1.5.5. Xenon separation

Another potential application of CMSM consists on the xenon separation/recovery from gas mixtures. Lagorsse *et al.* [135] proposed the use of CMSM for on-line recycling xenon in closed anaesthetic breathing circuits. Very high CO_2/Xe and N_2/Xe ideal selectivities were obtained in combination with high permeabilities. Simulation results indicated that a xenon recovery above 97 % can be achieved.

1.6. Motivation and thesis outline

Carbon molecular sieve membranes have been proposed as energy-efficient candidates for gas separation due to their high selectivity, permeability and stability in chemically aggressive environments. However, when exposed to water vapor and oxygen they exhibit pore blockage and oxygen chemisorption, respectively. This aging phenomenon significantly hinders the performance and seriously limits its industrial applicability. The aim of this work is to prepare stable high separation performance carbon molecular sieve membranes targeting industrial applications and identify the roots of the non-aging property displayed by the CMSM prepared from regenerated cellulose precursor.

The present thesis is divided in five chapters as follows:

Chapter I presents an introduction to the work.

Chapter II reports the carbonization and characterization of supported composite carbon membranes derived from resorcinol-formaldehyde resin loaded with boehmite nanoparticles.

Chapter III reports the preparation and characterization of new CMSM displaying extraordinary separation performance, not showing any noticeable pore blockage when treating humidified streams up to *ca.* 80 % relative humidity.

Chapter IV studies the preparation and characterization of stable CMSM derived from regenerated cellulose films obtained through an ionic liquid process.

Finally, Chapter V summarizes the main conclusions of this thesis and presents ideas/suggestions for future work research.

Appendix A shows additional characterization results concerning the carbon molecular sieve membranes with extremely high separation performance and stability presented in Chapter III.

Appendix B presents the published article “Preparation and characterization of carbon molecular sieve membranes based on resorcinol-formaldehyde resin”.

Appendix C presents the patent “A carbon molecular sieve membrane, method of preparation and uses thereof”, resulting from the development and characterization of CMSM with extremely high separation performance and stability.

1.7. References

[1] R.W. Spillman, Economics of Gas Separation Membranes, Chemical Engineering Progress, 85 (1989) 41-62.

[2] P. Bernardo, E. Drioli, G. Golemme, Membrane Gas Separation: A Review/State of the Art, Industrial & Engineering Chemistry Research, 48 (2009) 4638-4663.

[3] P. Bernardo, G. Clarizia, 30 Years of Membrane Technology for Gas Separation, Chemical Engineering Transactions, 32 (2013) 1999-2004.

[4] S. Hanft, Membrane Technology for Liquid and Gas Separations, BCC Research, Report 1-56965-895-1, 2014.

[5] R.W. Baker, Future Directions Of Membrane Gas Separation Technology, Industrial & Engineering Chemistry Research, 41 (2002) 1393-1411.

[6] H.F. Mark, Encyclopedia of polymer science and engineering, Second Edition, John Wiley & Sons, New York, 1987.

[7] M. Mulder, Basic Principles of Membrane Technology, Kluwer Academic Publishers, The Netherlands, 1996.

[8] W.N.W. Salleh, A.F. Ismail, T. Matsuura, M.S. Abdullah, Precursor Selection and Process Conditions in the Preparation of Carbon Membrane for Gas Separation: A Review, Separation & Purification Reviews, 40 (2011) 261-311.

[9] S.P. Nunes, K.V. Peinemann, Gas Separation with membranes, in: S.P. Nunes, K.V. Peinemann (Eds.) Membrane Technology in the Chemical Industry, Wiley-VCH, Germany, 2006.

[10] S.C.A. Kluiters, Status review on membrane systems for hydrogen separation, in: Intermediate report EU project MIGREYD NNE5-2001-670 Energy Research Centre, The Netherlands, 2004, pp. 1-29.

[11] A. Mushtaq, H.B. Mukhtar, A.M. Shariff, H.A. Mannan, A Review: Development of Polymeric Blend Membrane for Removal of CO_2 from Natural Gas, International Journal of Engineering & Technology, 13 (2013) 53-60.

[12] A.F. Ismail, D. Rana, T. Matsuura, H.C. Foley, Carbon-based Membranes for Separation Processes, Springer, New York, 2011.

[13] A.F. Ismail, L.I.B. David, A review on the latest development of carbon membranes for gas separation, Journal of Membrane Science, 193 (2001) 1-18.

[14] S.C. Rodrigues, R. Whitley, A. Mendes, Preparation and characterization of carbon molecular sieve membranes based on resorcinol–formaldehyde resin, Journal of Membrane Science, 459 (2014) 207-216.

[15] G. Dong, H. Li, V. Chen, Challenges and opportunities for mixed-matrix membranes for gas separation, Journal of Materials Chemistry A, 1 (2013) 4610-4630.

[16] M.A. Aroon, A.F. Ismail, T. Matsuura, M.M. Montazer-Rahmati, Performance studies of mixed matrix membranes for gas separation: A review, Separation and Purification Technology, 75 (2010) 229-242.

[17] S. Kulprathipanja, R.W. Neuzil, N.N. Li, Separation of gases by means of mixed matrix membranes, US patent 5127925 A, 1992.

[18] R. Mahajan, R. Burns, M. Schaeffer, W.J. Koros, Challenges in forming successful mixed matrix membranes with rigid polymeric materials, Journal of Applied Polymer Science, 86 (2002) 881-890.

[19] D.Q. Vu, W.J. Koros, S.J. Miller, Mixed matrix membranes using carbon molecular sieves: I. Preparation and experimental results, Journal of Membrane Science, 211 (2003) 311-334.

[20] M. Anson, J. Marchese, E. Garis, N. Ochoa, C. Pagliero, ABS copolymer-activated carbon mixed matrix membranes for CO_2/CH_4 separation, Journal of Membrane Science, 243 (2004) 19-28.

[21] J. Kim, J.W. Grate, P. Wang, Nanobiocatalysis and its potential applications, Trends in Biotechnology, 26 (2008) 639-646.

[22] B. Zornoza, C. Téllez, J. Coronas, Mixed matrix membranes comprising glassy polymers and dispersed mesoporous silica spheres for gas separation, Journal of Membrane Science, 368 (2011) 100-109.

[23] T.C. Merkel, B.D. Freeman, R.J. Spontak, Z. He, I. Pinnau, P. Meakin, A.J. Hill, Ultrapermeable, Reverse-Selective Nanocomposite Membranes, Science, 296 (2002) 519-522.

[24] J.S. Taurozzi, C.A. Crock, V.V. Tarabara, C_{60}-polysulfone nanocomposite membranes: Entropic and enthalpic determinants of C_{60} aggregation and its effects on membrane properties, Desalination, 269 (2011) 111-119.

[25] G. Clarizia, C. Algieri, A. Regina, E. Drioli, Zeolite-based composite PEEK-WC membranes: Gas transport and surface properties, Microporous and Mesoporous Materials, 115 (2008) 67-74.

[26] S. Kim, T.W. Pechar, E. Marand, Poly(imide siloxane) and carbon nanotube mixed matrix membranes for gas separation, Desalination, 192 (2006) 330-339.

[27] S. Basu, A. Cano-Odena, I.F.J. Vankelecom, Asymmetric Matrimid®/$[Cu_3(BTC)_2]$ mixed-matrix membranes for gas separations, Journal of Membrane Science, 362 (2010) 478-487.

[28] L.M. Robeson, Polymer membranes for gas separation, Current Opinion in Solid State and Materials Science, 4 (1999) 549-552.

[29] D.F. Mohshim, H.b. Mukhtar, Z. Man, R. Nasir, Latest development on membrane fabrication for natural gas purification: A Review, Journal of Engineering, 2013 (2013) 1-7.

[30] A.F. Ismail, K.C. Khulbe, T. Matsuura, Gas separation membranes: polymeric and inorganic, Springer International Publishing, Switzerland, 2015.

[31] L.M. Robeson, Correlation of separation factor versus permeability for polymeric membranes, Journal of Membrane Science, 62 (1991) 165-185.

[32] L.M. Robeson, The upper bound revisited, Journal of Membrane Science, 320 (2008) 390-400.

[33] A. Javaid, Membranes for solubility-based gas separation applications, Chemical Engineering Journal, 112 (2005) 219-226.

[34] M. Kiyono, W.J. Koros, P.J. Williams, Correlation Between Pyrolysis Atmosphere and Carbon Molecular Sieve Membrane Performance Properties, in: S.T. Oyama, S. Stagg-Williams (Eds.) Inorganic, Polymeric and Composite Membranes, Elsevier, Oxford, 2011.

[35] M.B. HÄgg, J.A. Lie, A. Lindbrathen, Carbon molecular sieve membranes: a promising alternative for selected industrial applications, Annals of the New York Academy of Sciences, 984 (2003) 329-345.

[36] R.W. Baker, Membrane Technology and Applications, Second Edition, John Wiley & Sons, California, 2004.

[37] J.D. Way, D.L. Roberts, Hollow Fiber Inorganic Membranes for Gas Separations, Separation Science and Technology, 27 (1992) 29-41.

[38] Y.H. Sim, H. Wang, F.Y. Li, M.L. Chua, T.-S. Chung, M. Toriida, S. Tamai, High performance carbon molecular sieve membranes derived from hyperbranched polyimide precursors for improved gas separation applications, Carbon, 53 (2013) 101-111.

[39] M.B. Rao, S. Sircar, Nanoporous carbon membranes for separation of gas mixtures by selective surface flow, Journal of Membrane Science, 85 (1993) 253-264.

[40] H. Marsh, F. Rodríguez-Reinoso, Activated Carbon, First Edition, Elsevier, Oxford, 2006.

[41] M.S. Dresselhaus, G. Dresselhaus, P.C. Eklund, R. Saito, M. Endo, Introduction to Carbon Materials, in: T.W. Ebbesen (Ed.) Carbon Nanotubes: Preparation and Properties, CRC Press Inc., New Jersey, 1997.

[42] A. Aqel, K.M.M. El-Nour, R.A.A. Ammar, A. Al-Warthan, Carbon nanotubes, science and technology part (I) structure, synthesis and characterisation, Arabian Journal of Chemistry, 5 (2012) 1-23.

[43] R.E. Franklin, The Interpretation of Diffuse X-Ray Diagrams of Carbon, Acta Crystallographica, 3 (1950) 107-121.

[44] R.E. Franklin, The Structure of Graphitic Carbons, Acta Crystallographica, 4 (1951) 253-261.

[45] M. Teixeira, M. Campo, D.A. Tanaka, M.A. Tanco, C. Magen, A. Mendes, Carbon–Al_2O_3–Ag composite molecular sieve membranes for gas separation, Chemical Engineering Research and Design, 90 (2012) 2338-2345.

[46] A.B. Fuertes, T.A. Centeno, Preparation of supported carbon molecular sieve membranes, Carbon, 37 (1999) 679-684.

[47] M. Kiyono, P.J. Williams, W.J. Koros, Effect of pyrolysis atmosphere on separation performance of carbon molecular sieve membranes, Journal of Membrane Science, 359 (2010) 2-10.

[48] S. Fu, G.B. Wenz, E.S. Sanders, S.S. Kulkarni, W. Qiu, C. Ma, W.J. Koros, Effects of pyrolysis conditions on gas separation properties of 6FDA/DETDA:DABA(3:2) derived carbon molecular sieve membranes, Journal of Membrane Science, 520 (2016) 699-711.

[49] A.M. Mendes, F.D. Magalhães, C.A.V. Costa, New Trends on Membrane Science, in: W.C. Conner, J. Fraissard (Eds.) Fluid Transport in Nanoporous Materials, Springer, The Netherlands, 2006.

[50] A.J. Burggraaf, Single gas permeation of thin zeolite (MFI) membranes: theory and analysis of experimental observations, Journal of Membrane Science, 155 (1999) 45-65.

[51] C.W. Jones, W.J. Koros, Carbon molecular sieve gas separation membranes - I. Preparation and characterization based on polyimide precursors, Carbon, 32 (1994) 1419-1425.

[52] M. Yoshino, S. Nakamura, H. Kita, K. Okamoto, N. Tanihara, Y. Kusuki, Olefin/paraffin separation performance of carbonized membranes derived from an asymmetric hollow fiber membrane of 6FDA/BPDA–DDBT copolyimide, Journal of Membrane Science, 215 (2003) 169-183.

[53] H. Suda, K. Haraya, Alkene/alkane permselectivities of a carbon molecular sieve membrane, Chemical Communications, (1997) 93-94.

[54] Y.K. Kim, H.B. Park, Y.M. Lee, Gas separation properties of carbon molecular sieve membranes derived from polyimide/polyvinylpyrrolidone blends: effect of the molecular weight of polyvinylpyrrolidone, Journal of Membrane Science, 251 (2005) 159-167.

[55] A.F. Ismail, K. Li, From Polymeric Precursors to Hollow Fiber Carbon and Ceramic Membranes, in: R. Mallada, M. Menéndez (Eds.), Inorganic Membranes: Synthesis, Characterization and Applications, First Edition, Elsevier, Oxford, 2008.

[56] M.B. Hägg, X. He, Carbon Molecular Sieve Membranes for Gas Separation, in: E. Drioli, G. Barbieri (Eds.) Membrane Engineering for the Treatment of Gases: Volume 2: Gas-separation Problems Combined with Membrane Reactors, First Edition, Royal Society of Chemistry, 2011.

[57] S.M. Saufi, A.F. Ismail, Fabrication of carbon membranes for gas separation—a review, Carbon, 42 (2004) 241-259.

[58] H.B. Park, Y.K. Kim, J.M. Lee, S.Y. Lee, Y.M. Lee, Relationship between chemical structure of aromatic polyimides and gas permeation properties of their carbon molecular sieve membranes, Journal of Membrane Science, 229 (2004) 117-127.

[59] Y.K. Kim, H.B. Park, Y.M. Lee, Carbon molecular sieve membranes derived from thermally labile polymer containing blend polymers and their gas separation properties, Journal of Membrane Science, 243 (2004) 9-17.

[60] Y.K. Kim, H.B. Park, Y.M. Lee, Preparation and characterization of carbon molecular sieve membranes derived from BTDA–ODA polyimide and their gas separation properties, Journal of Membrane Science, 255 (2005) 265-273.

[61] A.B. Fuertes, D.M. Nevskaia, T.A. Centeno, Carbon composite membranes from Matrimid® and Kapton® polyimides for gas separation, Microporous and Mesoporous Materials, 33 (1999) 115-125.

[62] K.M. Steel, W.J. Koros, An investigation of the effects of pyrolysis parameters on gas separation properties of carbon materials, Carbon, 43 (2005) 1843-1856.

[63] P.S. Tin, T.-S. Chung, S. Kawi, M.D. Guiver, Novel approaches to fabricate carbon molecular sieve membranes based on chemical modified and solvent treated polyimides, Microporous and Mesoporous Materials, 73 (2004) 151-160.

[64] J.A. Lie, M.B. Hägg, Carbon membranes from cellulose: Synthesis, performance and regeneration, Journal of Membrane Science, 284 (2006) 79-86.

[65] M.C. Campo, F.D. Magalhães, A. Mendes, Carbon molecular sieve membranes from cellophane paper, Journal of Membrane Science, 350 (2010) 180-188.

[66] L.I.B. David, A.F. Ismail, Influence of the thermastabilization process and soak time during pyrolysis process on the polyacrylonitrile carbon membranes for O_2/N_2 separation, Journal of Membrane Science, 213 (2003) 285-291.

[67] Y.D. Chen, R.T. Yang, Preparation of Carbon Molecular Sieve Membrane and Diffusion of Binary Mixtures in the Membrane, Industrial & Engineering Chemistry Research, 33 (1994) 3146-3153.

[68] C. Song, T. Wang, X. Wang, J. Qiu, Y. Cao, Preparation and gas separation properties of poly(furfuryl alcohol)-based C/CMS composite membranes, Separation and Purification Technology, 58 (2008) 412-418.

[69] M.G. Sedigh, F. Xu, T.T. Tsotsis, M. Sahimi, Transport and Morphological Characteristics of Polyetherimide-Based Carbon Molecular Sieve Membranes, Industrial & Engineering Chemistry Research, 38 (1999) 3367-3380.

[70] M.G. Sedigh, M. Jahangiri, P.K.T. Liu, M. Sahimi, T.T. Tsotsis, Structural characterization of polyetherimide-based carbon molecular sieve membranes, AIChE Journal, 46 (2000) 2245-2255.

[71] E. Barbosa-Coutinho, V.M.M. Salim, C.P. Borges, Preparation of carbon hollow fiber membranes by pyrolysis of polyetherimide, Carbon, 41 (2003) 1707-1714.

[72] H. Kumazawa, J.S. Wang, T. Fukuda, E. Sada, Permeation of carbon dioxide in glassy poly(ether imide) and poly(ether ether ketone) membranes, Journal of Membrane Science, 93 (1994) 53-59.

[73] A.B. Fuertes, T.A. Centeno, Carbon molecular sieve membranes from polyetherimide, Microporous and Mesoporous Materials, 26 (1998) 23-26.

[74] H.-J. Lee, H. Suda, K. Haraya, Characterization of the post-oxidized carbon membranes derived from poly(2,4-dimethyl-1,4-phenylene oxide) and their gas permeation properties, Separation and Purification Technology, 59 (2008) 190-196.

[75] H.-J. Lee, H. Suda, K. Haraya, D.-P. Kim, Influence of oxidation temperature on the gas permeation and separation properties in a microporous carbon membrane, Korean Journal of Chemical Engineering, 23 (2006) 435-440.

[76] H.-J. Lee, M. Yoshimune, H. Suda, K. Haraya, Gas permeation properties of poly(2,6-dimethyl-1,4-phenylene oxide) (PPO) derived carbon membranes prepared on a tubular ceramic support, Journal of Membrane Science, 279 (2006) 372-379.

[77] M. Yoshimune, I. Fujiwara, H. Suda, K. Haraya, Gas transport properties of carbon molecular sieve membranes derived from metal containing sulfonated poly(phenylene oxide), Desalination, 193 (2006) 66-72.

[78] M. Teixeira, M.C. Campo, D.A.P. Tanaka, M.A.P. Tanco, C. Magen, A. Mendes, Composite phenolic resin-based carbon molecular sieve membranes for gas separation, Carbon, 49 (2011) 4348-4358.

[79] A.B. Fuertes, I. Menendez, Separation of hydrocarbon gas mixtures using phenolic resin-based carbon membranes, Separation and Purification Technology, 28 (2002) 29-41.

[80] F.K. Katsaros, T.A. Steriotis, A.K. Stubos, A. Mitropoulos, N.K. Kanellopoulos, S. Tennison, High pressure gas permeability of microporous carbon membranes, Microporous Materials, 8 (1997) 171-176.

[81] T.A. Centeno, A.B. Fuertes, Supported carbon molecular sieve membranes based on a phenolic resin, Journal of Membrane Science, 160 (1999) 201-211.

[82] T.A. Centeno, A.B. Fuertes, Carbon molecular sieve membranes derived from a phenolic resin supported on porous ceramic tubes, Separation and Purification Technology, 25 (2001) 379-384.

[83] H.-J. Lee, H. Suda, K. Haraya, S.-H. Moon, Gas permeation properties of carbon molecular sieving membranes derived from the polymer blend of polyphenylene oxide (PPO)/polyvinylpyrrolidone (PVP), Journal of Membrane Science, 296 (2007) 139-146.

[84] W.N.W. Salleh, A.F. Ismail, Fabrication and characterization of PEI/PVP-based carbon hollow fiber membranes for CO_2/CH_4 and CO_2/N_2 separation, AIChE Journal, 58 (2012) 3167-3175.

[85] V.M. Linkov, R.D. Sanderson, E.P. Jacobs, Carbon membranes from precursors containing low-carbon residual polymers, Polymer International, 35 (1994) 239-242.

[86] H. Hatori, T. Kobayashi, Y. Hanzawa, Y. Yamada, Y. Iimura, T. Kimura, M. Shiraishi, Mesoporous carbon membranes from polyimide blended with poly(ethylene glycol), Journal of Applied Polymer Science, 79 (2001) 836-841.

[87] X. Zhang, H. Hu, Y. Zhu, S. Zhu, Carbon molecular sieve membranes derived from phenol formaldehyde novolac resin blended with poly(ethylene glycol), Journal of Membrane Science, 289 (2007) 86-91.

[88] W. Qiu, K. Zhang, F.S. Li, K. Zhang, W.J. Koros, Gas Separation Performance of Carbon Molecular Sieve Membranes Based on 6FDA-mPDA/DABA (3:2) Polyimide, ChemSusChem, 7 (2014) 1186-1194.

[89] S. Xiao, R.Y.M. Huang, X. Feng, Synthetic 6FDA–ODA copolyimide membranes for gas separation and pervaporation: Functional groups and separation properties, Polymer, 48 (2007) 5355-5368.

[90] A.M.W. Hillock, W.J. Koros, Cross-Linkable Polyimide Membrane for Natural Gas Purification and Carbon Dioxide Plasticization Reduction, Macromolecules, 40 (2007) 583-587.

[91] T.-S. Chung, J. Ren, R. Wang, D. Li, Y. Liu, K.P. Pramoda, C. Cao, W.W. Loh, Development of asymmetric 6FDA-2,6DAT hollow fiber membranes for CO_2/CH_4 separation: Part 2. Suppression of plasticization, Journal of Membrane Science, 214 (2003) 57-69.

[92] J.D. Wind, D.R. Paul, W.J. Koros, Natural gas permeation in polyimide membranes, Journal of Membrane Science, 228 (2004) 227-236.

[93] S.S. Hosseini, T.S. Chung, Carbon membranes from blends of PBI and polyimides for N_2/CH_4 and CO_2/CH_4 separation and hydrogen purification, Journal of Membrane Science, 328 (2009) 174-185.

[94] C.J. Anderson, S.J. Pas, G. Arora, S.E. Kentish, A.J. Hill, S.I. Sandler, G.W. Stevens, Effect of pyrolysis temperature and operating temperature on the performance of nanoporous carbon membranes, Journal of Membrane Science, 322 (2008) 19-27.

[95] M. Yoshimune, I. Fujiwara, K. Haraya, Carbon molecular sieve membranes derived from trimethylsilyl substituted poly(phenylene oxide) for gas separation, Carbon, 45 (2007) 553-560.

[96] M. Teixeira, S.C. Rodrigues, M. Campo, D.A.P. Tanaka, M.A.L. Tanco, L.M. Madeira, J.M. Sousa, A. Mendes, Boehmite-phenolic resin carbon molecular sieve membranes - Permeation and adsorption studies, Chemical Engineering Research and Design, 92 (2014) 2668-2680.

[97] W. Wei, G. Qin, H. Hu, L. You, G. Chen, Preparation of supported carbon molecular sieve membrane from novolac phenol–formaldehyde resin, Journal of Membrane Science, 303 (2007) 80-85.

[98] H. Ma, K. Yoon, L. Rong, Y. Mao, Z. Mo, D. Fang, Z. Hollander, J. Gaiteri, B.S. Hsiao, B. Chu, High-flux thin-film nanofibrous composite ultrafiltration membranes containing cellulose barrier layer, Journal of Materials Chemistry, 20 (2010) 4692-4704.

[99] W.N.W. Salleh, A.F. Ismail, Effect of stabilization condition on carbon hollow fiber membranes properties, Separation Science and Technology, 48 (2013) 1030-1039.

[100] W.N.W. Salleh, A.F. Ismail, Effect of stabilization temperature on gas permeation properties of carbon hollow fiber membrane, Journal of Applied Polymer Science, 127 (2013) 2840-2846.

[101] H.-H. Tseng, K. Shih, P.-T. Shiu, M.-Y. Wey, Influence of support structure on the permeation behavior of polyetherimide-derived carbon molecular sieve composite membrane, Journal of Membrane Science, 405-406 (2012) 250-260.

[102] N. Panapitiya, S. Wijenayake, D. Nguyen, C. Karunaweera, Y. Huang, K. Balkus, I. Musselman, J. Ferraris, Compatibilized Immiscible Polymer Blends for Gas Separations, Materials, 9 (2016) 1-23.

[103] W.N.W. Salleh, A.F. Ismail, Carbon membranes for gas separation processes: Recent progress and future perspective, Journal of Membrane Science and Research, 1 (2015) 2-15.

[104] X. He, M.-B. Hägg, Hollow fiber carbon membranes: From material to application, Chemical Engineering Journal, 215–216 (2013) 440-448.

[105] J.C. Chen, I.R. Harrison, Modification of polyacrylonitrile (PAN) carbon fiber precursor via post-spinning plasticization and stretching in dimethyl formamide (DMF), Carbon, 40 (2002) 25-45.

[106] E. Schindler, F. Maier, Manufacture of porous carbon membranes, US patent 4919860 A, 1990.

[107] A. Soffer, J. Gilron, S. Saguee, R. Hed-Ofek, H. Cohen, Process for the production of hollow carbon fiber membranes, European patent 0671202 A2, 1995.

[108] V.C. Geiszler, W.J. Koros, Effects of Polyimide Pyrolysis Conditions on Carbon Molecular Sieve Membrane Properties, Industrial & Engineering Chemistry Research, 35 (1996) 2999-3003.

[109] N. Tanihara, H. Shimazaki, Y. Hirayama, S. Nakanishi, T. Yoshinaga, Y. Kusuki, Gas permeation properties of asymmetric carbon hollow fiber membranes prepared from asymmetric polyimide hollow fiber, Journal of Membrane Science, 160 (1999) 179-186.

[110] P.J. Williams, W.J. Koros, Gas separation by Carbon Membranes, in: N.N. Li, A.G. Fane, W.S.W. Ho (Eds.), Advanced Membrane Technology and Applications, John Wiley & Sons, New Jersey, 2008.

[111] K. Steel, Carbon Membranes for Challenging Separations, PhD thesis, University of Texas, Austin, 2000.

[112] A.B. Fuertes, Effect of air oxidation on gas separation properties of adsorption-selective carbon membranes, Carbon, 39 (2001) 697-706.

[113] A.B. Fuertes, Adsorption-selective carbon membrane for gas separation, Journal of Membrane Science, 177 (2000) 9-16.

[114] K. Kusakabe, M. Yamamoto, S. Morooka, Gas permeation and micropore structure of carbon molecular sieving membranes modified by oxidation, Journal of Membrane Science, 149 (1998) 59-67.

[115] R. Singh, W.J. Koros, Carbon molecular sieve membrane performance tuning by *dual* temperature *secondary* oxygen doping (DTSOD), Journal of Membrane Science, 427 (2013) 472-478.

[116] M.A. Ahmad, Preparation of carbon molecular sieves from palm shell: effect of benzene deposition conditions, Adsorption, 15 (2009) 489-495.

[117] M. Bikshapathi, A. Sharma, A. Sharma, N. Verma, Preparation of carbon molecular sieves from carbon micro and nanofibers for sequestration of CO_2, Chemical Engineering Research and Design, 89 (2011) 1737-1746.

[118] A. Soffer, M. Azariah, A. Amar, H. Cohen, D. Golub, S. Saguee, H. Tobias, Method of improving the selectivity of carbon membranes by chemical carbon vapor deposition, US patent 5695818 A, 1997.

[119] C. Liang, G. Sha, S. Guo, Carbon membrane for gas separation derived from coal tar pitch, Carbon, 37 (1999) 1391-1397.

[120] M.M. Dubinin, Water vapor adsorption and the microporous structures of carbonaceous adsorbents, Carbon, 18 (1980) 355-364.

[121] S. Lagorsse, M.C. Campo, F.D. Magalhães, A. Mendes, Water adsorption on carbon molecular sieve membranes: Experimental data and isotherm model, Carbon, 43 (2005) 2769-2779.

[122] C.W. Jones, W.J. Koros, Characterization of Ultramicroporous Carbon Membranes with Humidified Feeds, Industrial & Engineering Chemistry Research, 34 (1995) 158-163.

[123] S. Lagorsse, F.D. Magalhães, A. Mendes, Aging study of carbon molecular sieve membranes, Journal of Membrane Science, 310 (2008) 494-502.

[124] I. Menendez, A.B. Fuertes, Aging of carbon membranes under different environments, Carbon, 39 (2001) 733-740.

[125] C.W. Jones, W.J. Koros, Carbon molecular sieve gas separation membranes - II. Regeneration following organic exposure, Carbon, 32 (1994) 1427-1432.

[126] S.A. Dastgheib, T. Karanfil, Adsorption of oxygen by heat-treated granular and fibrous activated carbons, Journal of Colloid and Interface Science, 274 (2004) 1-8.

[127] J.A. Menéndez, J. Phillips, B. Xia, L.R. Radovic, On the Modification and Characterization of Chemical Surface Properties of Activated Carbon: In the Search of Carbons with Stable Basic Properties, Langmuir, 12 (1996) 4404-4410.

[128] X. He, Development of Hollow Fiber Carbon Membranes for CO_2 separation, PhD thesis, Norwegian University of Science and Technology, Norway, 2011.

[129] J. Yao, W. Yu, Tensile Strength and Its Variation for PAN-Based Carbon Fibers. II. Calibration of the Variation from Testing, Journal of Applied Polymer Science, 104 (2007) 2625-2632.

[130] A. Sedghi, R.E. Farsani, A. Shokuhfar, The effect of commercial polyacrylonitrile fibers characterizations on the produced carbon fibers properties, Journal of Materials Processing Technology, 198 (2008) 60-67.

[131] M.G.A. Vieira, M.A. Silva, L.O. Santos, M.M. Beppu, Natural-based plasticizers and biopolymer films: A review, European Polymer Journal, 47 (2011) 254-263.

[132] A. Mendes, M. Andrade, M. Boaventura, S.C. Rodrigues, A carbon molecular sieve membrane, method of preparation and uses thereof, Patent WO 2017068517 A1, 2017.

[133] G. Gholami, M. Soleimani, M.T. Ravanchi, Application of carbon membranes for gas separation: A Review, Journal of Industrial Research & Technology, 3 (2013) 53-58.

[134] B. Belaissaoui, Y.L. Moullec, H. Hagi, E. Favre, Energy Efficiency of Oxygen Enriched Air Production Technologies: Cryogenic vs Membranes, Energy Procedia, 63 (2014) 497-503.

[135] S. Lagorsse, F.D. Magalhães, A. Mendes, Xenon recycling in an anaesthetic closed-system using carbon molecular sieve membranes, Journal of Membrane Science, 301 (2007) 29-38.

Chapter II

Chapter 2 – Preparation and characterization of carbon molecular sieve membranes based on resorcinol-formaldehyde resin[1]

2.1. Abstract

Carbon molecular sieve membranes (CMSM) were prepared on α-alumina supports by carbonization of a resorcinol-formaldehyde resin loaded with boehmite. Two series of carbon membranes produced at 500 °C and 550 °C carbonization end temperatures were prepared. The influence of the carbonization end temperature on the structure, morphology and performance of the membranes was examined by scanning electron microscopy, thermogravimetric analysis, CO_2 adsorption and permeation to N_2, O_2, He, H_2 and CO_2 at temperatures from 25 °C to 120 °C. SEM photographs showed carbon membranes with a thin and very uniform layer and a thickness of *ca.* 3 μm. Carbon dioxide adsorption isotherms revealed that all produced carbon membranes have a well-developed microporous structure. Nevertheless, membranes carbonized at 550 °C have more ultramicropores and a narrower pore size distribution. The permselectivity of CMSM prepared at this temperature surpasses the Robeson upper bound for polymeric membranes, especially regarding ideal selectivities of pairs O_2/N_2 (O_2 permeation rate: 9.85×10^{-10} $mol\cdot m^{-2}\cdot s^{-1}\cdot Pa^{-1}$ and ideal selectivity: >11.5), H_2/N_2 (H_2 permeation rate: 5.04×10^{-8} $mol\cdot m^{-2}\cdot s^{-1}\cdot Pa^{-1}$ and ideal selectivity: >586) and He/N_2 (He permeation rate: 4.68×10^{-8} $mol\cdot m^{-2}\cdot s^{-1}\cdot Pa^{-1}$ and ideal selectivity: >544).

[1] S.C. Rodrigues, R. Whitley, A. Mendes, Preparation and characterization of carbon molecular sieve membranes based on resorcinol-formaldehyde resin, Journal of Membrane Science, 459 (2014) 207-216.

2.2. Introduction

Carbon molecular sieve membranes have emerged as promising candidates for gas separation applications because of their attractive characteristics such as superior thermal resistance, chemical stability in corrosive environments, high permeabilities, as well as excellent selectivities compared to polymeric membranes [1-3]. Carbon membranes are prepared by carbonization of polymeric precursors under controlled inert atmosphere [4, 5]; the polymeric precursor should withstand high temperature treatment without much shrinkage [6] and should have a high carbon yield [1]. After the carbonization step, CMSM present an amorphous nanoporous skeleton [6, 7]; Figure 2.1 shows an high resolution transmission electron microscopy (HRTEM) image of a carbon molecular sieve membrane showing no ordered structural building units [8].

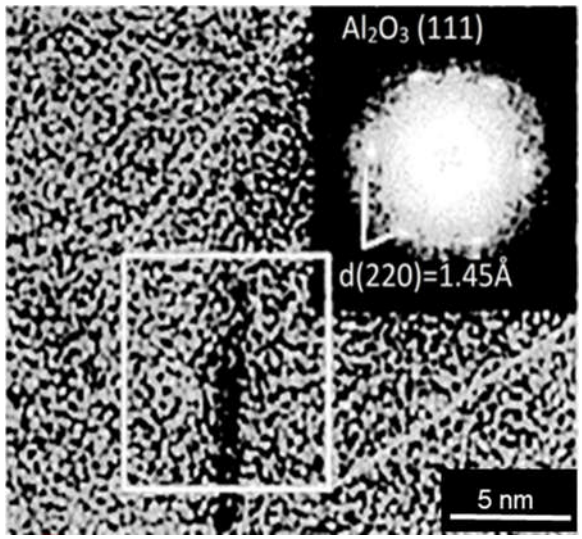

Figure 2.1. HRTEM image of a composite carbon molecular sieve membrane derived from phenolic resin incorporated with ceramic particles of boehmite (carbonized at 550 °C) [8].

CMSM have a slit-like pore structure, which provides a unique combination of micropores (0.7-2.0 nm) and ultramicropores (less than 0.7 nm) networks [9, 10]. The larger pores are responsible for sorption and ultramicropores are accountable for the molecular sieving mechanism since they approach the molecular dimensions of diffusing

gas molecules and consequently allow the passage of smaller species of a gas mixture and obstruct the larger ones [2, 5]. The exceptional gas separation performance of CMSM is made possible due to the combination of this molecular sieving transport with a solution-diffusion mechanism [4, 6, 11].

Some parameters such as carbonization conditions (heating rate, end temperature, soaking time and gas atmosphere) and pre-/post-treatments conditions (thermostabilization, oxidation and chemical vapor deposition) determine the microstructure and gas permeance properties of the carbon molecular sieve membranes [12-15]. But above all, polymer precursor has a crucial function in determining the final structure of the carbon membranes since different polymer precursors carbonized in the same conditions lead to carbon membranes with different properties [2, 16].

Research efforts have been focused on carbon molecular sieve membranes for gas separation obtained from the carbonization of various polymeric precursors such as polyimides [15-21], cellulose [22, 23], polyacrylonitrile [24], poly(furfuryl alcohol) [25, 26] and phenolic resins [4, 8, 27, 28]. Nevertheless, the search for ways to produce carbon membranes with excellent separation properties and stability, without losing the economical processability of polymeric membranes, still presents a major challenge in this field. Resorcinol-formaldehyde resin (Figure 2.2) makes an excellent precursor material for the production of CMSM due to its considerable fixed-carbon yield, high inherent purity and low-cost [29-32]. However, very few studies have been reported on the production of carbon molecular sieve membranes from resorcinol-formaldehyde resin. Tanaka *et al.* [33] prepared microporous carbon membranes on a porous α-alumina support by a partial carbonization of a resorcinol-formaldehyde resin for pervaporation applications. Dong *et al.* [34] prepared microporous carbon membranes on α-alumina supports carbonizing resorcinol-formaldehyde polymer precursor and quaternary ammonium compounds (tetramethylammonium bromide and tetrapropylammonium) for dehydration of water/ethanol and water/isopropanol mixtures by pervaporation.

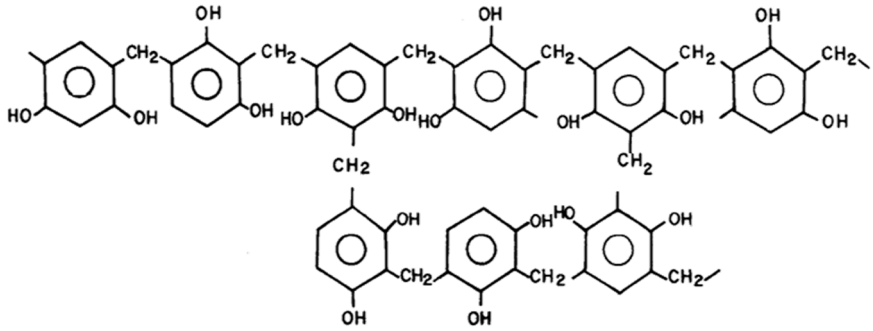

Figure 2.2. Structure of resorcinol-formaldehyde resin.

Yoshimune *et al.* [35] obtained highly mesoporous carbon membranes by carbonizing sol-gel derived mesoporous resorcinol-formaldehyde membranes.

In general, the methods described in the literature to obtain supported carbon membranes are complex and the coating-carbonization cycle must be repeated several times to achieve crack-free CMSM, which needs time and special care. Only a few researchers have reported the development of defect-free membranes by a single dipping-drying-carbonization step [1, 4, 8, 36-40]. The addition of boehmite particles with needle shape to the CMSM precursor, recently proved to be effective for producing crack-free supported membranes in a single dipping-drying-carbonization step. Boehmite (γ-AlO(OH)) is an aluminium oxide hydroxide, and it has been recently used by our research team to prepare carbon molecular sieve membranes [4, 8]. During carbonization, boehmite nanoparticles dehydrate and Al_2O_3 nanowires are formed and homogeneously distributed in the carbon matrix. Teixeira *et al*. [8] prepared composite carbon membranes from a Resol phenolic resin loaded with boehmite nanoparticles in a single coating-drying-carbonization step. Composite carbon membranes obtained exhibited high permeability to C_3H_6 and considerable C_3H_6/C_3H_8 ideal selectivity, well above the state-of-the-art plot for polymeric membranes for this separation. O_2/N_2, He/N_2 and CO_2/N_2 ideal selectivities of 5, 34 and 30 were achieved. In this study, the boehmite nanoparticles key role was identified: these needle shape particles control the polymeric precursor rheology.

This work proposes the incorporation of low-cost nanoparticles (boehmite) in a low-cost resorcinol-formaldehyde resin to prepare composite carbon molecular sieve membranes in a single dipping-drying-carbonization step. Defect-free supported carbon membranes were prepared successfully and reproducibly at different carbonization end temperatures of 500 °C (CMSM 500) and 550 °C (CMSM 550). Dry films of the composite top layer were prepared, and morphological characterization of the material was performed by scanning electron microscopy (SEM) and thermogravimetric analysis (TGA). Pore size distributions were obtained from the adsorption equilibrium isotherms of carbon dioxide at 0 °C. Permeation experiments were performed to assess the permeability towards N_2, O_2, CO_2, He and H_2 as well as the ideal selectivities for separations of industrial relevance.

2.3. Experimental

2.3.1. Materials

A resorcinol-formaldehyde resin, used as precursor, was provided by Continental Portugal. *N*-methyl-2-pyrrolidone (NMP) was supplied by Acros Organics. Boehmite nanoparticles (10 % Boehmite solution, particle size 8-20 nm) were supplied by Kawaken Fine Chemicals Co. Ltd. The α-alumina tubular supports were purchased from Inopor. Non-porous alumina tubes were bought from Omega Engineering Limited. The permanent gases were supplied by Air Liquide (99.999 % pure).

2.3.2. Tubular ceramic supports preparation

The ends of the porous Al_2O_3 supports were attached to non-porous Al_2O_3 tubes using a high temperature ceramic adhesive (Ceramabond^{TM} 569, Aremco Products) and sealed with a glass sealant at 1150 °C. The supports have a mean pore size of 200 nm (located in the outer part of the tube), an external diameter of 10 mm and a length of 70 mm. An effective length of approximately 50 mm was left for dip coating.

2.3.3. Preparation of carbon molecular sieve membranes

Resorcinol-formaldehyde resin was diluted in NMP to prepare a 15 wt. % resin solution with a viscosity of *ca.* 0.04 Pa·s and a pH of 4.6. A composite coating solution of 14 wt. % of resorcinol-formaldehyde resin, 0.5 wt. % of boehmite nanoparticles, 0.6 wt. % of ethylenediamine monohydrate and 85.6 wt. % of NMP was prepared. Ethylenediamine monohydrate was used as a basic catalyst of the polymerization reaction. Supported membranes were then prepared by dip coating the alumina tubular supports in the coating solution using a vacuum pump. The resorcinol/formaldehyde resin-based membranes were dried in a rotating oven at 70 °C overnight to avoid a quick release of the solvent during the carbonization stage that could damage the carbon matrix, causing cracks or defects. Subsequently, the membranes were left at 90 °C for 7 h.

The carbonization of the precursor was accomplished in a quartz tube (80 mm in diameter and 1.5 m in length) inside a tubular horizontal Termolab TH furnace. To guarantee temperature homogeneity along the quartz tube, the furnace has three separating heating elements controlled by a Eurotherm PID temperature controller. Figure 2.3 gives a schematic overview of the furnace.

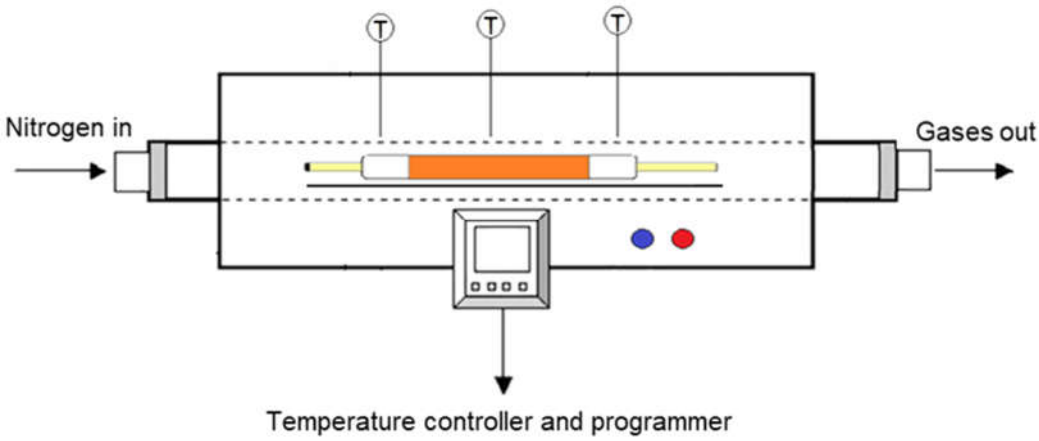

Figure 2.3. Schematic overview of the furnace setup.

The carbonization was performed under N_2 atmosphere, flow rate of 170 ml·min^{-1} and a heating rate of 1 °C·min^{-1}. Figure 2.4 shows the temperature history to prepare the carbon molecular sieve membranes from resorcinol-formaldehyde resin.

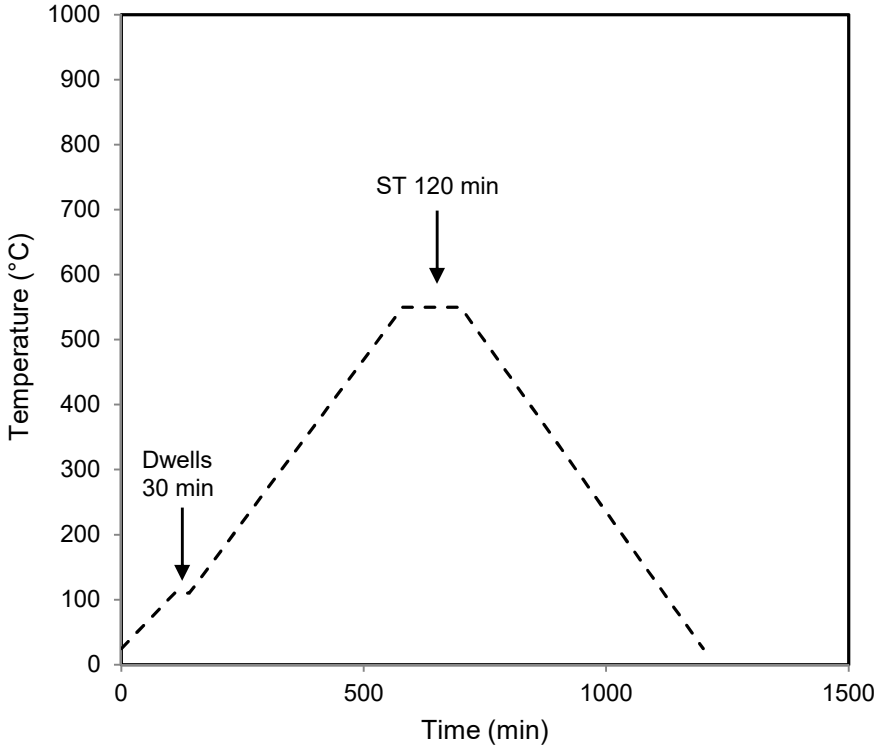

Figure 2.4. Temperature history to prepare CMSM from resorcinol-formaldehyde resin. End temperature: 550 °C.

First, the temperature was raised from ambient to 110 °C at a rate of 1 °C·min^{-1} and held at this temperature for 30 min; subsequently, the temperature was increased from 110 °C to the desired carbonization end temperature (again at a heating rate of 1 °C·min^{-1}) and held at temperature for 2 h; afterwards, the membranes were allowed to cool to room temperature.

2.3.4. Scanning electron microscopy analysis and energy dispersive X-ray spectroscopy analysis

The samples were fixed onto aluminum sample holders with Araldite™ cement, sputter-coated with palladium-gold (Bal-Tec-SCD 050) and observed in a scanning electron microscope (SEM, FEI Quanta 400FEG).

2.3.5. Thermogravimetric analysis

TGA were carried out in a Netzsch TG 209 F1 Iris thermogravimetric balance with a resolution of 0.1 μg. It was analyzed the dipping solution used for the preparation of the CMSM. The sample was previously dried in the oven at 110 °C for 72 h in order to remove most of the solvent. The characteristic curve was determined from 20 °C to 900 °C under N_2 atmosphere with a heating rate of 10 °C·min^{-1}.

2.3.6. Pore size characterization

The pore size distribution and the porosity volume of the produced CMSM were obtained based on the adsorption equilibrium isotherm of CO_2 at 0 °C determined in a magnetic suspension balance as described elsewhere [41].

2.3.7. Permeation experiments

The permeation properties of the produced CMSM were obtained by probing the membrane with pure gases. Briefly, N_2, O_2, He, H_2 and CO_2 were introduced shell side at 0.10-0.50 MPa relative feed pressure (Horiba Stec, model UR7340) and the permeated flowrate at room pressure was determined by one of three flow meters (Bronkhorst, ranges: 0-1, 0-10 and 0-100 $mL_N \cdot min^{-1}$) [8].

All results obtained are averages based on the measurements of at least three membrane samples prepared and tested under the same conditions.

2.4. Results and Discussion

2.4.1. Scanning electron microscopy and energy dispersive X-ray spectroscopy analysis

The morphology and qualitative elemental composition of carbon molecular sieve membranes were determined by scanning electron microscopy and energy dispersive X-ray spectroscopy (EDS), respectively. SEM microphotographs of cross-section of a supported CMSM 550 are showed in Figure 2.5.

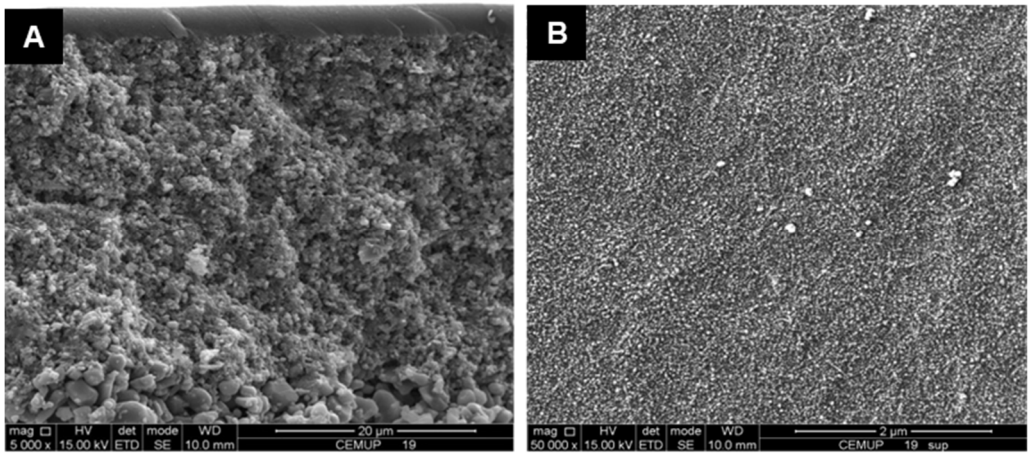

Figure 2.5. SEM photographs of one-coated resorcinol-formaldehyde based carbon membrane carbonized at 550 °C: **(A)** cross section, **(B)** surface view.

Figure 2.5-A indicates that two different parts can be distinguished: the top thin layer and the porous alumina support. A defect-free carbon film of *ca.* 3 µm thickness was uniformly formed on the top of the α-alumina tubular support. Figure 2.5-B shows that Al_2O_3 nanoparticles were well distributed in the carbon matrix. EDS analysis revealed also an uniform carbon and Al_2O_3 composition along the layer thickness (data not shown).

2.4.2. Thermogravimetric analysis

TGA was used to assess the thermal decomposition kinetics and stability of polymer in an inert atmosphere. TGA was performed on the dry dipping solution used for the preparation of the CMSM. The characteristic curve was obtained under N_2 atmosphere and is plotted in Figure 2.6.

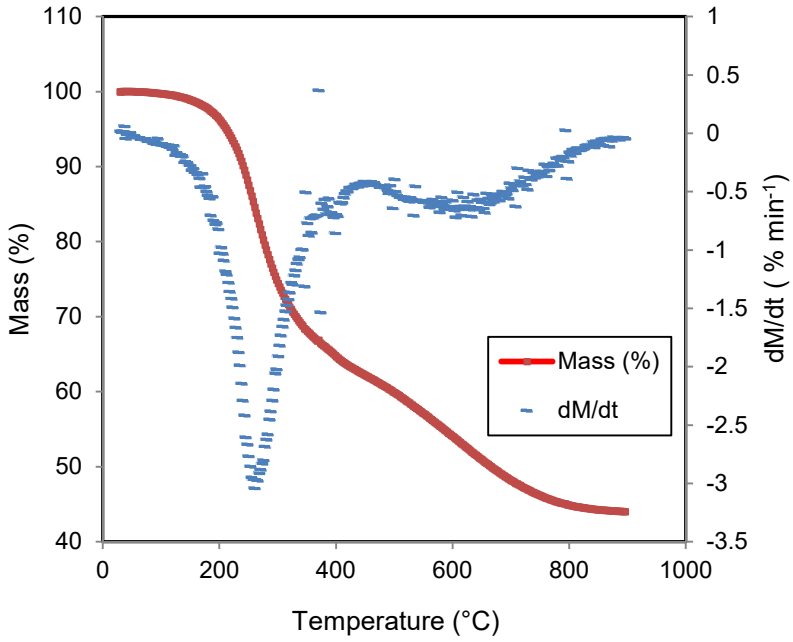

Figure 2.6. Thermogravimetric analysis of the composite dipping solution containing 14 wt. % of resin and 0.5 wt. % boehmite nanoparticles used to prepare carbon molecular sieve membranes.

Figure 2.6 shows that from room temperature to 175 °C the composite film loses about 2 % of its original weight. This loss is attributed to release of adsorbed water from the precursor. Between 175 °C and 350 °C the sample loses ca. 30 % of its original weight, which should be related to the degradation of the resorcinol-formaldehyde resin. It has been reported that at this temperature gases from the amine decomposition generate micropores in the carbonized resorcinol/formaldehyde resin-based membrane [42]. Between 500 °C and 800 °C a lower weight loss of 15 % is observed; at 900 °C the total

weight loss is approximately 44 %; this weight loss is in accordance with the literature [35].

2.4.3. Structural properties and pore size distribution

The adsorption of nitrogen at -196 °C is the most frequently used technique to assess the microporosity of carbonaceous materials. However, when ultramicroporosity is involved some diffusional limitations occur and adsorption of carbon dioxide at 0 °C is a good alternative to overcome this problem [43, 44]. The adsorption equilibrium isotherm of CO_2 at 0 °C for CMSM 500 and CMSM 550 is plotted in Figure 2.7.

Dubinin-Raduschkevisch (DR) equation is commonly used to describe the adsorption in micropores:

$$\frac{W}{W_0} = \exp\left[-\left(\frac{RT\ln\frac{P_0}{P}}{E_0}\right)^2\right] \tag{2.1}$$

where W is the micropore volume, P is the pressure, W_0 is the total micropore volume, E_0 is the characteristic energy for adsorption , P_0 is the vapor pressure of the free liquid, R is the gas constant and T is the absolute temperature. However, the DR equation only provides a reasonable description of adsorption in micropores when the characteristic curve obtained from CO_2 adsorption is linear. For handling non-linear characteristic curves, a more general equation was proposed, the Dubinin-Astakhov (DA) equation:

$$\frac{W}{W_0} = \exp\left[-\left(\frac{RT\ln\frac{P_0}{P}}{E_0}\right)^n\right] \tag{2.2}$$

where n is an adjustable parameter. DR equation results from DA equation for the particular case of n=2.

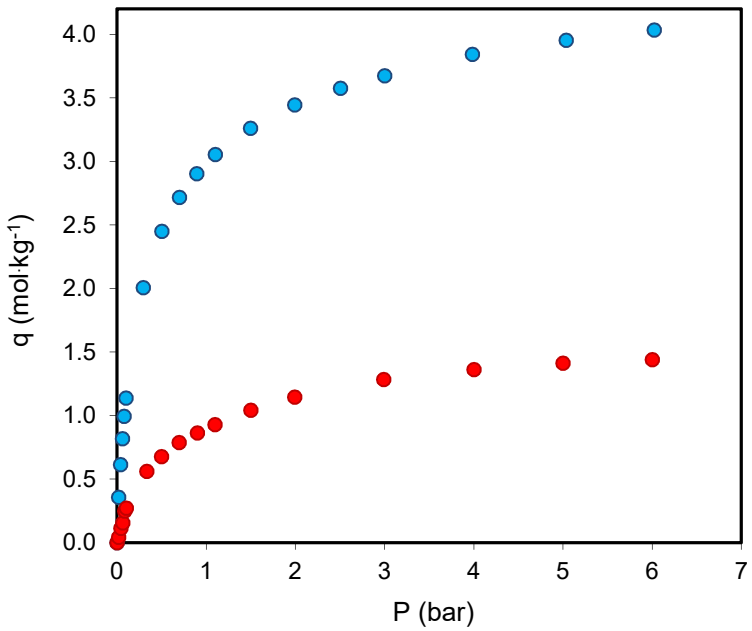

Figure 2.7. Adsorption equilibrium isotherm of CO_2 at 0 °C for CMSM 500 (red) and CMSM 550 (blue).

In the present work, the characteristic curves obtained from the CO_2 adsorption isotherm on CMSM 500 and CMSM 550 are not very linear, indicating that DR equation could not provide reasonable descriptions. Therefore, micropore volume and the characteristic energy for adsorption were determined by fitting the Dubinin-Astakhov equation to experimental data. Figure 2.8 presents the characteristic curve for CMSM 550. It can be seen that DA equation with n=2.6 fits very well the experimental data.

It is important to note that the slope of the plot is related to E_0 and the intercept is related to W_0. Table 2.1 presents a summary of the structural parameters for the studied samples. Generally, empiric correlations developed by Stoeckli are used to estimate the mean pore width. However, Stoeckli equation can only be used when the DR equation applies. For that reason, the mean pore width (l) in the present work was determined by a weighted average. For CMSM 550, the micropore volume of 0.40 $cm^3 \cdot g^{-1}$ is slightly higher when compared with other reported values [4, 21, 41, 45, 46]. However, the mean pore width (obtained by a weighted average) has the usual value found for carbon molecular sieves [4, 45, 46]. For CMSM 500, the mean pore width (obtained by a

weighted average) is a little higher when compared with other values in the literature [4, 8, 45, 46].

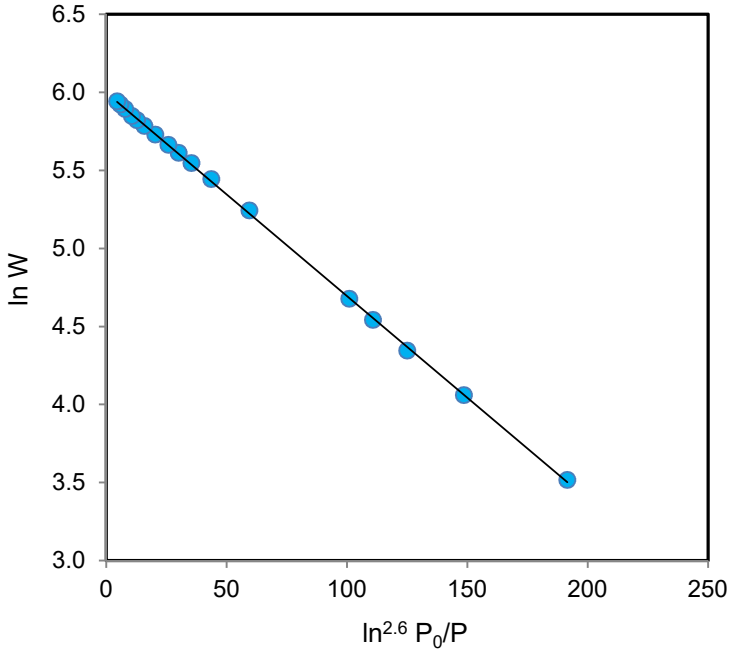

Figure 2.8. CO_2 characteristic curve for CMSM 550 (points – experimental data; solid line DA – fitting).

Table 2.1. Structural parameters for carbon molecular sieve membranes carbonized at 500 °C and 550 °C.

Parameter	CMSM 500	CMSM 550
W_0 ($cm^3 \cdot g^{-1}$)	0.13	0.40
E_0 ($kJ \cdot mol^{-1}$)	11.14	12.06
l (nm)	0.68	0.58

Pore size distribution for all carbon molecular sieve membranes was obtained using the method proposed by Do *et al*. [43, 47] for the determination of micropore size distribution in carbonaceous materials. Figures 2.9 and 2.10 show the pore size distribution obtained for CMSM 550 and CMSM 500, respectively.

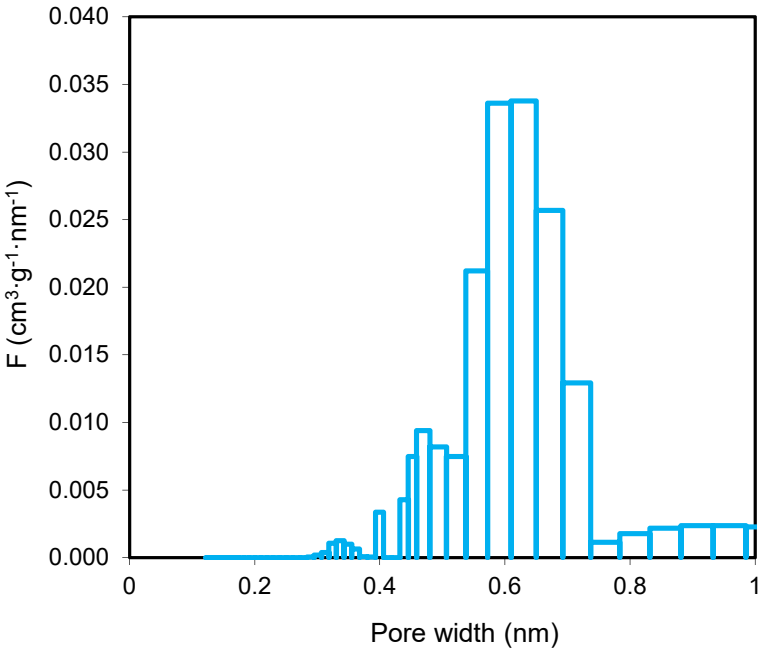

Figure 2.9. Micropore size distribution for CMSM 550.

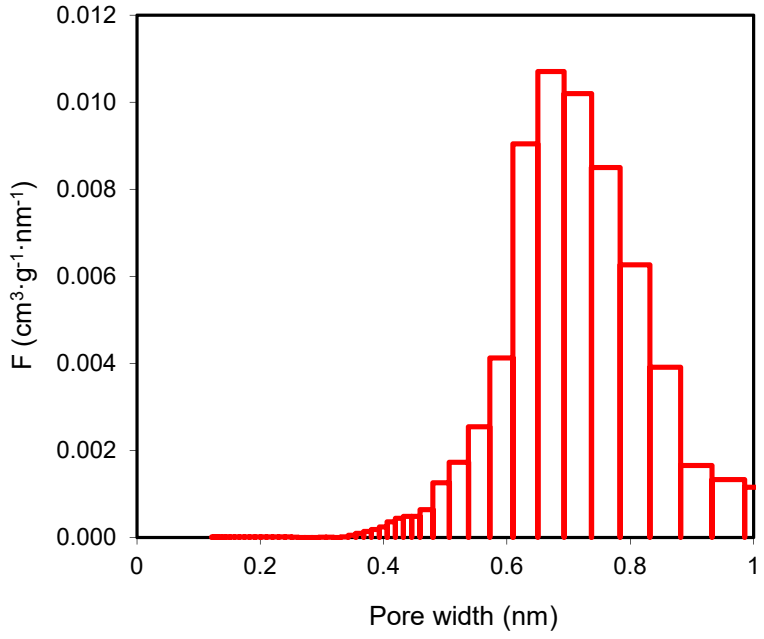

Figure 2.10. Micropore size distribution for CMSM 500.

It can be seen that the studied carbon membranes present ultramicropores (0.3-0.7 nm range) and larger micropores (0.7-1.0 nm). However, CMSM 500 have a large number of micropores with larger dimensions when compared to CMSM 550. On the other hand, CMSM 550 have a large number of micropores with narrower pore size distributions.

These small changes in the number and size of both ultramicropores and larger micropores influence the permeability and permselectivity performance of both membranes, as will be shown in the section 2.4.4.

2.4.4. Single gas permeation experiments

The permeance of the supported CMSM obtained at 500 °C and 550 °C was assessed for N_2 (0.364 nm), O_2 (0.346 nm), He (0.260 nm), H_2 (0.290 nm) and CO_2 (0.335 nm) – the values in brackets correspond to the kinetic diameter of the gases [48]. The produced CMSM were exposed to the room conditions for 6 days. Afterwards, the samples were heated at various temperatures (140 °C, 160 °C and 200 °C) during 2 h under N_2 atmosphere with a heating rate of 0.7 °C·min^{-1}. The relative feed pressure was varied between 0.10 MPa and 0.50 MPa while the permeate was kept at *ca.* 0.10 MPa (atmospheric pressure). Gas permeation experiments were carried out from 25 °C to 120 °C.

The effect of the carbonization end temperature on the permeability of two sets of resorcinol-formaldehyde carbon membranes is summarized in Figure 2.11. It can be concluded that the devised preparation process originates membranes with very similar permeation properties. Moreover, the samples carbonized at higher temperature (CMSM 550) have generically smaller gas permeation rate; for example, the permeability to N_2 became around 3 times smaller when compared to CMSM 500 samples. This can be attributed to the ultramicropores shrinkage [49, 50]. CMSM 500 also have a larger mean pore width, l= 0.68 nm compared to CMSM 550, l= 0.58 nm (Table 2.1). However,

CMSM 550 have a larger volume of ultramicropores (comparing Figures 2.9 and 2.10). This leads to a higher permeance of CMSM 550 than of CMSM 500 to He.

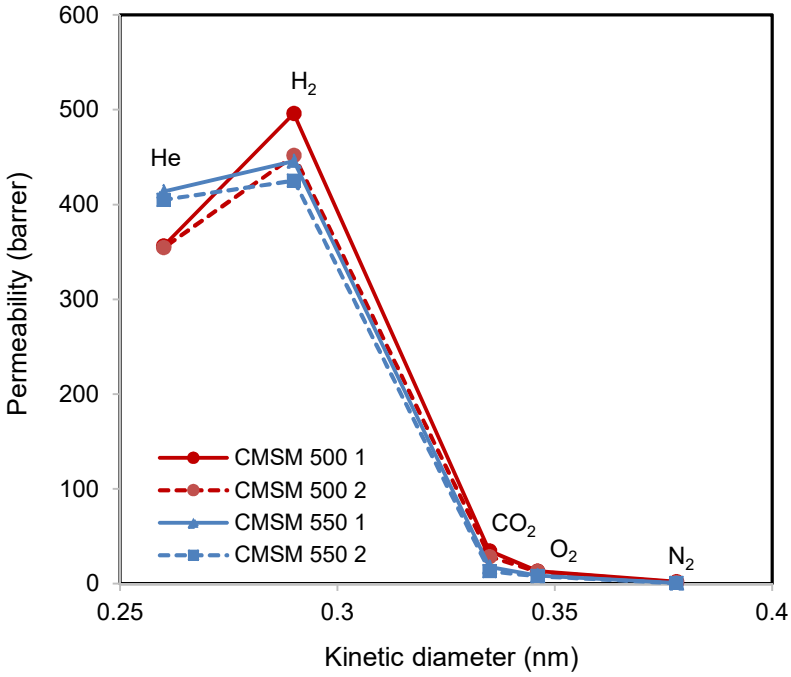

Figure 2.11. Permeability as a function of the kinetic diameter of gas molecules for two sets of supported carbon membranes obtained at different end carbonization temperatures. Lines were added for readability.

The performance of a membrane towards a separation is characterized by the permeability to the target species as well as the corresponding selectivities. Under all tested conditions, it was observed that the best compromise between permeability and selectivity was achieved for the membranes carbonized at 550 °C, activated at 140 °C and measured at 120 °C. Therefore, these results will be further discussed here.

Figure 2.12/Table 2.2 and Figure 2.13/Table 2.3 show the permeance as a function of the relative feed pressure for CMSM 500 and CMSM 550, respectively.

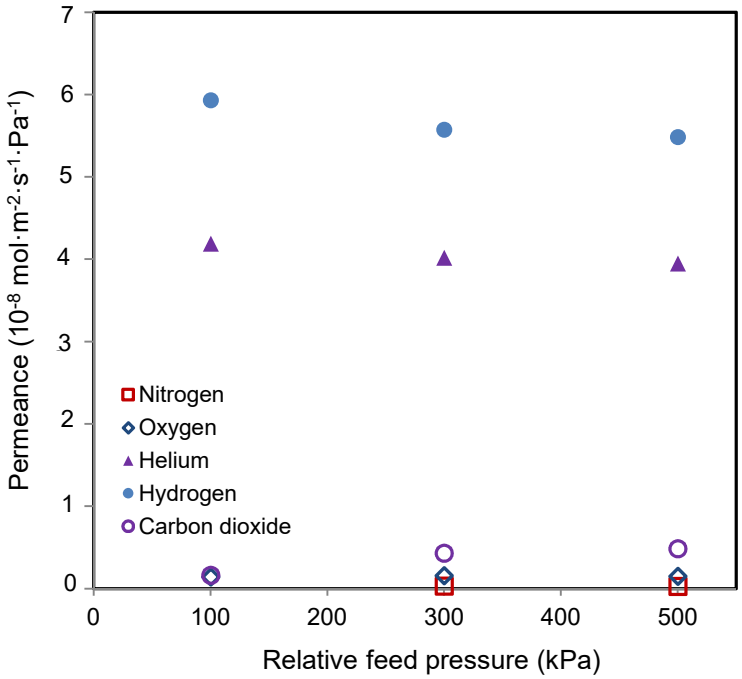

Figure 2.12. Gas permeance as a function of the relative feed pressure for CMSM 500. Membranes were activated at 140 °C for 2 h under N_2 atmosphere before permeation experiments.

Table 2.2. Permeance properties as a function of the relative feed pressure for CMSM 500. Membranes were activated at 140 °C for 2 h under N_2 atmosphere before permeation experiments.

Feed pressure (kPa)	Permeance (mol·m^{-2}·s^{-1}·Pa^{-1})				
	N_2	O_2	He	H_2	CO_2
500	2.465×10^{-10}	1.513×10^{-9}	3.947×10^{-8}	5.484×10^{-8}	4.831×10^{-9}
300	*	1.562×10^{-9}	4.017×10^{-8}	5.571×10^{-8}	4.310×10^{-9}
100	*	1.403×10^{-9}	4.189×10^{-8}	5.931×10^{-8}	1.615×10^{-9}

*Below the detection limit

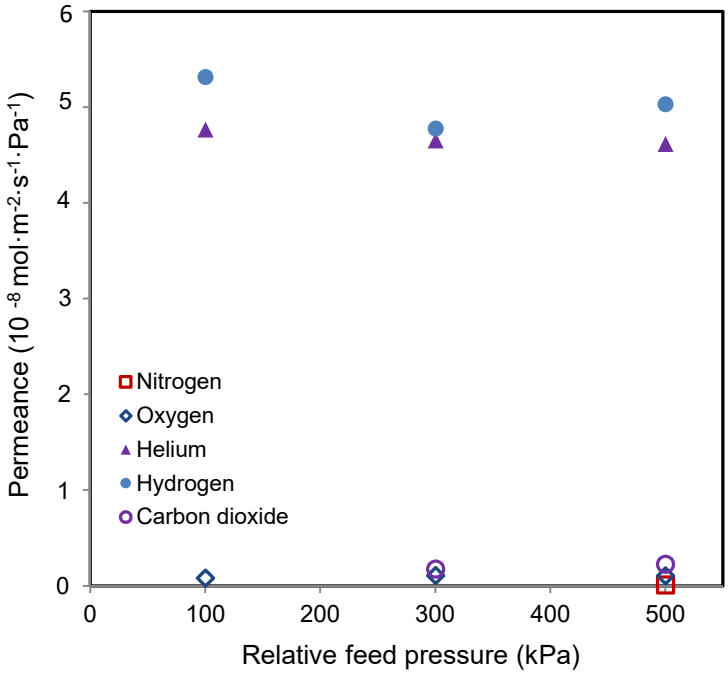

Figure 2.13. Gas permeance as a function of the relative feed pressure for CMSM 550. Membranes were activated at 140 °C for 2 h under N_2 atmosphere before permeation experiments.

Table 2.3. Permeance properties as a function of the relative feed pressure for CMSM 550. Membranes were activated at 140 °C for 2 h under N_2 atmosphere before permeation experiments.

Feed pressure (kPa)	Permeance (mol·m^{-2}·s^{-1}·Pa^{-1})				
	N_2	O_2	He	H_2	CO_2
500	<8.530×10^{-11}	1.062×10^{-9}	4.614×10^{-8}	5.029×10^{-8}	2.256×10^{-9}
300	*	1.075×10^{-9}	4.653×10^{-8}	4.775×10^{-8}	1.774×10^{-9}
100	*	8.173×10^{-10}	4.766×10^{-8}	5.312×10^{-8}	< 8.530×10^{-10}

*Below detection limit

The permeance toward all gases is pressure-dependent: Nishiyama *et al.* [42] and Lagorsse *et al.* [45] reported that this behavior seems to become more evident as the intensity of the adsorbate-adsorbent interactions increases. Since CO_2 shows a more pronounced permeance increase with pressure, CO_2 should have more affinity to the resorcinol-formaldehyde based carbon membranes than the other gases.

The effect of temperature on the permeance of CMSM 550 to the probing gases is illustrated in Figure 2.14.

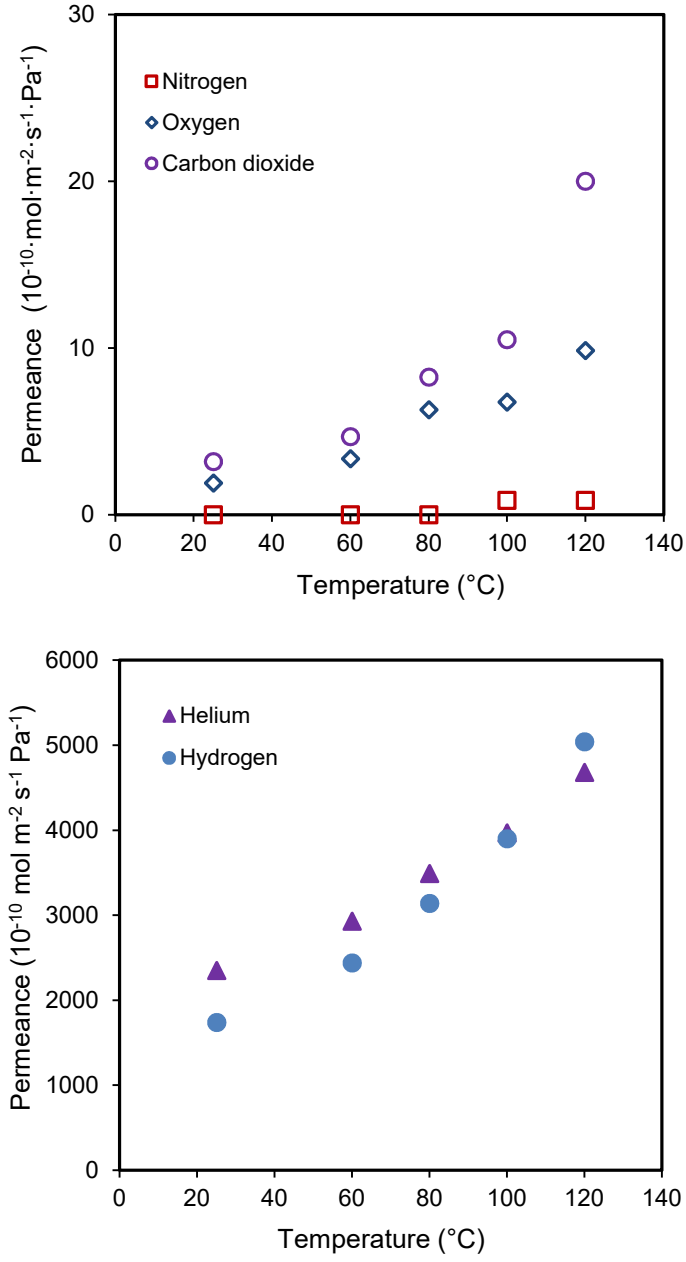

Figure 2.14. Gas permeance as a function of temperature for CMSM 550 (N_2, O_2, CO_2 - top figure; He, H_2 - bottom figure). Membranes were activated at 140 °C for 2 h under N_2 atmosphere before permeation experiments.

It can be seen that membrane permeance increases as the temperature increases. This reveals that the gas transport through the carbon molecular sieve membranes is an activated diffusion process, as expected for a molecular sieve mechanism [2].

From the change of CMSM permeance with temperature, the apparent activation energy can be estimated according to the following Arrhenius equation:

$$\ln(P) = -\frac{E_a}{RT} + \ln\left(\frac{D_0}{RT}\right) \tag{2.3}$$

where D_0 is a pre-exponential factor, E_a is the apparent activation energy, P is the permeability, R is the gas constant and T is the absolute temperature.

The estimated apparent activation energies for O_2, He, H_2 and CO_2 are 17.0, 7.0, 10.8 and 18.2 kJ·mol^{-1}, respectively. These values are relatively close to other values reported in literature [51]. The apparent activation energy for N_2 was not calculated because permeation data is only available for temperatures above around 100 °C (see Figure 2.14), and therefore there were not enough data to make the corresponding Arrhenius plot. Ideal selectivities obtained for both carbon molecular sieve membranes sets are shown in Table 2.4.

Table 2.4. Ideal selectivities for CMSM 500 and CMSM 550. Membranes were activated at 140 °C for 2 h under N_2 atmosphere before permeation experiments being performed.

Sample	Ideal Selectivity			
	O_2/N_2	He/N_2	H_2/N_2	CO_2/N_2
CMSM 500	5.9	221.0	158.0	15.4
CMSM 550	>11.5	>554.0	>586.0	>23.3

It can be seen that ideal selectivity for all gas pairs increase significantly when membrane carbonization end temperature increases from 500 °C to 550 °C. Small differences observed in pore size distribution and mean pore width are very important and strongly influence the diffusion of molecules with closer sizes such as N_2, O_2 and CO_2.

The obtained permeabilities and ideal selectivities were inserted into the semi-empirical plots devised by Robeson in 2008 [52]. Figures 2.15, 2.16, 2.17 and 2.18 illustrate the upper bound limits for O_2/N_2, He/N_2, H_2/N_2 and CO_2/N_2, respectively.

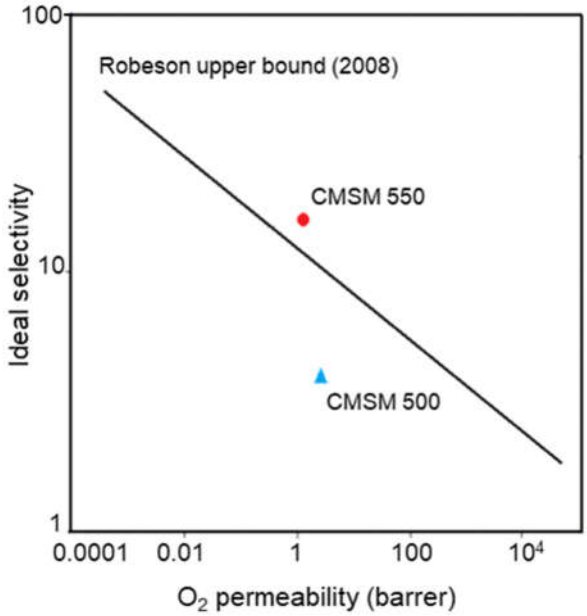

Figure 2.15. Robeson upper bound plot for O_2/N_2 gas pair showing the data for CMSM 500 and CMSM 550.

CMSM 550 showed promising results for the separation of O_2/N_2 (permeability: 8.7 barrer; and ideal selectivity: >11.5), H_2/N_2 (permeability: 445.6 barrer; and ideal selectivity: >586) and He/N_2 (permeability: 413.8 barrer; and ideal selectivity: >544). Finally, Figure 2.19 compares these results with permeation data of CMSM produced from other low-cost precursors (phenol-formaldehyde resins).

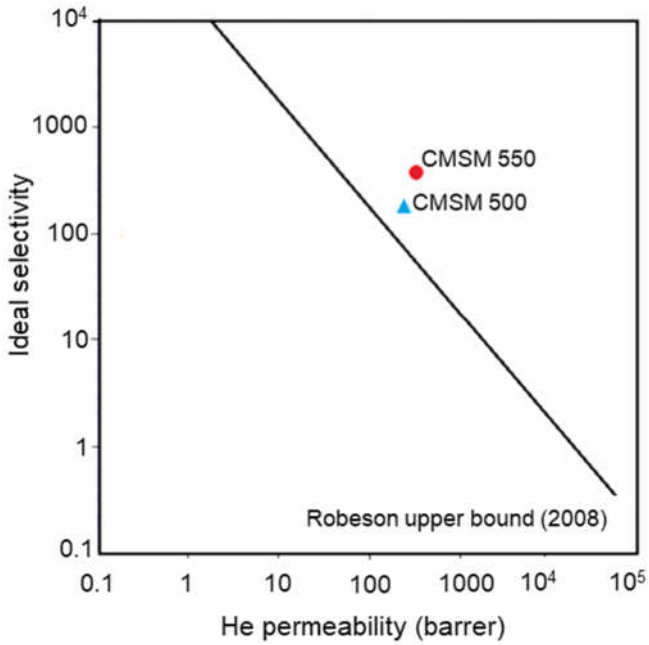

Figure 2.16. Robeson upper bound plot for He/N_2 gas pair showing the data for CMSM 500 and CMSM 550.

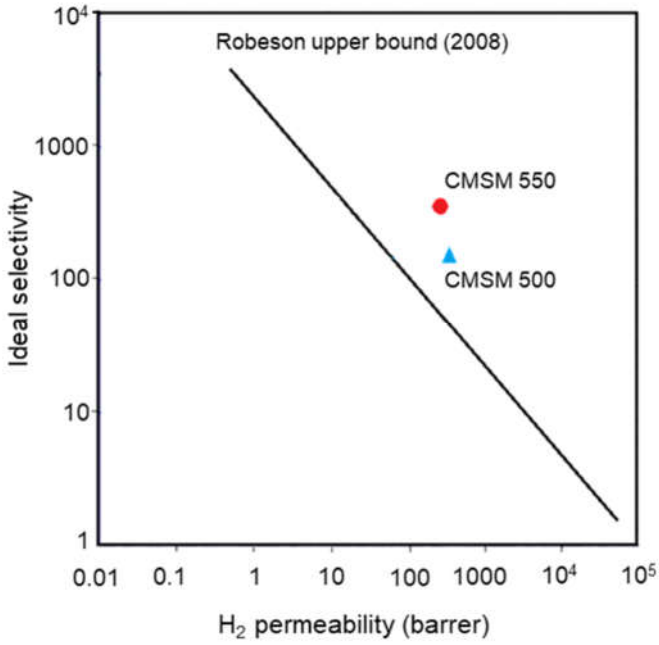

Figure 2.17. Robeson upper bound plot for H_2/N_2 gas pair showing the data for CMSM 500 and CMSM 550.

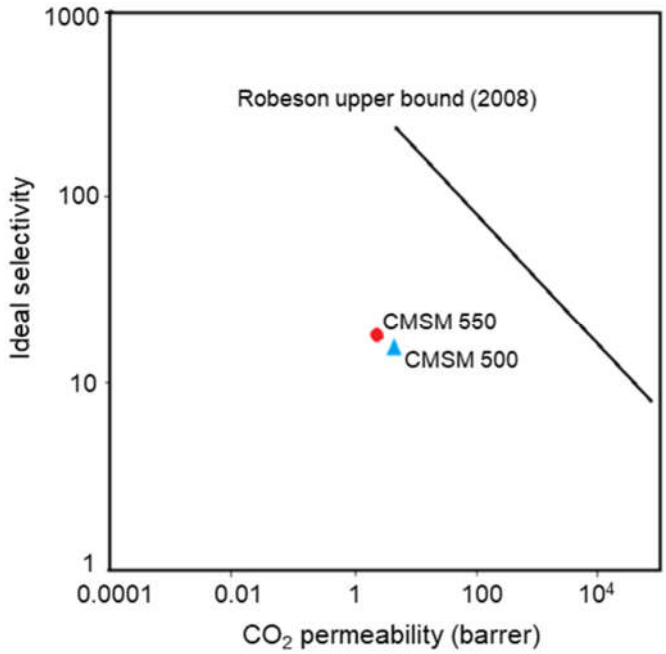

Figure 2.18. Robeson upper bound plot for CO_2/N_2 gas pair showing the data for CMSM 500 and CMSM 550.

It can be concluded that CMSM 550 exhibits higher ideal selectivities towards O_2/N_2, He/N_2 and H_2/N_2 and higher permeabilities towards H_2 and He when compared to similar studies [1, 4, 8, 36, 37, 53-57]. However, lower permeabilities were obtained towards O_2 [36, 53, 54, 56].

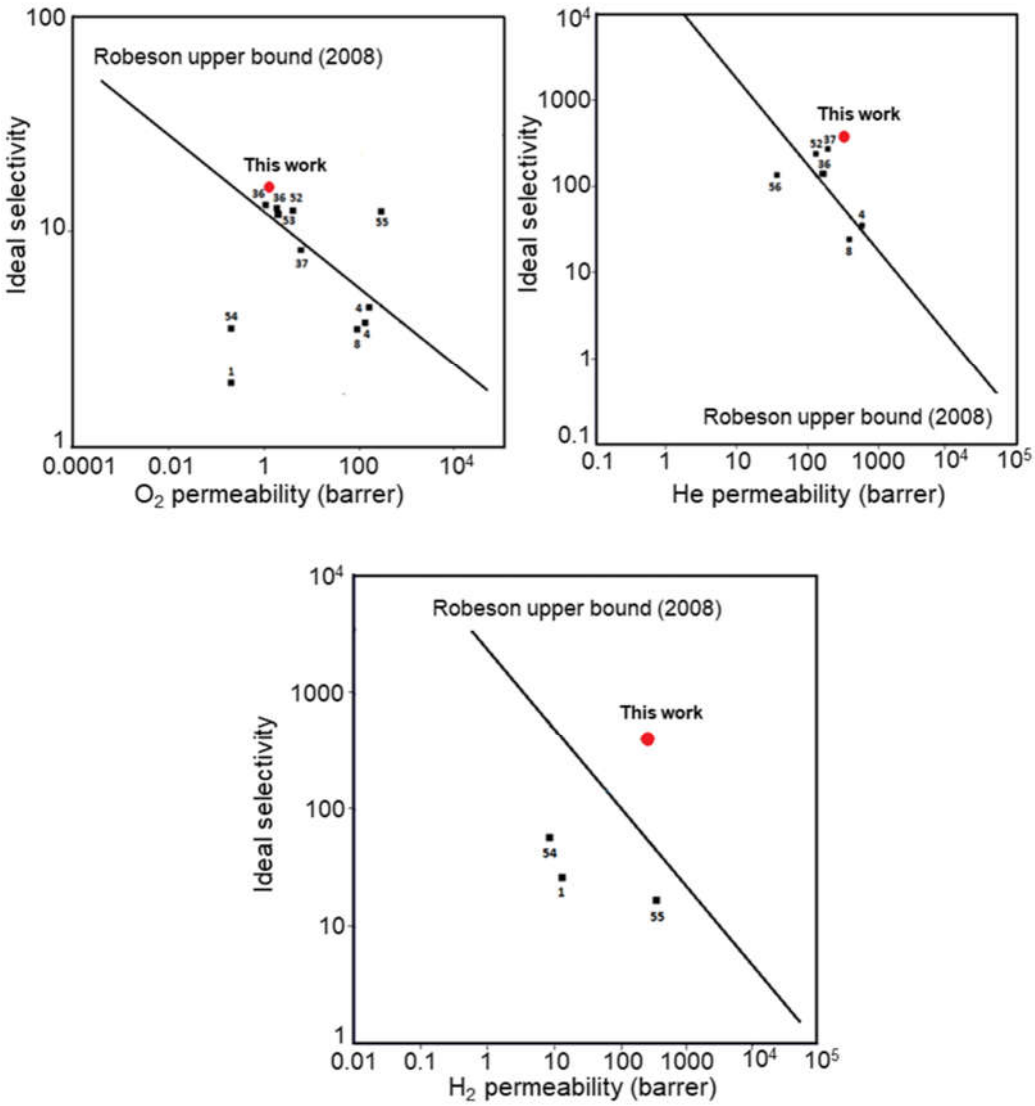

Figure 2.19. Robeson upper limits and comparison with pure gas permeation results obtained with low-cost phenol-formaldehyde resins derived carbon membranes. All selectivities are relative to N_2.

2.5. Conclusions

Carbon molecular sieve membranes were successfully prepared in a single dipping-drying-carbonization sequence. Membranes with reproducible properties were prepared from resorcinol-formaldehyde resin, a low-cost precursor, loaded with boehmite nanoparticles. The effect of the carbonization end temperature was assessed and better separation properties were found for sample CMSM 550, carbonized in an inert atmosphere at 550 °C. For improving their permeation stability, membranes were contacted with ambient air for 6 days and activated at 140 °C under N_2 atmosphere. Carbon molecular sieve membranes carbonized at 550 °C end temperature showed large number of micropores with a narrower pore size distributions and much higher ideal selectivities and relatively similar gas permeation rates than those produced at 500 °C.

The Robeson upper bound for polymeric membranes was overtaken by CMSM 550, regarding O_2/N_2 (O_2 permeation rate: 9.85×10^{-10} $mol\cdot m^{-2}\cdot s^{-1}\cdot Pa^{-1}$ and ideal selectivity: >11.5), H_2/N_2 (H_2 permeation rate: 5.04×10^{-8} $mol\cdot m^{-2}\cdot s^{-1}\cdot Pa^{-1}$ and ideal selectivity: >586) and He/N_2 (He permeation rate: 4.68×10^{-8} $mol\cdot m^{-2}\cdot s^{-1}\cdot Pa^{-1}$ and ideal selectivity: >544) separations. CMSM 550 are superior to many reported carbon membranes produced from other low-cost precursors, indicating that CMSM produced from resorcinol-formaldehyde resin have potential for gas separation.

2.6. Acknowledgments

The authors would like to acknowledge the funding provided by the Portuguese Foundation for Science and Technology (FCT) through the projects PTDC/EQU-EQU/114944/2009 and PTDC/EQU-EQU/104217/2008. The authors are also grateful to the European Union´s Seventh Framework Programme (FP7/2007) for Fuell Cells and Hydrogen Joint Technology for funding under grant agreement number 303476. The authors are thankful to CEMUP for the SEM/EDS analysis.

2.7. References

[1] W. Wei, G. Qin, H. Hu, L. You, G. Chen, Preparation of supported carbon molecular sieve membrane from novolac phenol-formaldehyde resin, Journal of Membrane Science, 303 (2007) 80-85.

[2] A.F. Ismail, L.I.B. David, A review on the latest development of carbon membranes for gas separation, Journal of Membrane Science, 193 (2003) 1-18.

[3] P.S. Tin, T.S. Chung, S. Kawi, M.D. Guiver, Novel approaches to fabricate carbon molecular sieve membranes based on chemical modified and solvent treated polyimides, Microporous Mesoporous Materials, 73 (2004) 151-160.

[4] M. Teixeira, M. Campo, D.A. Tanaka, M.A. Tanco, C. Magen, A. Mendes, Carbon Al_2O_3 Ag composite molecular sieve membranes for gas separation, Chemical Engineering Research and Design, 90 (2012) 2338-2345.

[5] A.B. Fuertes, T.A. Centeno, Preparation of supported carbon molecular sieve membranes, Carbon, 37 (1999) 679-684.

[6] Y.H. Sim, H. Wang, F.Y. Li, M.L. Chua, T.S. Chung, M. Toriida, S. Tamai, High performance carbon molecular sieve membranes derived from hyperbranched polyimide precursors for improved gas separation applications, Carbon, 53 (2013) 101-111.

[7] M. Kiyono, P.J. Williams, W.J. Koros, Effect of pyrolysis atmosphere on separation performance of carbon molecular sieve membranes, Journal of Membrane Science, 350 (2010) 2-10.

[8] M. Teixeira, M.C. Campo, D.A. Tanaka, M.A. Tanco, C. Magen, A. Mendes, Composite phenolic resin-based carbon molecular sieve membranes for gas separation, Carbon, 49 (2011) 4348-4358.

[9] S. Lowell, J.E. Shields, M.A. Thomas, M. Thommes, Characterization of Porous Solids and Powders: Surface Area, Pore Size and Density. Kluwer Academic Publishers, The Netherlands, 2004, Chapter 4, pp.26.

[10] A. J. Burggraaf, L. Cot. Fundamentals of Inorganic Membrane Technology. Elsevier Science, The Netherlands, 1996, Chapter 4, pp.71.

[11] M.B. Rao, S. Sircar, Nanoporous carbon membranes for separation of gas mixtures by selective surface, Journal of Membrane Science, 85 (1993) 253-264.

[12] C.W. Jones, W.J. Koros, Carbon molecular sieve gas separation membranes I. Preparation and characterization based on polyimide precursors, Carbon, 32 (1994) 1419-1425.

[13] M. Yoshino, S. Nakamura, H. Kita, K. Okamoto, N. Tanihara, Y. Kusuki, Olefin/paraffin separation performance of carbonized membranes derived from an asymmetric hollow fiber membrane of 6FDA/BPDA–DDBT copolyimide, Journal of Membrane Science, 215 (2003) 169-183.

[14] H. Suda, K. Haraya, Alkene/alkane permselectivities of a carbon molecular sieve membrane, Chemical Communications, (1997) 93–94.

[15] Y.K. Kim, H.B. Park, Y.M. Lee, Gas separation properties of carbon molecular sieve membranes derived from polyimide/polyvinylpyrrolidone blends: effect of the molecular weight of polyvinylpyrrolidone, Journal of Membrane Science, 251 (2005)159-167.

[16] H.B. Park, Y.K. Kim, J.M. Lee, S.Y. Lee, Y.M. Lee, Relationship between chemical structure of aromatic polyimides and gas permeation properties of their carbon molecular sieve membranes, Journal of Membrane Science, 229 (2004) 117-27.

[17] Y.K. Kim, H.B. Park, Y.M. Lee, Carbon molecular sieve membranes derived from thermally labile polymer containing blend polymer and their gas separation properties, Journal of Membrane Science, 243 (2004) 9-17.

[18] Y.K. Kim, H.B. Park, Y.M. Lee, Preparation and characterization of carbon molecular sieve membranes derived from BTDA-ODA polyimide and their gas separation properties, Journal of Membrane Science, 255 (2005) 265-273.

[19] A.B. Fuertes, D.M. Nevskaia, T.A. Centeno, Carbon composite membranes from Matrimid® and Kapton® polyimides for gas separation, Microporous Mesoporous Materials, 33 (1999) 115-125.

[20] K.M. Steel, W.J. Koros, An investigation of the effects of pyrolysis parameters on gas separation properties of carbon materials, Carbon, 43 (2005) 1843-1856.

[21] P.S. Tin, T.S. Chung, S. Kawi, M.D. Guiver, Novel approaches to fabricate carbon molecular sieve membranes based on chemical modified and solvent treated polyimides, Microporous Mesoporous Materials, 73 (2004) 151-160.

[22] J.A. Lie, M.B. Hägg, Carbon membranes from cellulose: synthesis, performance and regeneration, Journal of Membrane Science, 284 (2006) 79-86.

[23] M. Campo, F.D. Magalhães, A. Mendes, Carbon molecular sieve membranes from cellophane paper, Journal of Membrane Science, 350 (2010) 180-188.

[24] L.B. David, A.F. Ismail, Influence of the thermastablization process and soak time during pyrolysis process on the polyacrylonitrile carbon membranes for O_2/N_2 separation, Journal of Membrane Science, 213 (2003) 285-291.

[25] Y.D. Cheng, R.T. Yang, Preparation of carbon molecular sieve membranes and diffusion of binary mixtures in the membrane, Industrial & Engineering Chemistry Research, 33 (1994) 3146-3153.

[26] C. Song, T. Wang, X. Wang, J. Qiu, Y. Cao, Preparation and gas separation properties of poly(furfuryl alcohol)-based C/CMS composite membranes, Separation and Purification Technology, 58 (2008) 412-418.

[27] A.B. Fuertes, I. Menendez, Separation of hydrocarbon gas mixtures using phenolic resin-based carbon membranes, Separation and Purification Technology, 28 (2002) 29-41.

[28] F.K. Katsaros, T.A. Steriotis, A.K. Stubos, A. Mitropoulos, N.K. Kanellopoulos, S. Tennison, High pressure gas permeability of microporous carbon membranes, Microporous Mesoporous Materials, 8 (1997) 171-176.

[29] S.J. Park, W.Y. Jung, Preparation and structural characterization of activated carbons based on polymeric resin, Journal of Colloid and Interface Science, 250 (2002) 196–200.

[30] J. Hayashi, M. Uchibayashi, T. Horikawa, K. Muroyama, V. Gomes, Synthesizing activated carbons from resins by chemical activation with K_2CO_3, Carbon, 40 (2002) 2727–2752.

[31] S. Tenison, Phenolic-resin-derived activated carbons, Applied Catalysis A, 173 (1998) 289-311.

[32] T. Yamamoto, T. Sugimoto, T. Suzuki, S. Mukai, H. Tamon, Preparation and characterization of carbon cryogel microspheres, Carbon, 40 (2002) 1345–1351.

[33] S. Tanaka, T. Yasuda, Y. Katayama, Y. Miyake, Pervaporation dehydration performance of microporous carbon membranes prepared from resorcinol/formaldehyde polymer, Journal of Membrane Science, 379 (2012) 52-54.

[34] Y.R. Dong, M. Nakao, N. Nishiyama, Y. Egashira, K. Ueyama. Gas permeation and pervaporation of water/alcohols through the microporous carbon membranes prepared from resorcinol/formaldehyde/quaternary ammonium compounds, Separation and Purification Technology, 73 (2010) 2-7.

[35] M. Yoshimune, T. Yamamoto, M. Nakaiwa, K. Haraya. Preparation of highly mesoporous carbon membranes via a sol-gel process using resorcinol and formaldehyde, Carbon, 46 (2008) 1031-1036.

[36] T.A. Centeno, A.B. Fuertes. Carbon molecular sieve membranes derived from a phenolic resin supported on porous ceramic tubes, Separation and Purification Technology, 25 (2001) 379-384.

[37] A.B. Fuertes, I. Menendez, Separation of hydrocarbons gas mixtures using phenolic resin-based carbon membranes, Separation and Purification Technology, 28 (2002) 29-41.

[38] A.B. Fuertes, Effect of air oxidation on gas separation properties of adsorption-selective carbon membranes, Carbon, 39 (2001) 697-706.

[39] A.B. Fuertes, Adsorption-selective carbon membrane for gas separation, Journal of Membrane Science, 177 (2000) 9-16.

[40] I. Menendez, A.B. Fuertes, Aging of carbon membranes under different environments, Carbon, 39 (2001) 733-740.

[41] M.C. Campo, F.D. Magalhães, A. Mendes, Comparative study between a CMS membrane and a CMS adsorbent: Part I-morphology, adsorption equilibrium and kinetics, Journal of Membrane Science, 346 (2010) 15-25.

[42] N. Nishiyama, Y.R. Dong, T. Zheng, Y. Egashira, K. Ueyama, Tertiary amine-mediated synthesis of microporous carbon membranes, Journal of Membrane Science, 280 (2006) 603-609.

[43] C. Nguyen, D.D. Do, Adsorption of supercritical gases in porous media: determination of micropore size distribution, Journal of Physical Chemistry, 103 (1999) 6900-6908.

[44] S.W. Rutherford, C. Nguyen, J.E. Coons, D.D. Do, Characterization of carbon molecular sieves using methane and carbon dioxide as adsorptive probes, Langmuir, 19 (2003) 8335-8342.

[45] S. Lagorsse, F.D. Magalhães, A. Mendes, Carbon molecular sieve membranes - sorption, kinetic and structural characterization, Journal of Membrane Science, 241 (2004) 275-287.

[46] D. Cazorla-Amarós, J. Alcaniz-Monge, M.A. Casa-Lillo, A. Linares-Solano, CO_2 as an adsorptive to characterize carbon molecular sieves and activated carbons, Langmuir, 14 (1998) 4589-4596.

[47] C. Nguyen, D.D. Do, K. Haraya, K. Wang, The structural characterization of carbon molecular sieve membrane (CMSM) via gas adsorption, Journal of Membrane Science, 220 (2003) 177-182.

[48] D.W. Breck. Zeolite Molecular Sieves, Structure, Chemistry and Use. John Wiley & Sons, New York, 1974.

[49] T.H. Ko, W.S. Kuo, Y. H. Chang, Raman study of the microstructure changes of phenolic resin during pyrolysis, Polymer Composites, 21 (2000) 745-750.

[50] T.A. Centeno, J.L. Vilas, A.B. Fuertes, Effects of phenolic resin pyrolysis conditions on carbon membrane performance for gas separation, Journal of Membrane Science, 228 (2004) 45-54.

[51] A.F. Ismail, D. Rana, T. Matsuura, H.C. Foley. Carbon-based Membranes for Separation Processes. Springer, New York, 2011, pp. 299-313.

[52] L. M. Robeson, The upper bound revisited, Journal of Membrane Science, 320 (2008) 390-400.

[53] I. Menendez, A.B. Fuertes, Aging of carbon membranes under different environments, Carbon, 39 (2001) 733-740.

[54] W. Zhou, M. Yoshino, H. Kita, K. Okamoto, Preparation and gas permeation properties of carbon molecular sieve membranes based on sulfonated phenolic resin, Journal of Membrane Science, 217 (2003) 55-67.

[55] W. Wei, H. Hu, L. You, G. Chen, Preparation of carbon molecular sieve membrane from phenol-formaldehyde novolac resin, Carbon, 40 (2002) 465-467.

[56] A.B. Fuertes, Effect of air oxidation on gas separation properties of adsorptive-selective carbon membranes, Carbon, 39 (2001) 697-706.

[57] W. Shusen, Z. Meiyun, W. Zhizhong, Asymmetric molecular sieve carbon membranes, Journal of Membrane Science, 109 (1996) 267-270.

Chapter III

Chapter 3.A – Carbon membranes with extremely high separation performance and stability[1]

3.1. Abstract

For some time carbon molecular sieve membranes have been promoted as energy-efficient candidates for gas separation due to their high selectivity, permeability and stability in chemically aggressive environments. Nevertheless, these membranes have not yet made it into commercial products due to a significant decrease in performance when exposed to humidity and/or oxygen. Here we show that carbon molecular sieve membranes with extremely high separation performance and stability even in the presence of humidity can be prepared from a renewable low-cost precursor with a single carbonization step. The membranes showed a linear water vapor adsorption isotherm, characteristic of a homogeneous distribution of hydrophilic sites on the pore surfaces, allowing for water molecules to hop continuously between sites and avoiding the formation of pore-blocking water clusters. These results are a breakthrough towards bringing this new type of membrane to a commercial level.

[1] S.C. Rodrigues, M. Andrade, J. Moffat, F.D. Magalhães, A. Mendes, Carbon membranes with extremely high separation performance and stability, submitted, (2017).

3.2. Introduction

Carbon molecular sieve membranes (CMSM) were first reported by Koresh and Soffer in the 80s [1, 2] and have been widely studied since. CMSM are prepared by controlled carbonization of a polymeric precursor. They have a unique slit-like microporous structure formed by disordered non-homogeneous graphene-like layers; the resulting pore network consists of relatively wide pores with short narrow constrictions [3]. The combination of the molecular sieving effect at the narrow constrictions with the adsorption and diffusion mechanism on the larger micropores provides the simultaneous high permeability and high selectivity performance that is distinctive of these materials [4]. Several parameters can be manipulated to tune the size of the pores to a particular gas separation including the choice of precursor, the pre-treatment, the carbonization conditions (temperature history and atmosphere), and the post-treatment of the resulting material [5].

In addition to presenting high permeability and selectivity, an ideal membrane should maintain its performance in the presence of humidity and oxygen, be stable under harsh thermal and chemical environments, be mechanically resistant, and have a low production cost. CMSM are already known to have high permeability towards gases and excellent selectivities, overcoming the Robeson upper bound for polymeric membranes and to be thermally and chemically stable [6, 7]. However, they exhibit pore blockage in the presence of water vapor, and oxygen chemisorption when exposed to air, even at room temperature. This significantly hinders the performance and seriously limits its industrial applicability [8]. In addition, they are brittle making manipulation and assembly into a functional module difficult [9].

Here we elucidate unique CMSM that do not show any noticeable pore blockage when treating a humidified stream with up to *ca*. 80 % relative humidity (RH). Furthermore, these membranes display high flexibility and extraordinary separation performance. As described below, these novel CMSM are produced in a single carbonization step and use a low-cost precursor obtained from a renewable source.

Figure 3.1 illustrates the empirical selectivity/permeability upper bounds for O_2/N_2 (Figure 3.1-A), CO_2/CH_4 (Figure 3.1-B) and H_2/CH_4 (Figure 3.1-C) separations, as defined by Robeson in 2008 for polymeric membranes [10], together with the results obtained in this work, and a comparison with some results reported in literature [6, 11-19]. One of the membranes produced, CMSM 600, is situated far above Robeson's upper bound, showing an O_2/N_2 ideal selectivity greater than 800, for a permeability to oxygen of 0.78 barrer, a CO_2/CH_4 ideal selectivity greater than 2600, for a permeability to CO_2 of 2.57 barrer, and a H_2/CH_4 ideal selectivity greater than 25 000, for a permeability to hydrogen of 25 barrer. The arrows in the charts indicate the superior ideal selectivities which are significantly higher than those reported previously.

Since CMSM were first reported, several important advancements have been reported, primarily concerning precursor selection and modifications, pre-/post-treatments and addressing the humidity pore blockage and oxygen chemisorption. The precursor determines the final structure of the CMSM as illustrated by Figure 3.2, where very different micropore shapes are visible. Numerous thermosetting polymeric precursors have been extensively studied, namely polyimide, phenolic resin, polyfurfuryl alcohol, polyacrylonitrile and cellulose [9]. Consistently, however, cellulose-based precursors provide membranes with especially high selectivities and permeabilities to several permanent gases [20]. Cellulose also has the advantage of being a low-cost biopolymer. In 1983 [2], the first carbon membranes were prepared from the carbonization of cellulose hollow fibers and their application to gas separation processes was patented in 1987 [21]. The same authors patented [22] later a full description of the production process for hollow fiber membranes from cellulose. For a period of time, an Israeli company, Carbon Membranes Ltd., produced mechanically stable hollow fiber dense membranes from cellulose cupra-ammonia precursors. This was the first and, so far, the only company worldwide to produce at an industrial scale high quality hollow fiber membranes; the company closed, however, in 2001.

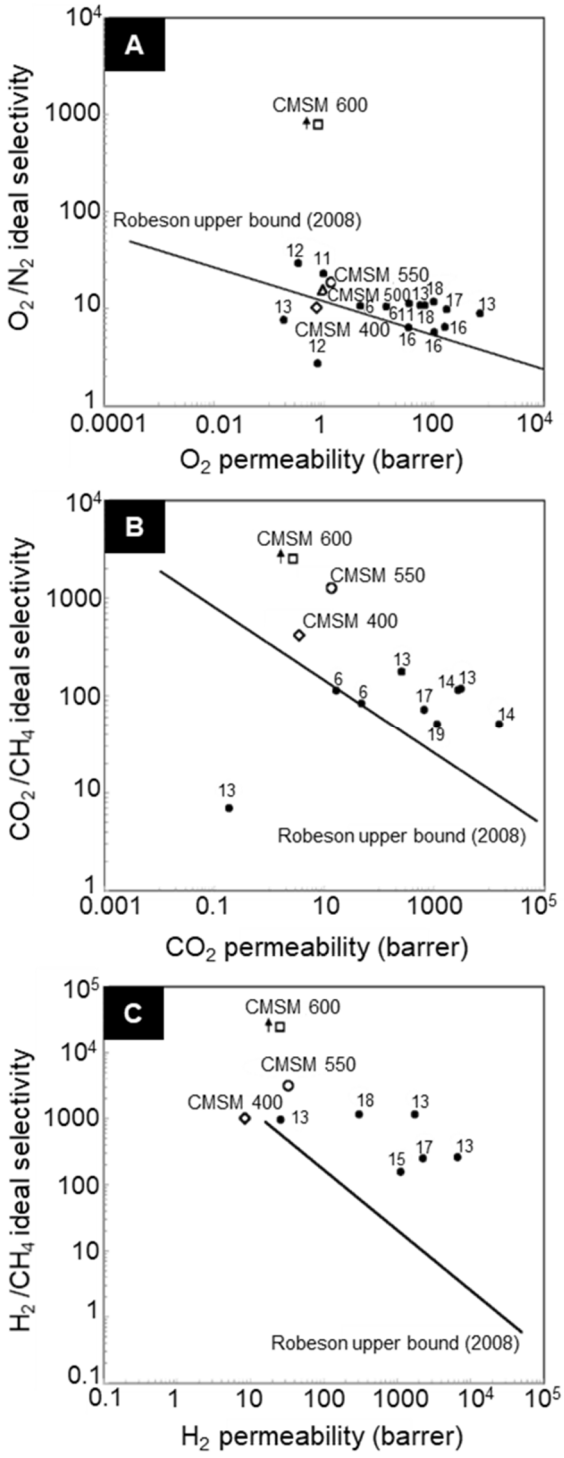

Figure 3.1. Robeson plots for **(A)** O_2/N_2, **(B)** CO_2/CH_4 and **(C)** H_2/CH_4 gas pairs showing the data for the cellophane-based CMSM. The data of reported literature are shown for comparison.

Before the carbonization step, treatments have been applied to provide additional dimensional stability to the polymeric matrix; these include air oxidation to make the polymer structure less prone to relaxation during carbonization, immersing membranes in chemical solutions to prevent pores to collapse, and use of catalysts for promoting carbonization at lower temperatures [23]. Precursors of polymer blends with inorganic particles of metals, zeolites, silica, boehmite and carbon nanotubes, have also been extensively used as a strategy for improving CMSM permeability and selectivity [9]. Chemical vapor deposition and post-oxidation have been applied to narrow and enlarge the pores, respectively [23]. Recently, Koros and Singh [24] patented a new oxygen doping method, where higher temperature and a trace amount of oxygen are used after carbonization for enhancing the selectivity of CMSM, while maintaining high permeance.

Many authors have concentrated their efforts on addressing the well-known CMSM aging effect, associated with the degradation of the membrane performance over time when exposed to humidity and oxygen. Water vapor is known to cause a pore blockage effect, where above a threshold partial pressure the CMSM loses reversibly most of its permeability [25, 26]. Jones and Koros [27] are among the few authors to address this challenge, coating their CMSM with a very thin film of Teflon® with encouraging results. For membranes coated with the protective layer, the permeability to oxygen only decreased 11 % under 83-85 % RH.

Many models have been developed to describe water vapor adsorption in carbon materials [28, 29]. In 2005 [30] the authors developed a model for water vapor adsorption/desorption on CMSM based on Do's model for activated carbons [31]. This model, which will be discussed below in more detail, describes the water adsorption as occurring on hydrophilic sites present in specific location within the pores, via hydrogen bonding. Sufficiently large clusters gain the ability to leave the primary adsorption site and to roll over the hydrophobic surface eventually clogging the pore at a constriction location. This model explains the water pore blockage effect as originated by the sparse

location of the hydrophilic sites within the pores, such as at the edges of the graphene-like layers.

The active sites at the edges of the graphene-like layers easily chemisorb oxygen forming oxygen functional groups [32] that reduce the CMSM open porosity. Treatments with hydrogen at high temperatures, where the hydrogen passivates the active sites, have been proposed by some authors. However, hydrogen passivation is not fully effective and many sites still exhibit sufficient reactivity to chemisorb oxygen [26]. CMSM have a great affinity to adsorb hydrocarbon molecules; in 1994, Koros [8] proposed the use of propylene as a cleaning agent after the exposition of CMSM to contaminants. A few years later, Menendez and Fuertes [33] concluded that propylene could be a protective treatment to prevent the chemisorption of oxygen. Furthermore, membrane permeabilities were not adversely affected by the propylene treatment.

3.3. Remarkable separation performance

Cellophane is a natural, renewable, low-cost polymer produced from wood cellulose by the viscose process. Briefly, cellulose is treated using aqueous sodium hydroxide to form 'alkali cellulose', which is then reacted with carbon disulphide to produce a solution of sodium cellulose xanthate, known as viscose. The aged viscose is then extruded through a slot die into a bath of dilute sulfuric acid and sodium sulfate to regenerate the cellulose as a film. The film is then passed through several baths to remove sulfur, to bleach the film and add softeners (normally, glycerin and urea) to prevent the film from becoming brittle. Cellophane was first reported as a promising precursor for CMSM by the authors in 2010 [34].

Membranes were prepared by carbonization of cellophane in one step according to the procedure described in the Supplementary Information (Chapter 3.B). Briefly, cellophane films were carbonized under a nitrogen atmosphere at various temperatures, namely 400 °C (CMSM 400), 500 °C (CMSM 500), 550 °C (CMSM 550) and 600 °C (CMSM 600). A slow heating rate of 0.5 °C·min^{-1} and several 30 min dwells

were implemented to avoid the formation of cracks and defects. Single gas permeation experiments were performed on the CMSM using several probe species at 25 °C: N_2 (0.364 nm), O_2 (0.346 nm), He (0.260 nm), H_2 (0.290 nm), CO_2 (0.335 nm), CH_4 (0.380 nm), C_3H_6 (0.450 nm), C_3H_8 (0.430 nm) and water vapor (0.268 nm) – the numbers in brackets are the kinetic diameters of the gases. Prior to permeation experiments, the CMSM were glued to steel O-rings and exposed to lab air for 4 days. Table 3.1 shows the permeabilities obtained for the CMSM prepared at different carbonization end temperatures.

Table 3.1. Permeabilities of CMSM at 25 °C.

Sample	Permeability (barrer)								
	N_2	O_2	He	H_2	CO_2	CH_4	H_2O	C_3H_6	C_3H_8
CMSM 400	0.07	0.73	5.43	8.35	3.39	0.008	12.07	n.d*	n.d*
CMSM 500	0.06	0.95	10.24	18.94	8.21	n.d*	15.96	n.d*	n.d*
CMSM 550	0.07	1.33	17.26	32.59	13.03	0.01	28.51	0.056	0.035
CMSM 600	<0.001	0.78	11.78	24.90	2.57	<<0.001	25.20	0.065	0.025

n.d* = not determined

In general, permeability decreases as the gas kinetic diameter increases, indicating that the CMSM have size-discrimination ability. Water vapor permeates faster than He despite being a larger species. This is believed to be associated with the hydrophilic character of these membranes, as it will be discussed later. The membrane is also more permeable to hydrogen than to helium, despite the larger size of hydrogen, due to its higher adsorption affinity [11]. A comparison between the membranes (Table 3.1), reveals that the permeabilities to all gases increase with carbonization end temperature up to 550 °C, decreasing thereafter. Thermogravimetric analysis (Figure S.1, Chapter 3.B) suggests that up to 550 °C most of the heteroatoms present in the precursor have been released in the form of volatile matter. Therefore, the increase in the permeability up to 550 °C is mostly related to pore network formation. At 600 °C, the decrease in the permeability suggests that carbon atoms are rearranging into a

constricted structure by a sintering mechanism [35]. Table 3.2 shows the obtained ideal selectivities for the CMSM. The separation performance is extremely high, particularly for the CMSM prepared at 600 °C.

Table 3.2. Ideal selectivities of CMSM at 25 °C.

Sample	Ideal Selectivity							
	O_2/N_2	H_2/N_2	H_2/CH_4	CO_2/N_2	CO_2/CH_4	He/N_2	H_2/O_2	C_3H_6/C_3H_8
CMSM 400	10.4	119.3	1043.8	48.4	423.8	77.6	11.4	n.d*
CMSM 500	15.8	315.7	n.d*	136.8	n.d*	170.7	19.9	n.d*
CMSM 550	19.0	465.6	3259.0	186.1	1303.0	246.6	24.5	1.6
CMSM 600	>800	>25 000	>>25 000	>2600	>>2600	>1200	44.5	2.6

n.d* = not determined

Despite the very high ideal selectivities displayed by these CMSM for most of the gas pairs, ideal selectivity towards C_3H_6/C_3H_8 is rather low when compared to other values reported in the literature (5-15 times lower) [16, 36-38]. To understand this apparent contradictory behavior, it was decided to prepare and characterize a carbon molecular sieve adsorbent (CMS) displaying particularly high C_3H_6/C_3H_8 ideal selectivity. The CMS was prepared from a phenolic resin precursor at 1100 °C. Table S.1 (Chapter 3.B) shows the C_3H_6/C_3H_8 and O_2/N_2 ideal selectivities for the CMSM and for the CMS, together with a brief comparison with literature values [16, 36-38]. It is apparent that when carbon molecular sieves show high O_2/N_2 ideal selectivities, low C_3H_6/C_3H_8 ideal selectivities are obtained and vice-versa. This suggests the existence of two extreme sieving mechanisms in carbon molecular sieves. Those mechanisms are rationalized as being: a) gate sieving for carbon molecular sieves having a gate-like pore shape, which are selective for spheroid gas species such as O_2, N_2, etc. and b) tubular sieving for carbon molecular sieves having a tubular pore shape, which are selective for linear gas species such as C_3H_6 and C_3H_8. To better understand the role of the pore morphology, high resolution transmission electron microscopy (HRTEM) images were taken of the

two carbon molecular sieve samples: Figure 3.2 shows the HRTEM images of a CMSM carbonized at 550 °C (Figure 3.2-A) and the CMS adsorbent (Figure 3.2-B).

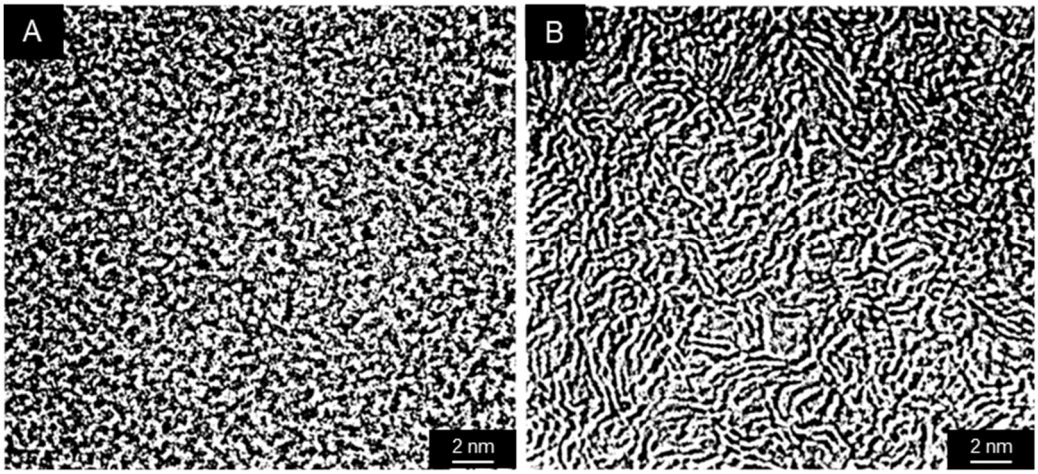

Figure 3.2. HRTEM images of the produced carbon molecular sieves: **(A)** CMSM 550, **(B)** CMS adsorbent.

As expected, the pore morphology of the two materials is very different: for the sample with high O_2/N_2 ideal selectivities, gate-like pores are present, characteristic of a gate sieving mechanism, whereas sample with high C_3H_6/C_3H_8 ideal selectivities present interconnected pores in the form of tubes, characteristic of a tubular sieving mechanism.

The CMSM separation performance was also evaluated for a gas mixture (50 % O_2/ 50 % N_2) at 25 °C, using CMSM prepared at 550 °C. The selectivity obtained from these bicomponent experiments was the same as the ideal selectivity computed from the single gas permeation runs (α = 19 for CMSM 550); this is because oxygen and nitrogen have similar adsorption isotherms.

3.4. Unique water vapor/oxygen stability

The adsorption of water vapor in carbon materials typically exhibits a type V isotherm [31], according to International Union of Pure and Applied Chemistry (IUPAC) designation, also known as S-shape isotherm; adsorption is almost nonexistent up to

relative pressures of *ca*. 0.3, but a significant uptake occurs at higher relative pressures. Some existing models assume that water adsorption on CMSM occurs essentially in three consecutive steps: i) water molecules adsorb onto hydrophilic functional groups, involving non-carbon species on the pore surface (*i.e.*, carboxyl, carboxylic anhydride, phenol, carbonyl, lactone, ether or quinone groups); ii) after an initial molecule becomes adsorbed, others attach to it through hydrogen bonding, forming clusters of several water molecules; iii) the resulting cluster composed by *m* water molecules has enough dispersion energy to be released from the hydrophilic group, rolling up until blocking a constriction of the pore network.

Permeation experiments in the presence of 75-77 % RH were undertaken using CMSM prepared at 550 °C, to determine membrane's performance stability in the presence of water vapor. Permeation data collected at 25 °C showed that humidity does not affect the membrane's ability to permeate and separate gases; the total flux increased *ca*. 2.5 times (the permeability to oxygen stays roughly constant) – Table 3.3. This increase is due to the very fast permeation of water vapor that occurs due to the membrane's high hydrophilicity as it will be shown later.

Table 3.3. Permeability of CMSM 550 sample to dry and humidified O_2 and N_2.

Sample	RH (%)	Dry feed		Humidified feed	
		Permeability to O_2 (barrer)	Permeability to N_2 (barrer)	Permeability to humidified O_2 (barrer)	Permeability to humidified N_2 (barrer)
CMSM 550	75-77	1.33	0.07	3.30	0.08

Water vapor adsorption/desorption isotherms at 25 °C were measured for the CMSM prepared at different carbonization end temperatures (Figure 3.3). All materials showed linear or quasi-linear adsorption isotherms, instead of the markedly S-shape curves normally displayed by CMSM [30]; the linear adsorption behavior (Fig.3.3-C) has never been reported. Since the hydrophilicity of a carbon material determines its

adsorption behavior toward water vapor, this indicates that these membranes do not have the same hydrophobic character as those previously reported elsewhere [31].

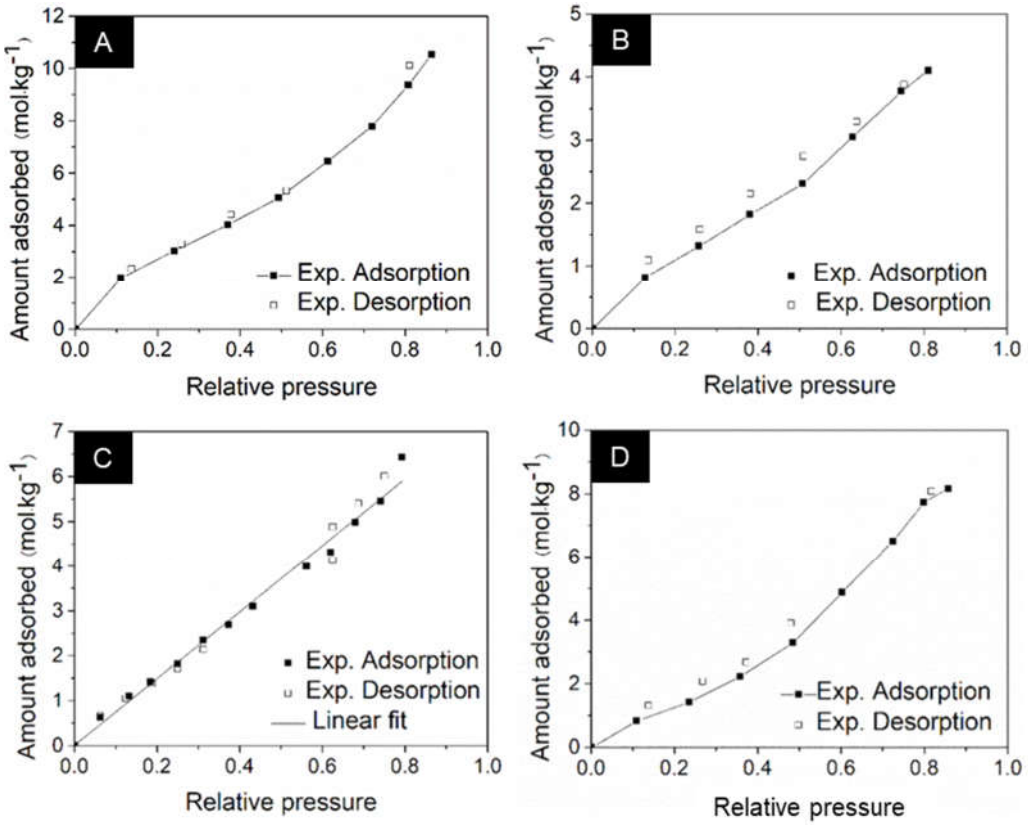

Figure 3.3. Water vapor adsorption/desorption equilibrium isotherms: **(A)** CMSM 400, **(B)** CMSM 500, **(C)** CMSM 550, **(D)** CMSM 600.

Linear water vapor adsorption/desorption isotherms are characteristic of carbon materials with hydrophilic sites homogeneously distributed throughout their inner surfaces, allowing water molecules to jump smoothly between polar sites and avoiding the formation of molecular water clusters. As a consequence, humidity exposure does not cause pore blockage. X-ray photoelectron spectroscopy (XPS) analysis performed on the CMSM indicates the presence of metallic and semi-metallic elements, incorporated in the membranes during cellophane film production, namely ionic sodium and silica nanoparticles (Table S.2). These elements homogeneously dispersed

throughout the pore surfaces and also the small size of the graphene-like platelets (Figure 3.2-A) with the typical hydrophilic sites at their edges provide a hydrophilic character to the pore walls that allows surface diffusion of water molecules, therefore minimizing cluster formation.

Fourier transform infrared spectroscopy (FTIR) analysis allowed detection of oxygen functional groups, such as hydroxyl, carbonyl, ether, ester and carboxylic, in the membranes' material (Figure S.2). However, these were already expected to be present and should not be associated with the peculiar water-adsorption behavior of the produced membranes.

The end carbonization temperature seems to have a noticeable influence on membrane surface chemistry. As it increases, the water vapor adsorption isotherm becomes increasingly linear (Fig. 3.3-A, Fig. 3.3-B and Fig. 3.3-C), indicating an increasingly hydrophilic character. Above 550 °C, however, the isotherm becomes curved again (Fig. 3.3-D), and at 900 °C it displays already a marked S-shape (Figure S.3). With the increase of the carbonization end temperature, the atomic concentration of ionic sodium on CMSM surface increases and, in contrast, the atomic concentration of oxygen decreases. The slight increase in atomic concentration of oxygen observed on CMSM 600 surface should be related to oxygen chemisorption (Table S.2). A carbonization end temperature of 550 °C appears to provide an optimum condition for the concentration of hydrophilic elements homogeneously distributed on CMSM surface.

Contact angle measurements performed on the different CMSM surfaces are coherent with the previous observations (Table S.3). The water contact angle decreases with an increase in carbonization end temperature between 400 °C and 550 °C, as the surface becomes more hydrophilic. At 600 °C, a slight increase in the water contact angle is observed, associated with higher hydrophobicity.

To determine the performance stability of the membranes in the presence of oxygen, membranes prepared at 550 °C and 600 °C were exposed to ambient air over several days, and their permeability to oxygen and nitrogen evaluated as a function of

exposure time (Table S.4). The results revealed that the permeability to oxygen decreased by *ca.* 66 % for CMSM 550 when increasing air exposure time from 2 to 5 days. For CMSM 600, permeability decreased by *ca.* 69 % when increasing exposure from 2 to 7 days. This shows that the prepared membranes are susceptible to oxygen chemisorption. However, up to a certain point, this process favors the selectivity of the membranes; when CMSM are exposed to ambient air before permeation tests, improved ideal selectivities are obtained compared to CMSM tested without air exposure (Table S.5). This is because oxygen chemisorbs on active sites in the pore surface during air exposure, forming oxygen-containing groups on the pore windows. As a consequence, the effective pore width narrows and improved selectivities are obtained.

As previously discussed, carbon membranes storage under a propylene atmosphere is a known strategy to protect them from oxygen chemisorption with minimal impact in the transport properties. Thus, immediately after carbonization, a CMSM 550 sample was stored under propylene at 2 bar for 10 days; a CMSM 550 control sample was also stored in contact with atmospheric air. Propylene was able to stabilize the membranes concerning oxygen chemisorption. After 3 days of air exposure, permeability to oxygen of the treated CMSM 550 decreased *ca*. 2 %, within the experimental error (Table S.5). Moreover, the membrane permeability was not unfavorably affected by the propylene treatment.

3.5. Morphological and structural characterization

The morphology of the membranes was analyzed by scanning electron microscopy (SEM) as shown in Figure S.4. Figure S.4-A indicates a uniform carbon membrane (CMSM 550) with *ca*. 9.5 µm thickness. The measured thicknesses from the cross-section views indicated that an increase in the carbonization end temperature led to a decrease in membrane thickness. SEM micrographs also revealed that all CMSM produced at different carbonization end temperatures present very similar surface

features. The observed microspheres clusters are a usual product of hydrothermal carbonization of cellulose at >220 °C (Figure S.4-B).

The flexibility of the disk-like membranes was assessed by bending them with a smaller bend radius indicating greater flexibility. It was observed that membrane flexibility tends to decrease as the carbonization end temperature increases; nevertheless, all prepared CMSM were flexible as shown in Figure S.5.

The pore size distribution of samples carbonized at 550 °C and 600 °C was obtained using the method proposed by Do *et al.* [39, 40] for carbonaceous materials (Figure S.6). The membranes present ultramicropores (0.3-0.7 nm) and micropores (0.7-1.0 nm). CMSM 550 presents a large volume of micropores with larger dimensions when compared to CMSM 600. On the other hand, CMSM 600 presents a large volume of ultramicropores compared to the samples prepared at 550 °C. These small changes in the amount and size of both larger micropores and ultramicropores have a significant influence on the permeability and selectivity of the membranes, as previously observed.

3.6. Foreseen industrial applications of the new CMSM

The cellophane based-CMSM, with their exceptional separation performance and stability, are promising materials for numerous industrial applications. Examples include: oxygen and nitrogen separation from air, CO_2 separation from flue gas, recovery of hydrogen from natural gas, separation of hydrogen from syngas, removal of CO_2 from natural gas, air dehumidification, natural gas dehydration and xenon separation from gas mixtures. Moreover, these CMSM might be considered in applications coupled with other processes, such as cryogenic distillation and pressure swing adsorption; this might be especially relevant for producing xenon for medical and space applications.

3.7. Acknowledgments

S.C. Rodrigues is grateful to the Portuguese Foundation for Science and Technology (FCT) for the doctoral grant (reference SFRH/BD/93779/2013) supported by funding POPH/FSE. M. Andrade is thankful to Comissão de Coordenação e Desenvolvimento Regional do Norte for the fellowship grant (reference LEPABE-2-ECO-INNOVATION-NORTE-01-0145-FEDER-000005). This work was financially supported by: Project EXPL/QEQ-PRS/0342/2013 from FCT; Project UID/EQU/00511/2013-LEPABE, by the FCT/MEC with national funds and when applicable co-funded by FEDER in the scope of the P2020 Partnership Agreement; Project NORTE-07-0124-FEDER-000026-RL1_Energy, by FEDER funds through Programa Operacional Factores de Competitividade – COMPETE, by the Programa Operacional do Norte (ON2) program and by national funds through FCT. The authors are thankful to CEMUP for the SEM and XPS analysis and to Dr. Whitley and Dr. Shubhra from Air Products and Chemicals for the pore size distribution experiments and, to INA for the HRTEM analyses.

3.8. References

[1] J.E. Koresh, A. Soffer, Mechanism of permeation through molecular-sieve carbon membrane. Part 1.-The effect of adsorption and the dependence on pressure, Journal of the Chemical Society, Faraday Transactions 1, 82 (1986) 2057-2063.

[2] J.E. Koresh, A. Sofer, Molecular Sieve Carbon Permselective Membrane. Part I. Presentation of a New Device for Gas Mixture Separation, Separation Science and Technology, 18 (1983) 723-734.

[3] A.F. Ismail, L.I.B. David, A review on the latest development of carbon membranes for gas separation, Journal of Membrane Science, 193 (2001) 1-18.

[4] R. Singh, W.J. Koros, Carbon molecular sieve membrane performance tuning by dual temperature secondary oxygen doping (DTSOD), Journal of Membrane Science, 427 (2013) 472-478.

[5] S.M. Saufi, A.F. Ismail, Fabrication of carbon membranes for gas separation - a review, Carbon, 42 (2004) 241-259.

[6] T.A. Centeno, A.B. Fuertes, Carbon molecular sieve membranes derived from a phenolic resin supported on porous ceramic tubes, Separation and Purification Technology, 25 (2001) 379-384.

[7] M.-B. Hägg, J.A. Lie, A. Lindbråthen, Carbon molecular sieve membranes: a promising alternative for selected industrial applications, Annals of the New York Academy of Sciences, 984 (2003) 329-345.

[8] C.W. Jones, W.J. Koros, Carbon molecular sieve gas separation membranes-II. Regeneration following organic exposure, Carbon, 32 (1994) 1427-1432.

[9] W.N.W. Salleh, A.F. Ismail, Carbon membranes for gas separation processes: Recent progress and future perspective, Journal of Membrane Science and Research, 1 (2015) 2-15.

[10] L.M. Robeson, The upper bound revisited, Journal of Membrane Science, 320 (2008) 390-400.

[11] H. Suda, K. Haraya, Gas permeation through micropores of carbon molecular sieve membranes derived from kapton polyimide, The Journal of Physical Chemistry B, 101 (1997) 3988-3994.

[12] M.B. Shiflett, H.C. Foley, Ultrasonic deposition of high-selectivity nanoporous carbon membranes, Science, 285 (1999) 1902-1905.

[13] H. Kita, M. Yoshino, K. Tanaka, K.-i. Okamoto, Gas permselectivity of carbonized polypyrrolone membrane, Chemical Communications, (1997) 1051-1052.

[14] W. Qiu, K. Zhang, F.S. Li, K. Zhang, W.J. Koros, Gas separation performance of carbon molecular sieve membranes based on 6FDA-mPDA/DABA (3:2) polyimide, ChemSusChem, 7 (2014) 1186-1194.

[15] A.K. Itta, H.-H. Tseng, M.-Y. Wey, Fabrication and characterization of PPO/PVP blend carbon molecular sieve membranes for H_2/N_2 and H_2/CH_4 separation, Journal of Membrane Science, 372 (2011) 387-395.

[16] M. Teixeira, M. Campo, D.A. Tanaka, M.A. Tanco, C. Magen, A. Mendes, Carbon-Al_2O_3–Ag composite molecular sieve membranes for gas separation, Chemical Engineering Research and Design, 90 (2012) 2338-2345.

[17] M.-Y. Wey, H.-H. Tseng, C.-k. Chiang, Effect of MFI zeolite intermediate layers on gas separation performance of carbon molecular sieve (CMS) membranes, Journal of Membrane Science, 446 (2013) 220-229.

[18] A. Soffer, D. Rosen, S. Saguee, J. Koresh, Carbon membranes, GB patent 2207666, 1989.

[19] Y.H. Sim, H. Wang, F.Y. Li, M.L. Chua, T.-S. Chung, M. Toriida, S. Tamai, High performance carbon molecular sieve membranes derived from hyperbranched

polyimide precursors for improved gas separation applications, Carbon, 53 (2013) 101-111.

[20] D. Grainger, M.-B. Hägg, Evaluation of cellulose-derived carbon molecular sieve membranes for hydrogen separation from light hydrocarbons, Journal of Membrane Science, 306 (2007) 307-317.

[21] A. Soffer, J. Koresh, S. Saggy, Separation device, US patent 4685940, 1987.

[22] A. Soffer, J. Gilron, S. Saguee, R. Hed-Ofek, H. Cohen, Process for the production of hollow carbon fibers membranes, European patent 0671202, 1995.

[23] A.F. Ismail, D. Rana, T. Matsuura, H.C. Foley, Carbon-based Membranes for Separation Processes, Springer, New York, 2011.

[24] R. Singh, W.J. Koros, Carbon molecular sieve membrane performance tuning by dual temperature secondary oxygen doping (DTSOD), US patent 2014/0000454 A1, 2015.

[25] C.W. Jones, W.J. Koros, Characterization of ultramicroporous carbon membranes with humidified feeds, Industrial & Engineering Chemistry Research, 34 (1995) 158-163.

[26] S. Lagorsse, F.D. Magalhães, A. Mendes, Aging study of carbon molecular sieve membranes, Journal of Membrane Science, 310 (2008) 494-502.

[27] W.J. Koros, C.W. Jones, Composite carbon fluid separation membranes, US patent 5288304, 1994.

[28] M.M. Dubinin, V.V. Serpinsky, Isotherm equation for water vapor adsorption by microporous carbonaceous adsorbents, Carbon, 19 (1981) 402-403.

[29] O. Talu, F. Meunier, Adsorption of associating molecules in micropores and application to water on carbon, AIChE Journal, 42 (1996) 809-819.

[30] S. Lagorsse, M.C. Campo, F.D. Magalhães, A. Mendes, Water adsorption on carbon molecular sieve membranes: Experimental data and isotherm model, Carbon, 43 (2005) 2769-2779.

[31] D.D. Do, H.D. Do, A model for water adsorption in activated carbon, Carbon, 38 (2000) 767-773.

[32] L.R. Radovic, Surface Chemistry of Activated Carbon Materials: State of the Art and Implications for Adsorption, in: J.A. Schwarz, C.C. I. (Eds.) Surfaces of Nanoparticles and Porous Materials, Marcel Dekker, New York, 1999.

[33] I. Menendez, A.B. Fuertes, Aging of carbon membranes under different environments, Carbon, 39 (2001) 733-740.

[34] M.C. Campo, F.D. Magalhães, A. Mendes, Carbon molecular sieve membranes from cellophane paper, Journal of Membrane Science, 350 (2010) 180-188.

[35] J. Koresh, A. Soffer, Study of molecular sieve carbons. Part 1.Pore structure, gradual pore opening and mechanism of molecular sieving, Journal of the Chemical Society, Faraday Transactions 1, 76 (1980) 2457-2471.

[36] X. Ma, B.K. Lin, X. Wei, J. Kniep, Y.S. Lin, Gamma-alumina supported carbon molecular sieve membrane for propylene/propane separation, Industrial & Engineering Chemistry Research, 52 (2013) 4297-4305.

[37] K.-i. Okamoto, S. Kawamura, M. Yoshino, H. Kita, Y. Hirayama, N. Tanihara, Y. Kusuki, Olefin/paraffin separation through carbonized membranes derived from an asymmetric polyimide hollow fiber membrane, Industrial & Engineering Chemistry Research, 38 (1999) 4424-4432.

[38] M. Teixeira, M.C. Campo, D.A.P. Tanaka, M.A.L. Tanco, C. Magen, A. Mendes, Composite phenolic resin-based carbon molecular sieve membranes for gas separation, Carbon, 49 (2011) 4348-4358.

[39] C. Nguyen, D.D. Do, Adsorption of supercritical gases in porous media: determination of micropore size distribution, The Journal of Physical Chemistry B, 103 (1999) 6900-6908.

[40] C. Nguyen, D.D. Do, K. Haraya, K. Wang, The structural characterization of carbon molecular sieve membrane (CMSM) via gas adsorption, Journal of Membrane Science, 220 (2003) 177-182.

Chapter 3.B – Supplementary Information

Carbon membranes with extremely high separation performance and stability[1]

S.1. Materials and methods

S.1.1. Preparation of carbon molecular sieve *membranes*

Transparent commercial cellophane paper (Sadipal Stationery Papers) was used as precursor film. Before carbonization, the precursor film was cut in disks with 48 mm diameter. The carbonization of the cellophane disks was accomplished in a quartz tube (80 mm in diameter and 1.5 m in length) inside a tubular horizontal Termolab TH furnace. To guarantee temperature homogeneity along the quartz tube, the furnace has three separating heating elements controlled by a Eurotherm PID temperature controller. The carbonization was performed under N_2 atmosphere with a flow rate of 170 ml·min^{-1}. The temperature history to prepare carbon molecular sieve membranes (CMSM) from cellophane precursor involved essentially slow heating rates with several dwells of 30 min to avoid a quick release of residual solvents and volatile matter that could damage the carbon matrix, causing cracks/defects, as described elsewhere [1]. The end temperature varied between 400 °C and 600 °C. After the end temperature was reached, the system was allowed to cool naturally until room temperature and the carbon membranes were removed from the tubular furnace.

[1] S.C. Rodrigues, M. Andrade, J. Moffat, F.D. Magalhães, A. Mendes, Carbon membranes with extremely high separation performance and stability, submitted, (2017).

S.1.2. Monocomponent permeation experiments

Prior to permeation experiments, CMSM were glued to steel O-rings. Epoxy glue (Araldite® Standard) was also applied along the interface of the steel O-ring and the carbon membrane, as described elsewhere [1]. A sintered metal disc covered with a filter paper was used as support for the film in the test cell. Single gases were tested at 25 °C, where the feed pressure was 1 bar and the permeate pressure was *ca*. 0.03 bar. The tests were performed in a standard pressure-rise setup with LabVIEW® data logging. The system included the membrane module connected to a vessel with a calibrated volume at the permeate side and connected also to a gas cylinder at the feed side. The feed gas could either be used dry or passed through a bubbler with distilled water prior to the membrane module (Figure S.7). The relative humidity was checked with a RH meter (Vaisala DMP74b) at an exit port. Oxygen, nitrogen, helium, hydrogen and carbon dioxide used in the present work were from Air Liquide (99.999 % pure). Propane and propene were from Praxair (99.5 % pure) and methane was from Linde (99.995 % pure).

The permeability of the CMSM towards a pure component *i*, P_i, was determined as described by the following equation:

$$P_i = \frac{F_i}{\Delta P_i / \delta} \tag{3.1}$$

where F_i is the flux of the species *i*, ΔP_i is the partial pressure difference of species *i* between the two sides of the membrane and δ is the membrane thickness (determined by scanning electron microscopy). The membrane permeability to pure component *i* was computed from the experimental data as follows:

$$P_i = \frac{\delta V_p v_M \Delta P_p}{RT t A (P_f - P_p)} \tag{3.2}$$

where V_p is the volume of the permeate tank, v_M is the molar volume of the gas at normal conditions, R is the gas constant, T is the absolute temperature, t is the time

to a certain increment in the permeate pressure ΔP_p, A is the effective area of the flat carbon membrane and P_f and P_p are the feed and permeate pressure, respectively. The permeability is expressed in barrer where 1 barrer = 3.39×10^{-16} mol·m·m^{-2}·s^{-1}·Pa^{-1}.

The ratio of two gases permeability is termed ideal permselectivity (often designated as ideal selectivity):

$$\alpha_{i,j} = \frac{P_i}{P_j} \tag{3.3}$$

S.1.3. Bicomponent permeation experiments

Analysis of separation of gas mixtures (50 % O_2/ 50 % N_2) was carried out at 25 °C for CMSM prepared at 550 °C. Briefly, the gas mixture at a pressure of 1 bar was introduced into the retentate side of the permeation cell. Argon was used as carrier gas and flowed through the permeate side (Pressure: 1 bar). The gas concentration in the permeate side was measured with a mass spectrometer (Pfeiffr, Omnistar) (Figure S.7).

S.1.4. Water vapor adsorption/desorption equilibrium isotherms

The adsorption and desorption equilibrium isotherms of water vapor were obtained by the gravimetric method using a suspension magnetic balance from Rubotherm® (±10^{-5} g precision) at 25 °C. The sample was fragmented into flakes and placed in the weighting basket. The system (illustrated in Figure S.8) basically consists on the magnetic suspension balance, 2 pressure sensors (Druck, range 0-7 bar and 0-350 mbar, 0.1 % FS), a vacuum pump (Edwards, RV5) and a thermostatic bath (Huber, CC1) for circulating the liquid at the desired temperature.

A temperature-controlled tank containing liquid water was used to fill the 5 L jacketed tank with water vapor at the desired pressure (Figure S.8). The tank containing liquid water was previously connected to the vacuum pump for dissolved gases removal and for removing the head gas volume.

S.1.5. Contact angle measurements

Contact angles were measured using the sessile drop method (DataPhysics OCA-Series) where water, ethylene glycol (Sigma-Aldrich, 99.8 %) and *n*-hexadecane (Sigma-Aldrich, ≥ 99 %) were employed as probing liquids. A needle connected to a micro syringe was used to place the liquid drops on the surfaces. For each drop 150 points were collected.

S.1.6. Pore size distribution (PSD)

The PSD of the produced CMSM were obtained based on the adsorption equilibrium isotherm of CO_2 at 0 °C determined in a fully automated 3-station instrument (Micromeritics). A bath within ± 0.1 °C was used for temperature control.

S.1.7. High-resolution transmission electron microscopy (HRTEM)

HRTEM was performed on the produced CMSM and CMS adsorbent in a FEI Titan Cubed microscope operated at 300 kV. This instrument was equipped with an image aberration corrector that provides 80 pm resolution.

S.1.8. Scanning electron microscopy (SEM)

Micrographs of the produced CMSM have been taken by SEM. A FEI Quanta 400FEG/EDAX Genesis X4M with 1.2 nm resolution was used.

S.1.9. Thermogravimetric analysis (TG)

Thermogravimetric analysis was used to assess the thermal decomposition kinetics and stability of precursor in inert atmosphere. TG was carried out in a Netzsch TG 209 F1 Iris thermogravimetric balance with a resolution of 0.1 µm. The amount of sample provided for the analysis was about 5 mg. The heating protocol to determine the characteristic curve [3] consisted on a first rise of the temperature from room

temperature to 110 °C at 25 °C·min^{-1} under nitrogen atmosphere, with two dwells at 50 °C (for 10 min) and 110 °C (for 7 min); subsequently, temperature was raised from 110 °C to 950 °C with a dwell at 950 °C (for 9 min) and finally the sample was kept at 950 °C for more 11 min under oxygen atmosphere.

S.1.10. Fourier transform infrared spectroscopy (FTIR)

The chemical structure of the samples was investigated by Fourier transform infrared spectroscopy. FTIR spectra of the cellulosic precursor and the different CMSM were measured on a Perkin Elmer Spectrum 100 spectrometer with universal attenuated total Reflectance (ATR). A total of 16 cumulative scans were taken with a resolution of 4 cm^{-1} in the frequency range 4000-650 cm^{-1}, in transmission mode.

S.1.11. X-ray photoelectron spectroscopy (XPS)

Surface chemical characterization of the membranes was carried out by X-ray photoelectron spectroscopy. XPS spectra were obtained using a Kratos Axis Ultra HSA spectrometer with a monochromatic Al kα ray source (1486.7 eV) operating at 15kV (90 W) and with VISION software for data acquisition and CASAXPS software for data analysis. Data acquisition was performed with a pressure lower than 10×10^{-6} Pa using a charge neutralization system. Survey spectra in the range 0-1300 eV were recorded at 80 eV of pass energy. High resolution spectra were recorded in FAT (Fixed Analyzer Transmission) mode with a pass energy of 40 eV. The binding energy scale was corrected by referring to the polyaromatic peak in the C1s spectrum as being 285 eV.

S.2. Supplementary text

S.2.1 Contact angle measurements

The evaluation of the surface energy (γ_s) of the CMSM and corresponding polar (γ_s^p) and dispersive (γ_s^d) components were carried out using the Owens-Wendt-Rable-Kaeble (OWRK) model [2]:

$$\gamma_s = \gamma_s^{\ d} + \gamma_s^{\ p} \tag{3.4}$$

$$\frac{1+\cos\theta}{2}\frac{\gamma_1}{\sqrt{\gamma_1^{\ d}}} = \sqrt{\gamma_s^p}\sqrt{\frac{\gamma_1^p}{\gamma_1^d}} + \sqrt{\gamma_s^d} \tag{3.5}$$

where γ_1, $\gamma_1^{\ p}$ and $\gamma_1^{\ d}$ are the superficial tension of the liquid and the corresponding polar and dispersive components, respectively. Table S.6 shows the surface energy, polar and dispersive component values of the liquid probes. Free surface energy and its components are important parameters for characterizing the surface properties of solids. According to Equation (3.4), the dispersive component of surface energy refers to London dispersion forces and the polar component refers mainly to hydrogen bonding. Table S.7 shows the obtained surface energy and the correspondent polar and dispersive components for each CMSM sample. It is observed that the free surface energy increases with the carbonization end temperature, peaking for sample CMSM 550; for sample CMSM 600 a decrease on free surface energy is observed. As expected, with the carbonization end temperature increase the polar component contribution for the total surface energy becomes higher when compared to the dispersive component. This happens due to the increase of polar interactions (hydrogen bonding) between water and carbon membrane surface as the carbonization end temperature increases.

S.2.2 Pore size distribution

The adsorption of nitrogen at -196 °C is the most frequently used technique to assess the microporosity of carbonaceous materials. However, when ultramicroporosity is involved some diffusional limitations occur and adsorption of carbon dioxide at 0 °C is a good alternative to overcome this challenge. Carbon dioxide was used as a probe molecule due to its small size and ability to highly adsorb in porous carbons. The adsorption equilibrium isotherms of CO_2 at 0 °C for CMSM 550 and CMSM 600 samples are plotted in Figure S.9.

Dubinin-Raduschkevisch (DR) equation is commonly used to describe the adsorption in micropores:

$$\frac{W}{W_0} = \exp\left[-\left(\frac{RT\ln\frac{P_0}{P}}{E_0}\right)^2\right] \tag{3.6}$$

where W is the micropore volume, P is the pressure, W_0 is the total micropore volume, E_0 is the characteristic energy for adsorption , P_0 is the vapor pressure of the free liquid, R is the gas constant and T is the absolute temperature. However, the DR equation only provides a reasonable description of adsorption in micropores when the characteristic curve obtained for CO_2 adsorption is linear. For handling non-linear characteristic curves, a more general equation was proposed, the Dubinin-Astakhov (DA) equation:

$$\frac{W}{W_0} = \exp\left[-\left(\frac{RT\ln\frac{P_0}{P}}{E_0}\right)^n\right] \tag{3.7}$$

where n is an adjustable parameter. DR equation results from DA equation for the particular case of n=2.

The characteristic curves obtained from CO_2 adsorption isotherms on CMSM 550 and CMSM 600 samples are not linear, indicating that DR equation is not applicable.

Therefore, micropore volume and the characteristic energy for adsorption were determined fitting the DA equation to the experimental data. A DA equation with *n*=2.4 fitted quite well the experimental data of both samples (Figure S.10): the slope of each plot is related to E_0 and the intercept is related to W_0. Table S.8 summarizes the obtained structural parameters for the studied samples. When the carbonization end temperature increases, the total pore volume increases, followed by a small decrease in average pore width, which is consistent with the work by Rodrigues *et al*. [4]. Therefore, at 600 °C, a more porous structure with a tighter size distribution is achieved which is in agreement with the obtained permeation results.

The skeleton density (obtained by helium picnometry) of the cellophane-based CMSM carbonized at 550 °C and 600 °C was 1.2 g·cm^{-3} and 2.1 g·cm^{-3}, respectively.

The pore size distributions of the two samples were obtained using the method proposed by Nguyen *et al*. [5, 6] for the determination of the micropore size distribution in carbonaceous materials. This method accounts for the enhancement of the potential energy of interaction between an adsorbate molecule and atoms within the pores. The Langmuir isotherm was used to describe the adsorption behavior inside the pores of size *r* while the heterogeneity of the system was assumed to be related to the pore size distribution, given by *f(r)* [5]. For the local Langmuir isotherm, the amount adsorbed in pores of radius *r*, *q(p,r)*, becomes:

$$q(p,r) = q^m(r)\frac{b_{pore}(r)P_{pore}(r)}{1+b_{pore}(r)P_{pore}(r)} \tag{3.8}$$

where q^m is the maximum capacity, P_{pore} is the pressure of the gas confined in the pore and b_{pore} is the adsorption affinity constant that can be calculated as described by Equation (3.9):

$$b_{pore} = b_S \exp\left(\frac{E_{pore} - E_{surface}}{RT}\right) \tag{3.9}$$

where b_s is the affinity factor related to adsorption in a flat surface, $E_{surface}$ is the potential energy when a molecule is adsorbed on a flat surface and E_{pore} is the potential

energy when a molecule is adsorbed inside a pore. A slit-like pore configuration was assumed. In a pore system some molecules are adsorbed on the surface and others remain in the gas phase within the pore (referred to as confined gas molecules). Therefore, P_{pore} is related to the bulk pressure and to the potential energy of molecules confined in the pore (E^{g}_{pore}):

$$P_{pore} = P_{bulk} \exp\left(\frac{-E^{g}_{pore}}{RT}\right) \tag{3.10}$$

The interaction potential energy between a molecule and the graphitic flat surface was calculated by the 10-4-3 Steele potential:

$$H(z) = 2\pi\rho_s\varepsilon_{sf}\sigma_{sf}^2\Delta\left[\frac{2}{5}\left(\frac{\sigma_{sf}}{z}\right)^{10} - \left(\frac{\sigma_{sf}}{z}\right)^{4} - \frac{\sigma_{sf}^4}{3\Delta(0.61\Delta + z)^3}\right] \tag{3.11}$$

where ρ_s is the density of carbon atoms in graphite, z is the distance between the center of the probe molecule and the center of a carbon atom in the pore wall, σ_{sf} and ε_{sf} are the solid-fluid interaction parameters estimated by the Lorentz-Berthelot mixture rules and Δ is the distance between the graphene layers. The micropore potential energy was then the addition of the contributions of both walls.

Assuming that *q(p,r)* is the isotherm equation for a pore of size *r*, the adsorbed concentration at pressure *P*, expressed as *q*(P), is the integral over all pore sizes of the adsorbed concentration for each pore size:

$$q(\mathrm{P}) = \int_0^{+\infty} \mathrm{q}(\mathrm{p}, r) f(r)\, dr \tag{3.12}$$

Substituting equation (3.8) in equation (3.12):

$$q(\mathrm{P}) = \int_0^{+\infty} q^{m}(r) \frac{b_{pore}(r)\mathrm{P}_{pore}(r)}{1 + b_{pore}(r)\mathrm{P}_{pore}(r)} f(r)\, dr \tag{3.13}$$

Minimizing the square of the difference between the CO_2 adsorption concentration at 0 °C as a function of the pressure between the experimental and the

model – equations (3.8), (3.10) and (3.13) – one obtains the pore size distributions. More details about this method can be found elsewhere [5, 6]. The resulting pore size distributions for CMSM 550 and CMSM 600 samples are plotted in Figure S.6.

S.3. Supplementary figures

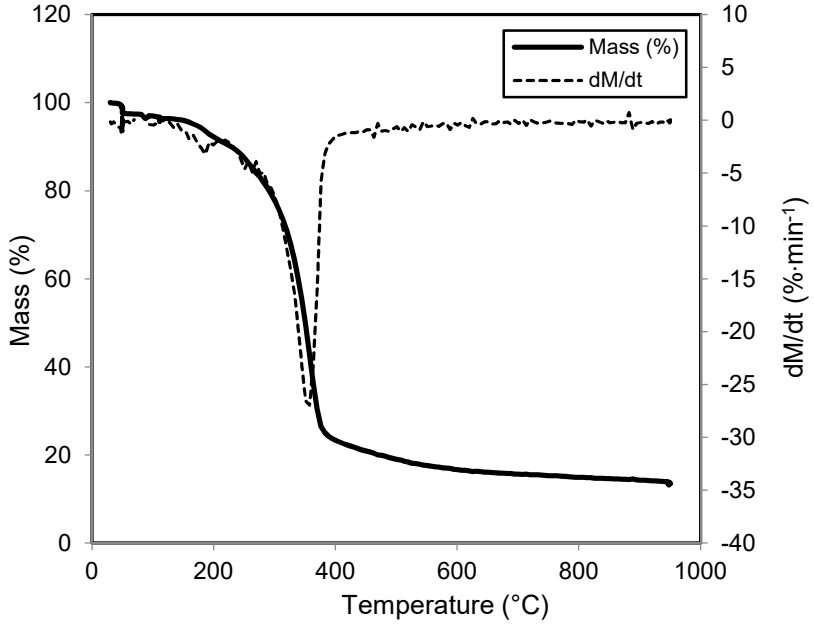

Figure S.1. Thermogravimetric analysis of the cellophane precursor.

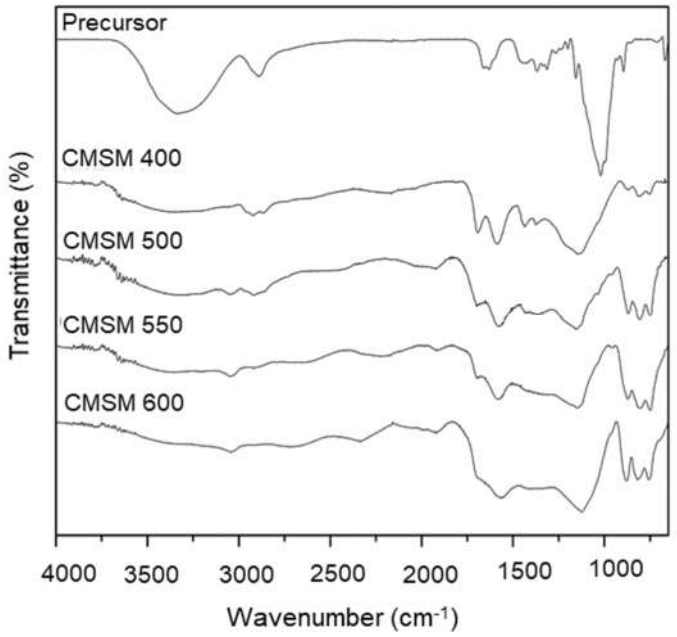

Figure S.2. FTIR spectra of the precursor and CMSM prepared at 400 °C, 500 °C, 550 °C and 600 °C.

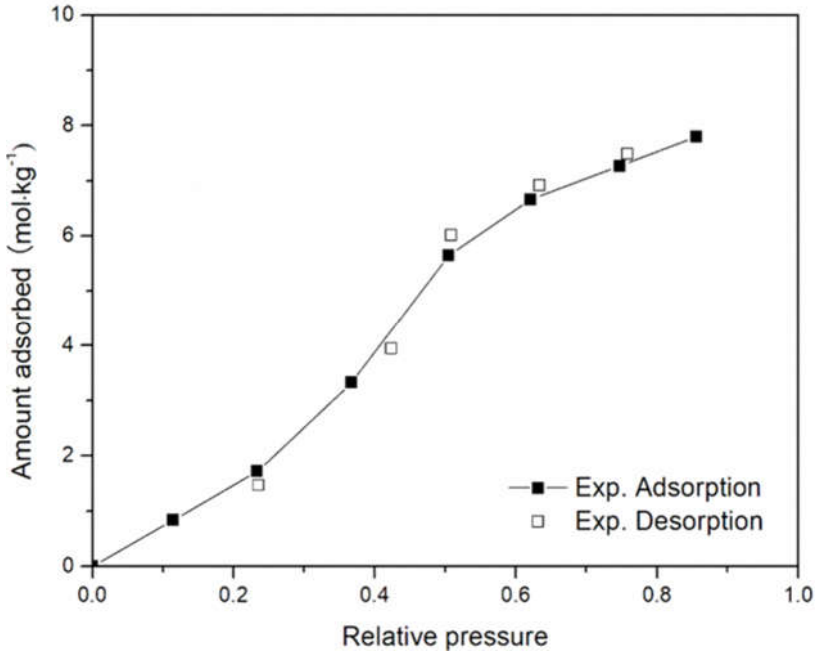

Figure S.3. Water vapor adsorption/desorption equilibrium isotherms on CMSM carbonized at 900 °C.

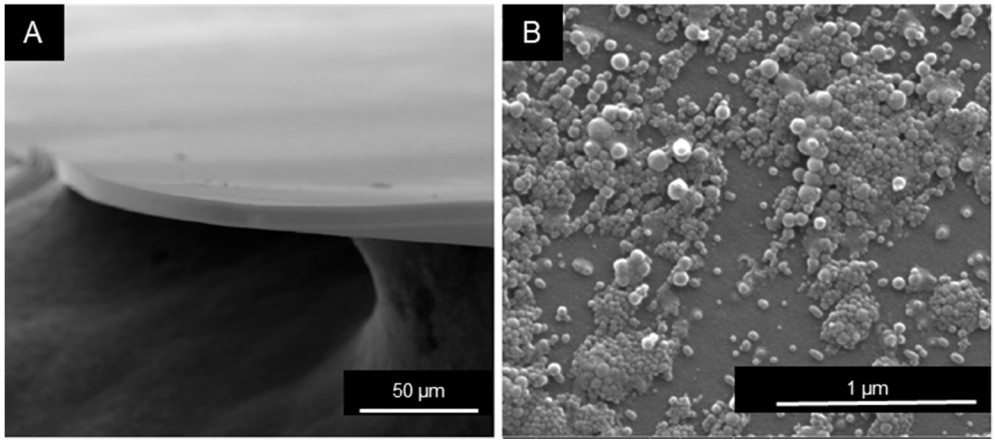

Figure S.4. Scanning electron micrographs of a cellophane based-CMSM: **(A)** cross-section (×1200 magnification), **(B)** surface view (×100 000 magnification). Carbonization end temperature: 550 °C.

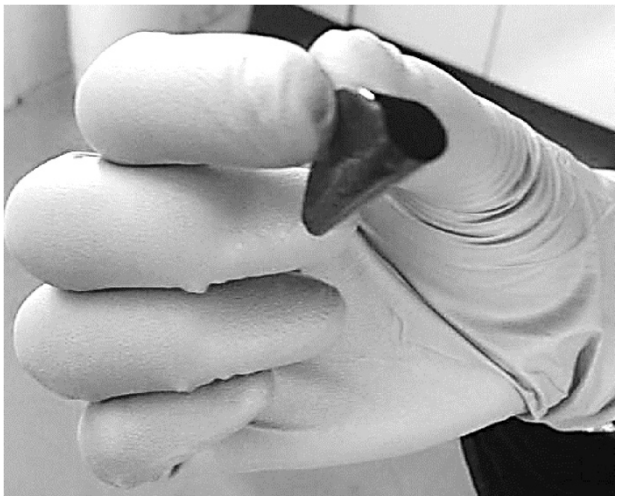

Figure S.5. Illustrative figure of the flexibility of the prepared carbon membranes; sample CMSM 550.

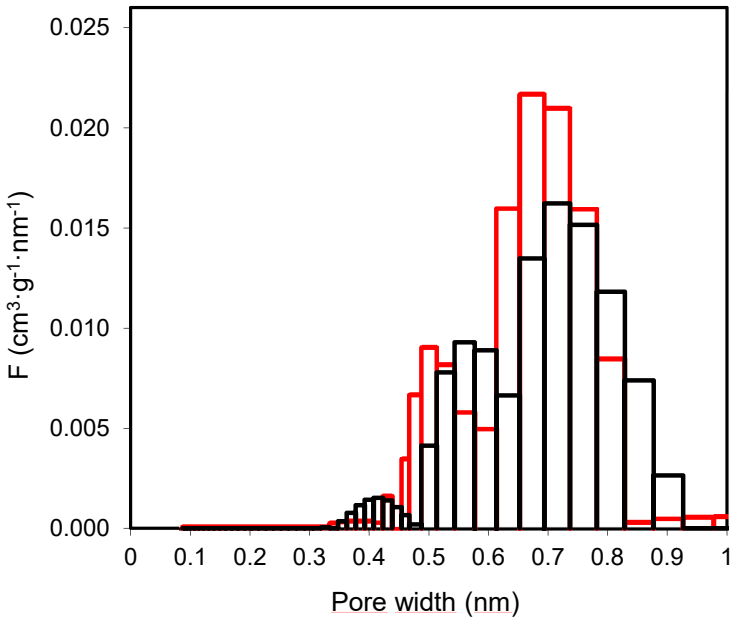

Figure S.6. Pore size distribution for CMSM 550 (black line) and CMSM 600 (red line).

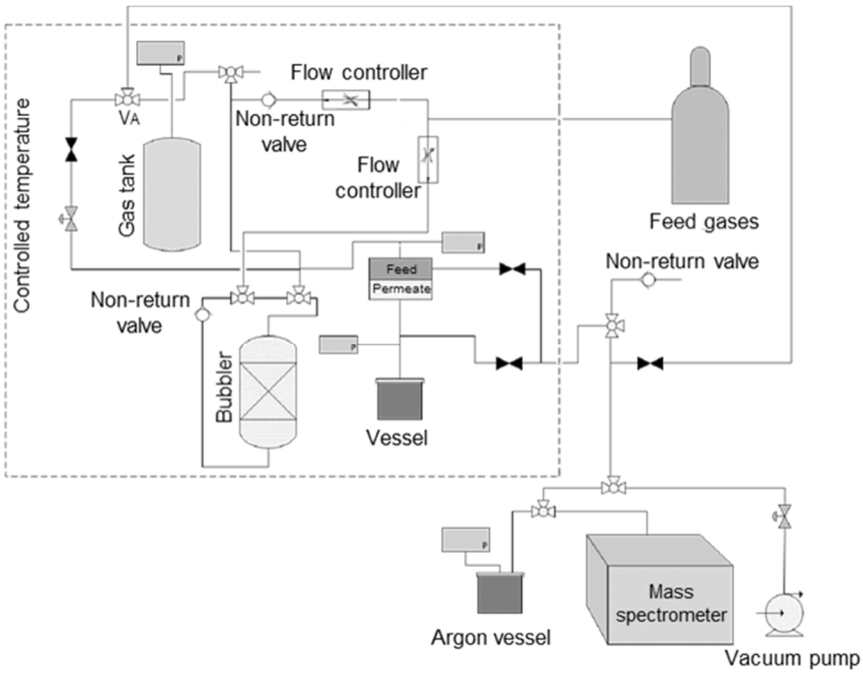

Figure S.7. Scheme of the experimental setup for measuring permeabilities in the presence and in the absence of controlled relative humidity.

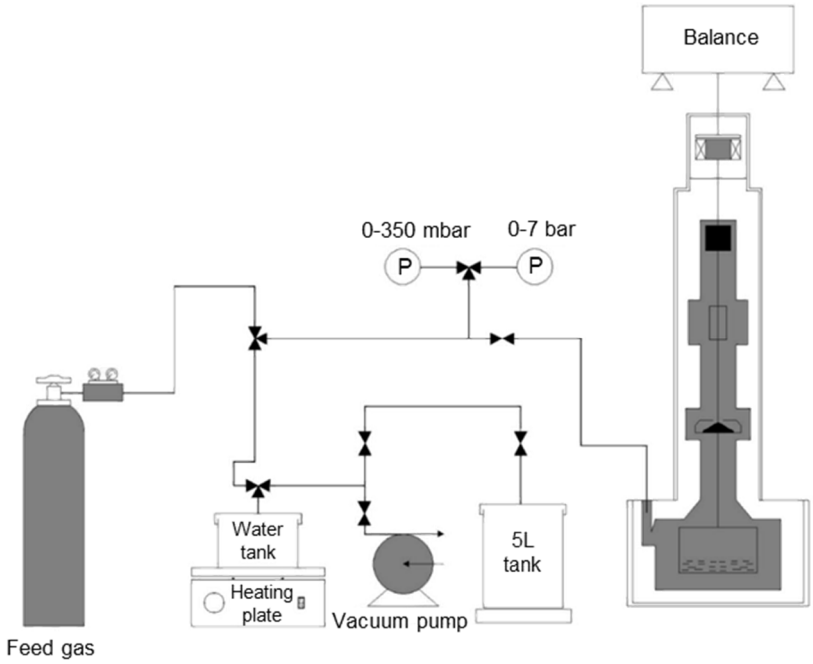

Figure S.8. Scheme of the gravimetric apparatus.

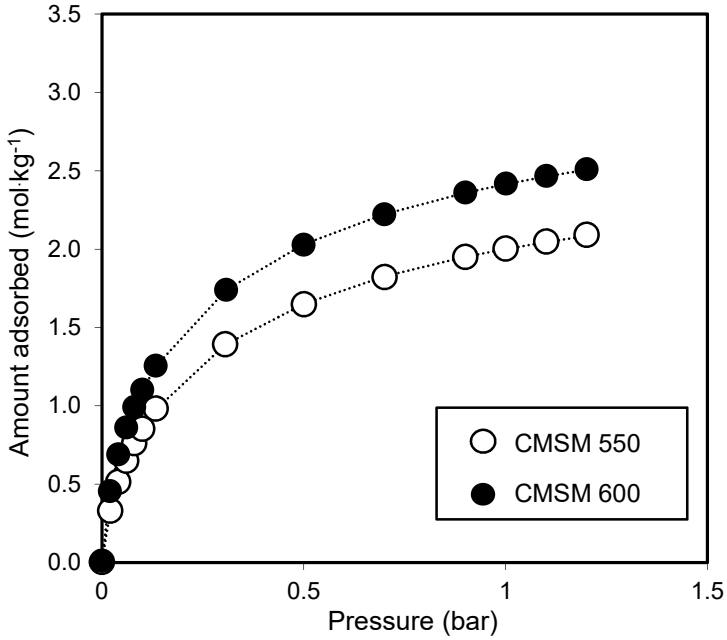

Figure S.9. Adsorption equilibrium isotherm of CO_2 at 0 °C for CMSM 550 and CMSM 600 samples.

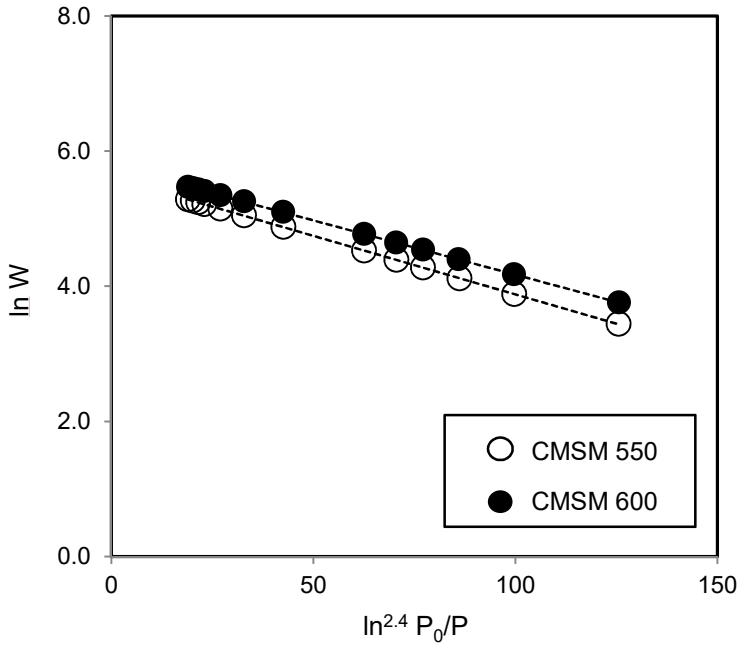

Figure S.10. CO_2 characteristic curve for CMSM 550 and CMSM 600 samples. The dashed lines represent the DA fitting.

S.4. Supplementary tables

Table S.1. C_3H_6/C_3H_8 and O_2/N_2 ideal selectivities obtained for CMSM and CMS adsorbent prepared in this work and a brief comparison with other carbon materials reported in literature.

Sample ID	C_3H_6/C_3H_8 ideal selectivity	O_2/N_2 ideal selectivity	Ref.
CMSM 550	1.6	19.0	This work
CMSM 600	2.6	>800	This work
CMS	84.3	13.2	This work
Carbon membrane	13.4	3.3	[7]
Carbon membrane	14.6	5.4	[8]
Carbon membrane	36.0	5.1	[9]
Carbon membrane	37.8	5.8	[10]

Table S.2. Atomic concentration of the elements present on the surface of the cellophane precursor and derived CMSM.

Membrane	%C	%O	%Na	%Si	%N	%S
Precursor	50.44	43.45	0.34	5.29	0.41	0.07
CMSM 400	65.31	24.89	1.01	8.23	0.40	0.17
CMSM 500	68.01	21.53	3.54	6.37	0.30	0.25
CMSM 550	68.28	20.32	7.94	3.23	0.11	0.12
CMSM 600	61.53	24.46	10.29	3.60	0.05	0.08

Table S.3. Measured contact angles for the produced cellophane-based CMSM samples.

Sample	Measured Contact Angles (°)		
	Water	Ethylene glycol	n-Hexadecane
CMSM 400	58 ± 2	29 ± 6	0 ± 0
CMSM 500	32 ± 5	25 ± 3	0 ± 0
CMSM 550	18 ± 1	14 ± 3	0 ± 0
CMSM 600	20 ± 1	14 ± 3	0 ± 0

Table S.4. O_2 and N_2 permeabilities and O_2/N_2 ideal selectivity of CMSM 550 and CMSM 600 after air exposure for different time periods.

Sample	Exposure time (days)	O_2 permeability (barrer)	N_2 permeability (barrer)	O_2/N_2 ideal selectivity
CMSM 550	2	2.20	0.12	18.5
	4	1.33	0.07	19.0
	5	0.74	n.d*	-
CMSM 600	2	1.15	n.d*	-
	4	0.78	<0.001	>800
	7	0.36	<0.001	>360

*n.d = not determined

Table S.5. O_2 and N_2 permeabilities and O_2/N_2 ideal selectivity of CMSM after storage in a propylene atmosphere.

Sample	Exposure time to air (days)	O_2 permeability (barrer)	N_2 permeability (barrer)	O_2/N_2 ideal selectivity
Control - CMSM 550	0	2.70	0.32	8.4
	2	2.20	0.12	18.5
	4	1.33	0.07	19.0
CMSM 550 in propylene	0	2.75	0.34	8.1
	1	2.75	n.d*	-
	3	2.69	n.d*	-

*n.d = not determined

Table S.6. Surface energy, polar and dispersive component values of the used probe liquids [11].

Liquid	Surface Energy ($mJ \cdot m^{-2}$)	Polar component ($mJ \cdot m^{-2}$)	Dispersive component ($mJ \cdot m^{-2}$)
Water	72.8	50.2	22.6
Ethylene glycol	48.8	16.0	32.8
n-Hexadecane	27.5	0.0	27.5

Table S.7. Obtained free surface energy and correspondent polar and dispersive component for the produced cellophane-based CMSM.

Sample	Surface Energy ($mJ \cdot m^{-2}$)	Polar component ($mJ \cdot m^{-2}$)	Dispersive component ($mJ \cdot m^{-2}$)
CMSM 400	45.66	19.26	26.40
CMSM 500	58.91	35.96	22.95
CMSM 550	65.50	42.95	22.56
CMSM 600	65.06	41.90	23.16

Table S.8. Structural parameters for CMSM carbonized at 550 °C and 600 °C.

Sample	W_0 ($cm^3 \cdot kg^{-1}$)	E_0 ($kJ \cdot mol^{-1}$)	l (nm)
CMSM 550	274.2	12.3	0.667
CMSM 600	322.5	12.7	0.635

S.5. References

[1] M.C. Campo, F.D. Magalhães, A. Mendes, Carbon molecular sieve membranes from cellophane paper, Journal of Membrane Science, 350 (2010) 180-188.

[2] D.K. Owens, R.C. Wendt, Estimation of the surface free energy of polymers, Journal of Applied Polymer Science, 13 (1969) 1741-1747.

[3] M. Ottaway, Use of thermogravimetry for proximate analysis of coals and cokes, Fuel, 61 (1982) 713-716.

[4] S.C. Rodrigues, R. Whitley, A. Mendes, Preparation and characterization of carbon molecular sieve membranes based on resorcinol–formaldehyde resin, Journal of Membrane Science, 459 (2014) 207-216.

[5] C. Nguyen, D.D. Do, Adsorption of supercritical gases in porous media: determination of micropore size distribution, The Journal of Physical Chemistry B, 103 (1999) 6900-6908.

[6] C. Nguyen, D.D. Do, K. Haraya, K. Wang, The structural characterization of carbon molecular sieve membrane (CMSM) via gas adsorption, Journal of Membrane Science, 220 (2003) 177-182.

[7] K.-i. Okamoto, S. Kawamura, M. Yoshino, H. Kita, Y. Hirayama, N. Tanihara, Y. Kusuki, Olefin/paraffin separation through carbonized membranes derived from an asymmetric polyimide hollow fiber membrane, Industrial & Engineering Chemistry Research, 38 (1999) 4424-4432.

[8] M. Teixeira, M.C. Campo, D.A.P. Tanaka, M.A.L. Tanco, C. Magen, A. Mendes, Composite phenolic resin-based carbon molecular sieve membranes for gas separation, Carbon, 49 (2011) 4348-4358.

[9] X. Ma, B.K. Lin, X. Wei, J. Kniep, Y.S. Lin, Gamma-alumina supported carbon molecular sieve membrane for propylene/propane separation, Industrial & Engineering Chemistry Research, 52 (2013) 4297-4305.

[10] M. Teixeira, M. Campo, D.A. Tanaka, M.A. Tanco, C. Magen, A. Mendes, Carbon-Al_2O_3–Ag composite molecular sieve membranes for gas separation, Chemical Engineering Research and Design, 90 (2012) 2338-2345.

[11] S. Wu, Polymer interface and adhesion, Marcel Dekker, New York, 1982.

Chapter IV

Chapter 4 – Preparation of carbon molecular sieve membranes from an optimized ionic liquid-regenerated cellulose precursor[1]

4.1. Abstract

Novel carbon molecular sieve membranes with high separation performance and stability in the presence of humidified streams were prepared from an optimized ionic liquid-regenerated cellulose precursor, in a single carbonization step. Membranes prepared at two different carbonization end temperatures (550 °C and 600 °C) were analyzed through scanning electron microscopy, thermogravimetric analysis, Fourier transform infrared spectroscopy, CO_2 adsorption and permeation experiments. The prepared membranes exhibited uniform thickness of approximately 20 μm and a well-developed microporous structure. The permeation performance of these carbon molecular sieve membranes was above the Robeson upper bound curve for polymeric membranes. In particular, the membrane prepared at 550 °C end temperature exhibited a permeability to O_2 of 5.16 barrer and O_2/N_2 ideal selectivity of 32.3 and a permeability to He of 126.36 barrer and He/N_2 ideal selectivity of 789.8; besides, permeation experiments performed in the presence of *ca.* 80 % relative humidity showed that humidity does not affect the membrane's ability to permeate and separate the tested permanent gases. These results open the door for the preparation of tailor made precursors that originate carbon molecular sieve membranes with extraordinary separation performances, mechanical resistance and stability.

[1] S.C. Rodrigues, M. Andrade, J. Moffat, F.D. Magalhães, A. Mendes, Preparation of carbon molecular sieve membranes from an optimized ionic liquid-regenerated cellulose precursor, submitted, (2017).

4.2. Introduction

Over the past few decades, membrane processes for gas separation have improved considerably. Compared to conventional separation techniques, membrane-based gas separation is more attractive because of its high adaptability, high reliability, low energy consumption and low capital cost, operation and maintenance, which makes it a more energy-saving and environmental friendly technology [1-4]. Moreover, carbon molecular sieve membranes (CMSM) have been considered promising candidates for gas separation due to their high corrosion resistance, high thermal stability and excellent permeabilities/permselectivities when compared to polymeric membranes [5-7]. CMSM are prepared from the carbonization of a polymeric precursor under controlled conditions (atmosphere and temperature history). After the carbonization step, CMSM display a highly aromatic structure comprising disordered sp^2 hybridized carbon sheets packed imperfectly. Pores are formed from packing imperfections between microcrystalline regions in the material [8]; the CMSM structure is turbostratic and described as “slit-like” with a bimodal pore size distribution with micropores connecting ultramicropores [8, 9]. Micropores provide sorption sites while ultramicropores (called constrictions) enable molecular sieving, making CMSM both highly permeable and highly selective - a distinct characteristic of these materials [10-12]. Despite all attractive characteristics displayed by CMSM, they display significant challenges related to their stability when exposed to specific environments [13-15]. In the presence of humidity, water initially adsorbs onto CMSM hydrophilic functional groups and once the first water molecule is adsorbed, adsorbate-adsorbate interactions promote the adsorption of further molecules through hydrogen bonding, originating clusters of several water molecules. The resulting cluster has enough dispersion energy to be released from the hydrophilic group, rolling up until blocking a constriction of the pore network [15]. Consequently, the membrane permeability decreases abruptly, making the carbon membrane useless; this aging effect has seriously limited the commercialization of CMSM.

Up to now, many polymeric precursors have been extensively studied to obtain CMSM with excellent separation performances and stability. These precursors include polyimides [16-20], polyacrylonitrile [21], poly(furfuryl alcohol) [22, 23], phenolic resins [24-28], resorcinol-formaldehyde resin [29-32] and cellulose [16, 33-35]. Recently, our group patented a process for obtaining, in a single carbonization step, CMSM that display no pore blockage effect in the presence of water vapor and display very high ideal permselectivities for several relevant industrial gas mixtures [36]; these novel carbon molecular sieve membranes were prepared from a commercial cellophane precursor – regenerated cellulose produced by the viscose process. Nevertheless, the obtained CMSM displayed low permeabilities to permanent gases and it was not possible to prepare a tailor made precursor.

Cellulose makes an excellent precursor material for the preparation of CMSM due to its considerable carbon yield, biodegradability, hidrophilicity and low-cost [37-39]. The chemical structure of cellulose consists in anhydroglucose linearly linked by (1,4)-β-D-glucosidic bounds, and the number of molecular glucose units defines its degree of polymerization [37, 40]. However, the strong inter and intra hydrogen bonds between cellulose macromolecular chains make it difficult to be dissolved in general solvents [39, 41]. The viscose technology uses a metastable solution of cellulose xanthogenate with hazardous byproducts like heavy metals and hydrogen sulfide [42-44]; moreover, it generates two kilograms of waste per kilogram of cellulose obtained [45, 46]. Other conventional cellulose solvent systems have numerous drawbacks such as limited dissolution capability, toxicity, high cost, uncontrollable side reactions, instability during cellulose processing and/or derivatization [38, 47] and negative environmental impacts [48].

Ionic liquids (IL), a group of salts with poorly coordinated ions and consequently low melting points, represent a promising alternative to existing cellulose-dissolving solvents. IL have been proposed as environmentally “green solvents”; they present a wide range of melting temperature (-40 °C to 400 °C), have low vapor pressure, excellent dissolution ability, high thermal stability (up to 400 °C), chemical stability,

ease of recyclability and are noninflammable [40, 49-51]. IL are made up of separate cationic and anionic species, but unlike common salts, they have a low tendency to crystallize due to their bulky and asymmetrical cation structure [50]; their properties for a specific need can be tuned combining suitable cations and anions [52]. Moreover, ionic liquids give the opportunity to produce tailor made regenerated cellulose precursor films that allow the preparation of carbon membranes with a high separation performance, mechanical resistance and stability.

In this work, we report the preparation and characterization of regenerated cellulose-based CMSM using an ionic liquid (1-ethyl-3-methyl imidazolium acetate) to dissolve cellulose and a spin coating method to cast the precursor membrane. Ionic liquid 1-ethyl-3-methyl imidazolium acetate (EMIMAc) is liquid at room temperature, has high dissolving power even in the presence of 10 wt. % of water, relatively low viscosity when compared to other ionic liquids, low toxicity and high hydrogen bond acceptor abilities. Hydrogen bond acceptor sites in the anion structure and lack of hydrogen bond donors in the ionic liquid cation favor the dissolution of cellulose. The acetate anion in 1-ethyl-3-methyl imidazolium acetate can form hydrogen bonds with hydroxyl protons of cellulose (Figure 4.1).

To the best of the authors' knowledge, this is the first time that regenerated cellulose films produced through an ionic liquid process are studied for preparation of CMSM. Defect-free CMSM were successfully and reproducibly prepared at two different carbonization end temperatures, 550 °C and 600 °C.

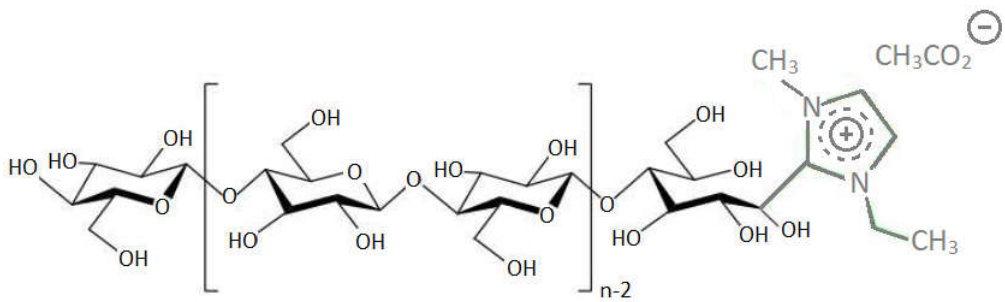

Figure 4.1. Schematic representation of cellulose and 1-ethyl-3-methylimidazolium acetate covalent binding (adapted from [42]).

4.3. Experimental

4.3.1. Materials

Wood pulp (cellulose) was provided by Innovia Films Ltd., displaying a degree of polymerization (DP) of 450. The ionic liquid 1-ethyl-3-methylimidazolium acetate (EMIMAc) and propylene glycol (≥99.5 %), used as plasticizer, were supplied by Sigma-Aldrich. Dimethyl sulfoxide (DMSO) was purchased from Fisher Scientific. The permanent gases were supplied by Air Liquide (99.999 % pure).

4.3.2. Preparation of regenerated cellulose precursor membranes

Wood pulp was dispersed in DMSO and EMIMAc (70:30 wt. % of DMSO:IL) to prepare a 9.2 wt. % cellulose solution. The mixture was heated at 90 °C under magnetic stirring until cellulose was completely dissolved. After dissolution, the resultant brownish solution was filtered with a wire mesh and placed in a vacuum oven at 40 °C for degassing during 2 hours. The obtained homogeneous solution was subsequently spin coated on rectangular glass plates with a spin-coater (POLOS^{TM}, SPIN150i) at a spinning speed of 2000 rpm, spin acceleration of 1000 rpm/s and a spinning time of 10 seconds. After coating, the films were immediately coagulated in distilled water (25 °C) to obtain a transparent regenerated cellulose film. The film was then intensely washed with distilled water for 60 min to remove the excess of ionic liquid. After that, the washed film was dipped in a softener bath containing 5 wt. % of propylene glycol for 1 min and then dried in an oven at 100 °C for 10 min. Figure 4.2 summarizes the preparation steps of the regenerated cellulose precursor membranes.

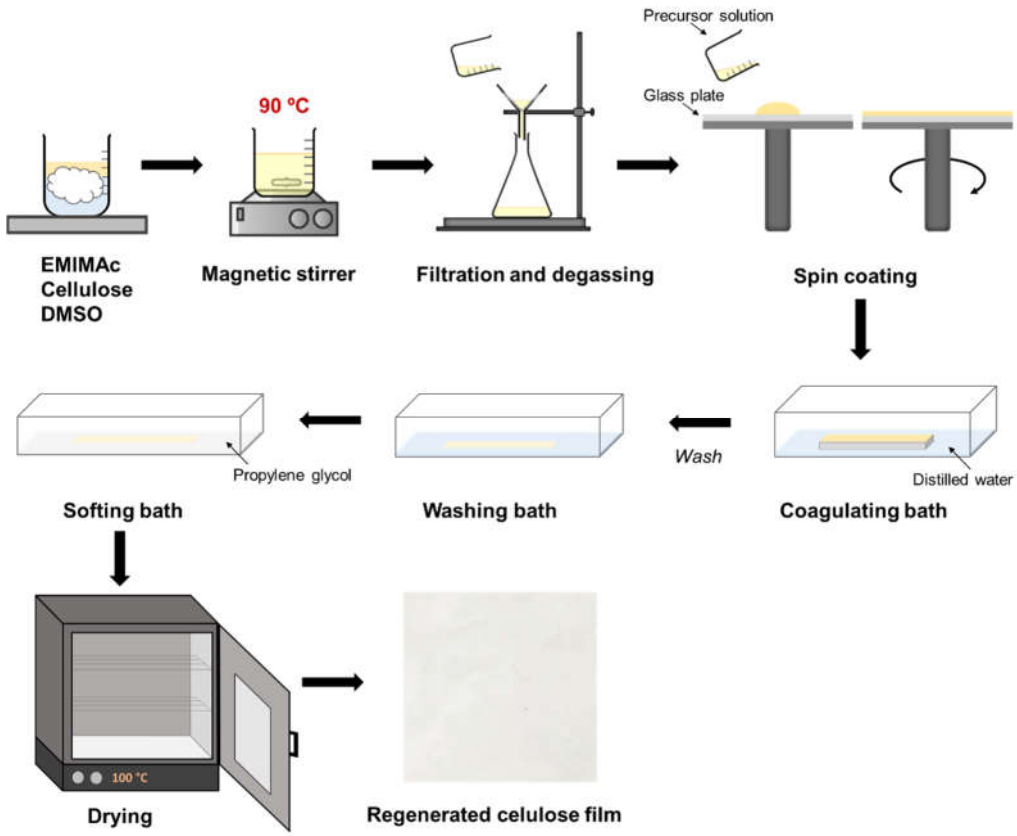

Figure 4.2. Preparation steps of the regenerated cellulose precursor membranes.

4.3.3. Preparation of regenerated cellulose-based carbon molecular sieve membranes

Previous to carbonization, the precursor membranes were cut in disks with 48 mm diameter. The carbonization was then accomplished in a quartz tube (80 mm in diameter and 1.5 m in length) inside a tubular horizontal Termolab TH furnace. To guarantee temperature homogeneity along the quartz tube, the furnace has three separating heating elements controlled by a Eurotherm PID temperature controller. Figure 4.3 gives a schematic overview of the setup for carbonization.

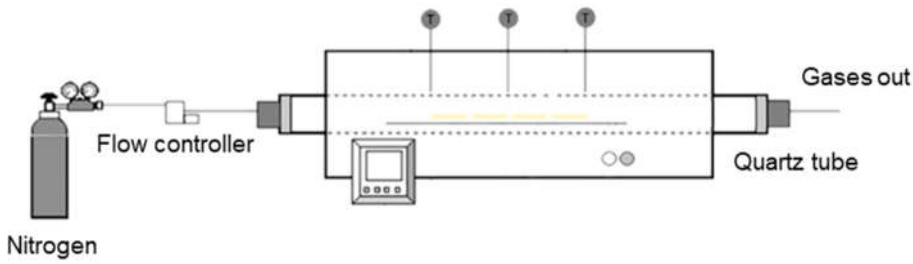

Figure 4.3. Carbonization setup used to prepare the regenerated cellulose-based CMSM.

The carbonization was performed under N_2 atmosphere, with flowrate of 170 ml·min^{-1} and a heating rate of 0.5 °C·min^{-1}. Figure 4.4 shows the heating history used to prepare the carbon molecular sieve membranes from regenerated cellulose films. The temperature history comprehends essentially slow heating rates with several dwells of 30 min to avoid a quick release of residual solvents/volatile matter that could damage the carbon matrix, causing cracks/defects. Two end temperatures were considered, 550 °C (CMSM 550) and 600 °C (CMSM 600); after the end temperature was reached, the system was allowed to cool naturally until room temperature, and the flat carbon membranes were finally removed from the carbonization furnace.

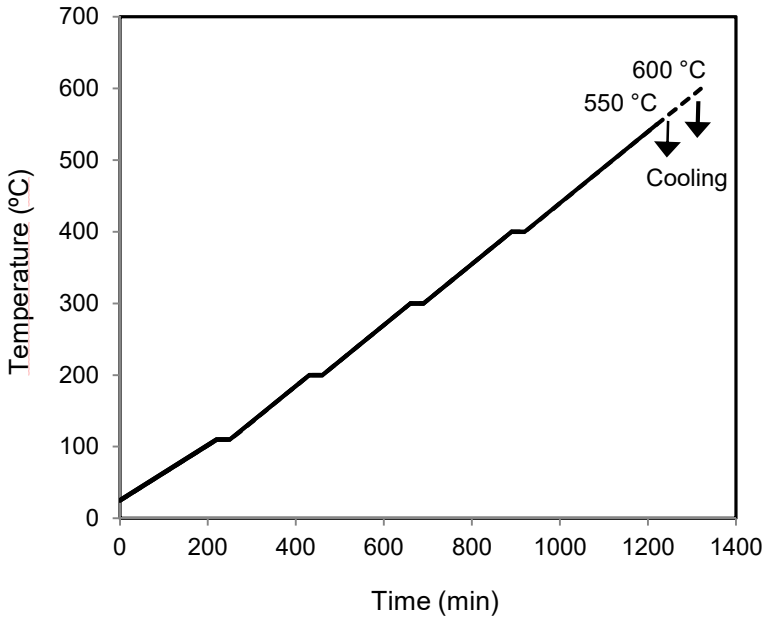

Figure 4.4. Carbonization protocol to prepare the regenerated cellulose-based CMSM.

4.3.4. Scanning electron microscopy

Micrographs of the regenerated cellulose precursor membrane and derived CMSM have been taken by scanning electron microscopy (SEM) using a high resolution scanning electron microscope JEOL JSM 6301F/Oxford INCA Energy 350 with X-ray microanalysis. All the samples were previously sputtered with gold/palladium using a SPI Module Sputter Coater equipment to allow better conductivity for SEM.

4.3.5. Thermogravimetric analysis

Thermogravimetric analysis (TGA) was carried out in a Netzsch TG 209 F1 Iris thermogravimetric balance with a resolution of 0.1 μm. The heating procedure [34] consisted on a first rise of the temperature from room temperature to 110 °C at 10 °C·min^{-1}, under nitrogen atmosphere, with two dwells at 50 °C (for 10 min) and 110 °C (for 7 min); subsequently, temperature rise from 110 °C to 950 °C with a dwell at 950 °C (for 9 min) and finally the sample was kept at 950 °C for more 11 min under oxygen atmosphere. Proximate analysis was performed to determine the percentage of moisture, volatile matter, carbon yield and ashes content of the precursor material [53]. After the first dwell at 110 °C, humidity is removed; up to the second dwell, volatile matter is released, and after the last dwell at 950 °C (under oxygen) all the fixed carbon is burned, leaving only ashes (if present).

4.3.6. Fourier transform infrared spectroscopy

The infrared spectra of the precursor and derived CMSM were recorded using a VERTEX 70 FTIR spectrometer (BRUKER) in transmittance mode with a high sensitivity DLaTGS detector at room temperature. Samples were measured in ATR mode, with a A225/Q platinum ATR diamond crystal with single reflection accessory. The spectra were recorded from 4000 to 500 cm^{-1} with a resolution of 4 cm^{-1}.

4.3.7. Pore size distribution

The pore size distribution (PSD) of the CMSM was obtained based on the adsorption equilibrium isotherm of carbon dioxide at 0 °C obtained by the volumetric method. This method is based on pressure variation of the gas after an expansion; assuming for the system an ideal gas behavior and knowing the pressure decrease, the concentration of the adsorbed solute can be determined [54, 55]. The apparatus used to perform these experiments is described elsewhere [55].

4.3.8. Permeation Experiments

Prior to permeation experiments, the CMSM were glued to steel O-rings as described elsewhere [34]. Single gases were tested at 25 °C, where the feed pressure was 1 bar and the permeate pressure was *ca*. 0.03 bar. The tests were performed in a standard pressure-rise setup with LabView® data logging. As shown in Figure 4.5, the system includes the membrane module connected to a vessel with a calibrated volume (at the permeate side) and to a gas cylinder (at the feed side). The feed gas could either be used dry or humidified; for humidified gas experiments, the feed gas was passed through a bubbler with distilled water prior to the membrane module and the relative humidity checked with a RH meter (Vaisala DMP74b) at an exit port.

The permeability, P_i, of the CMSM towards a pure component *i* was determined accordingly to:

$$P_i = \frac{F_i}{\Delta P_i / \delta} \tag{4.1}$$

where F_i is the flux of species *i*, ΔP_i the partial pressure difference of species *i* between the two sides of the membrane and δ the membrane thickness (determined by scanning electron microscopy). The membrane permeability to pure component *i* was computed from the experimental data as follows:

$$P_i = \frac{\delta V_p v_M \Delta P_p}{RTtA(P_f - P_p)} \tag{4.2}$$

where V_p is the volume of the permeate tank, v_M is the molar volume of the gas at normal conditions, R is the gas constant, T is the absolute temperature, t is the time to a certain increment in the permeate pressure ΔP_p, A is the effective area of the flat carbon membrane and P_f and P_p are the feed and permeate pressure, respectively. The ratio of two gases permeability coefficients is the ideal selectivity [56]:

$$\alpha_{i,j} = \frac{P_i}{P_j} \tag{4.3}$$

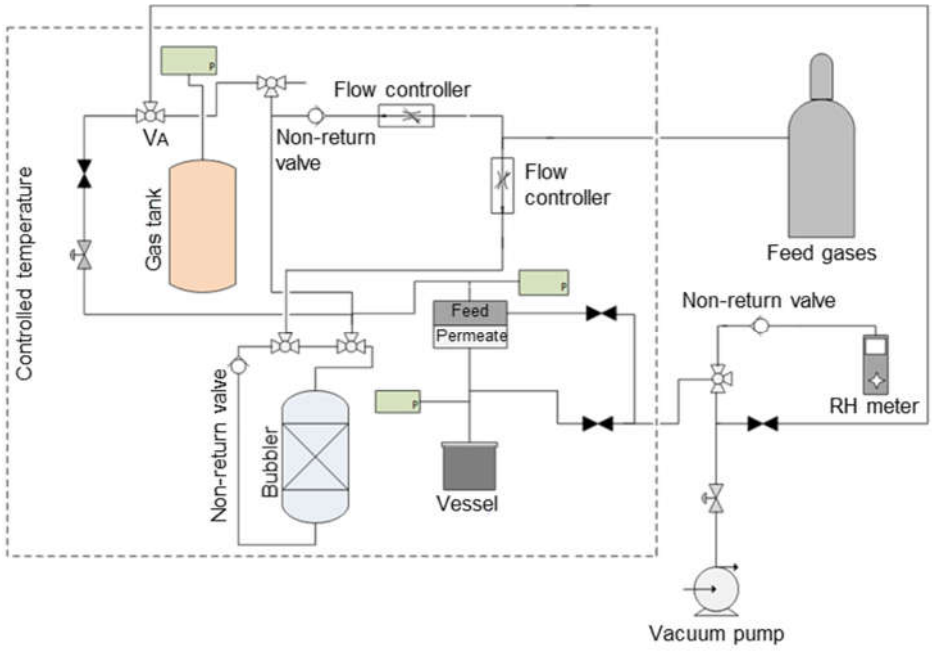

Figure 4.5. Scheme of the experimental setup for gas permeation experiments.

4.4. Results and Discussion

4.4.1. Preparation of regenerated cellulose-based carbon molecular sieve membranes

The prepared regenerated cellulose-based CMSM are identified in Table 4.1. The precursor disks shrank during the carbonization step and the shrinkage fraction (SH) of each CMSM was determined as follows:

$$SH = \frac{D_{before} - D_{after}}{D_{before}} \times 100 \tag{4.4}$$

where D_{before} is the membrane diameter before carbonization and D_{after} is the membrane diameter after the carbonization step.

Table 4.1. Identification of CMSM derived from regenerated cellulose.

Sample	Before carbonization		Carbonization temperature (°C)	After carbonization			Physical properties
	D (mm)	*δ* (μm)		*D* (mm)	*SH* (%)	*δ* (μm)	
Precursor	48.0	35.6	-	-	-	-	Transparent, flexible
CMSM 550	48.0	35.6	550	33.0	31.3	20.1	Black, bright, brittle
CMSM 600	48.0	35.6	600	28.0	41.7	18.0	Black, bright, brittle

From Table 4.1, it can be observed that shrinkage increased with the carbonization end temperature. Similarly, the increase in the carbonization end temperature led to a decrease in the membrane thickness (*δ*, measured by SEM). Figure 4.6 shows a membrane before and after carbonization.

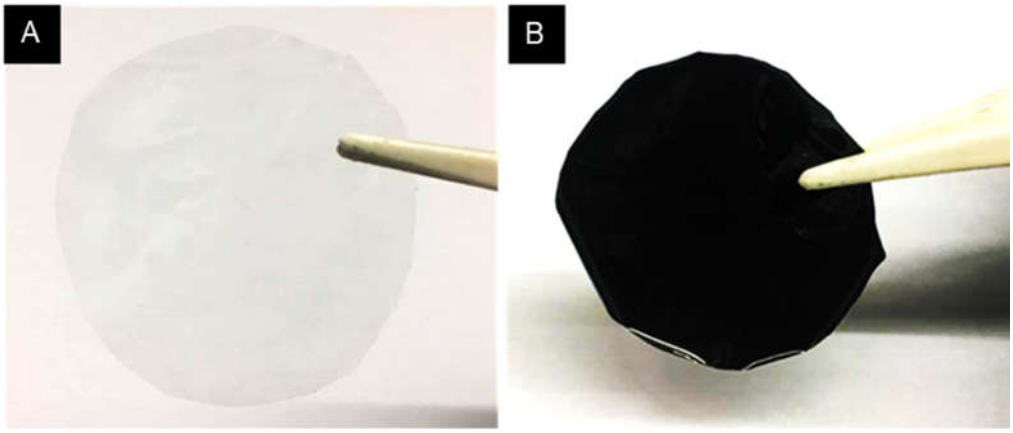

Figure 4.6. Regenerated cellulose membrane before **(A)** and after **(B)** carbonization.

4.4.2. Scanning electron microscopy

The structure of the membranes was examined by SEM. In a previous study, the research team prepared CMSM from commercial cellophane paper (a regenerated cellulose film produced by the viscose process) [36, 57]. Figure 4.7 shows scanning electron micrographs of surface and cross-sectional views of a CMSM prepared in this work and a cellophane-based CMSM, both carbonized at 550 °C. The surface of the sample prepared in this work is very smooth, with no apparent defects (Figure 4.7-A) indicating that spin coating is an effective technique for casting the precursor membrane. Microspheres (also called “condensed benzene rings”) [36, 58] were observed on the surface of cellophane-based CMSM (Figure 4.7-B) [57] but they were not observed on the surface of CMSM prepared through the ionic liquid process.

4.4.3. Thermogravimetric analysis

Thermogravimetric analysis was used to assess the thermal decomposition kinetics and stability of the precursor in inert atmosphere. TGA was performed on the dry regenerated cellulose film used to prepare the CMSM.

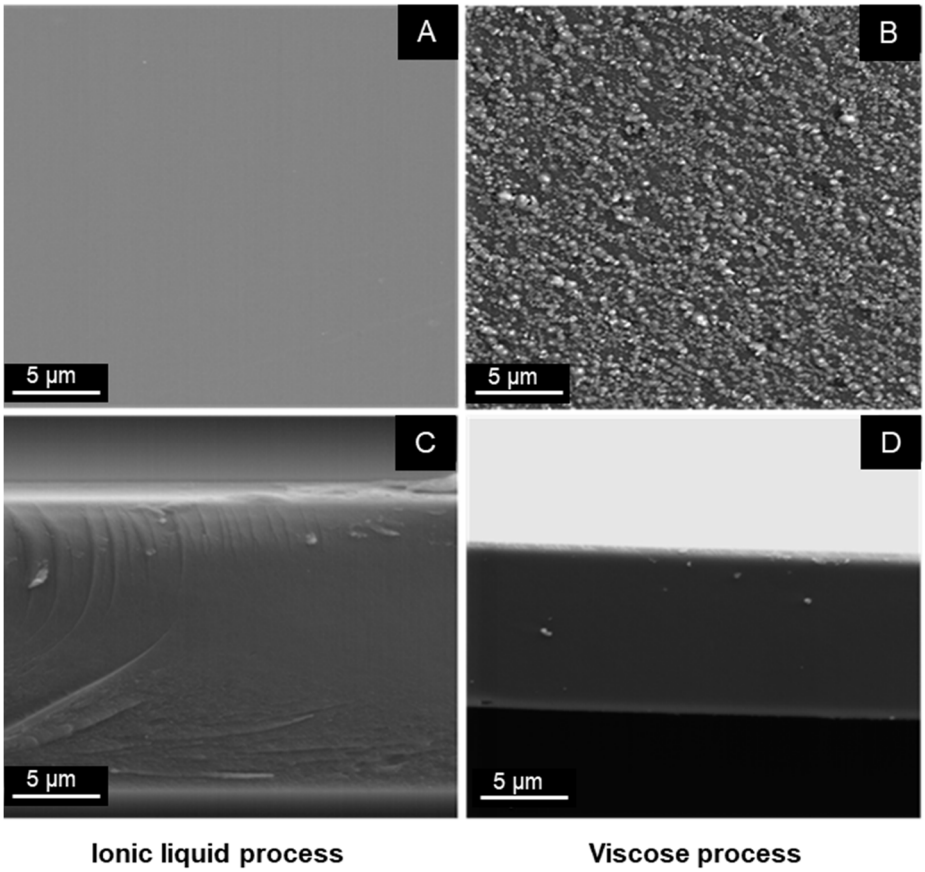

Figure 4.7. (A), **(B)** Surface images and **(C)**, **(D)** cross-sectional SEM images of CMSM obtained from regenerated cellulose films prepared through two different processes: ionic liquid and viscose. Magnification: × 5000. Carbonization end temperature: 550 °C.

The characteristic curve was obtained under N_2 atmosphere and is plotted together with the correspondent mass loss derivative curve in Figure 4.8. Up to 100 °C, the first derivative of mass loss curve shows a negative peak related with release of humidity present in the sample. The strong peak around 350 °C corresponds to the larger mass loss and indicates the degradation of the polymer [59] - an abrupt weight loss indicates the onset of the pore network formation [60]. A small weight loss is observed at *ca*. 415 °C and the mass still decreasing after this temperature until 950 °C, but at a much slower rate; at 950 °C the total weight loss was approximately 83 %. The regenerated cellulose precursor showed a higher weight loss and at lower

temperatures when compared to other polymer precursors commonly used in the preparation of CMSM [24, 26, 29, 60].

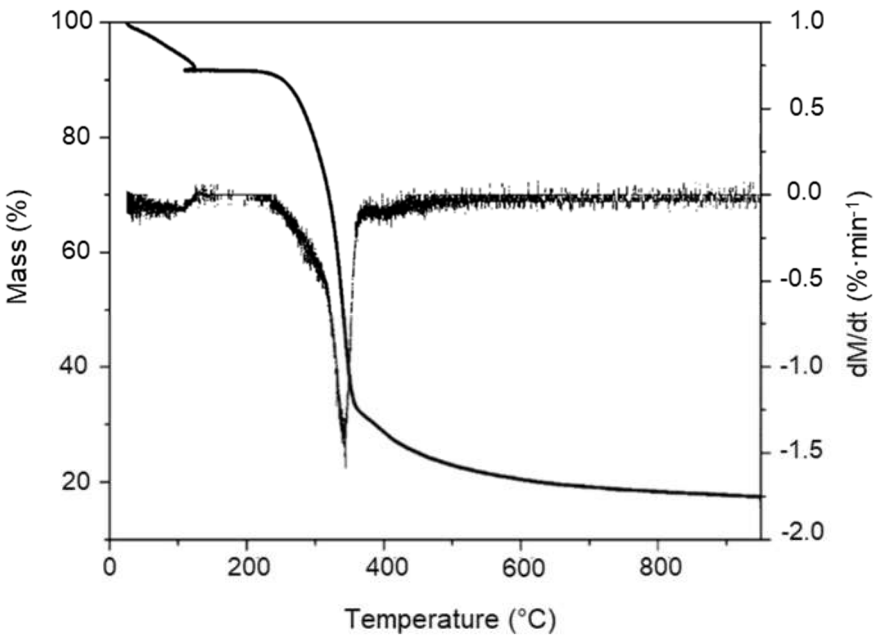

Figure 4.8. Thermogravimetric plot and correspondent derivative curve of the regenerated cellulose precursor.

Proximate analysis was also performed to determine humidity, volatile matter, fixed carbon and ashes content. Table 4.2 offers a summary of the results obtained. It was concluded that regenerated cellulose precursor is ash free, presenting *ca*. 75 wt. % of volatile matter and *ca*. 17 wt. % of fixed carbon.

Table 4.2. Proximate analysis (dry basis) of the regenerated cellulose precursor.

Proximate analysis (wt. %)			
Humidity	*Volatile matter*	*Carbon yield*	*Ashes*
8	75	17	0

4.4.4. Fourier transform infrared spectroscopy

The chemical structure of the samples was investigated by Fourier transform infrared spectroscopy. Figure 4.9 shows FTIR spectra of the precursor film and derived carbon membranes prepared at 550 °C and 600 °C carbonization end temperature. Band assignments for Figure 4.9 are summarized in Table 4.3.

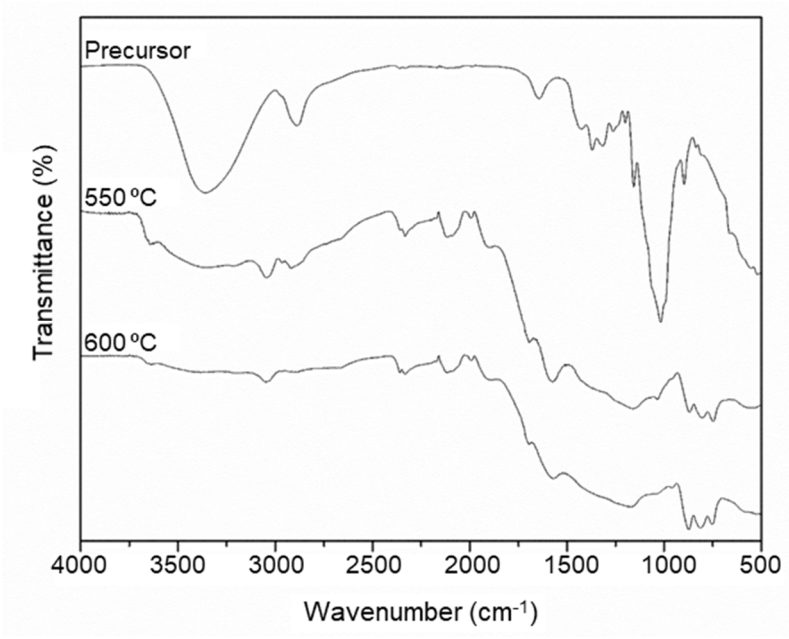

Figure 4.9. FTIR spectra of the regenerated cellulose precursor and derived CMSM.

The precursor spectra show a broad band at 3351 cm^{-1} which is ascribed to the O-H stretching vibrations in hydroxyl or carboxyl groups [61]. The precursor possesses aliphatic structures as it can be deduced from the band at 2887 cm^{-1}, which corresponds to stretching vibrations of aliphatic C-H [61, 62]. The band at about 1643 cm^{-1} can be assigned to C=C stretching vibrations and the one at 1423 cm^{-1} is attributed to CH_2 bending vibrations [63]; the bands at 1261 cm^{-1}, 1199 cm^{-1} and 1156 cm^{-1} correspond at C-O-C antisymmetric stretching vibrations and the peak at 1018 cm^{-1} is assigned to C-O stretching vibrations [64] (C-OH group of secondary alcohols existing in the

cellulose chain backbone). The peak detected at 897 cm^{-1} is characteristic of β-(1,4)-glycosidic linkages between glucose units (C-O-C stretching vibrations) [63].

Table 4.3. FTIR spectra bands assignments.

Wavenumber (cm^{-1})	**Functional group**	**Assignment**
3637,3354,3351	-OH	OH stretching
3047	=CH	=C-H stretching
2965,2919,2887	$-CH_3$ and $-CH_2-$	Aliphatic C-H stretching
2171	-N≡C	N≡C stretching
1985,1895	Substituted benzene ring	Several bands from overtones and combinations
1693	C=O	C=O stretching
1643	C=C	C=C stretching
1574	COO^-	COO^- antisymmetric stretching
1423	CH_2	CH_2 bending
1261,1199,1159,1156,897	C-O-C	C-O-C stretching
1034,1018	C-OH	C-O stretching
870,802,746	1,2,4-Trisubstituted benzenes; *o*-Disubstituted benzenes	Aromatic C-H out-of-plane bending

Regarding the carbon molecular sieve membranes, the spectra of the samples prepared at the two different carbonization end temperatures are similar. However, band intensities are weaker in CMSM obtained at 600 °C than those prepared at 550 °C; this implies that the degree of carbonization in CMSM increases with the carbonization end temperature. Absorption bands at 3637 cm^{-1} and 3354 cm^{-1}, characteristic of O-H stretching vibrations in hydroxyl or carbonyl groups, were observed [61]; at 3047 cm^{-1} a band ascribed to =C-H stretching was also identified [64]. The peaks at 2965 cm^{-1} and 2919 cm^{-1} are related to stretching vibrations of aliphatic C-H (CH_3 and CH_2 groups, respectively) [61, 62, 64]; however, it was observed that for samples carbonized at 600 °C these two bands disappeared. The band identified at 2171 cm^{-1}, for both samples, is ascribed to N≡C stretching vibrations [64]; moreover, two bands

characteristic of substituted benzene rings were detected at 1995 cm^{-1} and 1895 cm^{-1} [64]. The band at about 1693 cm^{-1} can be assigned to C=O stretching vibrations corresponding to carbonyl, quinone, ester or carboxyl [65]; the band at about 1574 cm^{-1} can be assigned to COO^- antisymmetric stretching [64], the one at 1159 cm^{-1} is attributed to C-O-C antisymmetric stretching vibrations and the one at 1034 cm^{-1} is assigned to C-O stretching vibrations [65]. The bands in the 870-746 cm^{-1} region are assigned to aromatic C-H out-of-plane bending vibrations [66].

4.4.5. Pore size distribution

In the present study, the microporosity of the CMSM was assessed based on the adsorption equilibrium isotherm of carbon dioxide at 0 °C. Figure 4.10 shows the adsorption equilibrium isotherm of CO_2 at 0 °C (Figure 4.10-A) and the CO_2 characteristic curve (Figure 4.10-B) for the sample carbonized at 550 °C, as an example. The Dubinin-Astakhov equation was used to fit the experimental data, obtaining then the micropore volume (W_0) and the characteristic energy of adsorption (E_0) [29, 67]. Dubinin-Astakhov equation with n=2.5 fits very well the experimental data (Figure 4.10-B). The mean pore width (l) was obtained by a weighted average. Table 4.4 summarizes the obtained structural parameters for each carbon membrane.

Table 4.4. Structural parameters of CMSM prepared by the ionic liquid and viscose processes.

	Ionic Liquid Process		**Viscose Process** [57]	
	CMSM 550	CMSM 600	CMSM 550	CMSM 600
W_0 ($cm^3 \cdot kg^{-1}$)	250.2	327.4	274.2	322.5
E_0 ($kJ \cdot mol^{-1}$)	11.8	11.9	12.3	12.7
l (nm)	0.711	0.700	0.667	0.635

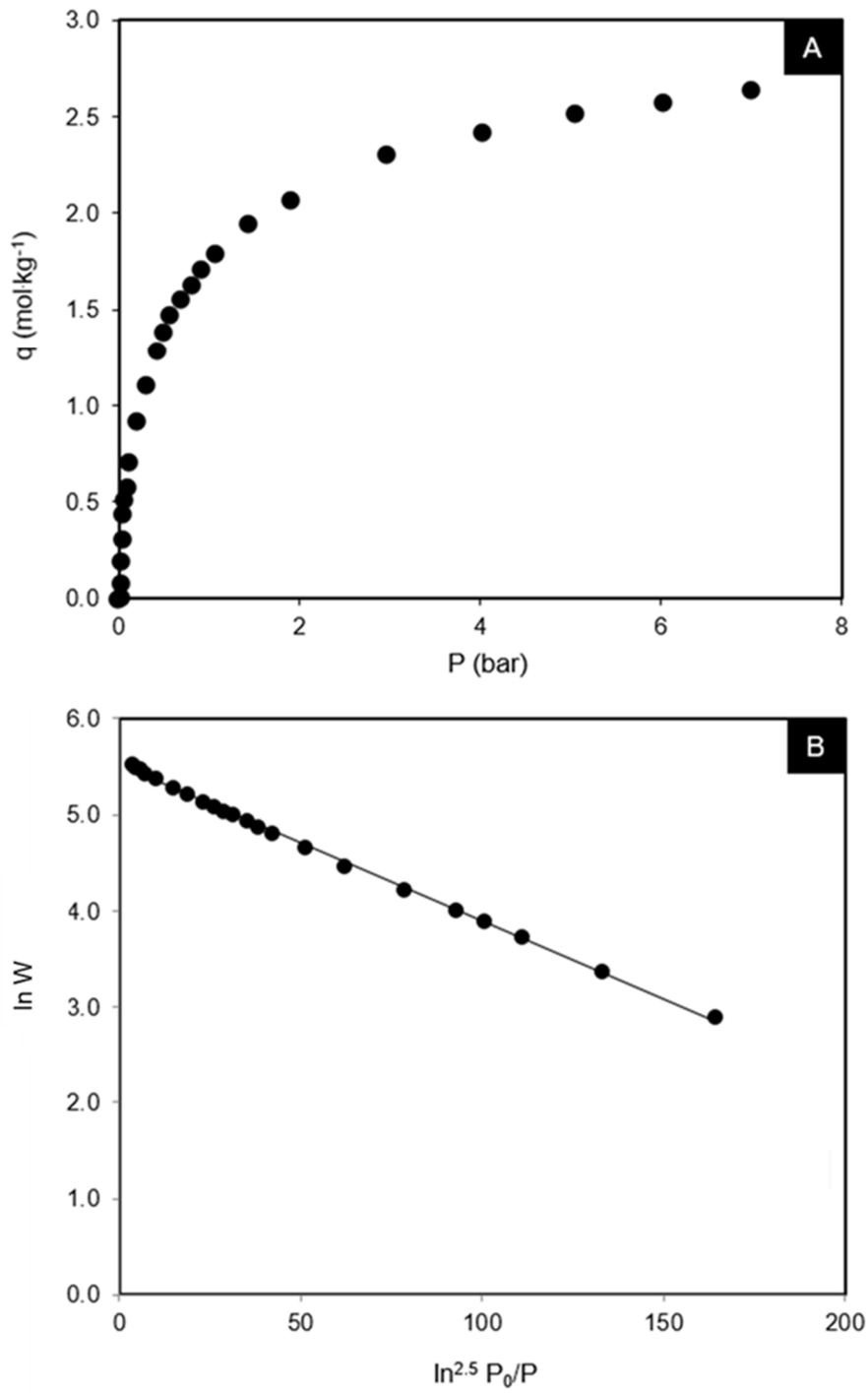

Figure 4.10. (A) Adsorption equilibrium isotherm of CO_2 at 0 °C and **(B)** CO_2 characteristic curve (points - experimental data; solid line - DA fitting). Carbonization end temperature: 550 °C.

The obtained micropore volume for CMSM 550 is typical for carbon molecular sieves; for CMSM 600, the micropore volume of 327.4 $cm^3 \cdot kg^{-1}$ is slightly higher [68, 69]. The obtained mean pore widths are slightly higher when compared to other reported values [29, 68-70]. Comparing the present values with the ones obtained for cellophane-based CMSM [57] (viscose process), it is possible to observe that these membranes have a higher mean pore width, which is in accordance with the obtained higher permeabilities as will be shown in section 4.4.6.

The skeleton density (obtained by helium picnometry) of the ionic liquid regenerated cellulose-based CMSM prepared at 550 °C and 600 °C was 1.4 $g \cdot cm^{-3}$ and 2.3 $g \cdot cm^{-3}$, respectively.

The pore size distribution was obtained using the structure-based method proposed by Nguyen *et al.* for the determination of the micropore size distribution in carbonaceous materials [71, 72]. A detailed description about this method can be found in Chapter 3.B. Figures 4.11 and 4.12 show the obtained micropore size distributions for CMSM 550 and CMSM 600, respectively, and a comparison with the PSD obtained for cellophane-based CMSM. From Figures 4.11 and 4.12, it can be seen that the CMSM prepared in this work at two different carbonization end temperatures present ultramicropores (0.4-0.7 nm range) and micropores (0.7-1.0 nm). The regenerated cellulose-based CMSM (ionic liquid process) prepared at 550 °C and 600 °C present a micropore size distribution slightly shifted to the right, towards higher pore sizes when compared to the cellophane-based; once more, this is in accordance with the obtained higher permeabilities and low ideal selectivities (section 4.4.6).

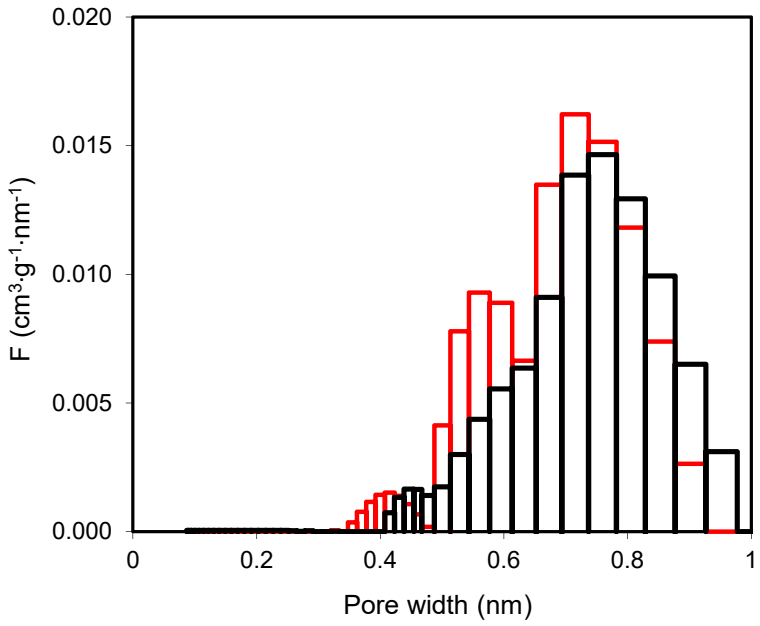

Figure 4.11. Micropore size distribution of regenerated cellulose-based CMSM. Ionic liquid process: black line; viscose process: red line. Carbonization end temperature: 550 °C.

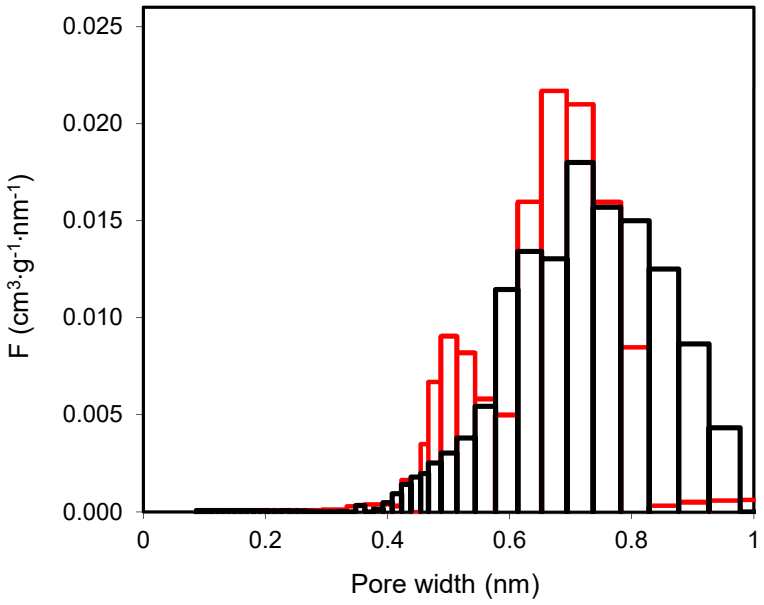

Figure 4.12. Micropore size distribution of regenerated cellulose-based CMSM. Ionic liquid process: black line; viscose process: red line. Carbonization end temperature: 600 °C.

4.4.6. Permeation Experiments

The membranes were tested for permeation using several probe species: N_2 (0.378 nm), O_2 (0.346 nm), CO_2 (0.335 nm), H_2 (0.290 nm) and He (0.260 nm) – the values in brackets correspond to the kinetic diameter of the gases [70]. Table 4.5 presents the obtained permeabilities and ideal selectivities for the regenerated cellulose-based CMSM prepared at 550 °C and 600 °C.

Table 4.5. Permeabilities and ideal selectivities for regenerated cellulose-based CMSM at 25 °C.

Gas species	CMSM 550		CMSM 600	
	Permeability (barrer)	Permselectivity X/N_2	Permeability (barrer)	Permselectivity X/N_2
N_2	0.16	-	0.09	-
O_2	5.16	32.3	2.19	24.3
CO_2	13.41	83.8	4.18	46.4
He	126.36	789.8	174.22	1935.8
H_2	n.d*	-	120.54	1339.3

*n.d. = not determined

Figure 4.13 shows the permeability towards several gas species against their kinetic diameter. It can be observed that there is a straightforward relation between the membrane permeability and the kinetic diameter of the permeant species, indicating that CMSM have size-discrimination ability and denoting the molecular sieving character of the prepared materials. The effect of carbonization end temperature on the separation performance of regenerated cellulose-based CMSM is also demonstrated in Figure 4.13 and Table 4.5. The samples carbonized at higher temperature (CMSM 600) have generally smaller gas permeation; for example, the membrane permeability towards N_2 became around 1.8 times smaller when compared to CMSM 550 - CMSM 550 have a larger mean pore width compared to CMSM 600 (Table 4.4). At 600 °C, carbon atoms are rearranging into a tighter structure, by a sintering mechanism [34, 73]. However, CMSM 600 have a larger volume of ultramicropores (Figures 4.11 and 4.12), leading to a higher permeability to He [29].

However, though this sample displays more pores they are smaller making the permeability of this sample to the other gases smaller than for sample CMSM 550.

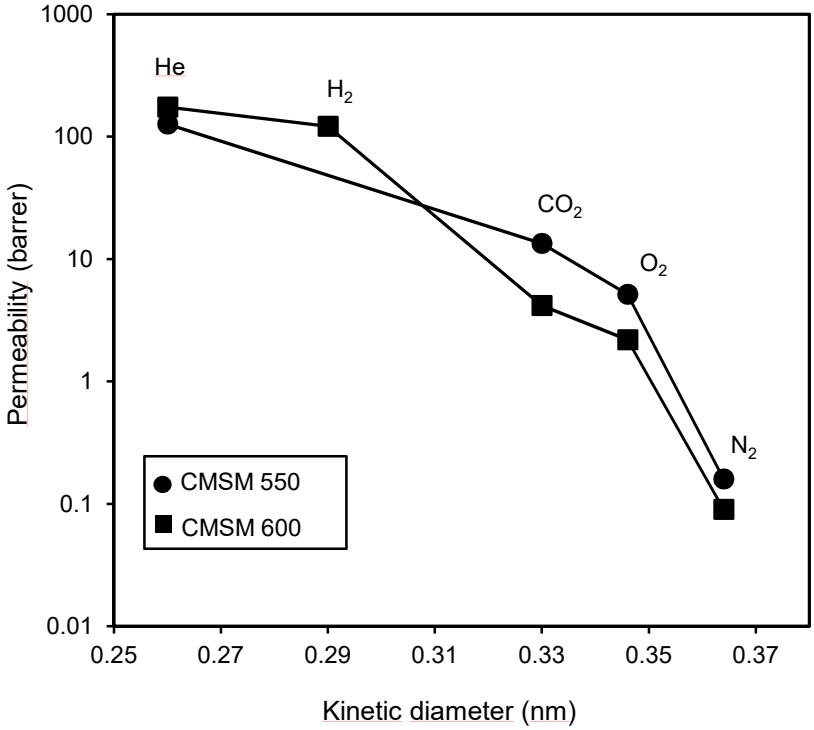

Figure 4.13. Permeability as a function of the gas kinetic diameter for regenerated cellulose-based membranes carbonized at 550 °C and 600 °C. Lines were added for readability.

The performance of a carbon membrane towards a separation is characterized by the gas permeability as well as the correspondent selectivity. In 2008 [74], Robeson proposed a selectivity/permeability upper bound for representative binary gas separations performed with polymeric membranes. Figures 4.14 to 4.17 illustrate the Robeson upper bounds for O_2/N_2 (Figure 4.14), He/N_2 (Figure 4.15), H_2/N_2 (Figure 4.16) and CO_2/N_2 (Figure 4.17), together with the results obtained in this work; a comparison with CMSM produced from other cellulosic precursors reported in literature [33, 34, 36, 57, 75, 76] is also included. For facilitating the comparison, a dashed line was drawn over the best sample of the present work, parallel to the Robeson line. All values below this line perform worse and vice-versa. The arrows in the charts indicate the superior

ideal selectivities. Robeson upper bounds are broadly recognized as the state-of-the-art curves for gas separation.

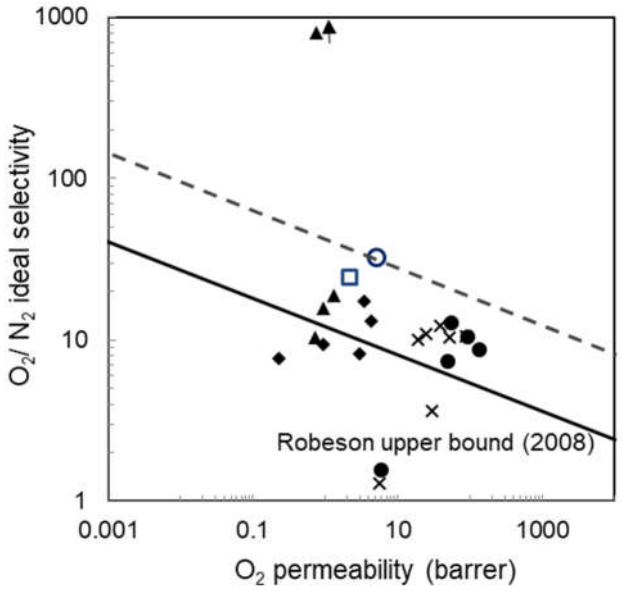

Figure 4.14. Robeson upper bound plot for O_2/N_2 gas pair showing the data for ○ CMSM 550, □ CMSM 600 and reported cellulose-based CMSM (♦[34];●[33];▲[36, 57]; ×[76]).

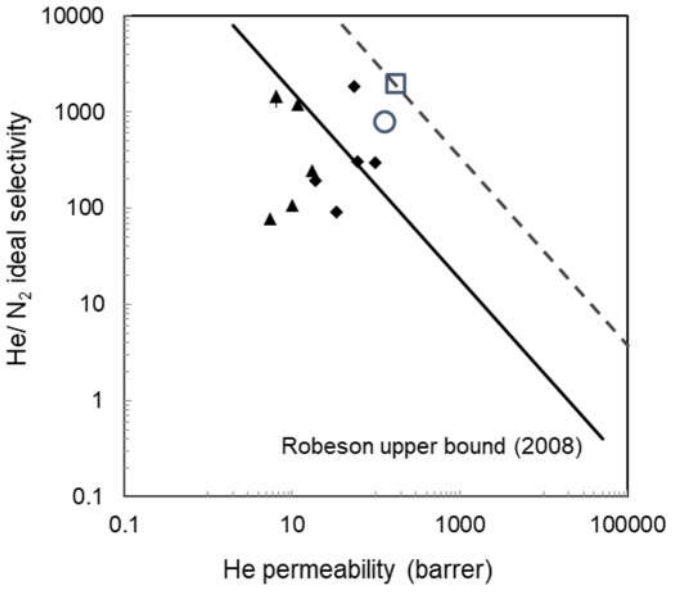

Figure 4.15. Robeson upper bound plot for He/N_2 gas pair showing the data for ○ CMSM 550 and □ CMSM 600 and reported cellulose-based CMSM (♦[34];▲[36, 57]; ×[76]).

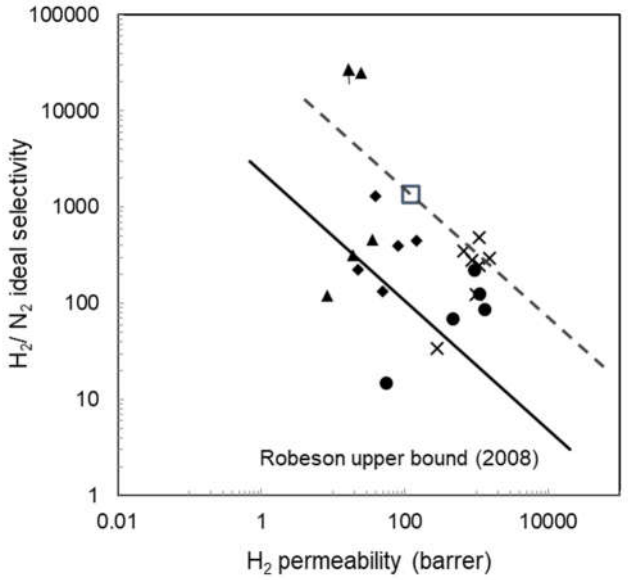

Figure 4.16. Robeson upper bound plot for H_2/N_2 gas pair showing the data for □ CMSM 600 and reported cellulose-based CMSM (♦[34];●[33];▲[36, 57]; ×[76]).

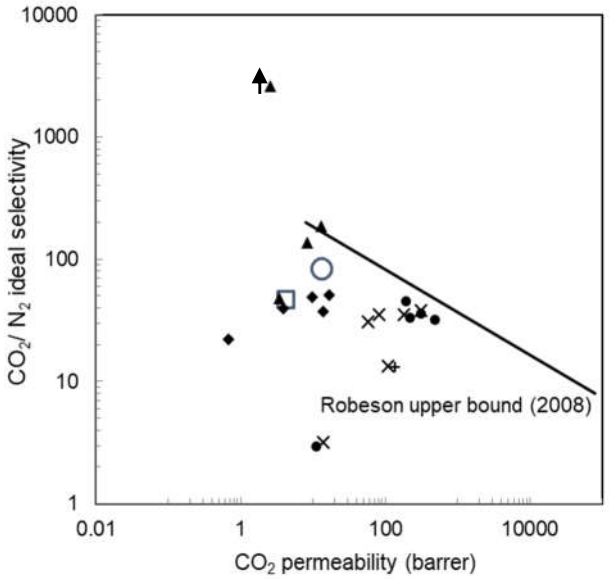

Figure 4.17. Robeson upper bound plot for CO_2/N_2 gas pair showing the data for ○ CMSM 550 and □ CMSM 600 and reported cellulose-based CMSM (♦[34];●[33];▲[36, 57]; +[75]; ×[76]).

It can be observed that the CMSM prepared in this work are plotted above the upper bound for O_2/N_2, He/N_2 and H_2/N_2 separations. Moreover, when these membranes are compared to the reported cellulosic-based CMSM, (see dashed line) they show a better permeability/permselectivity balance (except for the cellophane-based CMSM prepared in our previous work) for most of the studied gas separations.

Relative humidity stability

Permeation experiments in the presence of 75-77 % RH were undertaken using the regenerated cellulose-based CMSM to determine its performance stability in the presence of water vapor. Table 4.6 shows the permeability of CMSM 550 and CMSM 600 samples to dry and humidified O_2 and N_2.

Table 4.6. Permeability of CMSM 550 and CMSM 600 to dry and humidified O_2 and N_2.

Sample	RH (%)	Dry feed		Humidified feed	
		Permeability to O_2 (barrer)	Permeability to N_2 (barrer)	Permeability to humidified O_2 (barrer)	Permeability to humidified N_2 (barrer)
CMSM 550	75-77	5.16	0.16	8.47	1.33
CMSM 600	75-77	2.19	0.09	5.96	0.85

Permeation data showed that humidity does not affect membrane ability to permeate and separate gases. For carbon membrane samples prepared at 550 °C, the total flux increased *ca.* 1.6 times (the permeability to oxygen stays constant); for carbon membrane samples prepared at 600 °C, the total flux increased *ca.* 2.7 times. This increase is due to the very fast permeation of water vapor that occurs due to the membrane high hidrophilicity. Previous studies by the authors demonstrated that the high hydrophilicity is characteristic of regenerated cellulose-based CMSM [57].

4.5. Conclusions

Carbon molecular sieve membranes with high separation performance and stability in the presence of humidity were successfully prepared in a single carbonization step, without need for pre nor post treatments steps. The carbon membranes were prepared from regenerated cellulose, a renewable low-cost precursor, using an ionic liquid as cellulose solvent and spin coating for casting the precursor film. Ionic liquids are environmentally friendly and more efficient solvents than current methodologies to dissolve and process cellulose. This was the first time that regenerated cellulose films produced through an ionic liquid process were studied for preparation of CMSM. The permeability versus kinetic diameter towards N_2, CO_2, O_2, H_2 and He exhibited a molecular sieve mechanism for the prepared membranes. The effect of carbonization end temperature was assessed, and better separation performances were found for CMSM 550 sample, carbonized in an inert atmosphere at 550 °C. The Robeson upper bound for polymeric membranes was overtaken by the prepared membranes regarding O_2/N_2, He/N_2 and H_2/N_2 separations.

The produced carbon molecular sieve membranes are stable and have a great potential for gas separation; therefore, they might be considered in relevant industrial applications such as separation of nitrogen from air, air dehumidification and separation of hydrogen from syngas.

4.6. Acknowledgments

S.C. Rodrigues is grateful to the Portuguese Foundation for Science and Technology (FCT) for the doctoral grant (reference SFRH/BD/93779/2013) supported by funding POPH/FSE. M. Andrade is thankful to POCI-01-0145-FEDER-006939 (Laboratory for Process Engineering, Environment, Biotechnology and Energy – UID/EQU/00511/2013) funded by the European Regional Development Fund (ERDF), through COMPETE2020 - Programa Operacional Competitividade e Internacionalização (POCI) and by national funds, through FCT - Fundação para a Ciência e a Tecnologia and

NORTE-01-0145-FEDER-000005 – LEPABE-2-ECO-INNOVATION, supported by North Portugal Regional Operational Programme (NORTE 2020), under the Portugal 2020 Partnership Agreement, through the European Regional Development Fund (ERDF) for the fellowship grant. The authors are thankful to Innovia Films Ltd. for generously providing wood pulp.

4.7. References

[1] Q. Liu, T. Wang, H. Guo, C. Liang, S. Liu, Z. Zhang, Y. Cao, D.S. Su, J. Qiu, Controlled synthesis of high performance carbon/zeolite T composite membrane materials for gas separation, Microporous and Mesoporous Materials, 120 (2009) 460-466.

[2] X. Ma, B.K. Lin, X. Wei, J. Kniep, Y.S. Lin, Gamma-alumina supported carbon molecular sieve membrane for propylene/propane separation, Industrial & Engineering Chemistry Research, 52 (2013) 4297-4305.

[3] T.C. Merkel, H. Lin, X. Wei, R. Baker, Power plant post-combustion carbon dioxide capture: An opportunity for membranes, Journal of Membrane Science, 359 (2010) 126-139.

[4] R. Faiz, K. Li, Polymeric membranes for light olefin/paraffin separation, Desalination, 287 (2012) 82-97.

[5] W. Wei, G. Qin, H. Hu, L. You, G. Chen, Preparation of supported carbon molecular sieve membrane from novolac phenol–formaldehyde resin, Journal of Membrane Science, 303 (2007) 80-85.

[6] A.F. Ismail, L.I.B. David, A review on the latest development of carbon membranes for gas separation, Journal of Membrane Science, 193 (2001) 1-18.

[7] P.S. Tin, T.-S. Chung, S. Kawi, M.D. Guiver, Novel approaches to fabricate carbon molecular sieve membranes based on chemical modified and solvent treated polyimides, Microporous and Mesoporous Materials, 73 (2004) 151-160.

[8] M. Kiyono, P.J. Williams, W.J. Koros, Effect of pyrolysis atmosphere on separation performance of carbon molecular sieve membranes, Journal of Membrane Science, 359 (2010) 2-10.

[9] P.J. Williams, W.J. Koros, Gas Separation by Carbon Membranes in: N.N. Li, A.G. Fane, W.S.W. Ho, T. Matsuura (Eds.) Advanced Membrane Technology and Applications, John Wiley & Sons, New Jersey, 2008.

[10] A.F. Ismail, D. Rana, T. Matsuura, H.C. Foley, Carbon-based Membranes for Separation Processes, Springer, New York, 2011.

[11] M.A.L. Tanco, D.A.P. Tanaka, Recent advances on carbon molecular sieve membranes (CMSMs) and reactors, Processes, 4 (2016) 1-29.

[12] A. Mendes, F.D. Magalhães, C.A.V. Costa, New trends on Membrane Science in: W.C. Conner, J. Fraissard (Eds.) Fluid Transport in Nanoporous Materials Springer, The Netherlands, 2006.

[13] C.W. Jones, W.J. Koros, Characterization of ultramicroporous carbon membranes with humidified feeds, Industrial & Engineering Chemistry Research, 34 (1995) 158-163.

[14] I. Menendez, A.B. Fuertes, Aging of carbon membranes under different environments, Carbon, 39 (2001) 733-740.

[15] S. Lagorsse, M.C. Campo, F.D. Magalhães, A. Mendes, Water adsorption on carbon molecular sieve membranes: Experimental data and isotherm model, Carbon, 43 (2005) 2769-2779.

[16] K.M. Steel, W.J. Koros, An investigation of the effects of pyrolysis parameters on gas separation properties of carbon materials, Carbon, 43 (2005) 1843-1856.

[17] X. Ma, R. Swaidan, B. Teng, H. Tan, O. Salinas, E. Litwiller, Y. Han, I. Pinnau, Carbon molecular sieve gas separation membranes based on an intrinsically microporous polyimide precursor, Carbon, 62 (2013) 88-96.

[18] X. Ning, W.J. Koros, Carbon molecular sieve membranes derived from Matrimid® polyimide for nitrogen/methane separation, Carbon, 66 (2014) 511-522.

[19] O. Salinas, X. Ma, E. Litwiller, I. Pinnau, High-performance carbon molecular sieve membranes for ethylene/ethane separation derived from an intrinsically microporous polyimide, Journal of Membrane Science, 500 (2016) 115-123.

[20] Y.-J. Fu, C.-C. Hu, D.-W. Lin, H.-A. Tsai, S.-H. Huang, W.-S. Hung, K.-R. Lee, J.-Y. Lai, Adjustable microstructure carbon molecular sieve membranes derived from thermally stable polyetherimide/polyimide blends for gas separation, Carbon, 113 (2017) 10-17.

[21] L.I.B. David, A.F. Ismail, Influence of the thermastabilization process and soak time during pyrolysis process on the polyacrylonitrile carbon membranes for O_2/N_2 separation, Journal of Membrane Science, 213 (2003) 285-291.

[22] Y.D. Chen, R.T. Yang, Preparation of carbon molecular sieve membrane and diffusion of binary mixtures in the membrane, Industrial & Engineering Chemistry Research, 33 (1994) 3146-3153.

[23] C. Song, T. Wang, X. Wang, J. Qiu, Y. Cao, Preparation and gas separation properties of poly(furfuryl alcohol)-based C/CMS composite membranes, Separation and Purification Technology, 58 (2008) 412-418.

[24] M.A.L. Tanco, D.A.P. Tanaka, S.C. Rodrigues, M. Texeira, A. Mendes, Composite-alumina-carbon molecular sieve membranes prepared from novolac resin and boehmite. Part I: Preparation, characterization and gas permeation studies, International Journal of Hydrogen Energy, 40 (2015) 5653-5663.

[25] A.B. Fuertes, I. Menendez, Separation of hydrocarbon gas mixtures using phenolic resin-based carbon membranes, Separation and Purification Technology, 28 (2002) 29-41.

[26] M. Teixeira, M.C. Campo, D.A.P. Tanaka, M.A.L. Tanco, C. Magen, A. Mendes, Composite phenolic resin-based carbon molecular sieve membranes for gas separation, Carbon, 49 (2011) 4348-4358.

[27] W. Zhou, M. Yoshino, H. Kita, K.-i. Okamoto, Carbon molecular sieve membranes derived from phenolic resin with a pendant sulfonic acid group, Industrial & Engineering Chemistry Research, 40 (2001) 4801-4807.

[28] M. Teixeira, S.C. Rodrigues, M. Campo, D.A. Pacheco Tanaka, M.A. Llosa Tanco, L.M. Madeira, J.M. Sousa, A. Mendes, Boehmite-phenolic resin carbon molecular sieve membranes—Permeation and adsorption studies, Chemical Engineering Research and Design, 92 (2014) 2668-2680.

[29] S.C. Rodrigues, R. Whitley, A. Mendes, Preparation and characterization of carbon molecular sieve membranes based on resorcinol–formaldehyde resin, Journal of Membrane Science, 459 (2014) 207-216.

[30] M. Yoshimune, T. Yamamoto, M. Nakaiwa, K. Haraya, Preparation of highly mesoporous carbon membranes via a sol–gel process using resorcinol and formaldehyde, Carbon, 46 (2008) 1031-1036.

[31] Y.-R. Dong, M. Nakao, N. Nishiyama, Y. Egashira, K. Ueyama, Gas permeation and pervaporation of water/alcohols through the microporous carbon membranes prepared from resorcinol/formaldehyde/quaternary ammonium compounds, Separation and Purification Technology, 73 (2010) 2-7.

[32] S. Tanaka, T. Yasuda, Y. Katayama, Y. Miyake, Pervaporation dehydration performance of microporous carbon membranes prepared from resorcinol/formaldehyde polymer, Journal of Membrane Science, 379 (2011) 52-59.

[33] J.A. Lie, M.-B. Hägg, Carbon membranes from cellulose: Synthesis, performance and regeneration, Journal of Membrane Science, 284 (2006) 79-86.

[34] M.C. Campo, F.D. Magalhães, A. Mendes, Carbon molecular sieve membranes from cellophane paper, Journal of Membrane Science, 350 (2010) 180-188.

[35] M.C. Campo, F.D. Magalhães, A. Mendes, Separation of nitrogen from air by carbon molecular sieve membranes, Journal of Membrane Science, 350 (2010) 139-147.

[36] A. Mendes, M. Andrade, M. Boaventura, S.C. Rodrigues, A carbon molecular sieve membrane, method of preparation and uses thereof, Patent WO 2017068517 A1, 2017.

[37] H. Wang, G. Gurau, R.D. Rogers, Ionic liquid processing of cellulose, Chemical Society Reviews, 41 (2012) 1519-1537.

[38] J. Pang, X. Liu, X. Zhang, Y. Wu, R. Sun, Fabrication of cellulose film with enhanced mechanical properties in ionic liquid 1-allyl-3-methylimidaxolium chloride (AmimCl), Materials, 6 (2013) 1270-1284.

[39] B. Ma, A. Qin, X. Li, C. He, Preparation of cellulose hollow fiber membrane from bamboo pulp/1-butyl-3-methylimidazolium chloride/dimethylsulfoxide system, Industrial & Engineering Chemistry Research, 52 (2013) 9417-9421.

[40] Z.C. Zhang, Catalytic transformation of carbohydrates and lignin in ionic liquids, Wiley Interdisciplinary Reviews: Energy and Environment, 2 (2013) 655-672.

[41] S. Mahmoudian, M.U. Wahit, A.F. Ismail, A.A. Yussuf, Preparation of regenerated cellulose/montmorillonite nanocomposite films via ionic liquids, Carbohydrate Polymers, 88 (2012) 1251-1257.

[42] S. Livazovic, Z. Li, A.R. Behzad, K.V. Peinemann, S.P. Nunes, Cellulose multilayer membranes manufacture with ionic liquid, Journal of Membrane Science, 490 (2015) 282-293.

[43] A. Pinkert, K.N. Marsh, S. Pang, M.P. Staiger, Ionic liquids and their interaction with cellulose, Chemical Reviews, 109 (2009) 6712-6728.

[44] H.-Z. Chen, N. Wang, L.-Y. Liu, Regenerated cellulose membrane prepared with ionic liquid 1-butyl-3-methylimidazolium chloride as solvent using wheat straw, Journal of Chemical Technology & Biotechnology, 87 (2012) 1634-1640.

[45] M.T. Clough, K. Geyer, P.A. Hunt, S. Son, U. Vagt, T. Welton, Ionic liquids: not always innocent solvents for cellulose, Green Chemistry, 17 (2015) 231-243.

[46] B. Kosan, C. Michels, F. Meister, Dissolution and forming of cellulose with ionic liquids, Cellulose, 15 (2008) 59-66.

[47] J.-H. Pang, X. Liu, M. Wu, Y.-Y. Wu, X.-M. Zhang, R.-C. Sun, Fabrication and characterization of regenerated cellulose films using different ionic liquids, Journal of Spectroscopy, 2014 (2014) 1-8.

[48] F. Hoelkeskamp, Process for production of cuprammonium cellulose articles, US patent 3110546 A, 1963.

[49] T. Welton, Room-Temperature Ionic Liquids. Solvents for Synthesis and Catalysis, Chemical Reviews, 99 (1999) 2071-2084.

[50] S. Mallakpour, M. Dinari, Ionic Liquid as Green Solvents: Progress and Prospects, in: A. Mohammad, Inamuddin (Eds.) Green Solvents II. Properties and Applications of Ionic Liquids, Springer Dordrecht, 2012.

[51] K.M. Gupta, J. Jiang, Cellulose dissolution and regeneration in ionic liquids: A computational perspective, Chemical Engineering Science, 121 (2015) 180-189.

[52] J. Wang, J. Luo, S. Feng, H. Li, Y. Wan, X. Zhang, Recent development of ionic liquid membranes, Green Energy & Environment, 1 (2016) 43-61.

[53] M. Ottaway, Use of Thermogravimetry for Proximate Analysis of Coals and Cokes, Fuel, 61 (1982) 713-716.

[54] D. Ferreira, R. Magalhães, P. Taveira, A. Mendes, Effective adsorption equilibrium isotherms and breakthroughs of water vapor and carbon dioxide on different adsorbents, Industrial & Engineering Chemistry Research, 50 (2011) 10201-10210.

[55] J.C. Santos, F.D. Magalhães, A. Mendes, Contamination of zeolites used in oxygen production by PSA: effects of water and carbon dioxide, Industrial & Engineering Chemistry Research, 47 (2008) 6197-6203.

[56] L.M. Robeson, Correlation of separation factor versus permeability for polymeric membranes, Journal of Membrane Science, 62 (1991) 165-185.

[57] S.C. Rodrigues, M. Andrade, F.D. Magalhães, A. Mendes, Carbon membranes with extremely high separation performance and stability, submitted, (2017).

[58] M. Sevilla, A.B. Fuertes, The production of carbon materials by hydrothermal carbonization of cellulose, Carbon, 47 (2009) 2281-2289.

[59] C.S.R. Freire, A.J.D. Silvestre, C.P. Neto, M.N. Belgacem, A. Gandini, Controlled heterogeneous modification of cellulose fibers with fatty acids: Effect of reaction conditions on the extent of esterification and fiber properties, Journal of Applied Polymer Science, 100 (2006) 1093-1102.

[60] Y.-J. Fu, K.-S. Liao, C.-C. Hu, K.-R. Lee, J.-Y. Lai, Development and characterization of micropores in carbon molecular sieve membrane for gas separation, Microporous and Mesoporous Materials, 143 (2011) 78-86.

[61] C. Araujo-Andrade, F. Ruiz, J.R. Martínez-Mendoza, H. Terrones, Infrared and Raman spectra, conformational stability, ab initio calculations of structure, and vibrational assignment of α and β glucose, Journal of Molecular Structure: THEOCHEM, 714 (2005) 143-146.

[62] J. Ibarra, E. Muñoz, R. Moliner, FTIR study of the evolution of coal structure during the coalification process, Organic Geochemistry, 24 (1996) 725-735.

[63] D. Ciolacu, F. Ciocacu, V.I. Popa, Amorphous cellulose - structure and characterization, Cellulose Chemistry and Technology, 45 (2011) 13-21.

[64] J.M. Chalmers, P.R. Griffiths, Handbook of vibrational spectroscopy, Wiley, Virginia, 2002.

[65] B.M. Kabyemela, T. Adschiri, R.M. Malaluan, K. Arai, Glucose and fructose decomposition in subcritical and supercritical water: detailed reaction pathway, mechanisms, and kinetics, Industrial & Engineering Chemistry Research, 38 (1999) 2888-2895.

[66] A.C. Lua, T. Yang, Effect of activation temperature on the textural and chemical properties of potassium hydroxide activated carbon prepared from pistachio-nut shell, Journal of Colloid and Interface Science, 274 (2004) 594-601.

[67] N.D. Hutson, R.T. Yang, Theoretical basis for the Dubinin-Radushkevitch (D-R) adsorption isotherm equation, Adsorption, 3 (1997) 189-195.

[68] D. Cazorla-Amorós, J. Alcañiz-Monge, M.A. de la Casa-Lillo, A. Linares-Solano, CO_2 as an adsorptive to characterize carbon molecular sieves and activated carbons, Langmuir, 14 (1998) 4589-4596.

[69] S. Lagorsse, F.D. Magalhães, A. Mendes, Carbon molecular sieve membranes: Sorption, kinetic and structural characterization, Journal of Membrane Science, 241 (2004) 275-287.

[70] M. Teixeira, M. Campo, D.A. Tanaka, M.A. Tanco, C. Magen, A. Mendes, Carbon-Al_2O_3-Ag composite molecular sieve membranes for gas separation, Chemical Engineering Research and Design, 90 (2012) 2338-2345.

[71] C. Nguyen, D.D. Do, K. Haraya, K. Wang, The structural characterization of carbon molecular sieve membrane (CMSM) via gas adsorption, Journal of Membrane Science, 220 (2003) 177-182.

[72] C. Nguyen, D.D. Do, Adsorption of supercritical gases in porous media: determination of micropore size distribution, The Journal of Physical Chemistry B, 103 (1999) 6900-6908.

[73] J. Koresh, A. Soffer, Study of molecular sieve carbons. Part 1.-Pore structure, gradual pore opening and mechanism of molecular sieving, Journal of the Chemical Society, Faraday Transactions 1: Physical Chemistry in Condensed Phases, 76 (1980) 2457-2471.

[74] L.M. Robeson, The upper bound revisited, Journal of Membrane Science, 320 (2008) 390-400.

[75] X. He, J.A. Lie, E. Sheridan, M.-B. Hägg, Preparation and characterization of hollow fiber carbon membranes from cellulose acetate precursors, Industrial & Engineering Chemistry Research, 50 (2011) 2080-2087.

[76] J.A. Lie, M.-B. Hägg, Carbon membranes from cellulose and metal loaded cellulose, Carbon, 43 (2005) 2600-2607.

Chapter V

Chapter 5 – General Conclusions and Future Work

5.1. General Conclusions

This thesis focused on the development and characterization of carbon molecular sieve membranes displaying high separation performance, no pore blocking effect when treating humidified gas streams, and showing minimal oxygen chemisorption. Carbon molecular sieve membranes were successfully prepared on α-alumina supports by carbonization of resorcinol-formaldehyde resin loaded with boehmite nanoparticles in a single dipping-drying-carbonization step. Resorcinol-formaldehyde resin was considered a suitable precursor material for the preparation of CMSM due to its high fixed-carbon yield and low-cost; boehmite nanoparticles (γ-AlO(OH)) have been proved to be effective for producing crack-free supported membranes in a single dipping-drying-carbonization step since they are able to control the precursor rheology.

Two series of supported carbon membranes were prepared at 500 °C and 550 °C and the effect of the carbonization end temperature on the membrane structure, morphology and performance was assessed through scanning electron microscopy, CO_2 adsorption equilibrium isotherm at 0 °C and monocomponent permeation experiments at temperatures from 25 °C to 120 °C. It was observed that the obtained carbon molecular sieve layer is quite uniform showing *ca.* 3 μm of thickness. The supported CMSM carbonized at 550 °C displayed higher ideal selectivities and relatively similar gas permeation rates when compared to those prepared at 500 °C. The Robeson upper bound for polymeric membranes was overtaken by the carbon membranes prepared at 550 °C, regarding O_2/N_2 (O_2 permeation rate: 9.85×10^{-10} $mol\cdot m^{-2}\cdot s^{-1}\cdot Pa^{-1}$ and ideal selectivity: >11.5), H_2/N_2 (H_2 permeation rate: 5.04×10^{-8} $mol\cdot m^{-2}\cdot s^{-1}\cdot Pa^{-1}$ and ideal selectivity: >586) and He/N_2 (He permeation rate: 4.68×10^{-8} $mol\cdot m^{-2}\cdot s^{-1}\cdot Pa^{-1}$ and ideal

selectivity: >544) separations; the developed membranes are superior to various reported CMSM prepared from phenol-formaldehyde resin precursors.

Cellophane is a low-cost precursor obtained from wood cellulose by the viscose process. It was first reported as a promising precursor for CMSM by the research team in 2010. In the present thesis, carbon molecular sieve membranes with exceptional separation performance, stability and mechanical resistance were prepared from commercial cellophane sheets. The effect of carbonization end temperature was assessed from 400 °C to 600 °C and the roots of the non-aging property displayed by these membranes were studied. The obtained membranes displayed high flexibility and an extraordinary separation performance. The carbon membranes prepared at 600 °C were situated far above Robeson's upper bound, showing an O_2/N_2 ideal selectivity greater than 800 for a permeability to oxygen of 0.78 barrer, a CO_2/CH_4 ideal selectivity greater than 2600 for a permeability to CO_2 of 2.57 barrer, and an H_2/CH_4 ideal selectivity greater than 25 000 for a permeability to hydrogen of 25 barrer. Despite the very high ideal selectivities displayed by these CMSM for most of the gas pairs, ideal selectivity to C_3H_6/C_3H_8 was relatively low. To understand this behavior, a carbon molecular sieve adsorbent with high C_3H_6/C_3H_8 selectivity was prepared from a phenolic resin at 1100 °C. High-resolution transmission electron microscopy analysis shown that depending on the selected precursor material, carbon molecular sieves with two extreme sieving mechanisms can be produced: i) gate sieving for carbon molecular sieves having a gate-like pore shape which are selective for spheroid gas species and ii) tubular sieving for carbon molecular sieves having a tubular shape pore which are selective for linear gas species.

Membrane´s performance stability in the presence of water vapor was evaluated up to *ca.* 80 % of RH and it was concluded that humidity does not affect the membrane's ability to permeate and separate the tested permanent gases. Moreover, the membranes showed a mostly linear water vapor adsorption/desorption isotherm instead of the markedly S-shape curves normally displayed by CMSM. Linear water adsorption/desorption isotherms are characteristic of carbon materials with

hydrophilic sites homogeneously distributed throughout their inner surfaces allowing water molecules to jump continuously between polar sites and avoiding the formation of pore-blocking water clusters. X-ray photoelectron spectroscopy revealed that these hydrophilic elements are ionic sodium and silica nanoparticles that are incorporated in the cellophane precursor film during its production. The carbonization end temperature had a noticeable influence on membrane surface chemistry and it was found that 550 °C provide an optimum condition for the concentration of hydrophilic elements homogeneously distributed on CMSM surface.

The prepared cellophane-based CMSM were susceptible to oxygen chemisorption. However, up to a certain point, this process favored the membrane's selectivity since CMSM exposed to ambient air before permeation experiments showed improved ideal selectivities compared with CMSM without air exposure. In addition, a simple propylene treatment was able to stabilize membranes concerning oxygen chemisorption. These results are a breakthrough towards bringing these membranes to a commercial level.

Ionic liquids are a promising alternative to existing cellulose-dissolving solvents. For the first time, regenerated cellulose films produced through an ionic liquid process were used to prepare flat carbon membranes in a single casting-drying-carbonization step; a spin coating method was used for the precursor membrane casting. Two different carbon membranes were prepared at 550 ^{o}C and 600 ^{o}C and the effect of the carbonization end temperature on the membrane structure, morphology and performance was studied. The permeability versus kinetic diameter towards N_2, CO_2, O_2, H_2 and He denoted the molecular sieving character of the prepared materials. The CMSM revealed good ideal selectivities with separation performances above the upper bound for polymeric membranes devised by Robeson in 2008. Additionally, it was concluded that humidity does not affect the membrane's ability to permeate and separate gases through permeation experiments performed in the presence of *ca.* 80 % RH. These promising results open the doors for preparing tailor made

precursors that originate carbon molecular sieve membranes with extraordinary separation performances and stability.

5.2. Future Work

Taking into account the results of the present thesis, as future work it would be important to improve the permeability of the regenerated cellulose-based carbon molecular sieve membranes. For that, several approaches can be considered, namely the optimization of the precursor solution and the carbonization conditions. Membranes with different cellulose concentrations should be prepared and the influence of cellulose concentration on membrane's separation properties studied. Similarly, different plasticizers with different concentrations must be considered and their effect on the membrane's structure, morphology and performance examined. Finally, different porogenic agents with different concentrations must be also added to the precursor solution to increase the membrane porosity; these porogens should essentially release water, hydrogen or carbon dioxide at high temperatures.

Concerning the optimization of the carbonization conditions, heating rate and flowrate of the inert gas should be carefully optimized. The heating rate is related to the release rate of volatiles and this release is related to the pore size distribution and the number of connecting pores on CMSM; therefore, to optimize the heating rate during CMSM carbonization, a study concerning the identification of the diameter of the released volatiles as a function of degradation temperature should be undertaken. Higher inert flowrates produce carbon membranes with improved permeabilities showing a minimal role on the selectivities; therefore a high flowrate should be also applied during the carbonization step.

Finally, hollow fiber carbon molecular sieve membranes should be prepared and characterized. This is the best configuration for producing CMSM for commercial applications because of the high packing density, easy module assembly and mechanical stability. The target is to develop a dual-layer hollow fiber carbon molecular

sieve membranes; the first layer should be thick and porous, prepared from regenerated cellulose reinforced with ceramic particles (namely boehmite nanoparticles) for mechanical stability, while the second layer should be thin and selective. Both layers must exhibit similar shrinkage ratio.

Appendix A

Appendix A – Complementary characterizations

Carbon membranes with extremely high separation performance and stability

CMSM with high separation performance and stability were prepared from cellophane precursor films in one single carbonization step. The resultant CMSM are identified in Table A.1. For a better understanding, the number after the membrane identification was relative to the carbonization end temperature used to prepare the CMSM. For example, the sample CMSM 400 was carbonized at 400 °C; the sample CMSM 500 was carbonized at 550 °C, and so on. The precursor disks (initially circles with a diameter of 48 mm, Figure A.1-A) shrank during the carbonization process, giving place to elliptic membranes (Figure A.1-B). This fact may be caused by a preferential orientation of the macromolecules in the cellophane precursor film [1].

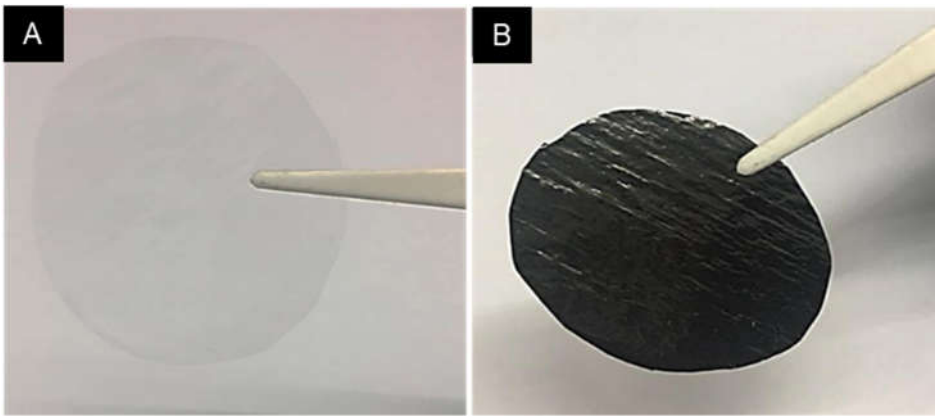

Figure A.1. Cellophane-based membranes: **(A)** before carbonization, **(B)** after carbonization.

Table A.1 presents two values of final diameters and shrinkage percentage, associated to the two characteristic dimensions of the final elliptical membranes. As expected, the shrinkage percentage increased with the increase of the carbonization end temperature.

Table A.1. Identification of carbon membranes derived from cellophane precursor.

Sample	Before Carbonization	Carbonization temperature	After Carbonization	
	D (mm)	(°C)	*D* (mm)	*SH* (%)
CMSM 400	48.0	400	32.0-30.0	33.3-37.5
CMSM 500	48.0	500	35.0-29.0	27.1-39.6
CMSM 550	48.0	550	33.5-28.0	41.7-30.2
CMSM 600	48.0	600	33.5-28.0	41.7-30.2

Table A.2 shows the thickness (δ, measured by scanning electron microscopy) of the precursor film and derived CMSM prepared at different carbonization end temperatures.

Table A.2. Thickness (δ) of cellophane film and derived CMSM.

Sample	δ_{before} (μm)	δ_{after} (μm)
CMSM 400	15.0-17.0	11.3
CMSM 500	15.0-17.0	9.7
CMSM 550	15.0-17.0	9.5
CMSM 600	15.0-17.0	9.2

It can be observed that an increase in the carbonization end temperature led to a decrease on the membranes thickness; this is in accordance with the membranes shrinkage macroscopically observed and previously discussed.

A.1. Raman spectroscopy analysis

Raman spectroscopy is a useful tool to obtain information on the microstructure of carbonaceous materials. Every band in Raman spectrum corresponds directly to a specific vibrational frequency of a band within a molecule. The vibrational frequency and hence the position of the Raman band are very sensitive to the orientation of the bands and weight of the atoms at either end of the band, which make it a popular choice for structural characterization.

Raman spectra of graphitic carbons consists of two bands: the G band (graphitic band) at 1575 cm^{-1} and the D band (disordered band) at 1355 cm^{-1} [2-4].The G band can

be attributed to the in-plane carbon stretching vibrations of ideal graphene sheets; the D band originates from a hybridized vibrational mode associated with graphene edges and indicates the presence of some disorder in the structure [5].

In the present work, Raman spectra were recorded with a Thermo Scientific Raman Microscope using a 523 nm laser as an excitation source in the range of 0 to 3500 cm^{-1}. Figure A.2 shows the Raman spectra of the precursor and CMSM. The spectra of CMSM carbonized from 400 °C to 600 °C feature two major peaks: the G-band centered at 1595 cm^{-1} and the D-band located at 1367 cm^{-1}, which reveal the presence of C sp^2 atoms in benzene or condensed benzene rings of amorphous (partially hydrogenated) carbon [3, 6, 7]. The Raman shift found for D-band is usually observed in amorphous carbon; the graphitic band is also slightly shifted, which is characteristic of carbon materials with disordered carbon.

Table A.3 shows the D and G band Raman intensities for all membranes. The intensity of G band increased with the increase of carbonization end temperature, indicating that the framework of CMSM becomes a more graphitized carbon at higher temperatures. The increase in the carbonization end temperature also increased the D band intensity, indicating more imperfections in the graphene structures that corresponds to an increase in amorphous carbon [8].

Table A.3. Raman intensity of D and G bands for cellophane-based CMSM.

Sample	**Raman Intensity**	
	G Band	*D Band*
CMSM 400	1075	825
CMSM 500	2150	1450
CMSM 550	2800	1950
CMSM 600	2650	1850

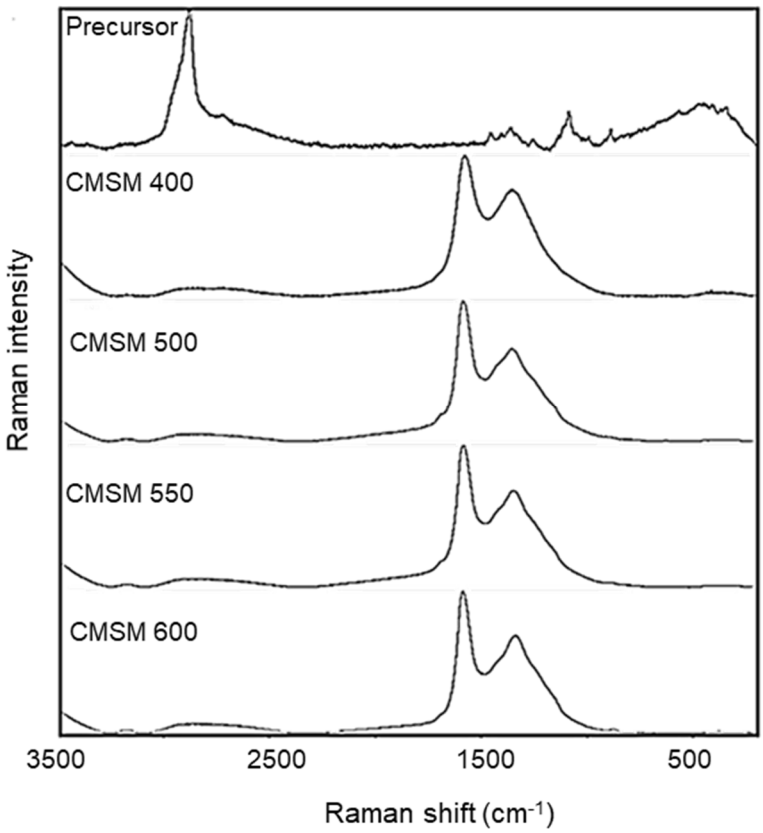

Figure A.2. Raman spectra of the cellophane precursor and derived CMSM.

A.2. Temperature programmed desorption analysis

Carbon structures contain heteroatoms such as hydrogen, oxygen, nitrogen, sulphur, etc. These heteroatoms are bounded to the edges of graphene layers originating a diversity of surface functional groups. The type and concentration of these functional groups have a significant influence on the CMSM performance. Temperature programmed desorption (TPD) is a thermal analysis technique for the characterization of surface functional groups on carbon materials. Figure A.3 summarizes the different surface functional groups found on carbon materials.

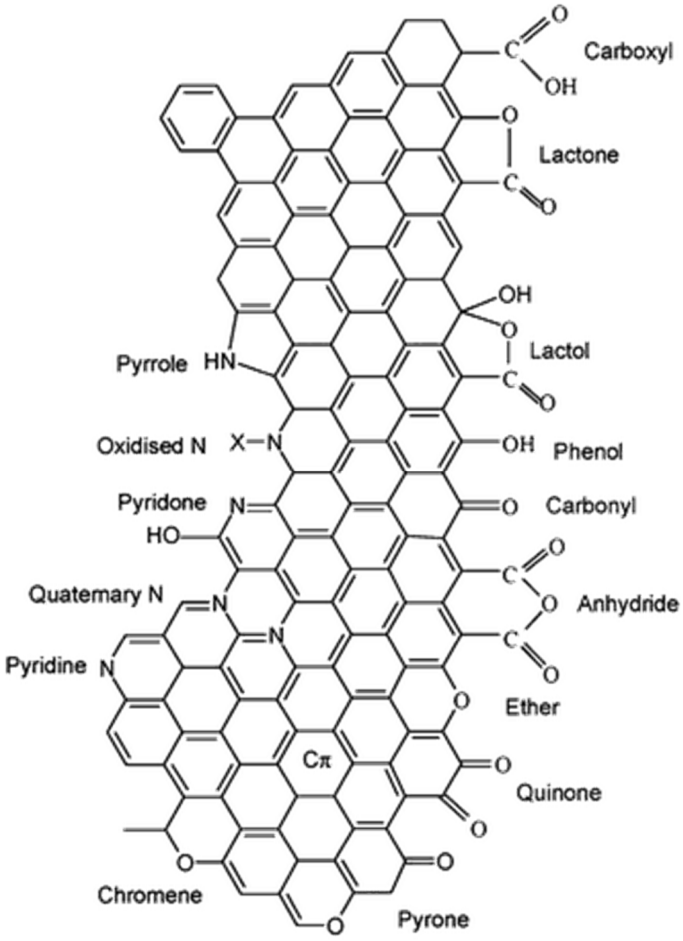

Figure A.3. Examples of oxygen and nitrogen functional groups found on carbon surfaces [12].

Surface complexes on carbon materials decompose upon heating by releasing CO and CO_2 at different temperatures. The nature of the groups can be then assessed by the decomposition temperature and the gas released. Table A.4 presents the functional groups related to their decomposition temperature and the emitted gas, by TPD.

In the present work, TPD experiments were carried out in a U-shaped quartz tube located inside an electrical furnace and connected to a Dycor Dymaxion Mass Spectrometer (Ametek Process Instruments) for samples prepared at 400 °C and 550 °C carbonization end temperatures. The studied samples (0.1 g) were heated to 1100 °C at 5 °C·min^{-1} using a constant He flow rate of 25 ml·min^{-1}.

Table A.4. Gaseous species emitted from functional groups on carbon by TPD.

Functional groups	Released gas	Temperature (°C)
Carboxylic	CO_2	250 [13] 100-400 [14] 200-250 [15]
Lactone	CO_2	627 [16, 17] 350-400 [15] 190-650 [18]
Phenol	CO	600-700 [15]
Carbonyl	CO	700-980 [18] 800-900 [15]
Ether	CO	700 [17]
Quinone	CO	700-980 [18] 800-900 [15]
Anhydride	CO+ CO_2	600 [19] 627 [13, 16, 17] 350-400 [15]

Figure A.4 shows the obtained TPD profiles, and Table A.5 indicates the amount of CO and CO_2 released during TPD for both carbon molecular sieve membranes.

Table A.5. Amount of CO and CO_2 released during TPD for CMSM 400 and CMSM 550 samples.

Sample	CO (μmol·g^{-1})	CO_2 (μmol·g^{-1})	CO/CO_2
CMSM 400	3615	2445	1.5
CMSM 550	1279	443	2.9

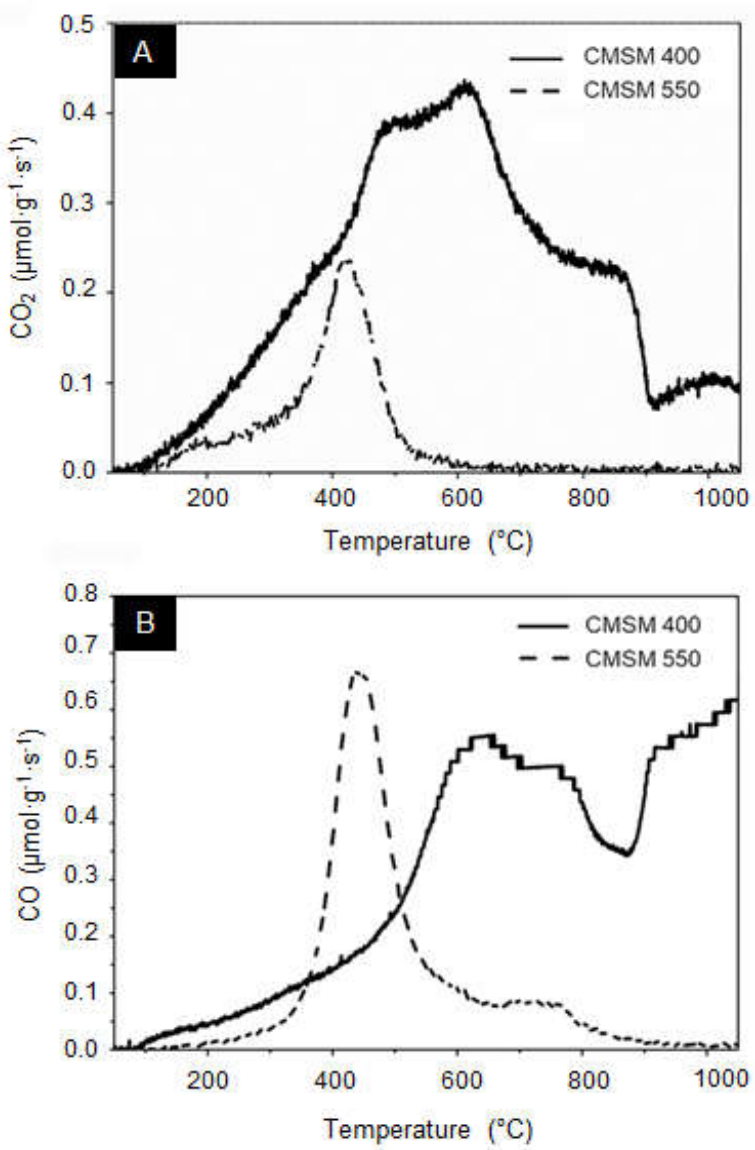

Figure A.4. TPD spectra of CMSM 400 and CMSM 550: **(A)** CO_2 evolution, **(B)** CO evolution.

It can be observed that an increase in the carbonization end temperature from 400 °C to 550 °C generates a decrease in the amount of surface oxygenated groups; this is evidenced by the larger released amount of CO_2 and CO of CMSM 550 sample when compared to CMSM 400. The CO/CO_2 ratio increased with the increase in the carbonization end temperature. The TPD peaks can be assigned to the different

functional groups by comparison with the data summarized in Figure A.4 and Table A.4 taken from the available literature. For CMSM 400 sample, the first CO_2 peak may be attributed to lactone groups. At around 630 °C a simultaneous CO_2 and CO peak is generated from carboxylic anhydrides. The peak at around 780 °C in the CO profile originates from quinone groups. For CMSM 550 sample, both CO and CO_2 peaks originate from the decomposition of carboxylic anhydrides.

A.3. X-ray photoelectron spectroscopy analysis

The atomic concentration of the elements found on the surface of the carbon molecular sieve membranes was assessed using x-ray photoelectron spectroscopy (XPS) and are presented in Table S.2 (Chapter 3.B). C, O and S are cellophane characteristic elements (hydrogen cannot be detected from XPS analysis). The presence of sodium and silica nanoparticles in cellophane and consequently in CMSM is justified by the production process of cellophane (discussed in Chapter 3.A). The N found is considered pollution or impurities due to membrane manufacturing [20, 21].

As expected, the O/C ratio decreases with the carbonization end temperature rise as the content of oxygen on membrane structure decreases significantly with carbonization step with the loss of CO, CO_2 and H_2O predominantly. It can be observed that the sodium concentration on the carbon membrane surface's increases as the carbonization temperature increases.

Comparison of C(1s) region

XP spectra of C(1s) region for the prepared CMSM at different carbonization end temperatures are shown in Figure A.5. Five peaks were used to fit the C(1s) region using consistent fitting protocols. Graphitic (C=C) and aliphatic carbon (C-C/C-H) appears at 285.0 eV binding energy (BE); the band at around 286.1 eV BE corresponds to C-O links and at around 287 eV BE is assigned to O-C-O/C=O; finally, the bands at around 289 eV BE and 290 eV BE are associated to –O-C=O and π-π* satellite, respectively [7, 20, 22].

Only one peak was used to fit the graphitic and aliphatic carbon atoms due to the close proximity of their binding energies [22, 23]. The appearance of π-π* shake-up satellite peak is the effect of polycondensed carbon cluster development that leads to the formation of a delocalized π electron system [22]. This π-π* shake-up indicates the development of sp^2 sites like in a graphitic structure [24] which is in accordance with Raman spectroscopy results previously discussed.

Integrated areas of individual components were computed to quantify the change in chemical composition of CMSM as a function of carbonization end temperature. Table A.6 shows the relative area of each component obtained by curve fitting of the C(1s) spectra for the different CMSM samples.

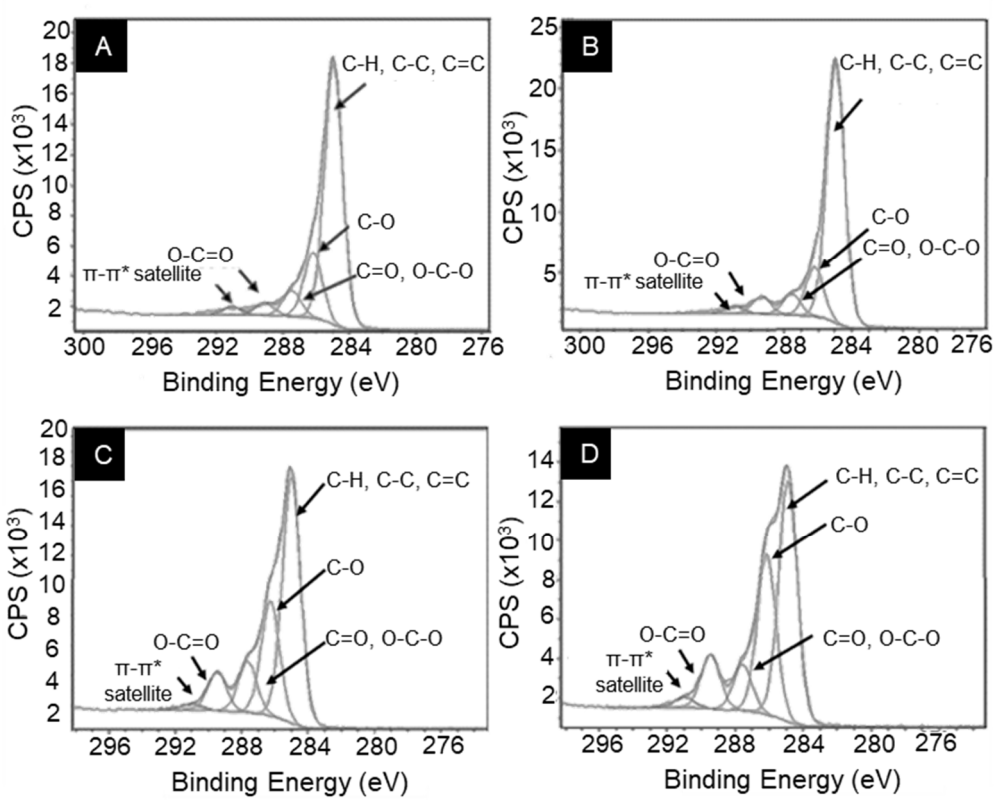

Figure A.5. Observed and deconvolved C(1s) XP spectra of the different CMSM: **(A)** CMSM 400, **(B)** CMSM 500, **(C)** CMSM 550, **(D)** CMSM 600.

Table A.6. Relative areas of the XPS C(1s) peaks for the different CMSM.

Sample	C-H/C-C/C=C	C-O	C=O/O-C-O	O-C=O	π-π*
CMSM 400	76.7	19.5	2.1	1.0	0.7
CMSM 500	80.8	15.3	1.8	1.5	0.6
CMSM 550	54.4	25.4	11.3	8.5	0.4
CMSM 600	51.2	34.0	2.7	11.5	0.6

The intensity of graphitic and aliphatic carbon peaks is the strongest in the C(1s) spectra for all the CMSM prepared at different carbonization end temperatures.

Comparison of O(1s) region

XP spectra of O(1s) regions for CMSM prepared at different carbonization end temperatures are shown in Figure A.6. Three peaks were used to fit the O(1s) region: a peak for C=O type oxygen (C=O and COOR; 531.5-532.4 eV BE), another for C-O type oxygen (C-OH, C-O-C and CO-O-R; 533.4-533.8 eV BE) and a third assigned to oxygen atoms in adsorbed oxygen and/or water (535.1-539.9 eV BE) [25-27]. For the membranes carbonized at 600 °C (CMSM 600), only two peaks were needed to fit O(1s) region (Figure A.6-D).

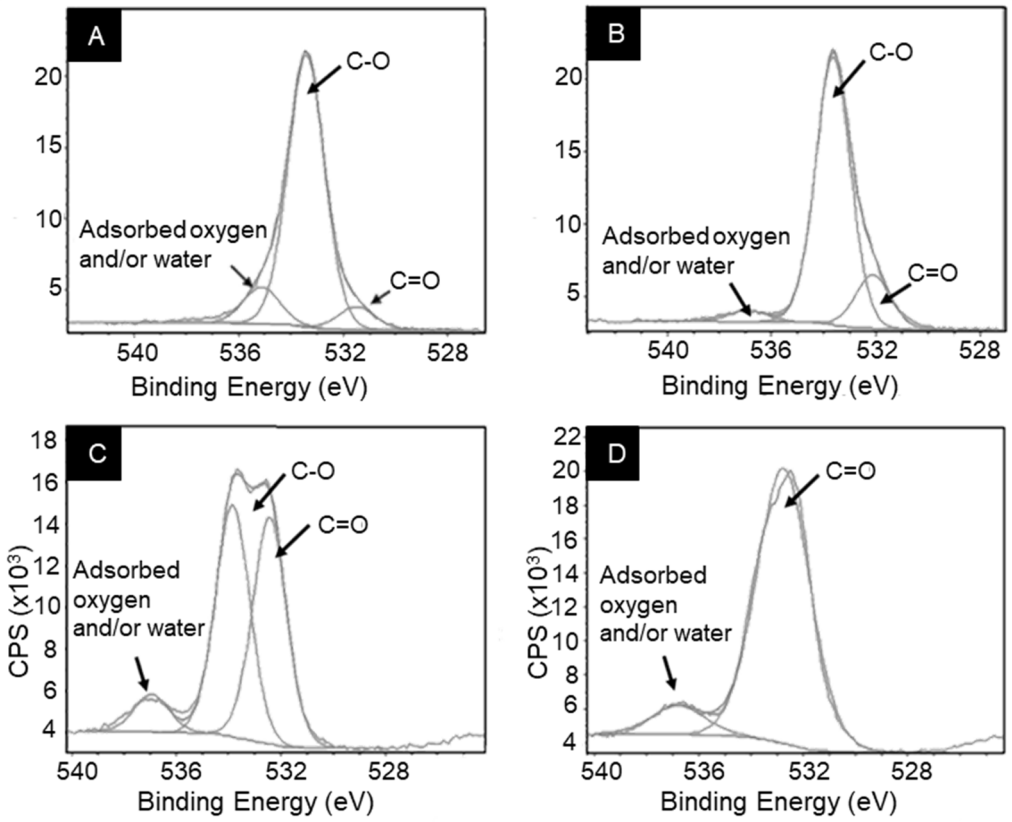

Figure A.6. Observed and deconvolved O(1s) XP spectra of the different CMSM: **(A)** CMSM 400, **(B)** CMSM 500, **(C)** CMSM 550, **(D)** CMSM 600.

Table A.7 shows the relative area of each component obtained by curve fitting of the O(1s) spectra for the different CMSM samples.

Table A.7. Relative areas of the XPS O(1s) peaks for the different CMSM.

Sample	C=O	C-O	Adsorbed oxygen and/or water
CMSM 400	7.1	81.9	11.0
CMSM 500	16.2	80.4	3.4
CMSM 550	45.8	46.6	7.6
CMSM 600	90.5	-	9.5

A significant increase in the relative area of the peak for C=O type oxygen and a substantial decrease in the relative area of the peak for C-O type oxygen is verified

when the carbonization end temperature increases from 400 °C to 600 °C. At 600 °C, C-O functional groups are not observed.

A.4. Fourier transform infrared spectroscopy analysis

As discussed in Chapter 3.B, the chemical structure of the samples was examined by Fourier transform infrared spectroscopy. Figure S.2 (Chapter 3.B) shows the FTIR spectra of the cellophane precursor and derived CMSM. The precursor spectrum shows a broad band in the 3800-3000 cm^{-1} region which is ascribed to the O-H stretching vibration [7, 8]. Cellophane possesses aliphatic structures as can be deduced from the band at 3000-2815 cm^{-1} which corresponds to stretching vibrations of aliphatic C-H [7]; the band at about 1640 cm^{-1} can be assigned to C=C stretching vibrations and at 1456 cm^{-1} is attributed to CH_2 bending vibrations. The bands at 1260 cm^{-1}, 1197 cm^{-1} and 1150 cm^{-1} correspond at C-O-C antisymmetric stretching vibrations and the peak at 1015 cm^{-1} is assigned to C-O stretching vibrations. The peak detected at 894 cm^{-1} is characteristic of β-(1,4)-glycosidic linkages between glucose units (C-O-C stretching vibrations) [28].

Regarding the CMSM, the spectra of the membranes prepared at different carbonization end temperatures are quite similar. For the samples prepared between 400 °C and 550 °C carbonization end temperature, an absorption band at 3379 cm^{-1} was observed, characteristic of O-H stretching vibrations in hydroxyl or carbonyl groups [29]. At 3038 cm^{-1} a band ascribed to =C-H stretching was also identified (except for the sample carbonized at 400 °C). The peak observed at 2921 cm^{-1} is related to stretching vibrations of aliphatic C-H (CH_2 group) [29-31]; however, it was observed that for samples carbonized at 600 °C this peak disappeared. A band characteristic of substituted benzene rings was also detected at 1916 cm^{-1} [30] (except for the sample carbonized at 400 °C). Besides, the band at about 1695 cm^{-1} can be assigned to C=O stretching vibrations corresponding to carbonyl, quinone, ester or carboxyl [32]; the band at about 1584 cm^{-1} can be assigned to COO^- antisymmetric stretching [30] and

the band at 1146 cm^{-1} is attributed to C-O-C antisymmetric stretching vibrations [32]. The bands in the 875-750 cm^{-1} region are assigned to aromatic C-H out-of-plane bending vibrations [7, 33, 34].

A.5. Inductively coupled plasma analysis

Inductively coupled plasma (ICP) is a powerful technique for detecting and analyzing trace and ultra-trace elements. In the present work, metallic elements in CMSM were estimated using an inductively coupled plasma mass spectrometer (Thermo, model X series) and an inductively coupled plasma-optical emission spectrometer (Horiba Jobin Yvon, model Activa M). The preparation of the samples for ICP analysis was performed by microwave-assisted digestion using nitric acid. Table A.8 shows the elements and respective concentration present within the cellophane precursor and CMSM. Sodium, chromium and manganese were found within the cellophane film and consequently on CMSM prepared at different carbonization end temperatures. As expected, the sodium concentration within the samples decreased with the increase of the carbonization end temperature; this is in accordance with XPS analysis already discussed (Table S.2, Chapter 3.B) that indicated that sodium concentration at sample's surface increased with the carbonization temperature increment.

Table A.8. Concentration of the elements present within the precursor and different produced CMSM.

Sample	Analyte ($\mu g \cdot L^{-1}$)		
	Na	Cr	Mn
Precursor	61.6	0.041	0.056
CMSM 400	56.6	0.036	0.040
CMSM 500	58.3	0.029	0.037
CMSM 550	51.8	0.035	0.042
CMSM 600	52.3	0.029	0.042

A.6. References

[1] M.C. Campo, F.D. Magalhães, A. Mendes, Carbon molecular sieve membranes from cellophane paper, Journal of Membrane Science, 350 (2010) 180-188.

[2] A.C. Ferrari, J. Robertson, Interpretation of Raman spectra of disordered and amorphous carbon, Physical Review B, 61 (2000) 14095-14107.

[3] J. Schwan, S. Ulrico, V. Batori, H. Ehrhart, Raman spectroscopy on amorphous carbon films, Journal of Applied Physics, 80 (1996) 440-447.

[4] A. Sadezky, H. Muckenhuber, H. Grothe, R. Niessner, U. Pöschl, Raman microspectroscopy of soot and related carbonaceous materials: Spectral analysis and structural information, Carbon, 43 (2005) 1731-1742.

[5] M. Šupová, J. Svítilová, Z. Chlup, M. Černý, Z. Weishauptová, T. Suchý, V. Machovič, Z. Sucharda, M. Žaloudková, Relation between mechanical properties and pyrolysis temperature of phenol formaldehyde resin for gas separation membranes, Ceramics-Silikáty, 56 (2012) 40-49.

[6] A.C. Ferrari, J. Robertson, Interpretation of Raman spectra of disordered and amorphous carbon, Physical Review B, 61 (2000) 14095-14107.

[7] M. Sevilla, A.B. Fuertes, The production of carbon materials by hydrothermal carbonization of cellulose, Carbon, 47 (2009) 2281-2289.

[8] S. Tanaka, T. Yasuda, Y. Katayama, Y. Miyake, Pervaporation dehydration performance of microporous carbon membranes prepared from resorcinol/formaldehyde polymer, Journal of Membrane Science, 379 (2011) 52-59.

[9] A.C. Lua, J. Su, Effects of carbonisation on pore evolution and gas permeation properties of carbon membranes from Kapton® polyimide, Carbon, 44 (2006) 2964-2972.

[10] L. Zhang, D. Ruan, J. Zhou, Structure and Properties of Regenerated Cellulose Films Prepared from Cotton Linters in NaOH/Urea Aqueous Solution, Industrial & Engineering Chemistry Research, 40 (2001) 5923-5928.

[11] R. Hussain, R. Qadeer, M. Ahmad, M. Saleem, X-ray diffraction study of heat-treated graphitized and ungraphitized carbon, Turkish Journal of Chemistry, 24 (2000) 177-183.

[12] J.L. Figueiredo, M.F.R. Pereira, The role of surface chemistry in catalysis with carbons, Catalysis Today, 150 (2010) 2-7.

[13] Y. Otake, R.G. Jenkins, Characterization of oxygen-containing surface complexes created on a microporous carbon by air and nitric acid treatment, Carbon, 31 (1993) 109-121.

[14] Q.L. Zhuang, T. Kyotany, A. Tomita, The change of TPD pattern of o_2-gasified carbon upon air exposure, Carbon, 32 (1994) 539-540.

[15] U. Zielke, K.J. Hüttinger, W.P. Hoffman, Surface-oxidized carbon fibers: I. Surface structure and chemistry, Carbon, 34 (1996) 983-998.

[16] Q.L. Zhuang, T. Kyotani, A. Tomita, DRIFT and TK/TPD analyses of surface oxygen complexes formed during carbon gasification, Energy & Fuels, 8 (1994) 714-718.

[17] Q.-L. Zhuang, T. Kyotany, A. Tomita, Abstracts Carbon, Granada, Spain, 94 (1994) p.466.

[18] B. Marchon, J. Carrazza, H. Heinemann, G.A. Somorjai, TPD and XPS studies of O_2, CO_2, and H_2O adsorption on clean polycrystalline graphite, Carbon, 26 (1988) 507-514.

[19] J. Driel, in: A. Capelle, F. de Vooys (Eds.) Activated Carbon-A Fascinating Material, Norit Amersfoort, The Netherlands, 1983, pp. 40-57.

[20] K. Ishimaru, T. Hata, P. Bronsveld, D. Meier, Y. Imamura, Spectroscopic analysis of carbonization behavior of wood, cellulose and lignin, Journal of Materials Science, 42 (2007) 122-129.

[21] M.I. Vázquez, J. Benavente, A study of temperature effect on chemical, structural and transport parameters determined for two different regenerated cellulose membranes, Journal of Membrane Science, 219 (2003) 59-67.

[22] Y.-R. Rhim, D. Zhang, D.H. Fairbrother, K.A. Wepasnick, K.J. Livi, R.J. Bodnar, D.C. Nagle, Changes in electrical and microstructural properties of microcrystalline cellulose as function of carbonization temperature, Carbon, 48 (2010) 1012-1024.

[23] L.A. Langley, D.E. Villanueva, D.H. Fairbrother, Quantification of surface oxides on carbonaceous materials, Chemistry of Materials, 18 (2006) 169-178.

[24] P.H. Gaskell, A. Saeed, P. Chieux, D.R. McKenzie, Neutron-scattering studies of the structure of highly tetrahedral amorphous diamondlike carbon, Physical Review Letters, 67 (1991) 1286-1289.

[25] H. Darmstadt, C. Roy, S. Kaliaguine, S.J. Choi, R. Ryoo, Surface chemistry of ordered mesoporous carbons, Carbon, 40 (2002) 2673-2683.

[26] H. Darmstadt, D. Pantea, L. Sümmchen, U. Roland, S. Kaliaguine, C. Roy, Surface and bulk chemistry of charcoal obtained by vacuum pyrolysis of bark: influence of feedstock moisture content, Journal of Analytical and Applied Pyrolysis, 53 (2000) 1-17.

[27] H. Darmstadt, C. Roy, S. Kaliaguine, ESCA characterization of commercial carbon blacks and of carbon blacks from vacuum pyrolysis of used tires, Carbon, 32 (1994) 1399-1406.

[28] D. Ciolacu, F. Ciolacu, V.I. Popa, Amorphous cellulose – structure and characterization, Cellulose Chemistry and Technology, 45 (2011) 13-21.

[29] C. Araujo-Andrade, F. Ruiz, J.R. Martínez-Mendoza, H. Terrones, Infrared and Raman spectra, conformational stability, ab initio calculations of structure, and vibrational assignment of α and β glucose, Journal of Molecular Structure: THEOCHEM, 714 (2005) 143-146.

[30] J.M. Chalmers, P.R. Griffiths, Handbook of vibrational spectroscopy, Wiley, Virginia, 2002.

[31] J. Ibarra, E. Muñoz, R. Moliner, FTIR study of the evolution of coal structure during the coalification process, Organic Geochemistry, 24 (1996) 725-735.

[32] B.M. Kabyemela, T. Adschiri, R.M. Malaluan, K. Arai, Glucose and fructose decomposition in subcritical and supercritical water: detailed reaction pathway, mechanisms, and kinetics, Industrial & Engineering Chemistry Research, 38 (1999) 2888-2895.

[33] W.N.R.W. Isahak, M.W.M. Hisham, M.A. Yarmo, Highly porous carbon materials from biomass by chemical and carbonization method: a comparison study, Journal of Chemistry, 2013 (2013) 1-6.

[34] A.C. Lua, T. Yang, Effect of activation temperature on the textural and chemical properties of potassium hydroxide activated carbon prepared from pistachio-nut shell, Journal of Colloid and Interface Science, 274 (2004) 594-601.

Appendix B

Journal of Membrane Science 459 (2014) 207–216

Contents lists available at ScienceDirect

Journal of Membrane Science

journal homepage: www.elsevier.com/locate/memsci

Preparation and characterization of carbon molecular sieve membranes based on resorcinol–formaldehyde resin

Sandra C. Rodrigues [a], Roger Whitley [b], Adélio Mendes [a,*]

[a] LEPABE – Faculdade de Engenharia, Universidade do Porto, Rua Dr. Roberto Frias, 4200-465 Porto, Portugal
[b] Air Products and Chemicals, Inc., Hamilton Blvd., Allentown, PA 18195-1501, USA

ARTICLE INFO

Article history:
Received 5 September 2013
Received in revised form
6 February 2014
Accepted 8 February 2014
Available online 28 February 2014

Keywords:
Carbon molecular sieve membrane
Resorcinol–formaldehyde resin
Boehmite nanoparticles
Gas separation

ABSTRACT

Carbon molecular sieve membranes (CMSM) were prepared on α-alumina supports by carbonization of a resorcinol–formaldehyde resin loaded with boehmite. Two series of carbon membranes produced at 500 °C and 550 °C carbonization end temperatures were prepared. The influence of the carbonization end temperature on the structure, morphology and performance of the membranes was examined by scanning electron microscopy, thermogravimetric analysis, CO_2 adsorption and permeation to N_2, O_2, He, H_2 and CO_2 at temperatures from 25 °C to 120 °C. SEM photographs showed carbon membranes with a thin and very uniform layer and a thickness of ca. 3 μm. Carbon dioxide adsorption isotherms revealed that all the produced carbon membranes have a well-developed microporous structure. Nevertheless, the membranes carbonized at 550 °C have more ultramicropores and a narrower pore size distribution. The permselectivity of CMSM prepared at this temperature surpasses the Robeson upper bound for polymeric membranes, especially regarding ideal selectivities of pairs O_2/N_2 (O_2 permeation rate: 9.85×10^{-10} mol m^{-2} s^{-1} Pa^{-1} and ideal selectivity: >11.5), H_2/N_2 (H_2 permeation rate: 5.04×10^{-8} mol m^{-2} s^{-1} Pa^{-1} and ideal selectivity: >586) and He/N_2 (He permeation rate: 4.68×10^{-8} mol m^{-2} s^{-1} Pa^{-1} and ideal selectivity: >544).

1. Introduction

Carbon molecular sieve membranes have emerged as promising candidates for gas separation applications because of their attractive characteristics such as superior thermal resistance, chemical stability in corrosive environments, high permeabilities, as well as excellent selectivities compared to polymeric membranes [1–3]. Carbon membranes are prepared by carbonization of polymeric precursors under controlled inert atmosphere [4,5]; the polymeric precursor should withstand high temperature treatment without much shrinkage [6] and should have a high carbon yield [1]. After the carbonization step, CMSM present an amorphous nanoporous skeleton [6,7]; Fig. 1 shows an HR-TEM photo of a carbon molecular sieve membrane showing no ordered structural building units [8].

CMSM have a slit-like pore structure, which provides a unique combination of micropore (0.7–2 nm) and ultramicropore (less than 0.7 nm) networks [9,10]. The larger pores are responsible for sorption and ultramicropores are accountable for the molecular sieving mechanism since they approach the molecular dimensions of diffusing gas molecules and consequently allow the passage of smaller species of a gas mixture and obstruct the larger ones [2,5]. The exceptional gas separation performance of CMSM is made possible due to the combination of this molecular sieving transport with a solution–diffusion mechanism [4,6,11].

Some parameters such as carbonization conditions (heating rate, end temperature, soaking time and gas atmosphere) and pre-/post-treatment conditions (thermostabilization, oxidation and chemical vapor deposition) determine the microstructure and gas permeance properties of the carbon molecular sieve membranes [12–15]. But above all, polymer precursor has a crucial function in determining the final structure of the carbon membranes since different polymer precursors carbonized in the same conditions lead to carbon membranes with different properties [2,16].

Research efforts have been focused on carbon molecular sieve membranes for gas separation obtained from the carbonization of various polymeric precursors such as polyimides [15–21], cellulose [22,23], polyacrylonitrile [24], poly(furfuryl alcohol) [25,26] and phenolic resins [4,8,27,28]. Nevertheless, the search for ways to produce carbon membranes with excellent separation properties and stability, without losing the economical processability of polymeric membranes, still presents a major challenge in this field.

* Corresponding author. Tel.: +1 351 22 508 1695; fax: +1 351 22 508 1449.
E-mail address: mendes@fe.up.pt (A. Mendes).

http://dx.doi.org/10.1016/j.memsci.2014.02.013
0376-7388

Resorcinol–formaldehyde resin (Fig. 2) makes an excellent precursor material for the production of CMSM due to its considerable fixed-carbon yield, high inherent purity and low cost [29–32].

However, very few studies have been reported on the production of carbon molecular sieve membranes from resorcinol–formaldehyde resin. Tanaka et al. [33] prepared microporous carbon membranes on a porous α-alumina support by a partial carbonization of a resorcinol–formaldehyde resin for pervaporation applications. Dong et al. [34] prepared microporous carbon membranes on α-alumina supports carbonizing resorcinol–formaldehyde polymer precursor and quaternary ammonium compounds (tetramethylammonium bromide and tetrapropylammonium) for dehydration of water/ethanol and water/isopropanol mixtures by pervaporation. Yoshimune et al. [35] obtained highly mesoporous carbon membranes by carbonizing sol–gel derived mesoporous resorcinol–formaldehyde membranes.

In general, the methods described in the literature to obtain supported carbon membranes are complex and the coating–carbonization cycle must be repeated several times to achieve crack-free CMSM, which needs time and special care. Only a few researchers have reported the development of defect-free membranes by a single dipping–drying–carbonization step [1,4,8, 36–40]. The addition of boehmite particles with needle shape to the CMSM precursor recently proved to be effective for producing crack-free supported membranes in a single dipping–drying–carbonization step. Boehmite (γ-AlO(OH)) is an aluminum oxide hydroxide, and it has been recently used by our research team to prepare carbon molecular sieve membranes [4,8]. During carbonization, boehmite nanoparticles dehydrate and Al_2O_3 nanowires are formed and homogeneously distributed in the carbon matrix. Teixeira et al. [8] prepared composite carbon membranes from a Resol phenolic resin loaded with boehmite nanoparticles in a single coating–drying–carbonization step. The composite carbon membranes obtained exhibited high permeability to C_3H_6 and considerable C_3H_6/C_3H_8 ideal selectivity, well above the state-of-the-art plot for polymeric membranes for this separation. O_2/N_2, He/N_2 and CO_2/N_2 ideal selectivities of 5, 34 and 30, respectively, were achieved. In this study, the boehmite nanoparticles' key role was identified: these needle-shaped particles control the polymeric precursor rheology.

This work proposes the incorporation of low cost nanoparticles (boehmite) in a low cost resorcinol–formaldehyde resin to prepare composite carbon molecular sieve membranes in a single dipping–drying–carbonization step. Defect-free supported carbon membranes were prepared successfully and reproducibly at different carbonization end temperatures of 500 °C (CMSM 500) and 550 °C (CMSM 550). Dry films of the composite top layer were prepared, and morphological characterization of the material was performed by scanning electron microscopy (SEM) and thermogravimetric analysis (TGA). Pore size distributions were obtained from the adsorption equilibrium isotherms of carbon dioxide at 0 °C. Permeation experiments were performed to assess the permeability toward N_2, O_2, CO_2, He and H_2 as well as the ideal selectivities for separations of industrial relevance.

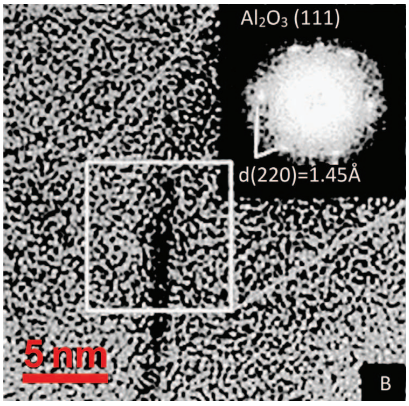

Fig. 1. HRTEM image of a composite carbon molecular sieve membrane derived from phenolic resin incorporated with ceramic particles of boehmite (carbonized at 550 °C) [24].

2. Experimental

2.1. Materials

A resorcinol–formaldehyde resin, used as precursor, was provided by Continental Portugal. *N*-methyl-2-pyrrolidone (NMP) was supplied by Acros Organics. Boehmite nanoparticles (10% Boehmite solution, particle size 8–20 nm) were supplied by Kawaken Fine Chemicals Co. Ltd. The α-alumina tubular supports were purchased from Inopor. Non-porous alumina tubes were bought from Omega Engineering Limited. The permanent gases were supplied by Air Liquide (99.999% pure).

2.2. Tubular ceramic supports preparation

The ends of the porous Al_2O_3 supports were attached to non-porous Al_2O_3 tubes and sealed with a glass sealant at 1150 °C. The supports have a mean pore size of 200 nm (located in the outer part of the tube), an external diameter of 10 mm and a length of 70 mm. An effective length of approximately 50 mm was left for dip-coating.

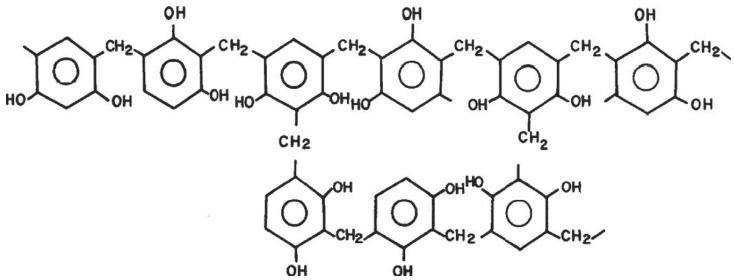

Fig. 2. Structure of a resorcinol–formaldehyde resin.

2.3. Preparation of carbon molecular sieve membranes

Resorcinol–formaldehyde resin was diluted in NMP to prepare a 15 wt% resin solution with a viscosity of ca. 0.04 Pa s and a pH of 4.6. A composite coating solution of 14 wt% of resorcinol–formaldehyde resin, 0.5 wt% of boehmite nanoparticles, 0.6 wt% of ethylenediamine monohydrate and 85.6 wt% of NMP was prepared. Ethylenediamine monohydrate was used as a basic catalyst of the polymerization reaction.

Supported membranes were then prepared by dip coating the alumina tubular supports in the coating solution using a vacuum pump. The resorcinol–formaldehyde resin-based membranes were dried in a rotating oven at 70 °C overnight to avoid a quick release of the solvent during the carbonization stage that could damage the carbon matrix, causing cracks or defects. Subsequently, the membranes were left at 90 °C for 7 h.

The carbonization of the precursor was accomplished in a quartz tube (80 mm in diameter and 1.5 m in length) inside a tubular horizontal Termolab TH furnace. To guarantee temperature homogeneity along the quartz tube, the furnace has three separating heating elements controlled by three PID control heating parameters. Fig. 3 gives a schematic overview of the furnace.

The carbonization was performed under N_2 atmosphere, flow rate of 170 mL min^{-1} and a heating rate of 1 °C min^{-1}. Fig. 4 shows the temperature history to prepare the carbon molecular sieve membranes from resorcinol–formaldehyde resin.

First, the temperature was raised from ambient to 110 °C at a rate of 1 °C min^{-1} and held at this temperature for 30 min; subsequently, the temperature was increased from 110 °C to the desired carbonization end temperature (again at a heating rate of 1 °C min^{-1}) and held at that temperature for 2 h; afterward, the membranes were allowed to cool to room temperature.

2.4. Scanning electron microscopy and energy dispersive X-ray spectroscopy analysis

The samples were fixed onto aluminum sample holders with Araldite™ cement, sputter-coated with palladium–gold (Bal–Tec – SCD 050) and observed in a scanning electron microscope (SEM, FEI Quanta 400FEG).

2.5. Thermogravimetric analysis

TGA were carried out in a Netzsch TG 209 F1 Iris thermogravimetric balance with a resolution of 0.1 μg. It was analyzed the dipping solution used to prepare the CMSM. The sample was previously dried in the oven at 110 °C for 72 h in order to remove most of the solvent. The characteristic curve was determined from 20 °C to 900 °C under N_2 atmosphere with a heating rate of 10 °C min^{-1}.

2.6. Pore size characterization

The pore size distribution and the porosity volume of the produced CMSM were obtained based on the adsorption equilibrium isotherm of CO_2 at 0 °C determined in a magnetic suspension balance as described elsewhere [41].

2.7. Permeation experiments

The permeation properties of the produced CMSM were obtained by probing the membrane with pure gases. Briefly, N_2, O_2, He, H_2 and CO_2 were introduced shell side at 0.11–0.15 MPa feed pressure (Horiba Stec, model UR7340) and the permeated flow rate at room pressure was determined by one of the three flow meters (Bronkhorst, ranges: 0–1, 0–10 and 0–100 mL_N min^{-1}) [8].

All the results obtained are averages based on the measurements of at least three membrane samples prepared and tested under the same conditions.

3. Results and discussion

3.1. Scanning electron microscopy and energy dispersive X-ray spectroscopy analysis

The morphology and qualitative elemental composition of carbon molecular sieve membranes were determined by scanning

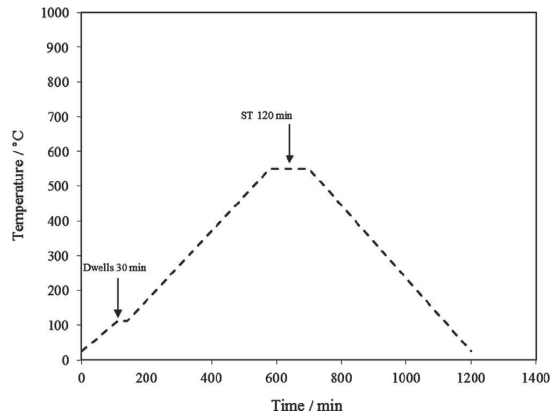

Fig. 4. Temperature history to prepare carbon molecular sieve membranes from resorcinol–formaldehyde resin. End temperature: 550 °C.

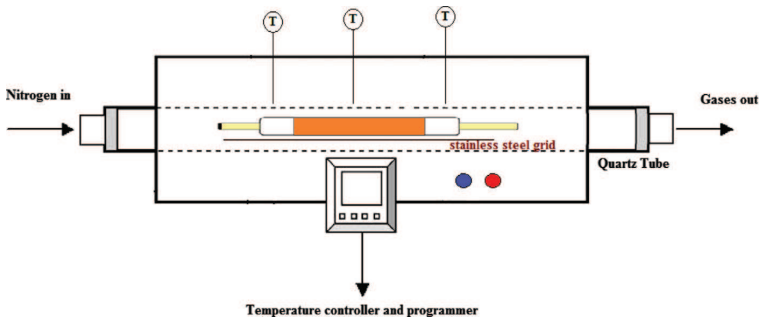

Fig. 3. Schematic overview of the furnace setup.

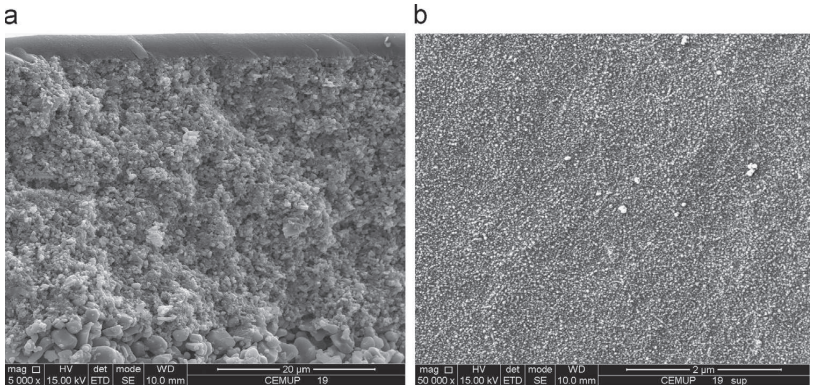

Fig. 5. SEM photographs of one-coated resorcinol–formaldehyde based carbon membrane carbonized at 550 °C: (a) cross section; (b) surface view.

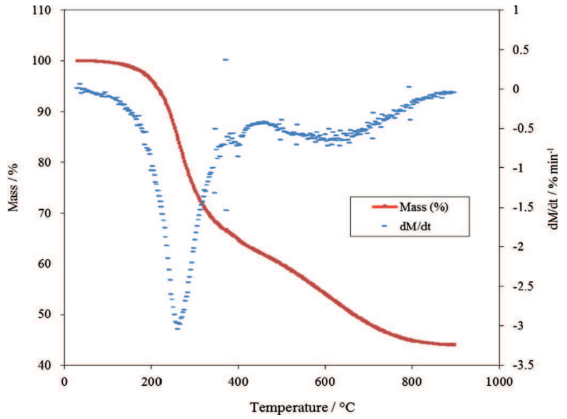

Fig. 6. Thermogravimetric analysis of composite dipping solution containing 14 wt% of resin and 0.5 wt% boehmite nanoparticles used to prepare CMSM.

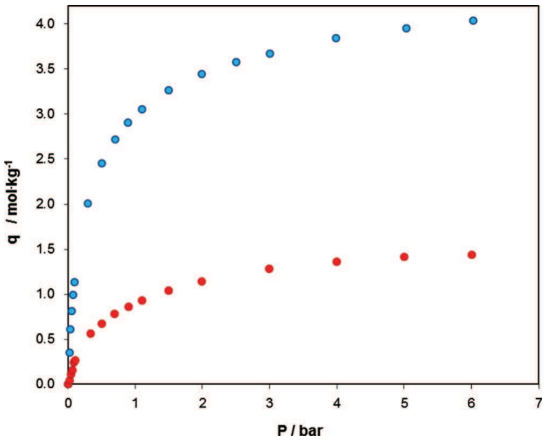

Fig. 7. Adsorption equilibrium isotherm of CO_2 at 0 °C for CMSM 500 and CMSM 550.

electron microscopy and energy dispersive X-ray spectroscopy (EDS), respectively. SEM microphotographs of cross-section of a supported CMSM 550 are shown in Fig. 5.

Fig. 5(a) indicates that two different parts can be distinguished: the top thin layer and the porous alumina support. A defect-free carbon film of ca. 3 μm thickness was uniformly formed on the top of the α-alumina tubular support. Fig. 5(b) shows that Al_2O_3 nanoparticles were well distributed in the carbon matrix. EDS analysis also revealed a uniform carbon and Al_2O_3 composition along the layer thickness (data not shown).

3.2. Thermogravimetric analysis

TGA was used to assess the thermal decomposition kinetics and stability of polymer in an inert atmosphere. TGA was performed on the dry dipping solution used for the preparation of the CMSM. The characteristic curve was obtained under N_2 atmosphere and is plotted in Fig. 6.

Fig. 6 shows that from room temperature to 175 °C the composite film loses about 2% of its original weight. This loss is attributed to the release of adsorbed water from the precursor. Between 175 °C and 350 °C the sample loses ca. 30% of its original weight, which should be related to the degradation of the resorcinol–formaldehyde resin. It has been reported that at this temperature gases from the amine decomposition generate micropores in the carbonized resorcinol–formaldehyde resin membrane [42]. Between 500 °C and 800 °C a lower weight loss of 15% is observed; at 900 °C the total weight loss is approximately 44%; this weight loss is in accordance with the literature [35].

3.3. Porosity assessment

The adsorption of nitrogen at −196 °C is the most frequently used technique to assess the microporosity of carbonaceous materials. However, when ultramicroporosity is involved some diffusional limitations occur and adsorption of carbon dioxide at 0 °C is a good alternative to overcome this problem [43,44]. The adsorption equilibrium isotherms of CO_2 at 0 °C for CMSM 500 and CMSM 550 are plotted in Fig. 7.

Dubinin–Raduschkevisch (DR) equation is commonly used to describe the adsorption in micropores:

$$\frac{w}{w_0} = \exp\left[-\left(\frac{RT\ln(P_0/P)}{E_0}\right)^2\right] \quad (1)$$

where W is the micropore volume, P is the pressure, W_0 is the total micropore volume, E_0 is the characteristic energy for adsorption, P_0 is the vapor pressure of the free liquid, R is the gas constant and T is the absolute temperature. However, the DR equation only provides a reasonable description of adsorption in micropores when the characteristic curve obtained from CO_2 adsorption is linear. Recently a more general equation was proposed, the Dubinin–Astakhov (DA) equation:

$$\frac{w}{w_0} = \exp\left[-\left(\frac{RT\ln(P_0/P)}{E_0}\right)^n\right] \quad (2)$$

where n is an adjustable parameter. DR equation results from DA equation for the particular case of $n=2$.

In the present work, the characteristic curves obtained from the CO_2 adsorption isotherm on CMSM 500 and CMSM 550 are not very linear, indicating that the DR equation could not provide reasonable descriptions. Therefore, micropore volume and the characteristic energy for adsorption were determined by fitting the Dubinin–Astakhov equation to experimental data. Fig. 8 presents the characteristic curve for CMSM 550.

It can be seen that the DA equation with $n=2.6$ fits very well the experimental data. It is important to note that the slope of the plot is related to E_0 and the intercept is related to W_0. Table 1 presents a summary of the structural parameters for the studied samples. Generally, empiric correlations developed by Stoeckli are used to estimate the mean pore width. However, Stoeckli equation can only be used when the DR equation applies. For that reason, the mean pore width in the present work was determined by a weighted average. For CMSM 550, the micropore volume of 0.40 $cm^3\,g^{-1}$ is slightly higher when compared with other reported values [4,21,41,45,46]. However, the mean pore width (obtained by a weighted average) has the usual value found for carbon molecular sieves [4,45,46]. For CMSM 500, the mean pore width (obtained by a weighted average) is a little higher when compared with other values in the literature [4,8,45,46].

Pore size distribution for all carbon molecular sieve membranes was obtained using the method proposed by Do et al. [43,47] for the determination of micropore size distribution in carbonaceous materials. Figs. 9 and 10 show the pore size distribution obtained for CMSM 550 and CMSM 500, respectively.

It can be seen that the studied carbon membranes present ultramicropores (0.3–0.7 nm range) and larger micropores (0.7–1 nm). However, CMSM 500 have a large number of micropores with larger dimensions when compared to CMSM 550. On the other hand, CMSM 550 have a large number of micropores with narrower pore size distributions.

These small changes in the number and size of both ultramicropores and larger micropores influence the permeability and permselectivity performance of both membranes, as will be shown in Section 3.4.

3.4. Single gas permeation experiments

The permeance of the supported CMSM obtained at 500 °C and 550 °C was assessed for N_2 (0.364 nm), O_2 (0.346 nm), He

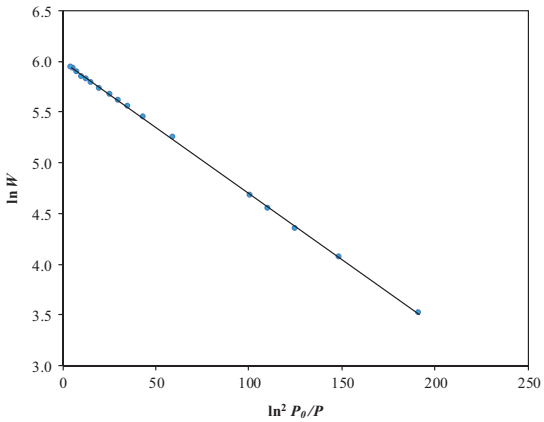

Fig. 8. CO_2 characteristic curve for CMSM 550 at 0 °C (points experimental data; solid line DA fitting).

Table 1
Structural parameters for carbon molecular sieve membranes carbonized at 500 °C and 550 °C.

Parameter	CMSM 500	CMSM 550
W_0 ($cm^3\,g^{-1}$)	0.13	0.40
E_0 ($kJ\,mol^{-1}$)	11.14	12.06
ℓ (nm)	0.68	0.58

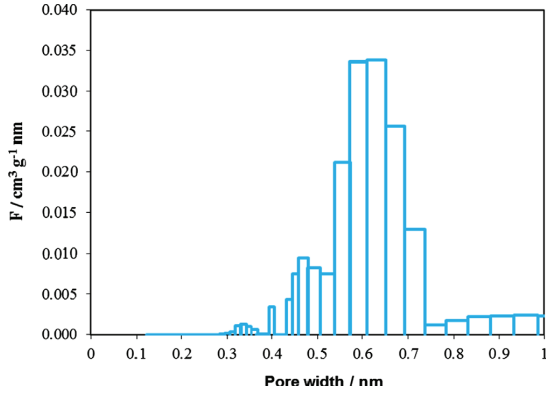

Fig. 9. Micropore size distribution for CMSM 550.

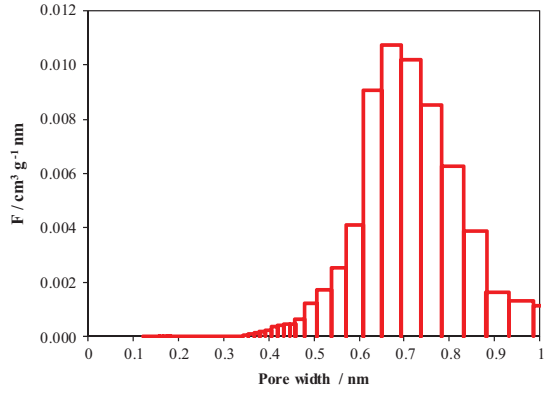

Fig. 10. Micropore size distribution for CMSM 500.

(0.260 nm), H_2 (0.290 nm) and CO_2 (0.335 nm) – the values in brackets correspond to the kinetic diameter of the gases [48].

The produced CMSM were exposed to the room conditions for 6 days. Afterward, the samples were heated at various temperatures (140 °C, 160 °C and 200 °C) for 2 h under N_2 atmosphere with a heating rate of 0.7 °C min^{-1}. The feed pressure was varied between 0.11 MPa and 0.15 MPa while the permeate was kept at ca. 0.10 MPa (atmospheric pressure). Gas permeation experiments were carried out at 25–120 °C.

The effect of carbonization end temperature on the permeability of two sets of resorcinol–formaldehyde carbon membranes is summarized in Fig. 11.

It can be concluded that the devised preparation process originates membranes with very similar permeation properties. Moreover, the samples carbonized at higher end temperature (CMSM 550) have generically smaller gas permeation rate; for example, the permeability to N_2 became around 3 times smaller when compared to CMSM 500 samples. This can be attributed to the ultramicropores shrinkage [49,50]. CMSM 500 also have a larger mean pore width, $\ell = 0.68$ nm compared to CMSM 550, $\ell = 0.58$ nm (Table 1). However, CMSM 550 actually have a larger volume of ultramicropores (comparing Figs. 9 and 10), which gives He a higher permeance in CMSM 550 than in CMSM 500.

The performance of a membrane toward a separation is characterized by the permeability to the target species as well as the corresponding selectivities. Under all tested conditions, it was observed that the best compromise between permeability and selectivity was achieved for the membranes carbonized at 550 °C, activated at 140 °C and measured at 120 °C. Therefore, these results will be further discussed here.

Fig. 12, Table 2 and Fig. 13, Table 3 show the permeances as a function of the feed pressure for CMSM 500 and CMSM 550, respectively.

The permeance toward all gases is pressure-dependent: Nishiyama et al. [42] and Lagorsse et al. [45] reported that this behavior seems to become more evident as the intensity of the adsorbate/adsorbent interactions increases. Since CO_2 shows a more pronounced

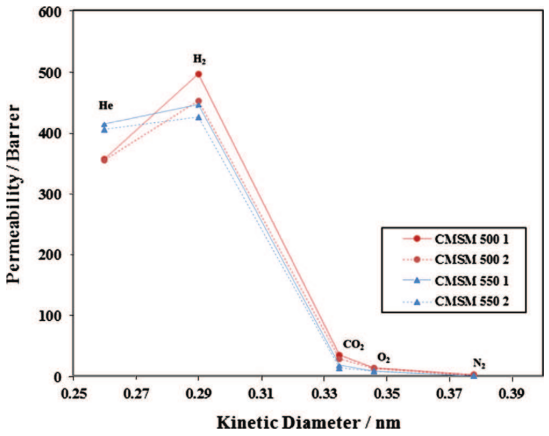

Fig. 11. Permeability as a function of kinetic diameter of gas molecules for two sets of supported carbon membranes obtained at different end carbonization temperatures.

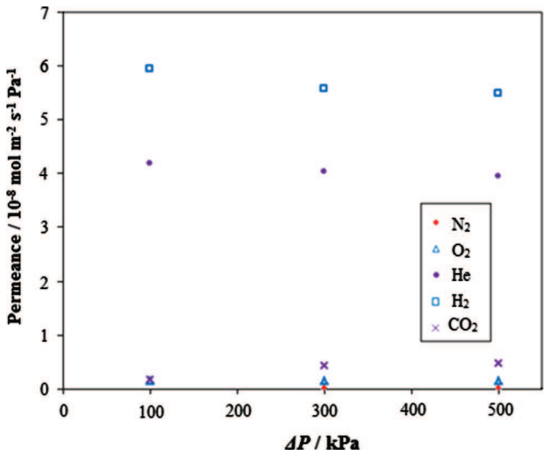

Fig. 12. Gases permeances as a function of feed pressure for CMSM 500. Membranes were activated at 140 °C for 2 h under N_2 atmosphere before permeation.

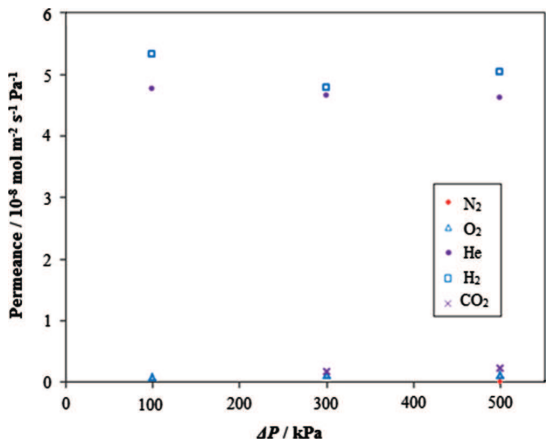

Fig. 13. Gases permeances as a function of feed pressure for CMSM 550. Membranes were activated at 140 °C for 2 h under N_2 atmosphere before permeation.

Table 2
Permeance properties as a function of the pressure difference for CMSM 500. Membranes were activated at 140 °C for 2 h under N_2 atmosphere before permeation.

Feed pressure (kPa)	Permeance (mol m^{-2} s^{-1} Pa^{-1})				
	N_2	O_2	He	H_2	CO_2
500	2.465×10^{-10}	1.513×10^{-9}	3.947×10^{-8}	5.484×10^{-8}	4.831×10^{-9}
300	[a]	1.562×10^{-9}	4.017×10^{-8}	5.571×10^{-8}	4.310×10^{-9}
100	[a]	1.403×10^{-9}	4.189×10^{-8}	5.931×10^{-8}	1.615×10^{-9}

[a] Below the detection limit.

Table 3
Permeance properties as a function of the pressure difference for CMSM 550. Membranes were activated at 140 °C for 2 h under N_2 atmosphere before permeation.

Feed pressure (kPa)	Permeance (mol m^{-2} s^{-1} Pa^{-1})				
	N_2	O_2	He	H_2	CO_2
500	$< 8.530 \times 10^{-11}$	1.062×10^{-9}	4.614×10^{-8}	5.029×10^{-8}	2.256×10^{-9}
300	[a]	1.075×10^{-9}	4.653×10^{-8}	4.775×10^{-8}	1.774×10^{-9}
100	[a]	8.173×10^{-10}	4.766×10^{-8}	5.312×10^{-8}	$< 8.530 \times 10^{-10}$

[a] Below detection limit.

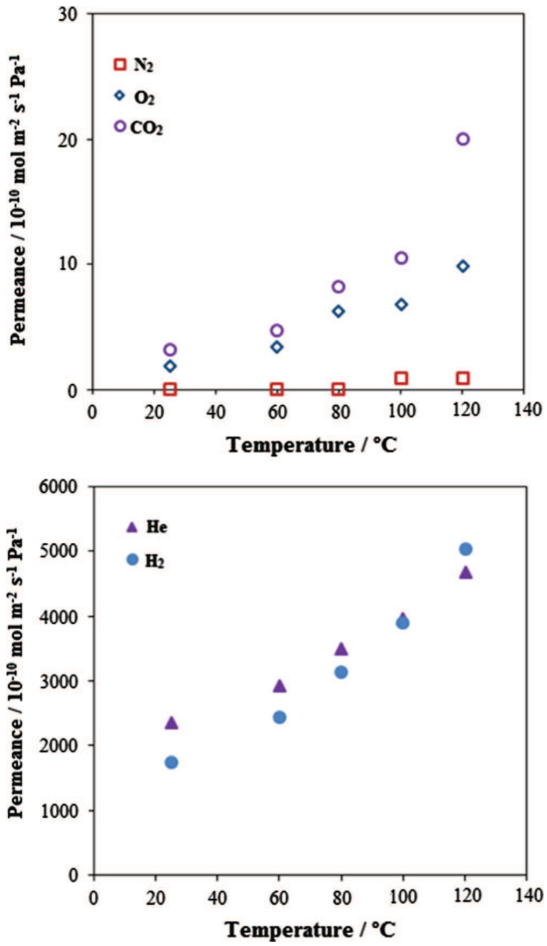

Fig. 14. Gases permeances as a function of temperature for CMSM 550. Membranes were activated at 140 °C for 2 h under N_2 atmosphere before permeation.

permeance increase with pressure, CO_2 should have more affinity to the resorcinol–formaldehyde based carbon membranes than the other gases.

The effect of temperature on the permeance of CMSM 550 to the probing gases is illustrated in Fig. 14.

It can be seen that membrane permeance increases as the temperature increases. This reveals that the gas transport through the carbon molecular sieve membranes is an activated diffusion process, as expected for a molecular sieve mechanism [2]. From the change of CMSM permeance with temperature, the apparent activation energy can be estimated according to the following Arrhenius equation:

$$\ln(P) = -\frac{E_a}{RT} + \ln\left(\frac{D_0}{RT}\right) \quad (3)$$

where D_0 is a pre-exponential factor, E_a is the apparent activation energy, P is the permeability, R is the gas constant and T is the absolute temperature.

The estimated apparent activation energies for O_2, He, H_2 and CO_2 are 17, 7, 10.8 and 18.2 kJ/mol, respectively. These values are relatively close to other values reported in literature [51]. The apparent activation energy for N_2 was not calculated because permeation data are just available for temperatures of 100 °C and

Table 4
Ideal selectivities for CMSM 500 and CMSM 550. Membranes were activated at 140 °C for 2 h under N_2 atmosphere before experiments were performed.

	Ideal selectivity			
	O_2/N_2	He/N_2	H_2/N_2	CO_2/N_2
CMSM500	5.9	221.0	158.0	15.4
CMSM550	> 11.5	> 544.0	> 586.0	> 23.3

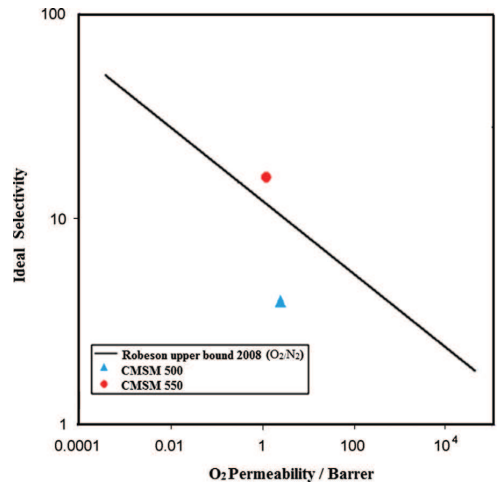

Fig. 15. Gas permeation results for O_2/N_2 in CMSM 500 and CMSM 550 and comparison with the respective upper bound plot.

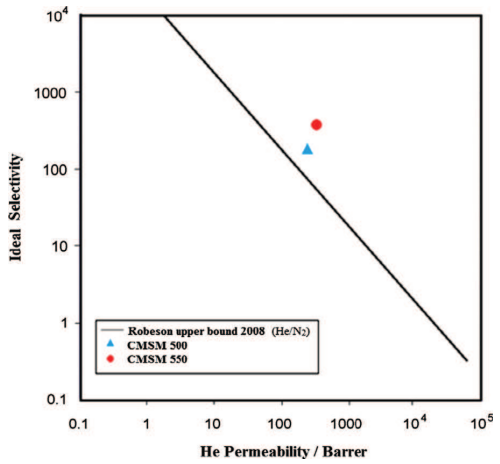

Fig. 16. Gas permeation results for He/N_2 in CMSM 500 and CMSM 550 and comparison with the respective upper bound plot.

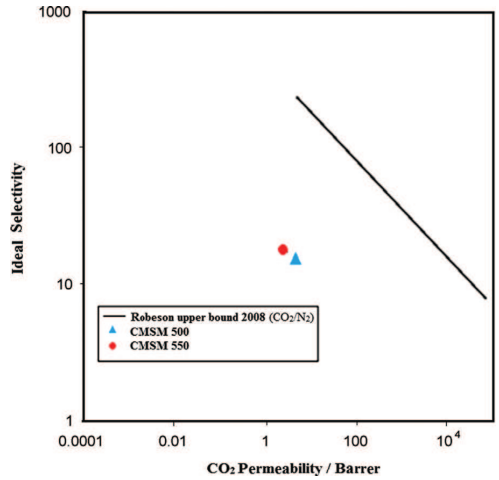

Fig. 18. Gas permeation results for CO_2/N_2 in CMSM 500 and CMSM 550 and comparison with the respective upper bound plot.

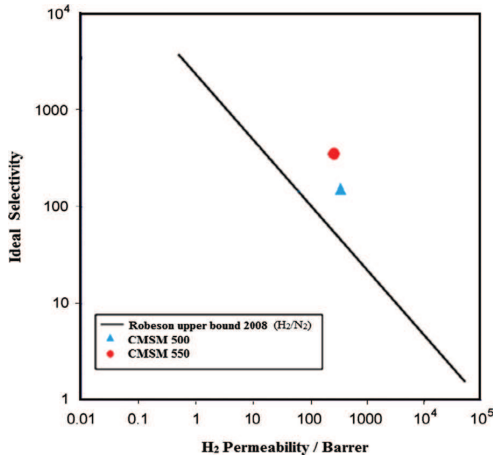

Fig. 17. Gas permeation results for H_2/N_2 in CMSM 500 and CMSM 550 and comparison with the respective upper bound plot.

above (see Fig. 14), and therefore there were not enough data to make the corresponding Arrhenius plot.

Ideal selectivities obtained for both carbon molecular sieve membrane sets are shown in Table 4.

It can be seen that ideal selectivity for all gas pairs increases significantly when the membrane carbonization end temperature increases from 500 °C to 550 °C. Small differences observed in pore size distribution and mean pore width are very important and strongly influence the diffusion of molecules with closer sizes such as N_2, O_2 and CO_2.

The obtained permeabilities and ideal selectivities were inserted into the semi-empirical plots devised by Robeson in 2008 [52]. The permeability is expressed in Barrer, which equals to 3.35×10^{-16} mol m m^{-2} s^{-1} Pa^{-1}. Figs. 15–18 illustrate the upper bound limits for O_2/N_2, He/N_2, H_2/N_2 and CO_2/N_2, respectively.

CMSM 550 showed promising results for the separation of O_2/N_2 (permeability: 8.7 Barrer; and ideal selectivity: >11.5), H_2/N_2 (permeability: 445.6 Barrer; and ideal selectivity: >586) and He/N_2 (permeability: 413.8 Barrer; and ideal selectivity: >544). Finally, Fig. 19 compares these results with permeation data of CMSM produced from other low cost precursors (phenol–formaldehyde resins).

It can be concluded that CMSM 550 exhibit higher ideal selectivities toward O_2/N_2, He/N_2 and H_2/N_2 and higher permeabilities toward H_2 and He when compared to similar studies [1,4,8,36,37,53–57]. However, lower permeabilities were obtained toward O_2 [36,53,54,56].

4. Conclusions

Carbon molecular sieve membranes were successfully prepared in a single dipping–drying–carbonization sequence. Membranes with reproducible properties were prepared from resorcinol–formaldehyde resin, a low cost precursor, loaded with boehmite nanoparticles. The effect of the carbonization end temperature was assessed and better separation properties were found for sample CMSM 550, carbonized in an inert atmosphere at 550 °C. For improving their permeation stability, membranes were contacted with ambient air for 6 days and activated at 140 °C under N_2 atmosphere. Carbon molecular sieve membranes carbonized at 550 °C end temperature showed a large number of micropores with a narrower pore-size distribution and much higher ideal selectivities and relatively similar gas permeation rates than those produced at 500 °C.

The Robeson upper bound for polymeric membranes was overtaken by CMSM 550, regarding O_2/N_2 (O_2 permeation rate: 9.85×10^{-10} mol m^{-2} s^{-1} Pa^{-1} and ideal selectivity: >11.5), H_2/N_2 (H_2 permeation rate: 5.04×10^{-8} mol m^{-2} s^{-1} Pa^{-1} and ideal selectivity: >586) and He/N_2 (He permeation rate: 4.68×10^{-8} mol m^{-2} s^{-1} Pa^{-1} and ideal selectivity: >544) separations. CMSM 550 are superior to many reported carbon membranes produced from other low cost precursors, indicating that CMSM produced from resorcinol–formaldehyde resin have potential for gas separation.

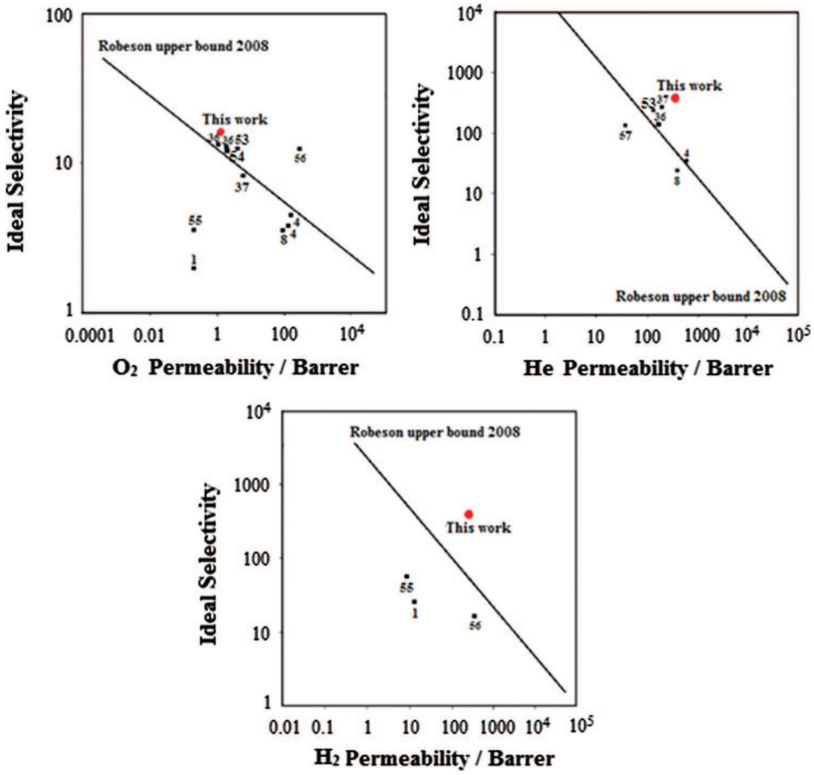

Fig. 19. Robeson upper limits and comparison with pure gas permeation results obtained with low cost phenol–formaldehyde resins derived carbon membranes. All selectivities are relative to N_2.

Acknowledgments

The authors would like to acknowledge the funding provided by the Portuguese Foundation for Science and Technology (FCT) through the Projects PTDC/EQU-EQU/114944/2009 and PTDC/EQU-EQU/104217/2008. The authors are also grateful to the European Union's Seventh Framework Programme (FP7/2007) for Fuel Cells and Hydrogen Joint Technology for funding under Grant agreement number 303476. The authors are thankful to CEMUP for the SEM/EDS analysis.

References

[1] W. Wei, G. Qin, H. Hu, L. You, G. Chen, Preparation of supported carbon molecular sieve membrane from novolac phenol–formaldehyde resin, J. Membr. Sci. 303 (2007) 80–85.
[2] A.F. Ismail, L.I.B. David, A review on the latest development of carbon membranes for gas separation, J. Membr. Sci. 193 (2003) 1–18.
[3] P.S. Tin, T.S. Chung, S. Kawi, M.D. Guiver, Novel approaches to fabricate carbon molecular sieve membranes based on chemical modified and solvent treated polyimides, Microporous Mesoporous Mater. 73 (2004) 151–160.
[4] M. Teixeira, M. Campo, D.A. Tanaka, M.A. Tanco, C. Magen, A. Mendes, Carbon Al_2O_3 Ag composite molecular sieve membranes for gas separation, Chem. Eng. Res. Des. 90 (2012) 2338–2345.
[5] A.B. Fuertes, T.A. Centeno, Preparation of supported carbon molecular sieve membranes, Carbon 37 (1999) 679–684.
[6] Y.H. Sim, H. Wang, F.Y. Li, M.L. Chua, T.S. Chung, M. Toriida, S. Tamai, High performance carbon molecular sieve membranes derived from hyperbranched polyimide precursors for improved gas separation applications, Carbon 53 (2013) 101–111.
[7] M. Kiyono, P.J. Williams, W.J. Koros, Effect of pyrolysis atmosphere on separation performance of carbon molecular sieve membranes, J. Membr. Sci. 350 (2010) 2–10.
[8] M. Teixeira, M.C. Campo, D.A. Tanaka, M.A. Tanco, C. Magen, A. Mendes, Composite phenolic resin-based carbon molecular sieve membranes for gas separation, Carbon 49 (2011) 4348–4358.
[9] S. Lowell, J.E. Shields, M.A. Thomas, M. Thommes, Characterization of Porous Solids and Powders: Surface Area, Pore Size and Density, Kluwer Academic Publishers, The Netherlands (2004) 26 (Chapter 4).
[10] A.J. Burggraaf, L. Cot, Fundamentals of Inorganic Membrane Technology, Elsevier Science, The Netherlands (1996) 71 (Chapter 4).
[11] M.B. Rao, S. Sircar, Nanoporous carbon membranes for separation of gas mixtures by selective surface, J. Membr. Sci. 85 (1993) 253–264.
[12] C.W. Jones, W.J. Koros, Carbon molecular sieve gas separation membranes I. Preparation and characterization based on polyimide precursors, Carbon 32 (1994) 1419–1425.
[13] M. Yoshino, S. Nakamura, H. Kita, K. Okamoto, N. Tanihara, Y. Kusuki, Olefin/paraffin separation performance of carbonized membranes derived from an asymmetric hollow fiber membrane of 6FDA/BPDA–DDBT copolyimide, J. Membr. Sci. 215 (2003) 169–183.
[14] H. Suda, K. Haraya, Alkene/alkane permselectivities of a carbon molecular sieve membrane, Chem. Commun. (1997) 93–94.
[15] Y.K. Kim, H.B. Park, Y.M. Lee, Gas separation properties of carbon molecular sieve membranes derived from polyimide/polyvinylpyrrolidone blends: effect of the molecular weight of polyvinylpyrrolidone, J. Membr. Sci. 251 (2005) 159–167.
[16] H.B. Park, Y.K. Kim, J.M. Lee, S.Y. Lee, Y.M. Lee, Relationship between chemical structure of aromatic polyimides and gas permeation properties of their carbon molecular sieve membranes, J. Membr. Sci. 229 (2004) 117–127.
[17] Y.K. Kim, H.B. Park, Y.M. Lee, Carbon molecular sieve membranes derived from thermally labile polymer containing blend polymer and their gas separation properties, J. Membr. Sci. 243 (2004) 9–17.
[18] Y.K. Kim, H.B. Park, Y.M. Lee, Preparation and characterization of carbon molecular sieve membranes derived from BTDA-ODA polyimide and their gas separation properties, J. Membr. Sci. 255 (2005) 265–273.
[19] A.B. Fuertes, D.M. Nevskaia, T.A. Centeno, Carbon composite membranes from Matrimid® and Kapton® polyimides for gas separation, Microporous Mesoporous Mater. 33 (1999) 115–125.
[20] K.M. Steel, W.J. Koros, An investigation of the effects of pyrolysis parameters on gas separation properties of carbon materials, Carbon 43 (2005) 1843–1856.

[21] P.S. Tin, T.S. Chung, S. Kawi, M.D. Guiver, Novel approaches to fabricate carbon molecular sieve membranes based on chemical modified and solvent treated polyimides, Microporous Mesoporous Mater. 73 (2004) 151–160.
[22] J.A. Lie, M.B. Hagg, Carbon membranes from cellulose: synthesis, performance and regeneration, J. Membr. Sci. 284 (2006) 79–86.
[23] M. Campo, F.D. Magalhaes, A. Mendes, Carbon molecular sieve membranes from cellophane paper, J. Membr. Sci. 350 (2010) 180–188.
[24] L.B. David, A.F. Ismail, Influence of the thermastablization process and soak time during pyrolysis process on the polyacrylonitrile carbon membranes for O_2/N_2 separation, J. Membr. Sci. 213 (2003) 285–291.
[25] Y.D. Cheng, R.T. Yang, Preparation of carbon molecular sieve membranes and diffusion of binary mixtures in the membrane, Ind. Eng. Chem. Res. 33 (1994) 3146–3153.
[26] C. Song, T. Wang, X. Wang, J. Qiu, Y. Cao, Preparation and gas separation properties of poly(furfuryl alcohol)-based C/CMS composite membranes, Sep. Purif. Technol. 58 (2008) 412–418.
[27] A.B. Fuertes, I. Menendez, Separation of hydrocarbon gas mixtures using phenolic resin-based carbon membranes, Sep. Purif. Technol. 28 (2002) 29–41.
[28] F.K. Katsaros, T.A. Steriotis, A.K. Stubos, A. Mitropoulos, N.K. Kanellopoulos, S. Tennison, High pressure gas permeability of microporous carbon membranes, Microporous Mesoporous Mater. 8 (1997) 171–176.
[29] S.J. Park, W.Y. Jung, Preparation and structural characterization of activated carbons based on polymeric resin, J. Colloid Interface Sci. 250 (2002) 196–200.
[30] J. Hayashi, M. Uchibayashi, T. Horikawa, K. Muroyama, V. Gomes, Synthesizing activated carbons from resins by chemical activation with K_2CO_3, Carbon 40 (2002) 2727–2752.
[31] S. Tenison, Phenolic-resin-derived activated carbons, Appl. Catal. A 173 (1998) 289–311.
[32] T. Yamamoto, T. Sugimoto, T. Suzuki, S. Mukai, H. Tamon, Preparation and characterization of carbon cryogel microspheres, Carbon 40 (2002) 1345–1351.
[33] S. Tanaka, T. Yasuda, Y. Katayama, Y. Miyake, Pervaporation dehydration performance of microporous carbon membranes prepared from resorcinol/formaldehyde polymer, J. Membr. Sci. 379 (2012) 52–54.
[34] Y.R. Dong, M. Nakao, N. Nishiyama, Y. Egashira, K. Ueyama, Gas permeation and pervaporation of water/alcohols through the microporous carbon membranes prepared from resorcinol/formaldehyde/quaternary ammonium compounds, Sep. Purif. Technol. 73 (2010) 2–7.
[35] M. Yoshimune, T. Yamamoto, M. Nakaiwa, K. Haraya, Preparation of highly mesoporous carbon membranes via a sol-gel process using resorcinol and formaldehyde, Carbon 46 (2008) 1031–1036.
[36] T.A. Centeno, A.B. Fuertes, Carbon molecular sieve membranes derived from a phenolic resin supported on porous ceramic tubes, Sep. Purif. Technol. 25 (2001) 379–384.
[37] A.B. Fuertes, I. Menendez, Separation of hydrocarbons gas mixtures using phenolic resin-based carbon membranes, Sep. Purif. Technol. 28 (2002) 29–41.
[38] A.B. Fuertes, Effect of air oxidation on gas separation properties of adsorption-selective carbon membranes, Carbon 39 (2001) 697–706.
[39] A.B. Fuertes, Adsorption-selective carbon membrane for gas separation, J. Membr. Sci. 177 (2000) 9–16.
[40] I. Menendez, A.B. Fuertes, Aging of carbon membranes under different environments, Carbon 39 (2001) 733–740.
[41] M.C. Campo, F.D. Magalhaes, A. Mendes, Comparative study between a CMS membrane and a CMS adsorbent: Part I – morphology, adsorption equilibrium and kinetics, J. Membr. Sci. 346 (2010) 15–25.
[42] N. Nishiyama, Y.R. Dong, T. Zheng, Y. Egashira, K. Ueyama, Tertiary amine-mediated synthesis of microporous carbon membranes, J. Membr. Sci. 280 (2006) 603–609.
[43] C. Nguyen, D.D. Do, Adsorption of supercritical gases in porous media: determination of micropore size distribution, J. Phys. Chem. 103 (1999) 6900–6908.
[44] S.W. Rutherford, C. Nguyen, J.E. Coons, D.D. Do, Characterization of carbon molecular sieves using methane and carbon dioxide as adsorptive probes, Langmuir 19 (2003) 8335–8342.
[45] S. Lagorsse, F.D. Magalhães, A. Mendes, Carbon molecular sieve membranes – sorption, kinetic and structural characterization, J. Membr. Sci. 241 (2004) 275–287.
[46] D. Cazorla-Amarós, J. Alcaniz-Monge, M.A. Casa-Lillo, A. Linares-Solano, CO_2 as an adsorptive to characterize carbon molecular sieves and activated carbons, Langmuir 14 (1998) 4589–4596.
[47] C. Nguyen, D.D. Do, K. Haraya, K. Wang, The structural characterization of carbon molecular sieve membrane (CMSM) via gas adsorption, J. Membr. Sci. 220 (2003) 177–182.
[48] D.W. Breck, Zeolite Molecular Sieves, Structure, Chemistry and Use, JohnWiley & Sons, New York, 1974.
[49] T.H. Ko, W.S. Kuo, Y.H. Chang, Raman study of the microstructure changes of phenolic resin during pyrolysis, Polym. Compos. 21 (2000) 745–750.
[50] T.A. Centeno, J.L. Vilas, A.B. Fuertes, Effects of phenolic resin pyrolysis conditions on carbon membrane performance for gas separation, J. Membr. Sci. 228 (2004) 45–54.
[51] A.F. Ismail, D. Rana, T. Matsuura, H.C. Foley, Carbon-Based Membranes for Separation Processes, Springer, New York (2011) 299–313.
[52] L.M. Robeson, The upper bound revisited, J. Membr. Sci. 320 (2008) 390–400.
[53] I. Menendez, A.B. Fuertes, Aging of carbon membranes under different environments, Carbon 39 (2001) 733–740.
[54] W. Zhou, M. Yoshino, H. Kita, K. Okamoto, Preparation and gas permeation properties of carbon molecular sieve membranes based on sulfonated phenolic resin, J. Membr. Sci. 217 (2003) 55–67.
[55] W. Wei, H. Hu, L. You, G. Chen, Preparation of carbon molecular sieve membrane from phenol–formaldehyde novolac resin, Carbon 40 (2002) 465–467.
[56] A.B. Fuertes, Effect of air oxidation on gas separation properties of adsorptive-selective carbon membranes, Carbon 39 (2001) 697–706.
[57] W. Shusen, Z. Meiyun, W. Zhizhong, Asymmetric molecular sieve carbon membranes, J. Membr. Sci. 109 (1996) 267–270.

Appendix C

(12) INTERNATIONAL APPLICATION PUBLISHED UNDER THE PATENT COOPERATION TREATY (PCT)

(19) World Intellectual Property Organization
International Bureau

(43) International Publication Date
27 April 2017 (27.04.2017)

WIPO | PCT

(10) International Publication Number
WO 2017/068517 A1

(51) International Patent Classification:
B01D 65/08 (2006.01) *B01D 69/10* (2006.01)
B01D 53/22 (2006.01) *B01D 69/14* (2006.01)
B01D 67/00 (2006.01) *B01D 71/02* (2006.01)

(21) International Application Number:
PCT/IB2016/056295

(22) International Filing Date:
19 October 2016 (19.10.2016)

(25) Filing Language: English

(26) Publication Language: English

(30) Priority Data:
108896 19 October 2015 (19.10.2015) PT

(71) Applicant: **UNIVERSIDADE DO PORTO** [PT/PT]; Praça Gomes Teixeira, S/N, 4º, S.419, 4099-002 Porto (PT).

(72) Inventors: **MAGALHÃES MENDES, Adélio Miguel**; Rua Veloso Salgado N5, 4 Andar, 4100-497 Porto (PT). **SILVA DE ANDRADE, Márcia Rafaela**; Rua Doutor Francisco Fernandes Duarte, 56 R/C Dte.Fte., 4700-267 Braga (PT). **FERREIRA DA SILVA BOAVENTURA, Marta**; Rua D.Carlos I, 63, 4430-258 Vila Nova De Gaia (PT). **VALE RODRIGUES, Sandra Cristina**; Rua de Boucinha 374, 4830-812 Póvoa De Lanhoso (PT).

(74) Agent: **TEIXEIRA DE CARVALHO, Anabela**; Patentree Edifício Net, Rua de Salazares 842, 4149-002 Porto (PT).

(81) Designated States *(unless otherwise indicated, for every kind of national protection available)*: AE, AG, AL, AM, AO, AT, AU, AZ, BA, BB, BG, BH, BN, BR, BW, BY, BZ, CA, CH, CL, CN, CO, CR, CU, CZ, DE, DJ, DK, DM, DO, DZ, EC, EE, EG, ES, FI, GB, GD, GE, GH, GM, GT, HN, HR, HU, ID, IL, IN, IR, IS, JP, KE, KG, KN, KP, KR, KW, KZ, LA, LC, LK, LR, LS, LU, LY, MA, MD, ME, MG, MK, MN, MW, MX, MY, MZ, NA, NG, NI, NO, NZ, OM, PA, PE, PG, PH, PL, PT, QA, RO, RS, RU, RW, SA, SC, SD, SE, SG, SK, SL, SM, ST, SV, SY, TH, TJ, TM, TN, TR, TT, TZ, UA, UG, US, UZ, VC, VN, ZA, ZM, ZW.

(84) Designated States *(unless otherwise indicated, for every kind of regional protection available)*: ARIPO (BW, GH, GM, KE, LR, LS, MW, MZ, NA, RW, SD, SL, ST, SZ, TZ, UG, ZM, ZW), Eurasian (AM, AZ, BY, KG, KZ, RU, TJ, TM), European (AL, AT, BE, BG, CH, CY, CZ, DE, DK, EE, ES, FI, FR, GB, GR, HR, HU, IE, IS, IT, LT, LU, LV, MC, MK, MT, NL, NO, PL, PT, RO, RS, SE, SI, SK, SM, TR), OAPI (BF, BJ, CF, CG, CI, CM, GA, GN, GQ, GW, KM, ML, MR, NE, SN, TD, TG).

Published:

— *with international search report (Art. 21(3))*

— *before the expiration of the time limit for amending the claims and to be republished in the event of receipt of amendments (Rule 48.2(h))*

(54) **Title**: A CARBON MOLECULAR SIEVE MEMBRANE, METHOD OF PREPARATION AND USES THEREOF

(57) **Abstract**: The present disclosure relates to a novel carbon molecular sieve membranes - CMSM. More particularly, the disclosure relates to the polymeric precursor and carbonization conditions needed for producing a high-selective, age-free CMSM. More specifically, the present subject-matter discloses a process for obtaining from a cellophane film and in a single carbonization step. The carbon molecular sieve membrane obtainable be the process describe displays no pore blockage in the presence of water vapor and displaying very high ideal permselectivities and permeabilities for industrially relevant gas mixtures.

WO 2017/068517 A1

D E S C R I P T I O N

A CARBON MOLECULAR SIEVE MEMBRANE, METHOD OF PREPARATION AND USES THEREOF

Technical field

[0001] The present disclosure relates to a novel carbon molecular sieve membranes (CMSM). More particularly, the disclosure relates to the polymeric precursor and carbonization conditions needed for producing a high-selective, age-free CMSM. More specifically, the present subject-matter discloses a process for obtaining from a cellophane precursor and in a single carbonization step a CMSM that displays no pore blockage in the presence of water vapor and displaying very high ideal permselectivities and permeabilities for industrially relevant gas mixtures.

Background

[0002] Carbon molecular sieve membranes (CMSM) were proposed first by Koresh and Soffer in 1980 and studied since them. Though the very promising high permselectivities and permeabilities displayed by these membranes, they still not commercial.

[0003] CMSM are prepared from the controlled carbonization of a polymeric precursor; pre- and post-treatments are normally applied to improve the separation performance and stability of the prepared membranes. This precursor plays a key role in the production of carbon molecular sieve membranes since different precursors carbonized in the same conditions bring carbon membranes with different properties. The carbonization conditions (carbonization end temperature, heating rate, atmosphere and soaking time) are also of extreme importance for the resulting CMSM performance since they tailor the pore size and structure of carbon membranes.

[0004] CMSM are known to have high permeability of gases, high selectivity and to be thermal and chemically stable. However, they present significant complications related to their performance stability. All reported and disclosed CMSM suffer pore blockage

in the presence of water vapor, normally above 30 % of RH, and display oxygen chemisorption that in some cases is most severe than in others. The chemisorbed oxygen reduces the pore size and affects the separation performance of the membrane. On the other hand when CMSM are exposed to humidity, water initially adsorbs onto hydrophilic sites and once the first water molecule is adsorbed, adsorbate-adsorbate interactions will promote the adsorption of further molecules through hydrogen bonds. When the resulting water cluster reaches the dispersive energy for rolling over the hydrophobic path, it eventually encounters a gas selective pore constriction blocking it. In consequence of this pore blockage, the membrane permeability decreases, normally abruptly, making it useless.

[0005] Jones and Koros [1] evaluated the performance of single-fiber test modules at various water activity levels (23 %-85 % of relative humidity) and observed that the membranes were unfavorably affected by exposure to water vapor. The membrane performance loss increased with the increase of the relative humidity in the stream. The same authors suggested, in 1995, a coating of the carbon membranes with a very thin film of highly porous and hydrophobic material such as Teflon [2]. This coating provided a protective barrier that reduced the adverse effects on the performance of the membrane caused by the humidity.

[0006] Carbon Membranes Ltd. (Israel) produced mechanically stable hollow fiber dense membranes from cellulose cupra-ammonia precursors [3]. A technique for repairing cracked hollow fibers was developed using a sealant [4] and a method for improving membrane selectivity was also carried out using chemical vapor deposition followed by activation [5]. However, these membranes presented aging problems when exposed to pure oxygen or air and exhibited pore blockage in the presence of humidity [6]. Eventually this company closed in 2001.

[0007] Various regeneration techniques are known in the art. These include thermal regeneration, ultrasonic regeneration, chemical regeneration, electrothermal regeneration and microwave regeneration. However, regeneration techniques are not favored since they are time consuming, expensive and often unsuccessful.

[0008] The prior art had never reported a CMSM stable in the presence of a humidified stream above 40 % RH. The present patent discloses the process and applications of a CMSM stable to oxygen and humidified streams, produced in a single carbonization step and displaying extremely high gas separation performances.

[0009] Cellophane is a thin, transparent sheet made of regenerated cellulose. "Cellophane" is in many countries a registered trademark of Innovia Films Ltd. Cellophane remains a trademark in many countries in Europe and elsewhere, in the United States it is, by court decision, a generic name.

[0010] Cellophane emerged from a series of efforts conducted during the late 19th century to produce artificial materials by the chemical alteration of cellulose, a natural polymer obtained in large quantities from wood pulp or cottonlinters. In 1892 English chemists Charles F. Cross and Edward J. Bevan patented viscose, a solution of cellulose treated with caustic soda and carbon disulfide. Viscose is best known as the basis for the man-made fiber rayon, but in 1898 Charles H. Stearn was granted a British patent for producing films from the substance.

[0011] These facts are disclosed in order to illustrate the technical problem addressed by the present disclosure.

General Description

[0012] It was surprisingly found , that contrary to what it was expected the membranes showed no noticeable pore blockage when treating humidified stream up to ca. 80 % RH, since the state of the art indicates otherwise. Preferably, the permeation of some species as well as separation factors was improved. Moreover, these membranes showed no noticeable oxygen chemisorption after a conventional treatment with propylene. This unprecedented result was obtained with a single carbonization step. This fact opens the door to a number of novel applications of these membranes. These new CMSM are advantageous for several industrial applications such as separation of nitrogen and oxygen from air, separation of hydrogen from syngas, removal of CO_2 from the natural gas wells, recover of hydrogen from natural

gas, CO_2 separation from flue gas, air dehumidification, natural gas dehydration, helium recovery/separation, ethene/ethane or xenon separation from gas mixtures. CMS membranes can be flat sheet or hollow fibers and supported or unsupported.

[0013] The present disclosure relates to a novel carbon molecular sieve membranes. More particularly, the disclosure relates to the polymeric precursor and carbonization conditions needed for producing a high-selective, age-free CMSM.

[0014] More specifically, the present subject-matter discloses a process for obtaining CMSM from a cellophane film and in a single carbonization step.

[0015] The carbon molecular sieve membrane obtainable by the process described displays no pore blockage in the presence of water vapor and displaying very high ideal permselectivities and permeabilities for industrially relevant gas mixtures.

[0016] The cellophane film/precursor used in the present disclosure was obtained by the viscose process.

[0017] An aspect of the present disclosure relates to a carbon molecular sieve membrane obtained by carbonization of a carbonaceous polymer precursor comprising hydrophilic surface elements, in particular homogeneously distributed, with a predetermined heating protocol up to a predetermined end carbonization temperature. The hydrophilic sites allow water molecules to jump along the surface from hydrophilic group in hydrophilic group avoiding the formation of water clusters and displaying a quasi-linear water vapor adsorption isotherm.

[0018] The carbon molecular sieve membrane pore size distribution is controlled independently by the carbonization end temperature.

[0019] In an embodiment for better results, the polymer precursor may be cellophane.

[0020] In an embodiment for better results, the hydrophilic surface elements can be metallic and semi-metallic elements and oxygen functional groups.

[0021] In an embodiment for better results, the metallic elements may be select of a list consisting of: lithium, sodium, potassium, magnesium, cupper, silicon, nickel, iron, calcium, barium and their oxides.

[0022] In an embodiment for better results, the hydrophilic surface elements are oxygen functional groups such as: hydroxyl, carbonyl, ether, esther and carboxylic.

[0023] In an embodiment for better results, the carbon molecular sieve membrane is age free - i.e. that displays no pore blockage - when submitted to a humidified stream comprising 50 % relative humidity (RH) - at 25 °C and 1 bar. Preferably, the carbon molecular sieve membrane is age free when submitted to a humidified stream comprising 80 % relative humidity (RH) - at 25 ° C and 1 bar. The measurement of the pore blockage can be performed by several methods, in this disclosure the pore blockage was measure as described in example 1.

[0024] In an embodiment for better results, the metallic elements are clusters of atoms, in particular clusters size in the range 1-20 atoms.

[0025] In an embodiment for better results, the carbon molecular sieve membrane of the present disclosure comprises large pores between 0.5-0.8 nm interconnected to pores between 0.3-0.5 nm. The measurement of the membrane pore size distribution can be performed by several methods, in this disclosure the pore size distribution was measured by the method proposed by Do et al. [7, 8] for carbonaceous materials.

[0026] In an embodiment for better results, the end carbonization temperature is between 500-625 °C, preferably between 525-600 °C, preferably between 500-575 °C.

[0027] In an embodiment for better results, the carbonization of the cellophane film has a heating rate between 0.1-10 C·min-1, preferably the cellophane film has a heating rate between 0.5-5°C·min-1, preferably 1 °C·min-1.

[0028] In an embodiment for better results, the carbonization of the cellophane film has one or more dwells, in particular comprising a first dwell at 110 °C.

[0029] In an embodiment for better results, the cellophane film is obtained by the viscose process.

[0030] In an embodiment for better results, the membrane thickness varies between 1-10 µm.

[0031] In an embodiment for better results, carbon molecular sieve membrane of the present disclosure may further comprising a support reinforced with inorganic particles, wherein the support comprises the same shrinkage ratio during the carbonization step compared with the carbon molecular sieve membrane, preferably inorganic particles of the support are boehmite and/or glass micro fibers.

[0032] In an embodiment for better results, the shrinkage ratio is controlled by adding further comprising phosphoric acid catalyst to the cellophane precursor.

[0033] In an embodiment for better results, the addition plasticizers improve the mechanical flexibility of the carbon molecular sieve membrane of the present disclosure. For better results the plasticizer concentration is between 5-15 wt.%, improving the control of the pore size distribution. Preferably the plasticizers may be select from a list consisting of: glycerol, PEG, monopropylene glycol, urea, and mixtures thereof.

[0034] Another aspect of the present disclosure relates to hollow fiber carbon comprising the carbon molecular sieve membrane of the present disclosure, wherein the membrane comprises a thickness between 1 - 10 μm.

[0035] Another aspect of the present disclosure relates to the use of the carbon molecular sieve membrane described in the present disclosure in a humidified gas streams comprising a constant gas permeation up to 80 % of relative humidity.

[0036] In carbon molecular sieve membrane described in the present disclosure may be use in gas separation, in particular for several applications as: air dehumidification, separation of nitrogen and oxygen from air, natural gas dehydration, separation of hydrogen from syngas, removal of CO2 from the natural gas wells, recover of hydrogen from natural gas, CO2 separation from flue gas, helium recovery/separation, ethene/ethane or xenon separation from gas mixtures.

[0037] Another aspect of the present disclosure relates to a method to obtain the carbon molecular sieve membrane described in the present disclosure comprising:

providing a cellophane precursor produced by the viscose process, comprising hydrophilic surface elements wherein the hydrophilic surface elements are metallic and semi-metallic and oxygen functional groups;

carbonizing the precursor with a predetermined heating protocol up to a predetermined end carbonization temperature, wherein the end carbonization temperature is between 500-625 °C, preferably the end temperature is between 525-575 °C, more preferably 550 °C.

[0038] In an embodiment for better results, the carbonization of the cellophane film has a heating rate between heating rate 0.1-10 C·min-1, preferably 0.5-5, more preferably 1 °C·min-1.

[0039] In an embodiment for better results, the carbonization of the cellophane precursor/film is in a controlled atmosphere, preferably of nitrogen or vacuum atmosphere.

[0040] In an embodiment for better results, the carbonization of the cellophane precursor film is in an atmosphere comprising a nitrogen flow rate ranging between 100-200 ml min-1.

[0041] In an embodiment for better results, the plasticizer has a concentration between 5-15 wt.%.

[0042] These and other features of the present invention will become readily apparent upon further review of the following specification and figures.

Brief Description of the Drawings

[0043] The following figures provide preferred embodiments for illustrating the description and should not be seen as limiting the scope of invention.

[0044] FIG.1 Temperature history to prepare carbon molecular sieve membranes.

[0045] FIG.2 Scanning electron images of a CMSM carbonized at 550 °C (A) cross-section; (B) surface view.

[0046] FIG. 3 Water vapor adsorption and desorption equilibrium data at 25 °C on a carbon molecular sieve membrane carbonized at 550 °C.

[0047] FIG. 4 Micropore size distribution for carbon molecular sieve membrane carbonized at 550 °C.

[0048] FIG.5 Gas permeation results for O_2/N_2 in carbon membranes carbonized at different temperatures and comparison with the respective upper bound limit.

[0049] FIG.6 HRTEM pictures of a (A) cellophane-based CMSM and (B) carbon molecular sieve membrane from Fraunhofer.

[0050] FIG. 7 TPD spectra of carbon molecular sieve membranes prepared at 400 °C and 550 °C and a comparison with the spectra of hollow fiber membranes by Carbon Membranes Ltd: (a) CO evolution; (b) CO_2 evolution.

[0051] FIG. 8 Illustrative figure of the high flexibility of the cellophane based-CMSM. Figure proving the high flexibility of a CMSM produced at 550 °C.

Detailed Description

[0052] Carbon molecular sieve membranes contain pores larger than the ultramicropores required for the molecular sieving process. These larger pores connect ultramicropores that perform the molecular sieving mechanism and allow for high permeabilities. Generally, an increase in the carbonization end temperature results in a decrease in the gas permeability and an increase in the ideal selectivity, since higher carbonization temperatures originate CMSM with smaller interplanar spacing between the graphite-like layers of carbon.

[0053] The carbonization process is a very important step during the production of carbon molecular sieve membranes and can be considered the heart of the carbon membrane fabrication process. The polymer precursor is heated to the desired end temperature in a controlled atmosphere at a specific heating rate, originating an

amorphous carbon membrane with a very narrow porosity that is responsible for the molecular sieve properties of the carbon membrane. Carbonization temperature lies between the decomposition temperature of the carbonaceous precursor and its graphitization temperature. The optimum carbonization temperature depends strongly on the type of the precursor. The choice of a suitable precursor is fundamental to guarantee the production of defect-free CMSM and it should withstand high temperature treatment without much shrinkage, should be thermosetting to avoid melting or softening during any stage of the carbonization process besides having a high carbon yield. Appropriate polymeric precursors include cellulose and derivatives thereof, polyfurfuryl alcohol, polyamides, polyimides, phenolic resins, acrylics, and the like. Other precursor materials may be useful for the preparation of carbon membranes and therefore the mentioned suitable precursors are not limiting.

[0054] CMSM suffer often quite fast oxidation in contact with ambient air and easily loses permeability (it may decrease orders of magnitude) due to water or other vapors adsorption as molecular clusters. Normally, the water vapor adsorption isotherm displays a S-shape behavior. This shape is related to the hydrophobic nature of the CMSM; for RH lower than ca. 30 %, the water molecules adsorb in hydrophilic sites and desorb permeating the membrane. However, above this humidity a catastrophic adsorption behavior is normally observed. Water molecules still adsorb in hydrophilic sites, but since the vapor concentration is high enough, other water molecules successively establish H-bonding until a *m* size cluster is reached. This behavior ends with a steep increase in the adsorbed water molecules and in pore blockage. Indeed, the resulting water clusters gain enough dispersion energy to detach from the hydrophilic site and move over the hydrophobic path towards pore constrictions, blocking them. Also, when CMSM are exposed to air, even at room temperature, oxygen atoms from air combine with some active sites forming oxygen surface groups that reduce the open porosity and increase the surface hydrophilicity.

[0055] To overcome the water vapor blockage problem and age-free behavior, the carbonized precursor shall have a hydrophilic character. Cellophane material was found to originate CMSM that meet these requirements. Cellophane is a natural

polymer of glucose, 100 % biodegradable and inexpensive, produced from wood cellulose by the viscose process. CMSM made from cellophane paper show hydrophilic sites homogeneously distributed in its inner surfaces that allow water molecules to jump smoothly between sites avoiding the formation of water clusters. These hydrophilic sites are made of metallic and semi-metallic elements that incorporated during the polymeric film production, namely ionic sodium and silica nanoparticles, and oxygen functional groups such as hydroxyl, carbonyl, ether, esther and carboxylic. CMS membranes carbonized from cellophane under optimized conditions show a linear or quasi-linear water vapor adsorption isotherm. This linear isotherm is characteristic of an adsorbent displaying hydrophilic sites homogeneously distributed. In the present subject-matter, permeation studies demonstrated that up saturation, humidity does not affect membrane ability to permeate and separate gases. Moreover, these membranes show no noticeable oxygen chemisorption after a conventional treatment with propylene.

[0056] Carbonization operating conditions have a significant impact on the final properties of carbon membrane. Generally, an increase in the carbonization end temperature results in a decrease in the gas permeability and an increase in the ideal selectivity; the same is valid for higher soaking times but its effect is much more moderate. Carbonization under vacuum commonly originates more selective and less permeable CMSM when compared to a carbonization under an inert atmosphere. The carbonization history controls then the pore size distribution but also the surface chemistry. For controlling these two characteristics independently it is necessary to have two independent factors. In the present disclosure, CMSM with different pore size distributions are obtained even if produced with the same carbonization history by varying the cellulose concentration in the cellophane precursor film. Moreover, plasticizers, which are incorporated during the cellophane film production to avoid the precursor embrittlement, similarly display a relevant role in the CMSM performance: they are also able to tailor the pore size distribution of the carbon membranes independently of the carbonization end temperature besides improving the mechanical flexibility of the final carbon film/hollow fiber.

[0057] In the present disclosure, surface chemistry studies demonstrate that the final carbonization temperature controls also the membrane surface chemistry. Carbonization is preferably carried out under an inert atmosphere, e.g. of nitrogen. The end carbonization temperature ranges between 400 °C and 900°C, preferably between 500 °C and 600 °C. The heating rate should be between 0.1 °C·min^{-1} and 10°C·min^{-1}, preferably between 0.5 °C and 5 °C·min^{-1} and more preferably 1 °C·min^{-1}. During the heating protocol various dwells are applied; these dwells are chosen according to the obtained thermogravimetric results, i.e. where the first derivative of mass loss shows a significant negative peak a dwell is applied. The first dwell, at ca. 110 °C, is very important for drying the membrane precursor and avoid the formation of cracks or defects in the carbon matrix and the subsequent dwells are needed to fine the pore size distribution. Dwells may be avoidable if heating rates are kept low. Once the end temperature is reached, the membranes are allowed to cool until room temperature before being removed from the furnace.

[0058] Carbon membranes can be divided in supported and unsupported. Unsupported membranes can be hollow fibers, flat membranes or capillary and supported membranes can be flat or tubular. The present carbon membranes can take any of these forms but are preferably unsupported or supported hollow fibers.

[0059] The disclosed CMSM are advantageous for industrial applications such as separation of nitrogen and oxygen from air, separation of hydrogen from syngas, removal of CO_2 from the natural gas wells, recover of hydrogen from natural gas, CO_2 separation from flue gas, air dehumidification, natural gas dehydration, helium recovery/separation, ethene/ethane and xenon separation from gas mixtures.

[0060] The invention will now be further described with reference to the following Examples, which are considered to be illustrative only, and non-limiting.

EXAMPLE 1

Extremely high performance CMSM for humidified O_2/N_2 separation

[0061] Cellophane paper with c.a. 20 µm thickness produced by the viscose process and containing 6.2 wt.% of moisture, 13.2 wt.% of plasticizers (glycerol and urea), 1.05 wt.% of sodium sulphate and 80.6 wt.% of cellulose was used as precursor.

[0062] Previous to the carbonization step, the precursor film was cut in disks with 48 mm in diameter. The carbonization of the cellophane films was accomplished in a quartz tube (80 mm in diameter and 1.5 m in length) inside a tubular horizontal Termolab TH furnace.

[0063] The basic protocol had an end temperature ranging between 500 °C and 900 °C, preferably between 525 °C and 575 °C, and more preferably 550 °C, without soaking time, a nitrogen flow rate ranging between 100-200 ml min^{-1} and a slow heating rate with some dwells to avoid a quick release of residual solvents and volatile matter that could damage the carbon matrix. The protocol is pictured in FIG.1. After the end temperature was reached, the system was allowed to cool naturally until room temperature and the carbon membranes were removed from the tubular furnace.

[0064] Micrographs of the produced carbon molecular sieve membranes were taken by scanning electron microscopy (SEM). FIG.2 presents the surface and cross-sectional views of an obtained CMSM; clusters of microspheres are observed. These microspheres are related to cellulose hydrothermal carbonization that happens at around 220 °C and originates more stable oxygen groups in the core (ether, quinone and pyrrone) and more hydrophilic oxygen groups in the shell (hydroxyl, carbonyl, carboxylic and esther).

To perform the permeation experiments, the carbon membranes were glued to steel o-rings. Epoxy glue (Araldite® Standard) was also applied along the interface of the steel o-ring and the carbon membrane. A sintered metal disc covered with a filter paper was used as support for the film in the test cell. Single gases were tested at 25 °C, feed pressure of 1 bar and vacuum at the permeate side. The tests were performed

in a standard pressure-rise setup with LabView® data logging. The system included the membrane module connected to a vessel with a calibrated volume at the permeate side and connected also to a gas cylinder at the feed side. The feed gas could either be used dry or passed through a bubbler with distilled water prior to the membrane module. The relative humidity was checked with a RH meter at an exit port. The permeability, P_i, of the CMSM towards to pure component i was determined as described by the following equation:

$$P_i = \frac{Flux_i}{\Delta P_i/\delta} \quad (1)$$

where $Flux_i$ is the flux of the species i, ΔP_i the partial pressure difference of species i across the membrane and δ the membrane thickness.

[0065] The ratio of two gases permeability coefficients is termed permselectivity (often designated as ideal selectivity):

$$\alpha\left(\frac{i}{j}\right) = \frac{P_i^*}{P_j^*} \quad (2)$$

[0066] Table 1 shows the permeation results for the produced CMSM when exposed to different levels of relative humidity for several hours.

TABLE 1

CMSM	RH Exposure	Pre-Exposure O_2 permeability (Barrer)	Post-Exposure O_2 permeability (Barrer)	Pre-Exposure N_2 permeability (Barrer)	Post-Exposure N_2 permeability (Barrer)	Pre-exposure O_2/N_2 Selectivity	Post-exposure O_2/N_2 Selectivity
CMSM 550	75-77 %	1.33	3.30	0.07	0.08	19.0	41.2

[0067] After CMSM contacting with a humidified oxygen stream (RH humidity relative- of 75-77 %), the overall permeability increased ca. 2.5 times (the permeability to oxygen stays roughly constant) and O_2/N_2 ideal selectivity increase from 19.0 to 41.2.

[0068] Carbon materials are generally poorly wetted by water presenting large contact angles. Contact angles measurements were performed in a surface energy evaluation system (DataPhysics OCA-Series) using the sessile drop method and water, ethylene glycol and *n*-hexadecane as probe liquids. A needle connected to a microsyringe was used to place the liquid drops on the surfaces. For each drop 150 points were collected. Table 2 shows the measured contact angles for a carbon molecular sieve membrane produced at 550 °C.

TABLE 2

Sample	Measured Contact Angles (deg)		
	Water	***Ethylene glycol***	***n-Hexadecane***
CMSM 550	17.7 ± 0.9	13.9 ± 3.3	0.0 ± 0.0

[0069] The prepared CMSM 550 sample shows the highest hydrophilic character displaying a small contact angle.

[0070] The adsorption and desorption equilibrium isotherms of water vapor were obtained for the produced carbon molecular sieve membranes by the gravimetric method using a suspension magnetic balance from Rubotherm® at 25 °C. The sample was fragmented into flakes in order to fill the weighting basket. FIG. 3 shows the experimental values as a function of relative pressure, considering 32 mbar the water vapor at 25 °C. The experimental adsorption/desorption branches are well described by a quasi-linear isotherm. The significant amount at very low relative pressures confirms the hydrophilic character of the developed carbon molecular sieve membranes.

[0071] The pore size distribution and the porosity volume were obtained for carbon molecular sieve membranes based on the adsorption equilibrium isotherm of CO_2 at 0 °C using a suspension magnetic balance from Rubotherm®. To perform the experiments the sample was also fragmented into flakes. FIG. 4 shows the obtained

pore size distribution and Table 3 the micropore volume, the mean pore width and the characteristic energy for adsorption.

TABLE 3

Parameter	CMSM 550
Micropore volume (cm^3 kg^{-1})	274.2
Mean pore width (nm)	0.435
Characteristic energy (kJ mol^{-1})	10.92

[0072] In an embodiment, CMSM 550 presents larger pores of 0.5-0.8 nm known as micropores (responsible for surface diffusion mechanism) interconnected to ultramicropores of 0.3-0.5 nm responsible for the molecular sieving properties of carbon membranes.

EXAMPLE 2

Extremely high performance CMSM for dry O_2/N_2 separation

[0073] Carbon molecular sieve membranes are prepared from cellophane according to Example 1, varying the carbonization end temperature between 575 °C and 625 °C, more preferably 600 °C. Table 4 shows the oxygen and nitrogen permeation results for the produced CMSM.

TABLE 4

Sample	Nitrogen Permeability (Barrer)	Oxygen Permeability (Barrer)	O_2/N_2 ideal selectivity
CMSM 600	<0.001	0.78	>800

[0074] The produced CMSM showed to be very selective to O_2/N_2 (ideal selectivity > 800) separation.

EXAMPLE 3

Other gas separations

[0075] Carbon molecular sieve membranes are prepared from cellophane precursor according to Example 1, varying the carbonization end temperature between 400 °C and 600 °C. Table 5 and 6 show the obtained permeabilities and ideal selectivities for several dry gases using CMSM produced at different carbonization end temperatures, respectively.

TABLE 5

CMSM	Permeability (Barrer)								
	N_2	O_2	He	H_2	CO_2	CH_4	H_2O	C_3H_6	C_3H_8
CMSM 400	0.07	0.73	5.43	8.35	3.39	0.008	12.1	n.d*	n.d*
CMSM 500	0.06	0.95	10.24	18.94	8.21	n.d*	16.0	n.d*	n.d*
CMSM 550	0.07	1.33	17.26	32.59	13.0	0.01	28.5	0.056	0.035
CMSM 600	<0.001	0.78	11.78	24.90	2.57	<<0.001	25.1	0.065	0.025

n.d* = not determined

TABLE 6

CMSM	Ideal Selectivity							
	O_2/N_2	H_2/N_2	H_2/CH_4	CO_2/N_2	CO_2/CH_4	He/N_2	H_2/O_2	C_3H_6/C_3H_8
CMSM 400	10.4	119.3	1044	48.4	423.8	77.57	11.4	n.d*
CMSM 500	15.8	315.7	n.d*	136.8	n.d*	170.7	19.9	n.d*
CMSM 550	19.0	465.6	3259	185.7	1300	246.6	24.5	1.6
CMSM 600	>800	>25 000	>>25 000	>2600	>>2600	>1200	44.5	2.6

n.d* = not determined

[0076] The results show that increasing the carbonization end temperature results in an increase in the carbon molecular sieve membrane selectivity.

[0077] The upper bound relationship for membrane gas separations correlates the log of the selectivity versus the log of the permeability of the more permeable gas for the best performing polymer membranes and it was devised by Robeson [9]. FIG.5 shows the permeation results of O_2 and N_2 in carbon membranes carbonized at 500 °C, 550 °C and 600 °C end temperatures and the upper bound limit. This figure illustrates that the CMSM prepared have a separation performance well above the referred upper bound limit.

[0078] The separation performance is extremely high, particularly for the carbon molecular sieve membrane produced at 600 °C. However, the C_3H_6/C_3H_8 ideal selectivity is extremely low when compared to other values reported in literature. After a brief research in the literature, it was perceived that when carbon molecular sieves shows high O_2/N_2 ideal selectivities, low C_3H_6/C_3H_8 ideal selectivities are then obtained and vice-versa (Table 7). This indicated the existence of two different sieving mechanisms for carbon molecular sieves: a gate sieving (for CMS with rounded shape pores) and a tunnel sieving (for CMS with needle shape pores). Figure 6 shows HRTEM pictures of a carbon molecular sieve membrane presenting a pore morphology of a gate sieving mechanism (Figure 6a) and a carbon molecular sieve membrane with a tunnel sieving mechanism (Figure 6b).

TABLE 7

Sample	C_3H_6/C_3H_8 ideal selectivity	O_2/N_2 ideal selectivity
CMSM 550	1.6	19
CMSM 600	2.6	>800
CMSM [as described in reference 10]	14.6	5.4
CMSM [as described in reference 11]	5.8	37.8
CMSM [as described in reference 12]	5.1	38
CMSM [as described in reference 13]	13	3.3

[0079] Contact angles measurements were performed in the different carbon molecular sieve membranes according to Example 1. Table 8 shows the measured contact angles for the different membranes.

TABLE 8

Sample	Measured Contact Angles (deg)		
	Water	*Ethylene glycol*	*n-Hexadecane*
CMSM 400	57.5 ± 2.3	28.5 ± 5.9	0.0 ± 0.0
CMSM 500	32.3 ± 4.6	24.9 ± 3.1	0.0 ± 0.0
CMSM 550	17.7 ± 0.9	13.9 ± 3.3	0.0 ± 0.0
CMSM 600	20.2 ± 0.8	13.9 ± 3.3	0.0 ± 0.0

[0080] The results show that with increasing the carbonization end temperature the produced carbon molecular sieve membranes become more hydrophilic until reaching a maximum at ca. 550 °C.

[0081] Temperature-programmed desorption (TPD) provides information on the surface functional groups on carbon materials. Surface complexes on carbon materials decompose upon heating by releasing CO and CO_2 at different temperatures. The nature of the groups can be assessed by the decomposition temperature and the gas released.

[0082] TPD experiments were carried out in a U-shaped quartz tube located inside an electrical furnace and connected to a Dycor Dymaxion Mass Spectrometer (Ametek Process Instruments). The samples (0.1 g) were heated to 1100 °C at 5 °C min^{-1} using a constant He flow rate of 25 ml min^{-1}. FIG. 7 shows the TPD profiles of the carbon molecular sieve membranes produced at 400 °C and 550 °C comparing with a hollow fiber membrane produced by Carbon Membranes Ltd.

[0083] The results show that the TPD spectra of CMSM 400 and CMSM 550 prepared from the same precursor film are quite distinct. For CMSM 400 sample, both CO and CO_2 peaks originate from the decomposition of carboxylic anhydrides. For CMSM 550 sample, the first CO_2 peak may be attributed to lactone groups and the higher temperature CO_2 peak may be result from carboxylic anhydrides. Considering the CO profile, this sample produced at 550 °C shows a first maximum around 650 °C related to carboxylic anhydrides. The second maximum appears at around 780 °C, which originates from quinone groups. Regarding the hollow fibers produced by Carbon Membranes Ltd, some different oxygen surface functional groups were found when compared to the obtained CMSM 550, namely phenol and carboxylic groups. Considering the CO_2 profile, lactone and carboxylic groups were identified. Phenol and quinone groups yield CO. Both CO and CO_2 originate a peak related to decomposition of carboxylic anhydrides.

[0084] One of the major limitations of carbon molecular sieve membranes is their brittleness which makes their manipulation and assembly into the functional modules very difficult. Although the flexibility of the produced cellophane-based CMSM of the present disclosure tended to decrease as the carbonization end temperature increase, all the prepared membranes are very flexible and could be bent as shown in Figure 8. When a cellophane-based CMSM of the present disclosure is bent, the minimal distance until fracture is c.a. 3 mm (obtained value for a carbon molecular sieve membrane prepared at 550 °C).

[0085] The term "comprising" whenever used in this document is intended to indicate the presence of stated features, integers, steps, components, but not to preclude the presence or addition of one or more other features, integers, steps, components or groups thereof.

[0086] All references recited in this document are incorporated herein in their entirety by reference, as if each and every reference had been incorporated by reference individually.

[0087] Where ranges are given, endpoints are included. Furthermore, it is to be understood that unless otherwise indicated or otherwise evident from the context and/or the understanding of one of ordinary skill in the art, values that are expressed as ranges can assume any specific value within the stated ranges in different embodiments of the invention, to the tenth of the unit of the lower limit of the range, unless the context clearly dictates otherwise. It is also to be understood that unless otherwise indicated or otherwise evident from the context and/or the understanding of one of ordinary skill in the art, values expressed as ranges can assume any subrange within the given range, wherein the endpoints of the subrange are expressed to the same degree of accuracy as the tenth of the unit of the lower limit of the range.

[0088] The disclosure should not be seen in any way restricted to the embodiments described and a person with ordinary skill in the art will foresee many possibilities to modifications thereof.

[0089] Where ranges are given, any value within the range may explicitly be excluded from any one or more of the claims. Any embodiment, element, feature, application, or aspect of the compositions and/or methods of the invention, can be excluded from any one or more claims.

[0090] The present disclosure should not be seen in any way restricted to the embodiments described and a person with ordinary skill in the art will foresee many possibilities to modifications thereof.

[0091] The above described embodiments are combinable. The following claims further set out particular embodiments of the disclosure.

[0092] All references recited in this document are incorporated herein in their entirety by reference, as if each and every reference had been incorporated by reference individually.

References

[1] C.W. Jones, W.J. Koros. Characterization of Ultramicroporous Carbon Membranes with Humidified Feeds. Ind. Eng. Chem. Res. 34 (1995) 158-163.

[2] W. J. Koros, C.W. Jones, Composite carbon fluid separation membranes, US Patent 5,288,304, (1994)

[3] A. Soffer, J. Gilron, S. Saguee, R. Hed-Ofek, H. Cohen, Process for the production of hollow carbon fibers membranes, Eur. Patent 671,202 (1995).

[4] A. Soffer, S. Saguee, D. Golub, H. Cohen, M. Azariah, Selective clogging of failed fibers, US Patent 5,575,963 (1996).

[5] A. Soffer, A. Moshe, A. Abraham, C. Haim, G. Dan, S. Shlomo, Method of improving the selectivity of carbon membranes by chemical carbon vapour deposition, US Patent 5,695,818 (1997).

[6] S. Lagorsse, F.D. Magalhães, A. Mendes, Aging study of carbon molecular sieve membranes, J. Membr. Sci. 310 (2008) 494-502.

[7] C. Nguyen, D.D. Do, Adsorption of supercritical gases in porous media: determination of micropore size distribution. *J. Phys. Chem.* 103 (1999) 6900-6908.

[8] C. Nguyen, D.D. Do, K. Haraya, K. Wang, The structural characterization of carbon molecular sieve membrane (CMSM) via gas adsorption. *J. Membr. Sci.* 220 (2003) 177-182.

[9] L.M. Robeson, The upper bound revisited, J. Membr. Sci. 320 (2008) 390-400.

[10] M. Teixeira, M.C. Campo, D.A. Tanaka, M.A. Tanco, C. Magen, A. Mendes, Composite phenolic resin-based carbon molecular sieve membranes for gas separation, Carbon 49 (2011) 4348-4358.[9] M. Teixeira, M. Campo, D.A.

[11]Tanaka, M.A. Tanco, C. Magen, A. Mendes, Carbon-Al_2O_3-Ag composite molecular sieve membranes for gas separation. *Chem. Eng. Res. Des.* 90 (2012) 2338-2345.

[12] X. Ma, B.K. Lin, X.Wei, J. Kniep, Y.S. Lin, Gamma-Alumina Supported Carbon Molecular Sieve for Propylene/Propane Separation. *Ind. Eng. Chem. Res.*52 (2013) 4297-4305.

[13] K-I. Okamoto, S. Kawamura, M. Yoshiro, H. Kita, Olefin/Paraffin Separation through Carbonized Membranes Derived from an Asymmetric Polyimide Hollow Fiber Membrane. *Ind. Eng. Chem. Res.*38 (1999) 4424-4432.

CLAIMS

1. Carbon molecular sieve membrane obtained by carbonization of a carbonaceous polymer precursor having hydrophilic surface elements with a predetermined heating protocol up to a predetermined end carbonization temperature.

2. Membrane according to the previous claim wherein the polymer precursor is cellophane.

3. Membrane according to the previous claims wherein the hydrophilic surface elements are metallic and semi-metallic elements and oxygen functional groups.

4. Membrane according to the previous claims wherein the metallic elements are select of a list consisting of: lithium, sodium, potassium, magnesium, cupper, silicon, nickel, iron, calcium, barium and their oxides.

5. Membrane according to the previous claims wherein the oxygen functional groups comprise hydroxyl, carbonyl, ether, esther and carboxylic.

6. Membrane according to the previous claims wherein the said carbon molecular sieve membrane is age free after exposed to a humidified stream comprising at least 50 % relative humidity (RH) - at 25 °C and 1 bar.

7. Membrane according to the previous claim wherein the said carbon molecular sieve membrane the said carbon molecular sieve membrane is age free after exposed to a humidified stream comprising at least 80 % relative humidity (RH) - at 25 °C and 1 bar.

8. Membrane according to the previous claims comprising large pores between 0.5-0.8 nm interconnected to pores between 0.3-0.5 nm.

9. Membrane according to the previous claims wherein the end carbonization temperature is between 500-625 °C.

10. Membrane according to the previous claim wherein the end carbonization temperature is between 525-600 °C.

11. Membrane according to the previous claim wherein the end carbonization temperature is between 500-575 °C.

12. Membrane according to any of the previous claims wherein the carbonization of the cellophane film has a heating rate between 0.1-10 C·min-1.

13. Membrane according to any of the previous claims wherein the carbonization of the cellophane film has a heating rate between 0.5-5°C·min-1, preferably 1 °C·min-1.

14. Membrane according to any of the previous claims wherein the carbonization of the cellophane film has one or more dwells, in particular comprising a first dwell at 110 °C.

15. Membrane according to the previous claims wherein the cellophane film is obtained by the viscose process.

16. Membrane according to the previous claims wherein the membrane thickness varies between 1-10 µm.

17. Membrane according to the previous claims further comprising a support reinforced with inorganic particles, wherein the support comprises the same shrinkage ratio during the carbonization step compared with the carbon molecular sieve membrane.

18. Membrane according to the previous claim wherein inorganic particles of the support are boehmite and/or glass micro fibers.

19. Hollow fiber carbon comprising the carbon membrane described in any of the previous claims, wherein the membrane comprises a thickness between 1 - 10 µm.

20. Use of the carbon molecular sieve membrane described in any of the previous claims in a humidified gas streams comprising a constant gas permeation up to 80 % of relative humidity.

21. Use of the carbon molecular sieve membrane according to the previous claim for the gas separation of the following mixtures: air dehumidification, nitrogen and oxygen from air, natural gas dehydration, separation of hydrogen from syngas, removal of CO2 from the natural gas wells, recover of hydrogen from natural gas, CO2 separation from flue gas, helium recovery/separation, ethene/ethane or xenon separation from gas mixtures.

22. Method to obtain a carbon molecular sieve membrane described in any of the previous claims comprising:
providing a cellophane precursor produced by the viscose process, comprising hydrophilic surface elements wherein the hydrophilic surface elements are metallic and semi-metallic and oxygen functional groups;
carbonizing the precursor with a predetermined heating protocol up to a predetermined end carbonization temperature, wherein the end carbonization temperature is between 500-625 °C.

23. Method according to the previous claim wherein the end temperature is between 525-575 °C, preferably 550 °C.

24. Method according to any of claims 22-23, wherein the carbonization of the cellophane film has a heating rate between heating rate 0.1-10 C·min-1, preferably 0.5-5, more preferably 1 °C·min-1.

25. Method according to any of claims 22-24, wherein the carbonization of the cellophane precursor is in a controlled atmosphere, preferably of nitrogen or vacuum atmosphere.

26. Method according to any of claims 22-25, wherein the carbonization of the cellophane precursor is in an atmosphere comprising a nitrogen flow rate ranging between 100-200 ml min^{-1}.

27. Method according to any of claims 22-26 ,wherein the cellophane precursor obtained by the viscose process comprises 5-10 wt.% of moisture, 0-15 wt.% of plasticizers, 0.5-2 wt.% of sodium sulphate and 80-90 wt.% of cellulose.

28. Method according to claims 22-27, wherein the plasticizer is between 5-15 wt.%.

29. Method according to claims 23-29, wherein the plasticizers is select from a list consisting of: glycerol, PEG, monopropylene glycol, urea, and mixtures thereof.

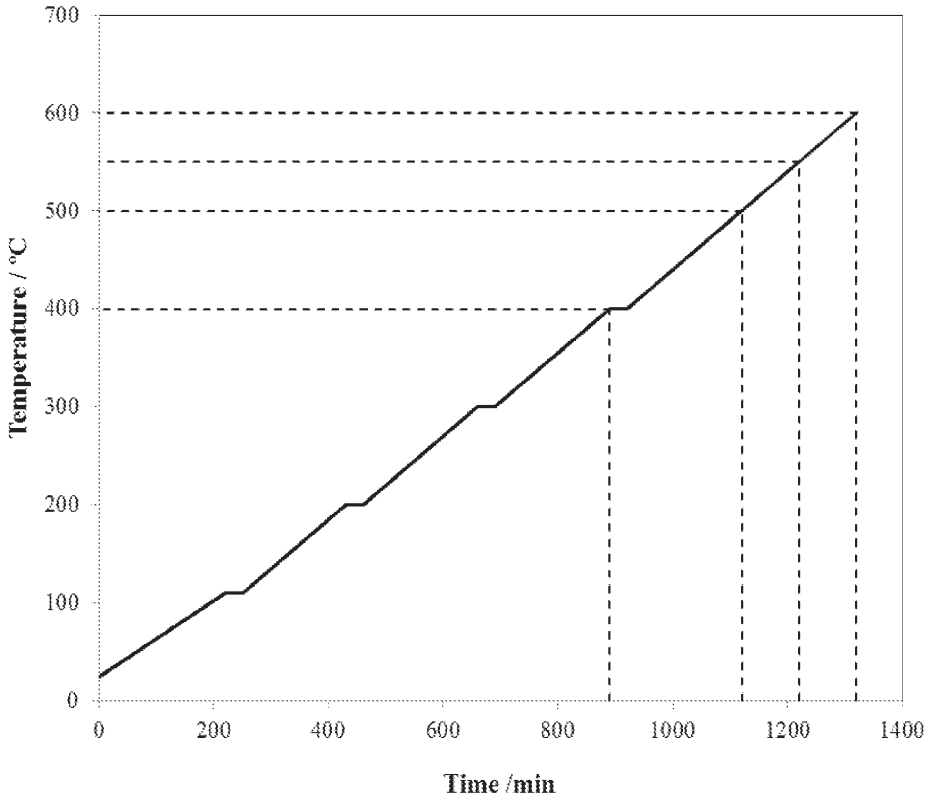
700
600
500
400
300
200
100
0
Temperature / °C
0
200
400
600
800
1000
1200
1400
Time /min

Fig. 1

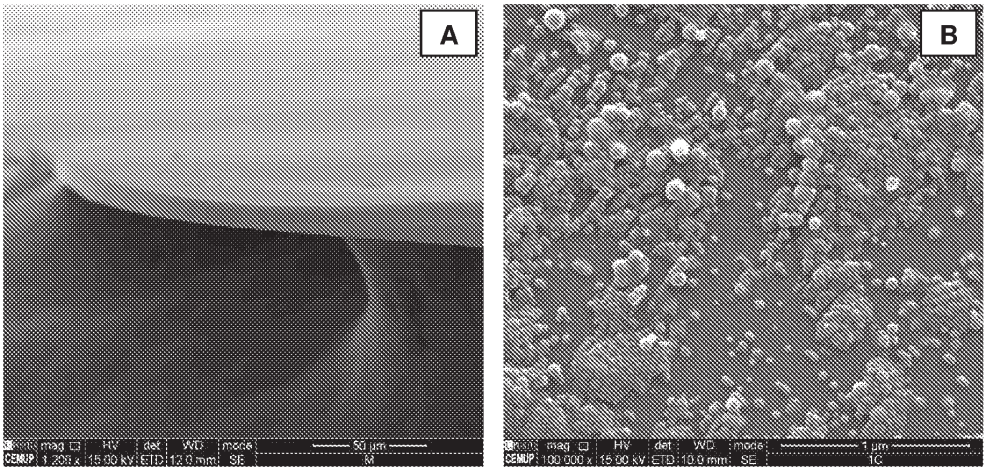

Fig. 2

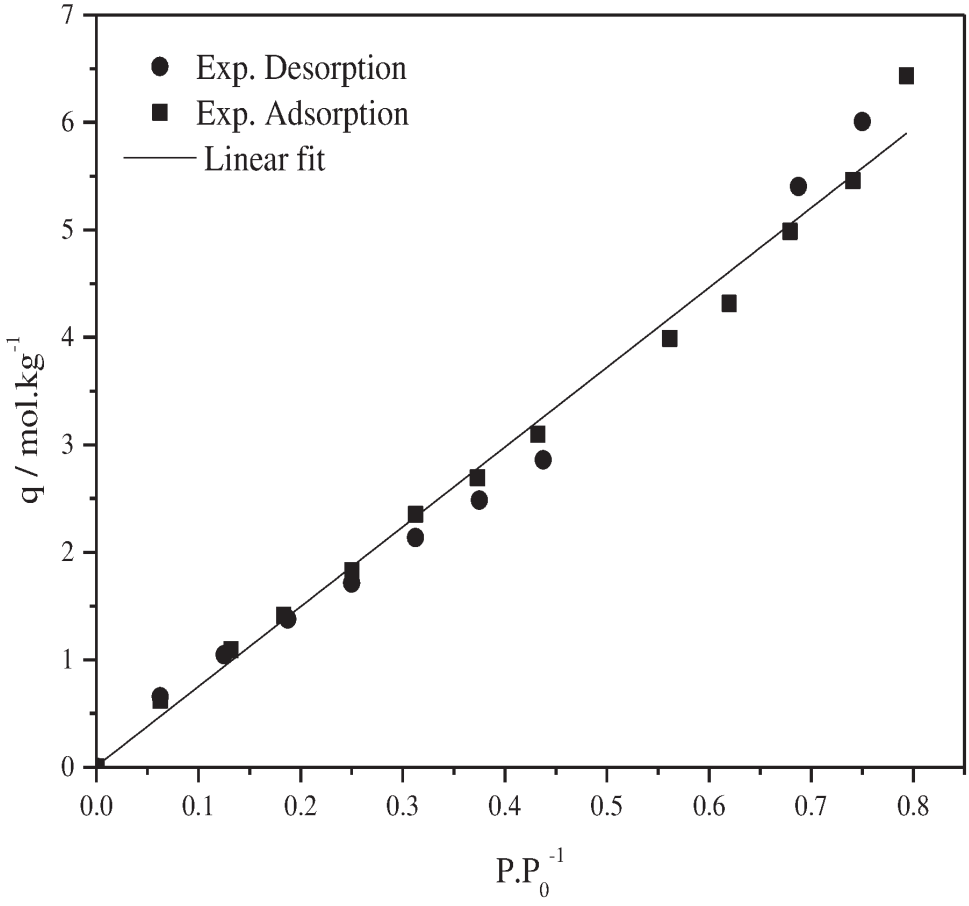
Exp. Desorption
Exp. Adsorption
Linear fit
q / mol.kg-1
P.P0-1
0
1
2
3
4
5
6
7
0.0
0.1
0.2
0.3
0.4
0.5
0.6
0.7
0.8

Fig. 3

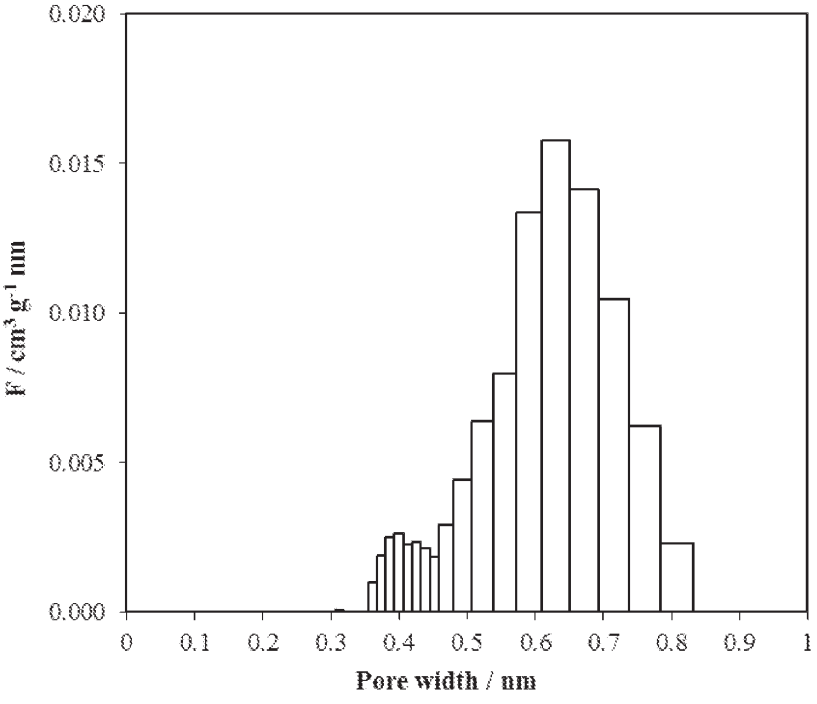
0.020
0.015
0.010
0.005
0.000
F / cm3 g-1 nm
0
0.1
0.2
0.3
0.4
0.5
0.6
0.7
0.8
0.9
1
Pore width / nm

Fig. 4

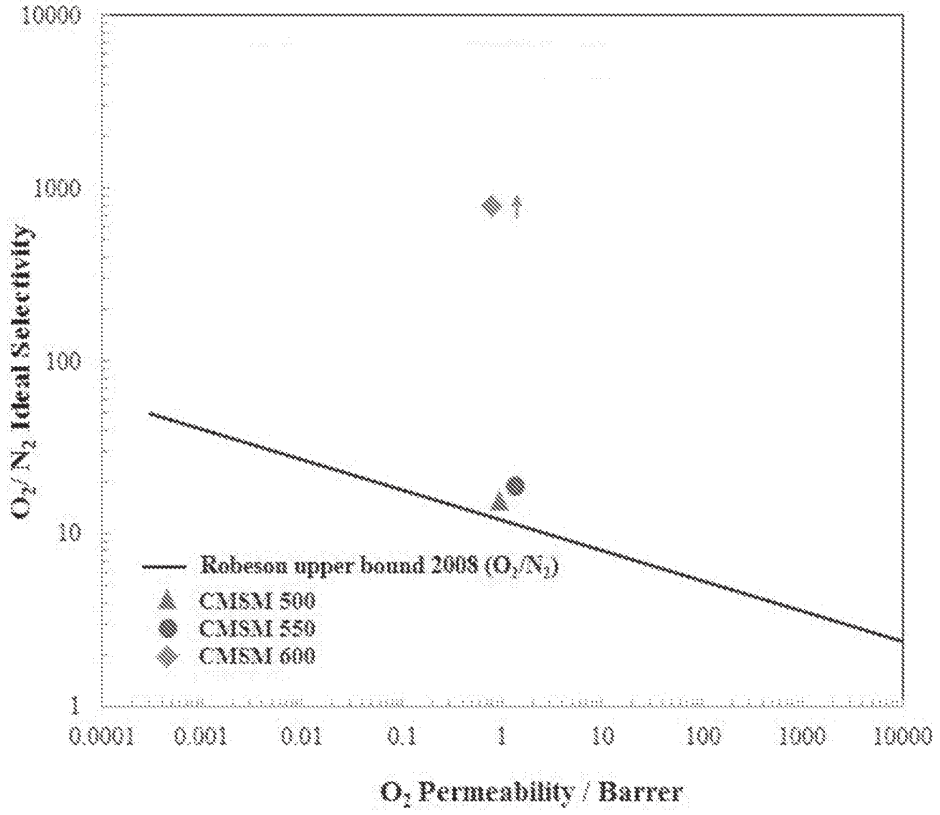
10000
1000
100
10
1
O_2/N_2 Ideal Selectivity
Robeson upper bound 2008 (O_2/N_2)
CMSM 500
CMSM 550
CMSM 600
0.0001
0.001
0.01
0.1
1
10
100
1000
10000
O_2 Permeability / Barrer

Fig. 5

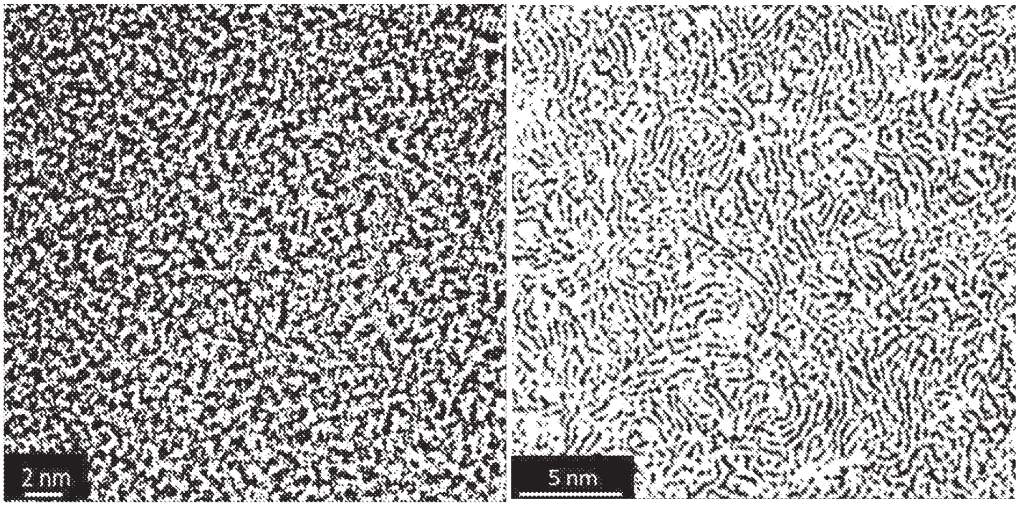
2 nm
5 nm

Fig. 6

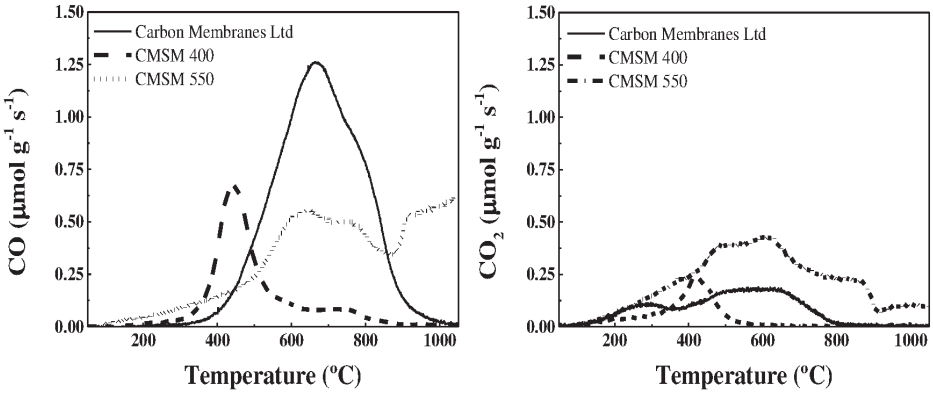
Carbon Membranes Ltd
CMSM 400
CMSM 550
CO (µmol g-1 s-1)
CO2 (µmol g-1 s-1)
Temperature (ºC)
1.50
1.25
1.00
0.75
0.50
0.25
0.00
200
400
600
800
1000

Fig. 7

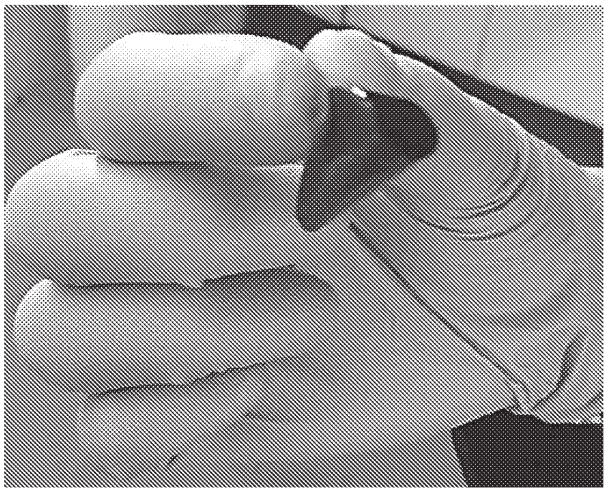

Fig. 8

INTERNATIONAL SEARCH REPORT

International application No
PCT/IB2016/056295

A. CLASSIFICATION OF SUBJECT MATTER
INV. B01D65/08 B01D53/22 B01D67/00 B01D69/10 B01D69/14 B01D71/02
ADD.
According to International Patent Classification (IPC) or to both national classification and IPC

B. FIELDS SEARCHED

Minimum documentation searched (classification system followed by classification symbols)
B01D

Documentation searched other than minimum documentation to the extent that such documents are included in the fields searched

Electronic data base consulted during the international search (name of data base and, where practicable, search terms used)
EPO-Internal, WPI Data

C. DOCUMENTS CONSIDERED TO BE RELEVANT

Category*	Citation of document, with indication, where appropriate, of the relevant passages	Relevant to claim No.
X	CAMPO M C ET AL: "Carbon molecular sieve membranes from cellophane paper", JOURNAL OF MEMBRANE SCIENCE, ELSEVIER BV, NL, vol. 350, no. 1-2, 15 March 2010 (2010-03-15), pages 180-188, XP026915560, ISSN: 0376-7388, DOI: 10.1016/J.MEMSCI.2009.12.026 [retrieved on 2010-01-04]	1-14, 16-26
Y	table 1 figure 2 table 3 page 181, column 2, line 10 - line 50	27-29
	----- -/--	

[X] Further documents are listed in the continuation of Box C.

[X] See patent family annex.

* Special categories of cited documents :

"A" document defining the general state of the art which is not considered to be of particular relevance

"E" earlier application or patent but published on or after the international filing date

"L" document which may throw doubts on priority claim(s) or which is cited to establish the publication date of another citation or other special reason (as specified)

"O" document referring to an oral disclosure, use, exhibition or other means

"P" document published prior to the international filing date but later than the priority date claimed

"T" later document published after the international filing date or priority date and not in conflict with the application but cited to understand the principle or theory underlying the invention

"X" document of particular relevance; the claimed invention cannot be considered novel or cannot be considered to involve an inventive step when the document is taken alone

"Y" document of particular relevance; the claimed invention cannot be considered to involve an inventive step when the document is combined with one or more other such documents, such combination being obvious to a person skilled in the art

"&" document member of the same patent family

Date of the actual completion of the international search	Date of mailing of the international search report
20 February 2017	08/03/2017

Name and mailing address of the ISA/	Authorized officer
European Patent Office, P.B. 5818 Patentlaan 2 NL - 2280 HV Rijswijk Tel. (+31-70) 340-2040, Fax: (+31-70) 340-3016	Hoyer, Michael

2

Form PCT/ISA/210 (second sheet) (April 2005)

C(Continuation). DOCUMENTS CONSIDERED TO BE RELEVANT

Category*	Citation of document, with indication, where appropriate, of the relevant passages	Relevant to claim No.
A	Sadipal: "Perforated Rolls / Roleaux perforés / Perforierte Rollen", , 15 March 2010 (2010-03-15), XP055344683, Retrieved from the Internet: URL:http://en.sadipal.com/upload/producte/papel-celo.pdf [retrieved on 2017-02-10] the whole document	1-29
A	246: "21 CFR 177.1200 - Cellophane", , 11 March 1989 (1989-03-11), XP055344697, Retrieved from the Internet: URL:https://www.gpo.gov/fdsys/pkg/CFR-2005-title21-vol3/pdf/CFR-2005-title21-vol3-sec177-1200.pdf [retrieved on 2017-02-10] the whole document	1-29
X	EP 0 671 202 A2 (ROTEM IND LTD [IL]; AGA AB [SE]) 13 September 1995 (1995-09-13) cited in the application claim 1 page 3, line 29 page 5, line 17	1,2
X	WO 00/53833 A1 (OSTTHUERINGISCHE MATERIALPRUEF [DE]; SCHULZE THOMAS [DE]; TAEGER EBERH) 14 September 2000 (2000-09-14) claim 1	1,2,15
Y	WO 2009/129984 A1 (MEMFOACT AS) 29 October 2009 (2009-10-29) paragraph [0042] paragraph [0055]	27-29

2

INTERNATIONAL SEARCH REPORT

Information on patent family members

International application No
PCT/IB2016/056295

Patent document cited in search report	Publication date	Patent family member(s)	Publication date
EP 0671202 A2	13-09-1995	CA 2144026 A1	08-09-1995
		EP 0671202 A2	13-09-1995
		IL 108883 A	10-03-1998
		JP H0847625 A	20-02-1996
		US 5925591 A	20-07-1999
WO 0053833 A1	14-09-2000	DE 19910012 C1	18-01-2001
		US 6881361 B1	19-04-2005
		WO 0053833 A1	14-09-2000
WO 2009129984 A1	29-10-2009	CA 2721860 A1	29-10-2009
		CN 102015082 A	13-04-2011
		EP 2276557 A1	26-01-2011
		JP 2011527935 A	10-11-2011
		KR 20110033111 A	30-03-2011
		US 2011072965 A1	31-03-2011
		WO 2009129984 A1	29-10-2009